

This item was submitted to Loughborough University as a PhD thesis by the author and is made available in the Institutional Repository (<https://dspace.lboro.ac.uk/>) under the following Creative Commons Licence conditions.



For the full text of this licence, please go to:
<http://creativecommons.org/licenses/by-nc-nd/2.5/>

LOUGHBOROUGH
UNIVERSITY OF TECHNOLOGY
LIBRARY

AUTHOR/FILING TITLE

HANSON, S

ACCESSION/COPY NO.

040129375

VOL. NO.

CLASS MARK

FOR REFERENCE ONLY
12 JUL 2000

27 JUN 1997

26 JUN 1998

14 JAN 2000

0401293750



BADMINTON PRESS
15 THE BALFOUR
LEICESTER LE1 1LD
ENGLAND
TEL 0116 259 2917
FAX 0116 259 6699

Interfaces between the Textural Components in Metallurgical Cokes

by

Svenja Hanson

A Doctoral Thesis

Submitted in partial fulfilment of the requirements
for the award of

Doctor of Philosophy

of the Loughborough University of Technology

January 1996

© by S.Hanson 1996

Loughborough University of Technology Library	
Date	Jan 96
Class	
Acc. No.	040129375

9/6451353

Abstract

The work presented in this thesis aims at furthering the understanding of the micro-texture of metallurgical cokes with regard to the interfacial properties of their optical components. Metallurgical coke, on the scale considered, can be understood as a composite of unfused carbon embedded in a porous matrix of fused material. The matrix is composed of textural units varying in size and shape depending on the rank of the coal or blend of coals carbonised. The quality of the interfaces between them and of those they form with the unfused material can reasonably be expected to influence macroscopic coke properties such as mechanical strength.

Three sample series of cokes were produced on an experimental scale under conditions resembling those in commercial coke ovens. They comprise a set of single coal cokes, individually carbonised and blended maceral concentrates and two sets of samples containing coking additives.

The samples were examined using polarized light microscopy with a magnification of $\times 1000$. A classification system for coke component interfaces according to their optical appearances was arrived at and different methods of quantitative interface analysis developed and evaluated. An interface quality index (IQI) was defined, which can be calculated from the counted data. It was found to be a suitable working construct for the purpose of comparing the quality of interfaces formed by individual textural components, groups thereof and for cokes as a whole.

The IQI could be related to the rank of the precursor coals, but this relation was thought to be a secondary effect of the rank dependence of the components themselves. On the basis of the data obtained interfacial behaviour is thought to be a characteristic property of the individual textural components. But other factors, such as the unit size of the components, the carbonisation conditions and the employment of coking additives, were also found to play important roles in the determination of total coke interface quality.

It has not yet been possible to definitively link the interface quality between the optical components to any properties of the cokes as a whole, although some weak trends with coke tensile strength and friability suggest that such relationships may eventually be established.

Acknowledgements

I would like to express my gratitude to my supervisor Prof. J.W. Patrick for the help and support I received throughout my work on this thesis.

I would also like to thank Dr. A. Walker and Mr. D. Hays for their academic and technical assistance on the project far beyond the call of duty, and for the friendship and patience shown in my many moments of doubt.

'Cheers' to my family and friends; I must have been a pain to live with for the last year. I promise I won't do it again !

Many thanks also to the ECSC (European Coal and Steel Community) who kindly funded the project 7220-EB/843.

Publications

The characterization of interfaces between textural components in metallurgical cokes
Barriocanal, C., Hanson, S., Patrick, J.W., Walker, A.
Fuel, 1994, vol.73 (12), p.1842

The quality of interfaces in metallurgical cokes containing petroleum coke
Barriocanal, C., Hanson, S., Patrick, J.W., Walker, A.
Fuel Processing Technology 45 (1995), 1-10, p.1

Interfaces between the optical components in metallurgical cokes - their classification
and relevance to coke properties
Barriocanal, C., Hanson, S., Patrick, J.W., Walker, A.
The 1995 IChemE Research Event, 5-6 Jan. 1995, Univ. of Edinburgh,
Vol.1, p. 312

Interfaces between coke constituents
Barriocanal, C., Hanson, S., Patrick, J.W., Walker, A.
Carbon 95, 22nd bien. Conf. on Carbon, 16-21 July 1995, Am. Carbon Soc.,
San Diego, p.756

Quality of interfaces between textural components in metallurgical cokes
Barriocanal, C., Hanson, S., Patrick, J.W., Walker, A.
Coal Science, Proc. 8th Int. Conf. on Coal Science, Oviedo (Spain), 1995,
vol. 1, p. 1061

Table of Contents

	Page Numbers
1 Introduction	1 - 3
2 Literature Review	4 - 62
2.1 The Origin and Properties of Coal	4 - 16
2.1.1 The Origin of Coal	
2.1.2 The Classification of Coal by Rank	
2.1.2.1 The Testing of Rank Parameters	
1 Proximate Analysis	
2 Ultimate Analysis	
3 Calorific Value	
4 Vitrinite Reflectance	
2.1.2.2 The Testing of Coking Property Parameters	
1 Crucible Swelling Number	
2 Gray King Coke Type	
3 Roga Index	
4 Dilatation	
2.1.3 The Classification of Coal by Type	
2.1.3.1 Coal Petrography	
2.1.3.2 The Properties of the Maceral Groups	
2.2 The Utilisation and Production of Coke	17 - 30
2.2.1 The Iron Blast-Furnace	
2.2.1.1 The Role of Coke in the Blast Furnace	
2.2.1.2 Coke Quality Criteria	
1 Chemical Tests	
2 Strength Tests	
2.2.2 Coke Making	
2.2.3 Coke Quality Prediction	
2.2.4 Coal Blending and Coking Additives	

2.3	The Fundamentals of Coal Carbonisation	31 - 48
2.3.1.1	The Pre-Plastic Stage	
2.3.1.2	The Plastic Stage	
2.3.1.3	The Post-Plastic Stage	
2.3.2	Theories of Coal Plasticity	
2.3.3	The Development of Coke Texture	
2.3.3.1	Rank Dependence of Optical Coke Components	
2.3.3.2	Development Routes of Optical Coke Components	
2.3.4	The Influence of Petrographic Composition	
2.3.4.1	The Reactivity of Inertinite	
2.4	Coke Microscopy	49 - 56
2.4.1	Optical Anisotropy	
2.4.1.1	Optical Anisotropy in Carbon Materials	
2.4.2	The Theory and Application of Polarized Light Microscopy	
2.4.3	The Texture of Cokes	
2.4.3.1	Historical	
2.4.3.2	Classification of Coke Textural Components	
2.5	Interfaces	57 - 61
2.5.1	The Analogy between Cokes and Composites	
2.5.2	Classification of Interfaces in Composites	
2.5.3	Interfaces in Metallurgical Cokes	
2.5.4	Interfaces involving Coking Additives	
2.6	Present Position	62
3	Experimental	63 - 72
3.1	The Cokes	63 - 69
3.1.1	Series 1	
3.1.2	Series 2	
3.1.2.1	Formulation of the Maceral Concentrate Blends	
3.1.3	Series 3	
3.2	Friability Testing	69

3.3	Sample Preparation for Microscopy	69 - 70
3.4	Polarized Light Microscopy	70 - 72
3.4.1	Coke Component Counts	
3.4.2	Interface Counts	
4	Discussion of Results	73 - 171
4.1	The Interface Classification System	73 - 89
4.1.1	Interface Classes	
4.1.2	Counting Methods for Quantitative Interface Analysis	
4.1.3	Interface Quality Index	
4.1.4	Rank Dependence of the Interface Distribution	
4.1.5	Textural Component Dependence of the Interface Distribution	
4.1.6	Influence of Carbonisation Method	
4.2	Statistical Appraisal of the Counting Methods	90 - 99
4.2.1	Mathematical Background	
4.2.2	Errors in Component and Interface Counts	
4.2.3	Interface Distribution Errors due to Variations in the Counting Method	
4.3	Binding Power Hypothesis	100 - 107
4.3.1	Formulation of the Binding Power Hypothesis	
4.3.2	Testing of the Binding Power Hypothesis	
4.3.3	Estimation of the Theoretical Component Binding Powers	
4.3.4	Prediction of Interface Quality Indices for Series 2	
4.4	Component Size Modelling	108 - 121
4.4.1	Interface Participation and Component Size	
4.4.2	Mathematics of the Component Size Model	
4.4.3	Calculation of Component Sizes for Series 1	
4.4.4	Estimation of Pore- and Single Component Interfaces	
4.4.5	Prediction of Interface Type Percentages in Series 2	

4.5	Effect of the Maceral Separation Process	122 - 124
4.5.1	Component Distribution	
4.5.2	Interface Distribution	
4.6	Relation between Coal Inertinite and Coke Inerts	125 - 129
4.6.1	Conversion of Maceral Group Weight Percentage to VolumePercentage	
4.6.2	Relation between Inerts and the Inertinite Derived Coke Fraction	
4.7	The Effect of Coke Inerts on Interfaces	130 - 141
4.7.1	Relative Importance of Interfaces with Inerts	
4.7.2	Variation of Interface Frequencies with Inert Levels	
4.7.3	Variation of IQI with Inert Levels	
4.8	The Effects of the Blending of Maceral Concentrates	142 - 150
4.8.1	Component Composition	
4.8.2	Interface Distribution	
4.8.3	Interface Quality Indices	
	1 Vitrinite Concentrates from Coal A2	
	2 Vitrinite Concentrates from Coal B2	
	3 Vitrinite Concentrates from Coal C2	
	4 Vitrinite Concentrates from Coal D2	
4.9	The Effect of Coking Additives on Coke Component Interfaces	151 - 167
4.9.1	Additive Incorporation	
4.9.2	Relative Participation in Interfaces	
4.9.3	Variation of Overall Interface Quality Index with Additive Levels:	
	1 Additive 1	
	2 Additive 2	
	3 Comparison of the Additives	
	4 Influence of Changes in Component Composition	
4.9.4	Individual Interface Quality Indices for Inerts and Additives	
	1 Inerts	
	2 Additives	
	3 Variation between Coals	
	4 Relation of Total to Individual Interface Quality Indices	

4.10	Interface Quality and Coke Properties	168 - 171
4.10.1	Tensile Strength of Series 1	
4.10.2	Friability of Series 2 and 3	
	1 Series 2	
	2 Series 3	
5	Discussion	172 - 187
5.1	The Nature and Origin of the Interfaces	172 - 183
5.1.1	The Formation of Transitional and Fused Interfaces	
5.1.2	Formation of Poor Interfaces (Micro-Cracks)	
5.1.3	Estimated Percentage of Particle Boundary derived Interfaces	
5.2	Theoretical Relation between Interfaces and Strength	183 - 187
5.2.1	Theory of Fracture and Stress Propagation	
5.2.2	Application of the Fracture Theory to Metallurgical Cokes	
6	Conclusions	188 - 191

References

Appendix 1

The Estimation of the Properties of the Pure Macerals

Appendix 2

Component Count Data

Appendix 3

Interface Count Data

List of Tables

	Page
T2.1 The Variation of Coal Properties with Coal Rank	6
T2.2 The British Coal Classification System (NCB Code Numbers)	7
T2.3 The International Coal Classification System	8
T2.4 Description of Coal Lithotypes	12
T2.5 The Origin of the Coal Macerals	14
T2.6 Comparison of the Different Methods of Testing Coke Strength	22
T2.7 Typical Values for the Coke Specifications in terms of Chemical and Strength Tests	23
T3.1 Properties of the Coals	64
T3.2 Petrographic Composition of the Coals and Maceral Concentrates in Series 2	65
T3.3 Composition of Blends in Series 2.1	68
T3.4 Weight Percentage of the Vitrinite Concentrates in the Blends in Series 2.2	68
T3.5 Classification of Textural Coke Components	71
T4.1 Description of the Classification System of Coke Component Interfaces	73
T4.2 Interface Quality Indices for Reactive-Inert Interfaces in Series 1	82
T4.3 Interface Quality Indices for Reactive-Reactive Interfaces in Series 1	83
T4.4 Ratio of Transitional and Fused Interfaces between Reactive Components in Series 1	85
T4.5 Interface Quality Indices from by Component Counts of Series 2.1	87
T4.6 Interface Quality Indices from by Component Counts of Series 2.2	88
T4.7 Ranking of the Average Interface Quality Indices for Reactive-Reactive Interfaces in Series S1 and S2	89
T4.8 Average Errors and Multiplication Factor for 95 % Confidence Limit for Component Counts	93

T4.9	Average Errors and Multiplication Factor for 95 % Confidence Limit for Interface Counts	93
T4.10	95 % Confidence Limits for Component and Interface Counts	94
T4.11	Comparison of the Interface Distributions in Series 1 counted by Simple and by, By-Component Counts	96
T4.12	Comparison of the Interface Distributions in Series 2 counted by Simple/Split and by, By-Component Counts	98
T4.13	Comparison of the Percentage of Reactive -Reactive, Reactive - Small -.Inerts and Reactive -Large Inerts counted by Split and by By-Component Counts	99
T4.14	Ratio of the Squares of the Interface Types formed with Small and Large Inerts in Series 1	103
T4.15	Estimated Component Binding Powers	105
T4.16	Predicted and Counted Interface Quality Indices for Inerts in Series 2	106
T4.17	Ratio of the Number of Interfaces to the Sum of the Volume Percent of the Interfacing Components (Series 1)	109
T4.18	Component Unit Side Length	
	a) First Estimates	114
	b) Edited Estimates	115
	c) Final Estimates	116
T4.19	Interface Combination Percentages Calculated from the Final Component Side Length Estimates	
	a) All Combinations	118
	b) Excepting Inert-Inert and Pore Interfaces	119
T4.20	Comparison of the Predicted and Counted Percentages of Reactive-Reactive, Reactive-Small Inerts and Reactive-Large Inerts Interfaces for Series 2	120
T4.21	Comparison of the Component Distributions for the Cokes from the Coals in Series 2 and their equivalent Vitrinite-Inertinite Concentrate Blends	123
T4.22	Comparison of the Interface Distributions for the Cokes from the Coals in Series 2 and their equivalent Vitrinite-Inertinite Concentrate Blends	124
T4.23	Potential Errors in Blend Inertinite Weight Percentage in Series 2	126

T4.24	Calculated and Counted Inerts in Sample Series 2.1	128
T4.25	Comparison of Inert Component Percentages and their Percentage Participation in Interfaces in Series 1	130
T4.26	Ratio of the Number of Interfaces of the Reactive Components with Inerts and their Combined Volume Percent for Series 2.1	137
T4.27	Counted and Calculated Component Distribution in Series 2.2	143
T4.28	Counted and Calculated Interface Distributions for Series 2.2	145
T4.29	Average Total Interface Quality Indices in Series 2.2	147
T4.30	Interface Quality Indices of Series 2.2 determined by Split Counts	148
T4.31	Ratio of Interface Frequency to the Combined Volume Percentage of the Interfacing Components for Series 3	154
T4.32	Total Interface Quality Indices for Series 3	155
T4.33	Deviation of the Textural Component Composition from the Additive-free Samples in Series 3	157
T4.34	Individual Interface Quality Indices for Small and Large Coal Derived Inerts	160
T4.35	Individual Interface Quality Indices for Small and Large Additive Particles	161
T4.36	Relative Contributions of the Interface Types to the Total Interface Quality Index	165/6
T5.1	Relation of Interface Distributions for Reactive-Reactive Components with the Percentage of Mosaic Type Components in Series 1 and 2	178

List of Figures

	Page
F2.1 Schematic View of the Temperature Regime in a Blast Furnace	18
F2.2 Schematic View of a Coke Oven	25
F2.3 Simplified Representation of Coke Strength in Relation to Coal Rank and Inert Content	27
F2.4 Reflectance and Dilatation Limits for Coal Blending (MOF Diagram)	28
F2.5 Causal Chain of the Phenomena in Coke Formation	31
F2.6 Volatile Matter of Coal in Relation to Softening and Decomposition Temperatures	32
F2.7 Optical Appearance and Inferred Structure of Mesophase Spheres	39
a) Phenomena observed when a Mesophase Sphere is rotated between Crossed Nicols	
b) Inferred Structure of the Mesophase Sphere	
F2.8 The Reorientation of the Lamellae when two Mesophase Spheres coalesce	41
F2.9 Structural and Optical Anisotropy of Graphite	50
F2.10 Schematic Representation of the Difference of Graphitisable and Non-graphitisable Carbons	51
F2.11 Colour Changes on Rotation of an Anisotropic Sample between Crossed Polars using a Half Wave Retarder Plate	54
F3.1 Schematic View of the Experimental Carbonisation Set-up	66
F3.2 Micrographs of the Optical Coke Components	72
F4.1 Micrographs of the Interface Types	74/5
F4.2 Distribution of the Textural Components and their Interfaces in Sample Series 1	79
a) Textural Component Distribution	
b) Interface Distribution	
F4.3 Average Interface Quality Indices for the Cokes in Series 1	80

F4.4	Overall Interface Quality versus Selected Coal Rank Parameters for the Cokes in Series 1 a) Carbon Content b) Total Dilatation	81
F4.5	Illustration of the 95% Confidence Limits for Component and Interface Counts	95
F4.6	Estimated Component Binding Powers	105
F4.7	Predicted and Counted Interface Quality with Small Inerts in Series 2	107
F4.8	Predicted and Counted Interface Quality with Large Inerts in Series 2	107
F4.9	Illustration of the Estimated Component Unit Sizes	117
F4.10	Percentage of Calculated Inerts versus the Difference between Calculated and Counted Inerts in Series 2.1	128
F4.11	Interface Distributions Split by Interface Types in Series 1 a) Reactive - Reactive Interfaces (R-R) b) Reactive - Small Inerts Interfaces (R-S) c) Reactive - Large Inerts Interfaces (R-L) d) All Interfaces	131/2
F4.12	Comparison of Average Interface Type Quality Indices with the Overall Interface Quality Index in Series 1 a) Interface Quality Index for Reactive-Reactive Interfaces (IQIr) b) Interface Quality Index for Reactive-Small Inerts Interfaces (IQIs) c) Interface Quality Index for Reactive-Large Inerts Interfaces (IQIL) d) Overall Interface Quality Index (IQIt)	133
F4.13	Variation of the Interface Frequency to Component Volume Ratio for Reactive-Inert Interfaces with Inerts Content in Series 2.1 a) GF b) CM c) MM d) FM e) ISO	135
F4.14	Variation of the Interface Type Quality Indices with the Inerts Content for Coal A2 a) Reactive - Small Inert Interfaces (IQIs) b) Reactive - Large Inert Interfaces (IQIL) c) Reactive - Total Inerts Interfaces (IQIt) d) Reactive - Reactive Interfaces (IQIr)	139

F4.15	Variation of the Interface Type Quality Indices with the Inerts Content for Coal B2	140
	a) Reactive - Small Inert Interfaces (IQIs)	
	b) Reactive - Large Inert Interfaces (IQII)	
	c) Reactive - Total Inerts Interfaces (IQIi)	
	d) Reactive - Reactive Interfaces (IQIr)	
F4.16	Variation of the Interface Type Quality Indices with the Inerts Content for Coal C2	141
	a) Reactive - Small Inert Interfaces (IQIs)	
	b) Reactive - Large Inert Interfaces (IQII)	
	c) Reactive - Total Inerts Interfaces (IQIi)	
	d) Reactive - Reactive Interfaces (IQIr)	
F4.17	Additive Derived Coke Fraction not Counted as Additive Component in Series 3	152
	a) Additive 1	
	b) Additive 2	
F4.18	Variation of the Individual Interface Quality Indices in Series 3	163
	a) Interfaces with Small Inerts (IQIs) in Samples with Additive 1	
	b) Interfaces with Small Inerts (IQIs) in Samples with Additive 2	
	c) Interfaces with Small Additive Particles (IQIas) in Samples with Additive 1	
	d) Interfaces with Small Additive Particles (IQIas) in Samples with Additive 2	
	e) Interfaces with Large Inerts (IQII) in Samples with Additive 1	
	f) Interfaces with Large Inerts (IQII) in Samples with Additive 2	
	g) Interfaces with Large Additive Particles (IQIal) in Samples with Additive 1	
	h) Interfaces with Large Additive Particles (IQIal) in Samples with Additive 2	
F4.19	Total Interface Quality versus Tensile Strength for the Cokes in Series 1	168
F4.20	Total Interface Quality versus Friability Test Weight Loss for the Cokes in Series 2	170
F4.21	The Relation between Friability Weight Loss and Overall Interface Quality Index for Samples in Series 3	171
F5.1	Sketches of the two Basic Mechanisms of the Development of Coke Microtexture [114]	174
	a) medium Rank, softening Coal	
	b) high Rank, non-softening Coal	

F5.2	Variation of the Percentage of Particle Boundary Derived Interfaces with a) Particle Size b) Average Reactive Component Size c) Inert Content	182
F5.3	Griffith Estimate for the Relation between the Stress applied and the Stress concentrated at a Crack Tip [116]	184

Glossary

General (Components and Interfaces)

C	Any Component	(subscript c)
R	Any Reactive Component	(subscript r)
S	Small Inerts	(subscript s)
L	Large Inerts	(subscript l)
I	Any Interface Type	

IQI	Interface Quality Index
IQIx	Interface Quality Index for an Individual Component Combination x
IQIt	Total Interface Quality Index for all Component Combinations in a Coke
BP	Binding Power (Theoretical IQI of an Individual Component)
P(X)	Percentage of Component\Interface X Counted
	Probability of Component\Interface X occurring
px	Fraction of Component\Interface X Counted

Statistics

p	Probability of an Event
P (r)	Probability of an Event occurring r number of times for a given Number of Trials (usually here: Number of Points of a Component\Interface Counted)
N	Number of Trials (usually here: Total Number of Points Counted)
μ	True (Theoretical) Mean
\bar{x}	Observed Mean
s ²	Variance
s	Standard Deviation
EAE	Expected Absolute Error
AAE	Actual Absolute Error
a	Multiplication Factor relating theoretical and actual 95% Confidence Limit

Component Size Model

a	Component Unit Side Length
V	Volume of Component
S	Surface Area of Component
ST	Total Surface Area of all Components in a Coke
A	Fraction of Surface Area in a Coke given by a Component
Ar	Fraction of Surface Area in a Coke given by Reactive Components
PAB	Probability of a Component A interfacing with a Component B
Pc	Probability of Interfaces between Units of the same Component
Pii	Probability of two Inerts interfacing
Pr	Probability of Units of different Reactive Components interfacing
Ps	Probability of Interfaces between Reactive Components and Small Inerts
Pl	Probability of Interfaces between Reactive Components and Large Inerts
Pp	Probability of Interfaces between Components and Pores

1 Introduction

Coke, in general terms, is a black to silver-grey porous carbon residue [1], which is the solid product of the destructive distillation of organic substances out of contact with air [2]. In this thesis the term coke will specifically refer to the high temperature carbonisation product of coal used in the iron- and steel industry.

The main industrial application of metallurgical coke is iron ore smelting in the blast-furnace. In 1991, for example, 5.3 Mt of the 6.2 Mt of coke consumed in the U.K. were used in blast-furnaces [3], which is roughly equivalent to 85 % of the total coke consumption. Inversely, coke, when used exclusively without the addition of substitutes such as heavy fuel oil or pulverized coal, accounts for about 39 % of the production costs of pig iron [4]. Coke is still considered indispensable for iron production, with a minimum of 300 - 350 kg / t hot metal considered possible, compared to the about 480 kg / t presently required [5].

Coke has three main functions in the blast furnace [6, 7]. Firstly, it acts as a fuel, generating heat by combustion. Secondly, it provides carbon and carbon monoxide for the reduction of the iron oxides. And finally it maintains burden permeability in the high temperature zones of the furnace, so that the molten iron and slag can drain into the hearth and the hot reducing gases can rise from the tuyeres up towards the stack. It is the third of these functions which defines the need for a solid fuel such as coke, capable of withstanding severe physical, chemical and thermal conditions, as none of the substitutes can as yet match the vital mechanical role coke plays in the blast furnace. This stresses the importance of coke strength, and it is hardly surprising that the structural properties of coke appertaining to it have excited much research interest [8, 9]. One of the difficulties in dealing with this topic is that structural ordering occurs at different levels of scale [10] ranging from the alignment of individual molecules into basic units through to the formation of large fissures, measurable in centimeters, due to differential stresses in the coke oven as the re-solidified semi-coke contracts.

The work presented here aims at understanding the structure of coke on the scale of tens to several hundreds of microns, the type of order perceived by viewing coke with a $\times 1000$ magnification under an optical microscope. Metallurgical coke on this scale can be considered as a composite of unfused carbon embedded in a porous matrix of fused material. The strength of this carbon/carbon composite, on theoretical grounds, can be expected to depend on its porous structure, the materials properties of the carbon forms present, and the quality of the interfaces between them [11]. The coke

matrix is composed of textural units varying in size and shape depending on the rank of the coals in the blend carbonised [12,13,14]. The system is complicated by the absence of a clear divide between fusing and inert components and the lack of a simple relationship between their quantitative occurrence and the petrographic constituents of the parent coal [15]. It is possible that a better understanding of the textural coke components, and eventually of the way they influence macroscopic coke properties, can be arrived at by assessing the way in which they interact with one another.

The studies described in this thesis relate to three series of cokes which were produced on an experimental scale under conditions resembling those in commercial coke ovens. The cokes were examined using polarized light microscopy (PLM) with the view to gaining further insight into the interfacial behaviour of their optical components.

The first sample series was predominantly used to devise a classification system for coke component interface types and to evaluate different methods of quantifying them. Careful inspection of the cokes led to a classification system distinguishing between 'good' and 'poor' interfaces. 'Good' interfaces can be subdivided into transitional (T) and fused (Fu), depending on whether there appears to be a smooth transition between the components via an intermediate material, or whether a clear boundary between them can be identified. 'Poor' interfaces divide into fissured (Fi) and unfused (Uf) according to the size of the area of no contact between the components relative to the size of the entire interfacial area.

One of the foremost questions considered is whether interfacial behaviour is characteristic for individual components or whether a component behaves differently when derived from coals of different rank. At the extremes two possibilities are envisaged. Either there is a direct link between component and interface distribution such that the interfacial behaviour of each component is an invariable characteristic of the same and the overall interface distribution can be predicted from the component distribution. Alternatively, the interfacial behaviour of a component could vary according to its origin and frequency of occurrence, so that it would be a function of some bulk property of the coal or blend carbonised and could be predicted from this.

Whereas the reactivity or binding power of the components is useful in predicting the interface quality achieved by individual component combinations, it does not indicate their impact on the overall coke interface quality, which also depends on the frequency with which they occur. As the sizes of the component units are perceived to be one of the likely factors governing the frequency of interfaces involving different component combinations, an attempt to estimate them is made. The model devised for this purpose is based on the assumption that the probability of an interface occurring

between two components is directly proportional to their combined surface areas available for interfacing

The second sample series was aimed at investigating the role of the petrographic composition of the coal or coal blend carbonised on coke component interfaces. Particular attention was given to the role of inerts and their relation to the inertinite derived fraction of the cokes. The cokes are carbonised from maceral concentrates rather than coals in order to be able to vary the petrographic composition more widely. Two possible effects are sought after. Firstly, it is investigated whether individual components have characteristic optimum inert levels, akin to those of the vitrinite types used for coke strength prediction [16]. Secondly, the possibility that there may be a limit to the ability of any component to incorporate inerts, beyond which it may become "saturated", is considered.

Finally, in the third sample series, the interfacial behaviour of the reactive coke components with coking additives is considered and a comparison is made with that of intrinsic, coal derived inerts. Apart from the interaction of the reactive coke components with these additives, it is of some interest whether their addition influences the interfacial behaviour between the reactives themselves and with the coal derived inerts, and, if this is the case, in what manner.

An attempt is also made to establish if the interface quality of the textural components is a truly independent parameter, which has a bearing on the macro-properties of the cokes. For this purpose the interface quality is related to coke strength in the case of series 1 and to the percentage weight loss on friability testing for series 2 and 3.

2 Literature Review

2.1 Origin and Properties of Coal

2.1.1 The Origin of Coal

Coal is an opaque, black or dark coloured combustible sedimentary rock [17]. Coal deposits were formed from the remains of plant materials by the combined action of heat and pressure in a process referred to as 'coalification'. It occurred where plant debris was prevented from rapid aerobic decay, e.g. by being submerged in swamps or estuaries, and was converted to peat in the absence of air. Subjection to heat and pressure on burial under successive layers of sediment led to the formation of coals with increasingly higher carbon content, starting with the 'soft' coals, brown coal, lignite and subbituminous coal, and finally yielding 'hard' coals, bituminous coal and anthracites. This progression in coal rank with time is commonly referred to as coalification series [18]. Most bituminous coals date from the Carboniferous period (some 280 to 345 million years ago), whereas the brown coals and lignites tend to date from the Tertiary and Cretaceous periods (3 to 136 million years ago) [17]. Although this holds generally true, there are significant departures. Some coals, like those in the Moscow basin [19], never developed beyond the brown coal rank despite their considerable age of about 330 million years. Also, it has been pointed out that this view is restricted to the coals occurring in the Northern Hemisphere, mostly Europe and North America, which still formed the single continent of Laurasia during the major coal forming periods [20]. Southern Hemisphere coals, collectively termed Gondwana coals after the continent which later broke up to form South America, Africa, Antarctica, India, Madagascar and Australia, were predominantly deposited during the Permian period (about 248 to 286 million years ago). The conditions of deposition differed insofar that the climate was cold temperate to Arctic, as opposed to the humid, subtropical climate which prevailed during the Carboniferous era in Laurasia, so that the coals from the two 'provinces' are derived from very different kinds of vegetation.

The coalification process is divided into two stages, a bio-chemical one, called diagenesis [18] or peatification [19] and a geochemical one, sometimes referred to as metamorphosis [18]. The former is thought to determine the coal type, in terms of petrographic composition, the latter establishes the coal rank [21]. The conditions for both to occur are rather stringent, which accounts for the relative rarity of coal compared to other sedimentary rocks formed in the same geological periods. The first prerequisite is the accumulation of peat in a gently subsiding aquatic environment

(geosyncline). This can occur under quite varied circumstances, in particular hydrological regimes, climate, nature of the sediment and rate of subsidence, so that coal types may vary considerably due to the vegetation type and the conditions of preservation and decomposition. During peatification the upper layers of the plant debris undergo extensive alteration by the action of bacteria, fungi and enzymes. Below a certain burial depth these actions cease and a process known as gelification sets in, the chemistry of which is not fully understood. This stage is characterized by swelling, degradation and infilling of cell lumina and the destruction of recognizable plant cellular structure. The geochemical stage represents the transformation of peat into coal, which is predominantly controlled by the increases in temperature and pressure that accompany the progressive burial by sediments in the subsiding basin. Time and temperature are now favoured as the factors determining coal rank, i.e. its position in the coalification series. There is therefore a link between burial depth and coal rank, although this is not always straightforward, due to local variations in geothermal gradient induced by differences in sediment conductivity, hydrodynamic regimes, crustal thinning and igneous activity. Though the role of pressure is still largely unresolved, it is thought to have an important influence on the physical properties of the coal, such as pore volume and moisture content.

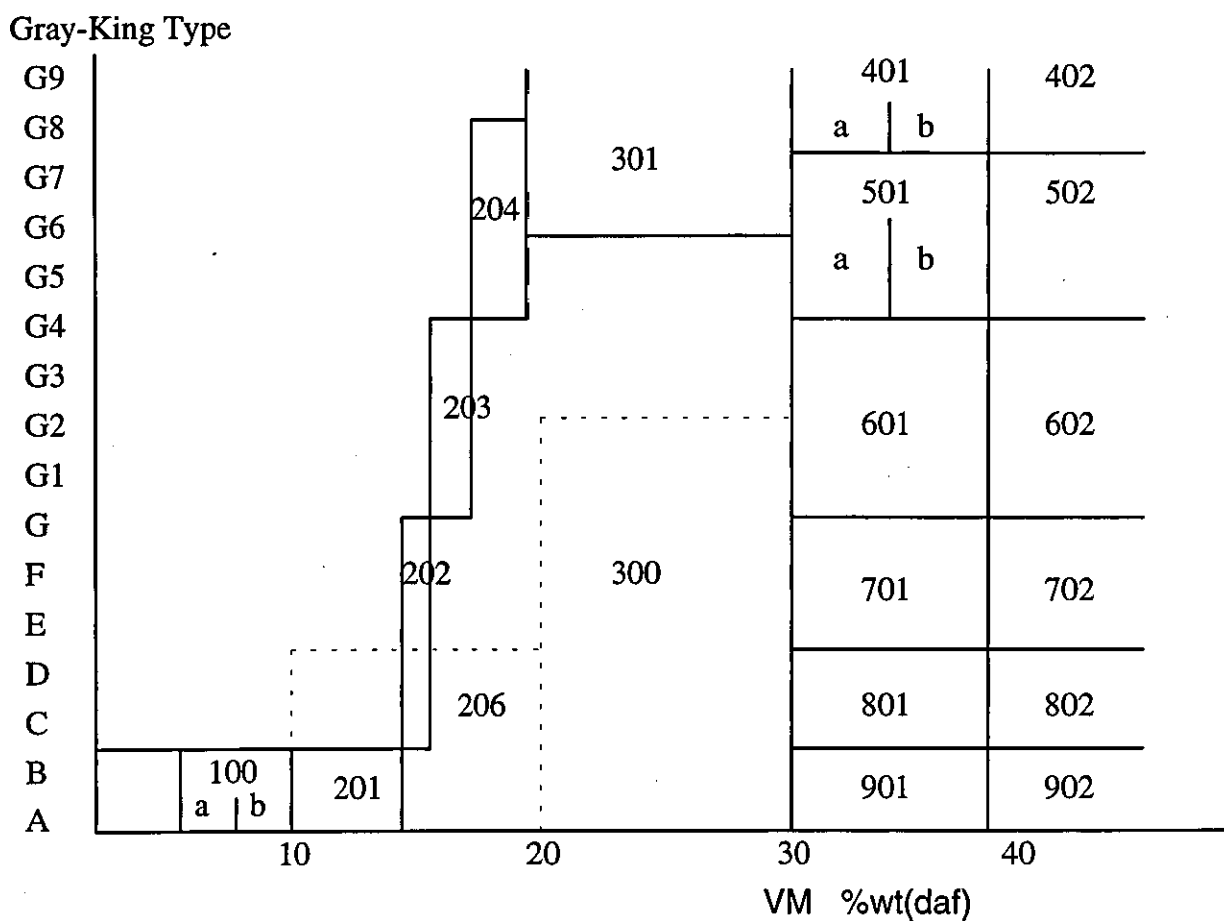
2.1.2 Classification of Coal by Rank

During coalification the chemical and physical properties of the coal are progressively altered. Among the physical changes are a reduction in moisture content, a decrease in porosity, changes in surface area and non-linear changes in optical properties such as refractive and absorptive indices [19]. The most important chemical change is the increase of coal aromaticity with rank, which results in an enrichment in carbon corresponding to the loss of CH, CH₂ and CH₃ groups. Plotting atomic ratios on van Krevelen type diagrams [18], that is the hydrogen/carbon ratio against the oxygen/carbon ratio, indicates that during the transformation from lignite to bituminous coal the predominant loss is that of oxygen relative to carbon, followed by the rapid loss of hydrogen at higher levels of coalification. Bulk properties such as moisture and volatile matter do not exhibit linear changes throughout the coalification series, but undergo sudden shifts known as 'coalification jumps'. A useful overview of the variation of coal properties with rank is given by Neavel [21] and is reproduced on the following page as table 2.1. The same author points out the limitations of classification by rank, as coal rank and type are not independent and results can be distorted by the presence of large fractions of non-vitrinite macerals.

Properties increasing with rank	Reflectance and optical anisotropy Carbon content Aromaticity Condensed - ring fusion Parallelisation of molecular moieties Calorific value
Properties decreasing with rank	Volatile matter Oxygen content Oxidizability Solubility
Properties increasing initially with rank, then decreasing	Hardness Plastic properties Hydrogen content
Properties decreasing initially with rank, then increasing	Surface area Porosity Density

Table 2.1 The Variation of Coal Properties with Coal Rank

There is no single property which can be used reliably over the whole range of the coalification series for classification purposes, which has led to a number of classification systems using different combinations of properties. The conflict between accuracy and simplicity has led to the parallel development of scientific and commercial classification systems [18]. Scientific classification systems, the best known of which is Seyler's Chart, are based either on elemental composition or on vitrinite reflectance, both of which are tedious and lengthy to determine. Most commercial classification systems contain a parameter of rank and one or two of coking properties [22]. The most commonly used rank parameters are carbon content (US) and volatile matter content (UK, France, International) in combination with calorific value for lower ranks. Coking property parameters are the Gray King coke type (UK, International), the crucible swelling number (France, International), the Roga index (International) and dilatation (International). The British classification system, known as NCB Code Numbers, and the International one, which will be referred to later in this chapter and are used in the experimental part of this work, are shown in tables 2.2 and 2.3. The standard testing procedures for classification purposes are outlined in the following sections.



100		Anthracite
200		Low Volatile Steam Coal
	201	Dry Steam Coal
	202	Coking Steam Coal, weakly caking
	203	Coking Steam Coal, medium caking
	204	Coking Steam Coal, strongly caking
	206	Scottish Navigation Coal
300		Medium Volatile Coal
	300	Scottish Medium Volatile Coal
	301	Coking Coal
400-900		High Volatile Coal
	400	Very Strongly Caking Coal
	500	Strongly Caking Coal
	600	Medium Caking Coal
	700	Weakly Caking Coal
	800	Very Weakly Caking Coal
	900	Non-caking Coal

Table 2.2 The British Coal Classification System (NCB Code Numbers)

GROUPS (determined by caking properties)			CODE NUMBERS										SUB-GROUPS (determined by caking properties)			
Group number	Alternative group parameters		The first figure of the code number indicates the class of the coal. [*] The second figure indicates the group of coal, determined by caking properties. The third figure indicates the sub-group, determined by caking properties.										Sub-group number	Alternative sub-group parameters		
	Crucible-swelling number	Roga index												Dilatometer	Gray-King	
3	>4	>45					435	535	635				5	>140	>G8	
										V _C				4	>50-140	G5-G8
							334	434	534							
							V _A	V _B								
							333	433	533	633	733			3	>0-50	G1-G4
2	2½-4	>20-45					332	432	532	632	732	832	2	≤0	E-G	
							332	432	532	632	732	832				
							323	423	523	623	723	823				
							322	422	522	622	722	822				
							321	421	521	621	721	821				
1	1-2	>5-20					321	421	521	621	721	821	1	Contraction only	B-D	
							212	312	412	512	612	712	812			
							211	311	411	511	611	711	811			
							210	310	410	510	610	710	810			
							209	309	409	509	609	709	809			
0	0-½	0-5					208	308	408	508	608	708	808	0	Non-softening	A
							207	307	407	507	607	707	807			
							206	306	406	506	606	706	806			
							205	305	405	505	605	705	805			
							204	304	404	504	604	704	804			
Class number →			0	1	2	3	4	5	6	7	8	9	As an indication, the following classes have an approximate volatile matter content of: Class 6 33-41% 7 33-44% 8 35-50% 9 42-50%			
Class parameters	Volatile matter →	%	0-3	>3-10 >3 >6.5 -6.5-10	>10-14	>14-20	>20-28	>28-33	>33	>33	>33	>33				
	Calorific parameter* →		-	-	-	-	-	-	>7 750	>7 200 -7 750	>6 100 -7 200	>5 700 -6 100				

* %wt on a dry ash-free basis

Table 2.3 The International Coal Classification System

2.1.2.1 The Testing of Rank Parameters

2.1.2.1.1 Proximate Analysis

Proximate analysis comprises the determination of moisture, ash and volatile matter content (VM).

The moisture content, as a weight percentage, is found by drying a coal sample at 105 °C in air until a constant weight is achieved. The moisture content is a drying weight loss and must not be confused with the water content of the coal, as water will still be contained as inherent moisture trapped in pores and in chemical compounds, which will only be released on pyrolysis.

The ash content is the weight of the solid residue left after combustion of a coal sample. It is usually determined in an electrical furnace which is charged cold and heated to a maximum temperature of 815 °C. Ash content is sensitive to the nature of the mineral matter in the coal, as some chemical alterations take place on heating, such as CO₂ removal from carbonates, loss of water from silicates or transformation of pyrites into ferric oxide [22], so that the method is no accurate measurement of mineral matter content. It can be used though to estimate the mineral matter content.

Volatile matter (VM) content is a measure of weight loss on carbonisation, due to the release of combustible gases, such as H₂, CO, CH₄ and other hydrocarbons, tarry vapours and non-combustible gases, namely water and CO₂. For the VM determination about 1 g of finely crushed coal contained in a crucible, with a well fitting lid to avoid oxidation, is placed in a very hot furnace (900 or 950 °C) for a short time (about 3 min) and the weight loss due to this treatment is determined. The moisture and ash content enable the VM to be calculated as a weight percentage on a dry, ash-free basis (wt% daf).

2.1.2.1.2 Ultimate Analysis

Ultimate analysis is an elemental analysis for the main chemical constituents of coal, that is carbon, hydrogen and oxygen. Other elements, such as sulphur, nitrogen, chlorine and phosphorus, are often additionally tested for, in particular where they are of some importance for a given application. Carbon and hydrogen percentages are determined by complete combustion of the coal at high temperatures (up to 1400°C). The combustion gases, H₂O and CO₂, are retained by absorption and the carbon and hydrogen content is deduced from the change of weight of the absorbents. Oxygen content is mostly deduced from the difference of the other elements tested for, but it can be determined by high temperature (about 1200 °C) pyrolysis in nitrogen. The pyrolysis products are passed over activated carbon at 200 °C, which converts them into CO. This is further converted to CO₂ and the oxygen content is derived from it.

2.1.2.1.3 Calorific Value

The calorific value (CV), or heat of combustion, is determined by measuring the temperature rise due to complete combustion in a constant volume bomb calorimeter in an atmosphere of oxygen. This is known as the gross CV, as the condensation energy of the water is included, and the net CV is calculated from it using the data obtained in the ultimate analysis on the basis of standard atmospheric conditions (96 % relative humidity, 30 °C). Both CVs are usually quoted on an ash-free basis.

2.1.2.1.4 Vitrinite Reflectance

Vitrinite reflectance analysis is based on the fact that the proportion of incident light reflected from a surface depends on its chemical composition and molecular structure [21]. It increases with the degree of molecular ordering, which in turn increases with coal rank, so that it can be used as a rank parameter. For reflectance analysis, polished vitrinite samples are viewed under a reflected light microscope. The system is calibrated using glass standards of known reflectance, from which the sample reflectances are calculated. The reflected light fraction from a small sample area (about 2 to 10 μm) is detected by a sensitive photomultiplier tube, which transmits a signal that is amplified and displayed digitally. In routine analysis the average of 100 points per specimen is usually taken. For each measurement the microscope stage is rotated through 360° and the maximum is recorded, so that a bias due to anisotropy effects is avoided. The value thus arrived at is known as mean maximum reflectance. A simpler, but less accurate, process in which the microscope stage is not rotated, yields a value known as mean (random) reflectance.

2.1.2.2 The Testing of Coking Property Parameters

2.1.2.2.1 Crucible Swelling Number

The crucible swelling test is a free swelling test, i.e. expansion of the coal is not restricted by containment, as in the other tests covered in this section. It measures the swelling of a small sample of coal on very rapid heating (about 400 °C / min) over an open flame or in a preheated electrical furnace. The resulting coke button is compared to a series of standards numbered from 0, no cohesion, to 9, swelling to fill out the entire crucible. The number assigned to the coke button is known as 'swelling index'.

2.1.2.2.2 Gray King Coke Type

In the method developed by Gray and King 20 g of finely crushed coal is slowly heated in a tube (5 °C / min between 300 and 600 °C) and the resulting coke is visually examined by comparing it to a number of standards. Letters from A (pulverulent) to G (same volume as original coal) are assigned to it. For strongly swelling coals (> G) it is then determined how many parts of electrode carbon by weight need to be included in the 20 g sample to obtain the appearance of a G type coal. This number is then added as a subscript from G₁ (slightly swollen) to G₉ (very strongly swollen).

2.1.2.2.3 Roga Index

The Roga test gives an impression of the caking power of the coal by means of a friability test. A sample of crushed coal mixed with anthracite is placed in a crucible and weighed down by a disk of specified weight. It is heated in an electric furnace at 850 °C for 15 minutes. After cooling it is weighed and screened on a 1 mm screen. Then the sample is subjected to an abrasion test by being rotated in a drum for 15 minutes at 50 rpm. During this it is screened and weighed at 5 minute intervals. An abrasion curve is plotted from the data thus obtained as the percent of coke < 1 mm versus time. From the plot the Roga index is determined as the area under the curve divided by the total area.

2.1.2.2.4 Dilatation

Dilatometer tests use a slow heating rate in an attempt to simulate the behaviour of coal in a coke oven. Many different dilatometers are currently used and these can be roughly divided into two groups according to their temperature range. The lower temperature ones investigate the behaviour of the coal during its plastic range, whereas the higher temperature ones extend beyond the resolidification temperature. The Audibert-Arnu dilatometer, which is the most commonly used one, is of the former kind. It determines the percentage of maximum dilatation on a small coal sample (2 g) compressed to a pencil, which is heated at a constant rate (3 °C / min). A plunger (piston) resting on the pencil records the swelling of the coal as a function of temperature. Initially, as the coal softens, contraction will occur and the total dilatation is measured from this minimum to the maximum height attained at resolidification.

2.1.3 The Classification of Coal by Type

2.1.3.1 Coal Petrography

Coal is a sedimentary rock comprised of constituents called macerals, and subordinatly of minerals and water and gases trapped in micro-pores. The macerals are derived from various plant tissues and exudates, which have been incorporated into the sedimentary strata, subjected to decay, compacted, hardened and chemically altered [21]. The term maceral was introduced by Stopes (1935) to denote the basic organic constituents of coals which can be recognized under the microscope. Macerals were considered to be analogous to the minerals of other rocks. They were defined as "organic substances or optically homogeneous aggregates of organic substances that possess distinctive physical and chemical properties" by Spackman [21]. Macerals can be described and classified on the basis of their different plant origins, which is known as coal petrography. Different types of coal are recognizable on the basis of their relative proportions and the textural or spacial associations of the macerals and minerals comprising them. It must be noted though that the specification of a coal type is insufficient for a definitive classification, as individual macerals are found at different stages of the coalification series, i.e. in coals of different rank.

Coal petrography has three sets of classifications differing in scale. Firstly, the lithotypes (rock-types), which are visible to the naked eye, then the micro-lithotypes, a term introduced by Seyler (1954) to denote typical associations of macerals in humic coals whose minimum band width had to exceed 50 μm [23], and finally the macerals themselves.

The nomenclature for the lithotypes was first proposed by Stopes in 1919 [18], who identified four bands of different appearances in coals and named them vitrain, clarain, durain and fusain. Their descriptions are given in table 2.4.

Lithotype	Appearance
Vitrain	coherent and uniform; brilliant, glossy; vitreous in texture
Clarain	definite, smooth surface; pronounced gloss or shine; surface lustre inherently banded
Durain	hard; close, firm texture, granular in appearance; fine lumpy or mat surface, dull to greasy lustre
Fusain	occurs chiefly as patches or wedges; powdery, readily detachable; fibrous strands; silky lustre

Table 2.4 Description of Coal Lithotypes

The micro-petrological terminology was also originally developed by Stopes and was later extended to become the Stopes-Heerlen-System. In it the macerals are ordered into three groups: Vitrinite, exinite (or liptinite) and inertinite. Within each group the macerals are distinguished by their morphology, optical properties, botanical affinities, technological properties and inferred mode of preservation [19]. The three maceral groups form the basis of coal petrography, as, from a technical point of view, it is of greater interest to gain an overview, rather than a detailed description of all the macerals and sub-groups of macerals, of which hundreds have been identified over the years and which are of interest mainly to the botanist or geologist.

A summary of the most frequently quoted macerals and their descriptions was given by Stach [23]. Of the three maceral groups vitrinite is the most important in amount, forming the familiar brilliant and black bands in coal. Two main macerals belong to this group, tellinite, derived from cell-wall material, and collinite, which is derived from the substance that fills cell cavities. Usually they are not distinguished, as their reflectances are very similar.

Exinite consist of macerals derived from spores, cuticles, resins and algae. The spores, which occur in tetrads, are nearly always compressed and show a tetrad-scar consisting of three rays. The leaves and needles of plants possess a protective skin of cutin, the cuticle, that is highly resistant to the process of decomposition and forms the maceral of cutinite. The maceral resinite covers all the resinous components of coal, including resinified essential oils in lignites and bituminous coals. The resin bodies, cell fillings and resin rodlets, are frequently found isolated and are elliptical or spindle-shaped. They are dark in appearance compared to spores and cuticles. The maceral alginite is formed from the algae *Pila* and *Reinschia*. They are the lowest reflecting, hence darkest, bodies on polished coal surfaces.

The inertinite group of macerals derives its name from showing no or little reaction in the coking process. They have the highest reflectance and originate from similar plant remains to vitrinite, but have been more strongly affected by oxygen during the biological stage of coalification. Several grades of transition exist between vitrinite and inertinite. Strongly fusinised tissue is thought to have been exposed to the atmosphere during the early coalification stages. Fusinite is practically a fossil charcoal and may have been formed as result of forest fires. The cell structure of wood may be well preserved in fusinites.

Another maceral in the inertinite group is sclerotinite, which is formed from fungal remains. Its name derived from the sclerotia of fungi.

The two micrinites, massive and fine, also belong to the inertinite group, even though the latter is not completely inert. Massive micrinite is composed of grains that are equal in size and is in reality a sediment of inert detritus. Fine or flocculent micrinite

is frequently, but not always, found associated with microspores and appears to be a degradation product of protoplasm.

A concise summary of the main macerals has recently been given by Murchison [24] and is reproduced as table 2.5.

Maceral Group	Maceral	Origin
Vitrinite	Telinite	Humified plant remains typically derived from woody, leaf or root tissue with well to poorly preserved cell structures
	Collinite	Humified material showing no trace of cellular structure, probably colloidal in origin
	Vitrodetrinite	Humified attrital or less commonly detrital plant tissue with particles typically being cell fragments
Exinite (Liptinite)	Sporinite	Outer casing of spores and pollens
	Cutinite	Outer waxy coating from leaves, roots and some related tissue
	Resinite	Resin filling of cells and ducts in wood; resinous exudations from damaged wood
	Fluorinite	Essential oils in part; some may be produced during phyco-chemical coalification and represent non-migrated petroleum
	Suberinite	Cork cell and related tissue
	Bituminite	Uncertain, but probable algal origin
	Alginite	Derived from some groups of green algae
	Exudatinitite	Veins of bitumen-related material expelled from organic matter during coalification
	Liptodetrinite	Detrital forms of liptinite that cannot be differentiated
Inertinite	Fusinite	Originates from wood and leaf tissue on oxidation
	Semifusinite	Wood or leaf tissue weakly altered by mouldering or by biochemical alteration
	Inertodetrinite	Similar to fusinite or semifusinite, but occurring as small fragments
	Macrinite	Humic tissue probably first gelified and then oxidised by processes similar to those producing semifusinite
	Sclerotinite	Moderately reflecting material of fungal origin, largely restricted to Tertiary coals
	Micrinite	Largely of secondary origin formed by disproportionation of lipid or lipid-like compounds

Table 2.5 The Origin of the Coal Macerals

2.1.3.2 The Properties of the Maceral Groups

The maceral groups are usually identified under an optical microscope using point counting methods. In incident light under oil immersion, vitrinite varies from dark to light grey in appearance, frequently showing signs of botanical structure. Exinite appears much darker being composed of megaspores, microspores, cuticles and resin bodies. Inertinite is the highest reflecting component and is again frequently characterized by cell structure [23].

The problem of maceral characterization lies in the difficulty of separating them, as they usually are finely dispersed in one another. Complete isolation has not as yet been achieved, but concentrations in excess of 90 % have been reported by various researchers, all be it for very small quantities of finely ground particles. The difference in density of the macerals is exploited for the purpose of concentration using either sink-float methods [25, 26] or more recently density gradient centrifugation [27].

The three maceral groups can be characterized chemically, as has been done by Dormans et al (1957) [25] by applying elemental mass balances to maceral concentrates. Some properties, such as volatile matter or density, can be deduced using the same method. They showed that for a given carbon content exinite possesses the highest hydrogen content, followed in decreasing order by vitrinite and micrinite. The order for oxygen content is reverse to that for hydrogen. The trend for volatile matter was found to reflect that for hydrogen, that for density follows that for oxygen. The elemental composition of fusinite appeared almost independent of rank. Plotting their results on a van Krevelen diagram demonstrated that the compositional differences between the maceral groups decrease with coal rank, so that for the highest ranks the maceral groups are almost identical. The same trends were found by Kroger et al [28] who conducted proximate and elemental analysis on vitrinite, exinite and micrinite concentrates of four coals and plotted the results for volatile matter, carbon, hydrogen and oxygen content against the volatile matter of the vitrinite concentrates. The ash content was found to be highest for micrinite, from which they concluded that demineralisation is least effective for it, probably because the mineral matter is more finely dispersed. Kroger and Pohl [29] studied the devolatilisation behaviour of the same concentrates in some detail. They found that the rate of weight loss due to the evolution of primary gases is similar for the maceral groups except for a temperature range around 400 to 550 °C, where rapid devolatilisation occurs and the macerals show distinct peaks. In this range the weight loss is most marked for exinite, followed by vitrinite and is least strong for micrinite. The total weight loss also varies. Vitrinite was found to lose on average 20 % more weight than micrinite. The devolatilisation weight loss of exinite appears to be more strongly rank dependent than that of the other macerals. For the lowest rank coal it was roughly double that of vitrinite, whereas it

lay slightly below the vitrinite weight loss for the highest rank coal investigated. This is in keeping with the importance of exinite macerals in the coking process, where they yield most of the valuable components of coal tar in low temperature carbonisation [23].

Dyrcaz et al [27] investigated the chemical and structural differences of maceral concentrates with purities above 90 % and represented their results by plotting them against the densities of the fractions analysed. This showed clearly that the chemical composition varies not only between the maceral groups, but also continuously within them with increasing density. They found that aromaticity and density are closely related. In the case of bituminous coals aromaticity increases linearly with density from the densities associated with exinites via those of vitrinite to those of inertinite. For sub-bituminous coals and anthracites the relationship is somewhat more complex, but nevertheless the structural differences between the maceral groups can be clearly shown by plotting their H/C ratios against aromaticity. The maceral groups occupy distinct areas on such a diagram, inertinite having the lowest H/C ratio and highest aromaticity and exinite the highest H/C ratio and lowest aromaticity, with vitrinite falling in between the two.

Gray and Champagne [30] comment on the differences in plasticity of the maceral groups in a discussion of the impact of petrographic composition on the coal to coke transformation. It is thought that exinite displays the greatest plasticity, becoming very fluid in the 410 - 425 °C temperature range. The plasticity of the inertinite group is described as negligible. As this is linked to the question of the reactivity of inertinite in terms of carbonisation, it will be discussed in some detail in section 2.3.4.1.

A good summary of the physical properties of the maceral groups is given by Loison et al [22]. They describe exinite as the lightest maceral group and as not very brittle, increasing the shock resistance of the lithotype it occurs in. Inertinite, which is thought to have undergone substantial oxidation prior to coalification, is the most dense of the maceral groups. Inertinite is hard, but friable, in contrast to vitrinite, which is described as fracturing easily. Vitrinite is intermediate in density between the other two groups.

2.2 The Utilisation and Production of Coke

The major industrial application of coke is iron ore smelting in the blast-furnace. At one time alternative production methods for steel seemed to threaten to replace the blast-furnace. But the most prominent of these, the direct reduction process, still only accounted for 1.4 % of the total steel production worldwide in 1990 [4], so that it can safely be assumed that the blast-furnace will remain to play a vital role in the steel industry.

2.2.1 The Iron Blast-Furnace

The object of the process of smelting is to remove oxygen from the iron ore and to melt the product. The pig iron thus produced contains about 4 - 5 % carbon, specified amounts of other elements, such as silicon and manganese, and as little sulphur as possible [31], which makes it suitable for further refinement into steel. Modern blast-furnaces are vertical shaft furnaces of circular cross-section, some 60 m or more in height, with an output capacity of 5000 to 12 000 t / day [6]. They comprise five sections: The hearth at the bottom, where liquid iron and slag collect, surmounted by the bosh, an inverted truncated cone. This is connected by a short vertical section, the bosh parallel (barrel, belly), to the stack, an upright truncated cone, which in turn supports the throat. A schematic view of a blast furnace indicating the temperature regime within it is given in figure 2.1.

Blast-furnaces are operated continuously. They are charged periodically from the top of the stack through a double bell-and-cone gas-trap system with alternating layers of mixed ore and flux, which mainly consists of limestone, and coke. Pre-heated air is blown through tuyeres, numbering between 12 and 36 depending on furnace size, into the hearth. The air blast may be enriched with additions such as steam, oxygen or various forms of hydrocarbon fuels to reduce the furnace burden [32]. At regular intervals the slag and the molten pig iron are run off through separate tap holes, which are afterwards re-sealed with refractory material. Sometimes the iron is run into moulds to form ingots of pig iron, but more typically it is conveyed molten to be converted into steel in nearby installations.

The slag (calcium - aluminium - silicate [32]) consists mainly of the reduction products of the earthy waste, also called gangue, which reacts with the limestone added for that purpose. It has a few applications, such as, as a railway ballast or as an aggregate in tar macadam or concrete, but by no means all of it can be made use of.

The gas leaving the top of the furnace still contains 20 - 25 % CO and is therefore too valuable a fuel gas to be wasted. Part of it is used in regenerator stoves for pre-heating the air blast. Typically three stoves per furnace are used, two are heated by burning

furnace gas and one for pre-heating air at any one time. The air supplied to the furnace achieves a temperature of between 1000 and 1350 °C. The remainder of the furnace gas is used on site for purposes like electricity generation and re-heating furnaces.

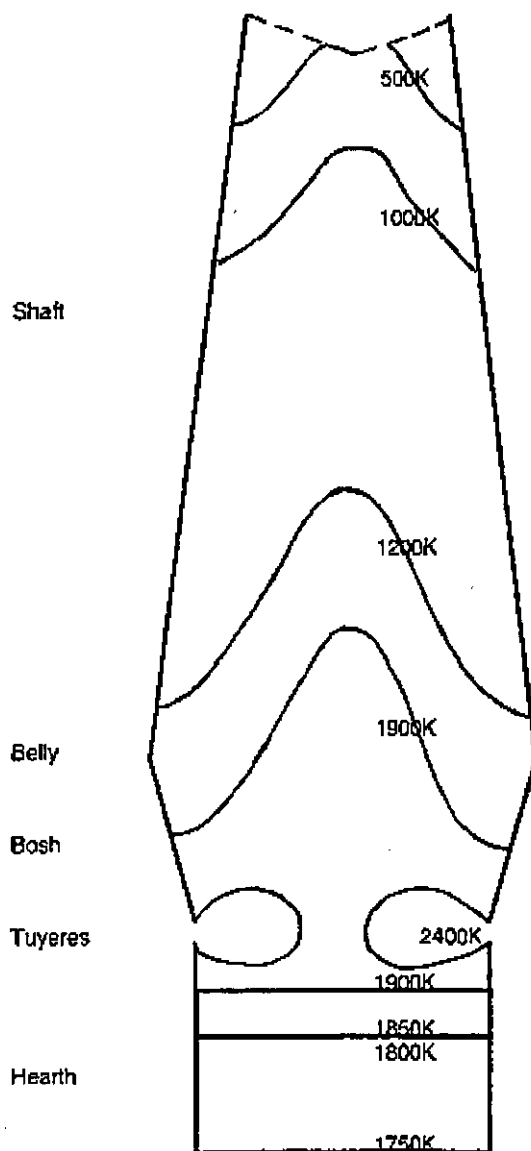
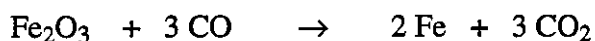


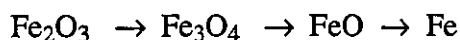
Figure 2.1 Schematic View of the Temperature Regime in a Blast Furnace

2.2.1.1 The Role of Coke in the Blast Furnace

Coke fulfills several important roles in the blast-furnace. Firstly, it acts as a fuel providing heat due to its partial combustion in the tuyere raceways, a zone extending 1 - 2 m from the tuyeres which is cleared by the air blast. In excess of half of the coke is consumed in that way [22] and temperatures between 1900 and 2400 °C are achieved [31]. The partial combustion product, carbon monoxide (CO) acts as the reducing agent which converts iron oxide (Fe₂O₃) into iron (Fe) in the fusion zone lying above. The overall reaction is given by



although it is thought to occur in three stages [33] :



Indirect or gaseous reduction in the iron ore layers and conversion of the resulting CO₂ to CO in the coke layers proceeds up to the 1200K isotherm, below which the coke gasification reaction ceases [34]. Some reduction of the higher iron oxides does still take place in the higher regions.

The third role of coke is to provide carbon that is dissolved into the liquid iron, saturating it as it percolates down into the hearth.

Finally, about 15 % of the coke descends into the bosh and hearth [22] where it is the only material that is still solid. This is where its mechanical properties become important, as it has to maintain a porous bed through which the gases can ascend and the liquid products can descend. By the time it reaches this zone it will have experienced severe mechanical, chemical and thermal attack, and it is the ability to withstand this sufficiently well which gives rise to most coke quality criteria.

2.2.1.2 Coke Quality Criteria

In its role as a chemical reductant the main coke requirement is that it should be as close to pure carbon as possible, as any impurity present, such as mineral matter, sulphur and moisture, increases the coke consumption per tonne of iron produced [35]. Much the same applies to its role as a fuel. As a support refractory it has been shown that the capability of the coke to maintain bed permeability depends on its size, and possibly shape, and the size distribution about the mean size. For maximum permeability a large size and narrow size range was found to be desirable [35]. As the coke is subjected to physical and chemical breakdown due to compression, impact, abrasion, chemical reaction and differential thermal expansion, a high level of

resistance to those degrading forces is required. Traditionally coke has been assessed on the basis of its cold strength, size and chemical composition. Although some tests have now been developed which are more closely related to the actual conditions in the blast furnace, such as reactivity to CO_2 and high temperature strength, they have not been standardized and as a rule are unsuitable for routine testing.

2.2.1.2.1 Chemical Tests

Tests regarding the chemical composition of coke are roughly the same as those performed on coals, i. e. proximate analysis (moisture, ash, volatile matter), elementary composition and calorific value. For the elementary composition most commonly the carbon, hydrogen and sulphur contents are analysed, occasionally also those of oxygen and nitrogen. The tests are virtually identical to those described in section 2.1.2.1 for coal.

2.2.1.2.2 Strength Tests

There are two types of strength tests, drum tests and shatter tests. The latter are rarely used these days except for foundry coke, so that drum tests only will be discussed here. In drum tests a specified amount of coke is rotated in a drum under standard conditions and its size distribution before and after testing is compared. These tests subject the coke to degradation by two distinct processes. In the early stages breakage occurs by impact along macro-fissures in the coke. In the later stages of the test size reduction by abrasion becomes dominant [36]. This leads to a distinctly bimodal size distribution, taken into account by most tests by defining two indices. The strength tests adopted in various countries are a product of custom, rather than being based on scientific principles [37].

The oldest and most widely used coke strength test is the Micum test. In it 50 kg of sized coke (> 63 mm through a round hole sieve) are rotated in a 1m x 1m drum for 100 revolutions at 25 rpm. Two indices are defined, the M40 and the M10, as the weight of the fractions larger than 40 mm and smaller than 10 mm respectively. The M40 is known as the index of fissuring, the M10 as a measure of abrasion resistance. The Irsid test uses the same apparatus as the Micum test, but a smaller coke size (> 20 mm) and a larger number of rotations (500). Both its indices, the I20 and the I10, indicate the cohesiveness of the coke. The I10 and M10 have been shown to correlate well [22]. The ASTM Tumbler test defines two indices, the stability factor, which is the weight fraction remaining above 1.06 in, and the hardness factor, which is the weight fraction remaining above 0.265 in. Its results do not correlate well with those from the Micum and Irsid tests. The JIS test subjects the coke to more severe treatment than either of the tests mentioned above due to a combination of larger drum

and smaller sample size. Its main indices are denoted as D30 15 and D 150 15, which are the weight fractions above 15 mm after 30 and 150 revolutions respectively (at 15 rpm). A good comparison between the different methods cited here is given by Loison et al [22], which is included as table 2.6.

Some typical values for the coke specifications in terms of chemical and strength tests are given in table 2.7.

	Micum	IRSID	ASTM tumbler	JIS
Lump size	> 63 mm (round)	> 20 mm (round)	51 - 76 mm (square)	> 50 mm (square)
Weight taken	200 kg	200 kg	11.3 kg	40 kg
Weight subjected to test	50 kg	50 kg	10 kg	10 kg
Drum characteristics	1×1m without internal axle (4 internal 100 mm angles)	as for Micum	914 × 457 mm (2 internal 51 mm angles)	1.5 × 1.5 m (6 internal 250 mm angles)
Rotations	100 at 25 rpm	500 at 25 rpm	1400 at 24 rpm	30 or 150 at 15 rpm
Sieves used	40, 20 and 10 mm , round-hole	20 and 10 mm , round-hole	27 and 6.75 mm , square-hole	50, 25 and 15 mm, square-hole
Strength indices	> 40 mm (M40) < 10 mm (M10)	> 20 mm (I20) < 10 mm (I10)	Stability Factor (> 27 mm) Hardness Factor (> 6.75 mm)	> 50 mm > 15 mm

Table 2.6 Comparison of the Different Methods of Testing Coke Strength

Tests on Metallurgical Coke		Typical	Values
		[37]	[6]
Chemical	Moisture	< 3 %	
	Ash	< 8 %	8 - 12 %
	Sulphur (organic / pyritic)	< 0.6 %	0.5 - 1.3 %
	Volatile Matter		< 1 %
Physical	Size (mean)	20 x 63 mm	50 mm
	(range 90 %)		45 - 55 mm *
			(30 - 70 mm)**
	Strength (M 40)	> 75	
	Abrasion Resistance (M10)	< 7	

* preferred values

** values typical of current practise

Table 2.7 Typical Values for the Coke Specifications in terms of Chemical and Strength Tests

2.2.2 Coke Making

Coke making or coking is a special case of a process generally referred to as carbonisation when applied to a special grade of coals or coal blends formulated to simulate the relevant properties of that grade. Carbonisation is defined as destructive distillation [38] or thermal degasification [4] of organic substances out of contact with air. Coal carbonisation processes are classified according to the temperatures the coal is heated to [38]. Low temperature processes (450 - 700 °C) mainly yield tar and reactive coke most suitable as a domestic fuel. Medium temperature processes (750 - 900 °C) also produce reactive coke, but their main by-products are gaseous, so that they were most widely used in the gas-making industry (town gas). With the substitution of domestic solid fuel by gas and electricity and the virtual disappearance of the gas-making industry after North Sea natural gas became easily available, low and medium temperature carbonisation have decreased greatly in importance. Therefore high temperature carbonisation (> 900 °C), which leads to a hard, unreactive coke, better known as metallurgical coke after its principle use, is exclusively dealt with here. Figure 2.2 shows a general view of a typical industrial coking plant. The coke is produced in batteries of up to 60 [39] or 80 [40] slot-type ovens, each capable of producing several thousand tons of coke per year (up to 20 000 t in modern designs). Presently an oven length of 18 m and height of 8 m are considered to be the size limit dictated by constraints in construction [4]. As coals and semi-cokes are poor heat conductors the ovens have to be kept narrow. Formerly 0.4 - 0.45 m was considered the maximum width to attain about 900 °C at the center of the charge with wall temperatures of 1200 °C. More recent developments, such as refractory materials allowing wall temperatures up to 1500 °C, have led to an increase in oven width, with 0.6 m presently made to work satisfactorily. The crushed, and possibly preheated, coal is charged through manholes along the top of the oven. At the end of the coking cycle, which typically lasts 15 hours, the coke is pushed out of the wider side of the oven and discharged into quenching cars, which take it to be cooled by water spray in a quench tower before being screened and loaded.

A coking plant requires extensive ancillary equipment, most importantly for the collection and refinement of by-products to obtain clean fuel gas, ammonia, crude benzole and coal tars [39], the description of which would be beyond the scope of this review.

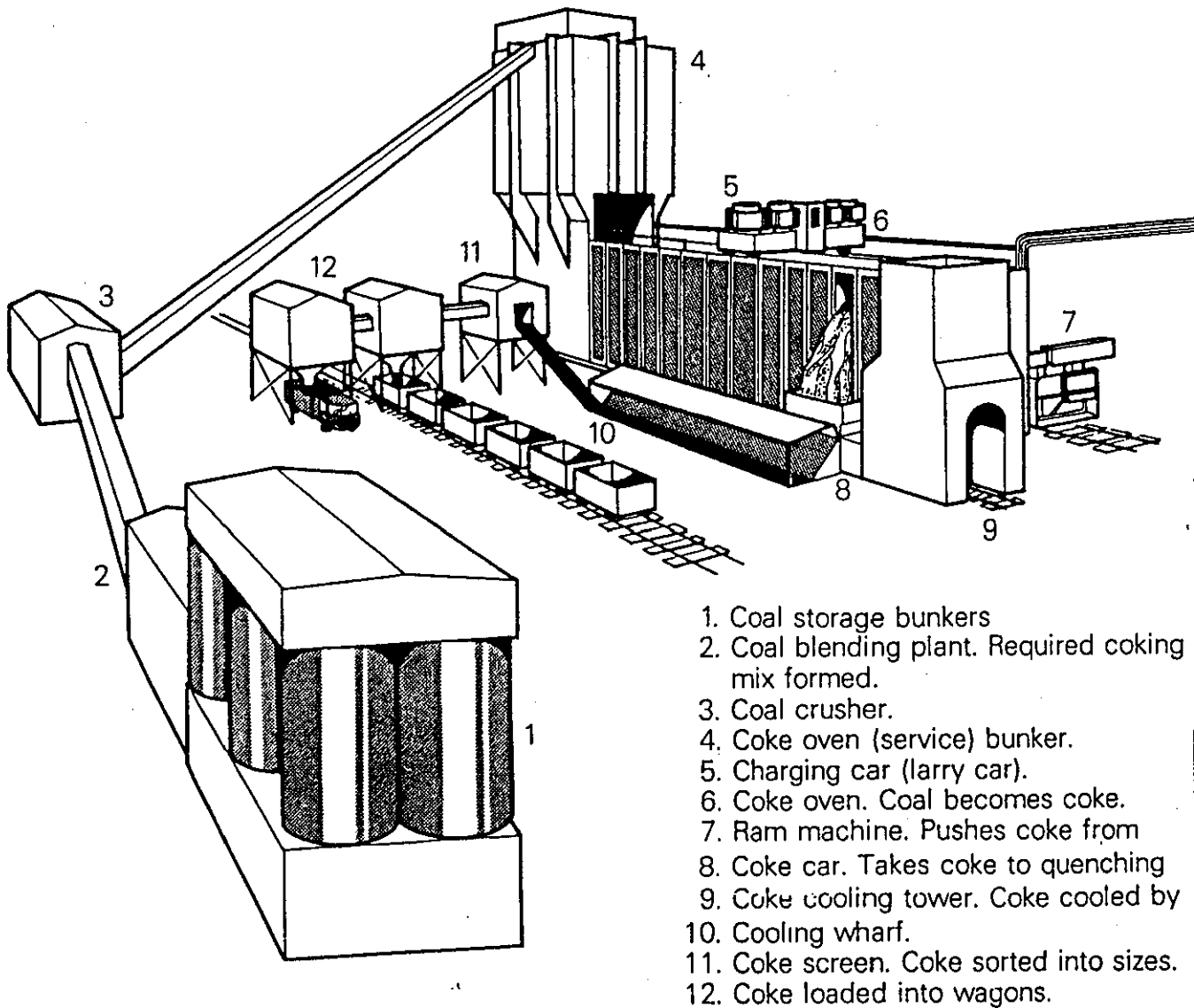


Figure 2.2 Schematic View of a Coke Oven [39]

2.2.3 Coke Quality Prediction

The relationship between coal and coke properties has probably been more thoroughly investigated than that of any other coal use, but no universal agreement on which criteria should be used to predict coke quality has been achieved. The evaluation of coal for a specific use is a form of classification by grade, which aims to establish its economic value. This is usually a complex function of the interaction of the process system considered and both, coal rank and type [21].

The chemical quality of a coke is a direct reflection of the quality of the feed coal(s). The two main chemical coke specification parameters, ash (or mineral matter) and sulphur content, have been successfully related to their weight percentages in the coal. Essentially all the inorganic constituents of the coal remain in the coke, so that the coke ash content can be estimated from the ash and volatile matter content of the coal [21].

$$\text{Ash (\%wt coke)} = \text{Ash (\% wt coal)} \times \{ 100 / [100 - 0.87 \times \text{VM (\% coal)}] \}$$

Not all of the coals sulphur remains in the coke. Multiplying the coal sulphur weight percent by 0.8 - 0.9 has been found to be a good estimate for the weight percent of sulphur in the coke [21].

The coke strength has proven difficult to predict, as no direct correlation with any single one of the coking property tests cited in section 2.1.2.2 has been found [21]. Many prediction models have been developed, the description of all of which would be beyond the scope of this review. They can be roughly divided into two categories as being predominantly based on petrographic data or on the plastic properties of the coal [22]. The first category of coke strength predictions is based on the concept of reactive, i.e. fusing, and inert, i.e. non-fusing, components in the coal. They assume that for each fusible component there is an optimum level of inerts for maximum strength and that the actual strength can be deduced from the deviation from this optimum. An example of this type of prediction is the method developed by Shapiro and Gray [16], in which they divide the fusible material into different vitrinite types according to their reflectance. From empirically determined data, each type is assigned a rank index for the actual inert level in the coal or coal blend and an optimum inert level. From the sums of these the ASTM stability factor is predicted. A similar, but somewhat simpler, method for the prediction the M40 index of coal blends from reflectance and maceral analysis is described by Marshall [35]. From empirical data the variation of M40 index with the percentage of inerts in the blend is plotted for different mean reflectances. He does, however, recognise the limitations of a purely petrography based model and points out that dilatometry is routinely used for

additional monitoring of the blends, as it is sensitive to variations in amount and size distribution of mineral matter and to the state of oxidation of the coals. A simplified version of this approach to coal strength prediction is shown in figure 2.3. The diagram shows that for any coal rank, as indicated by the average reflectance of its vitrinite, there is a maximum of coke strength in terms of ASTM stability which can be obtained when the optimum balance between reactive and inert material is achieved. An inert percentage other than the optimum gives a weaker coke. Figure 2.3 is a simplification insofar as the optimum is not indicated by absolute values, which would differ for each vitrinite reflectance, so that a much more complex map of iso-stability lines is needed for a realistic representation.

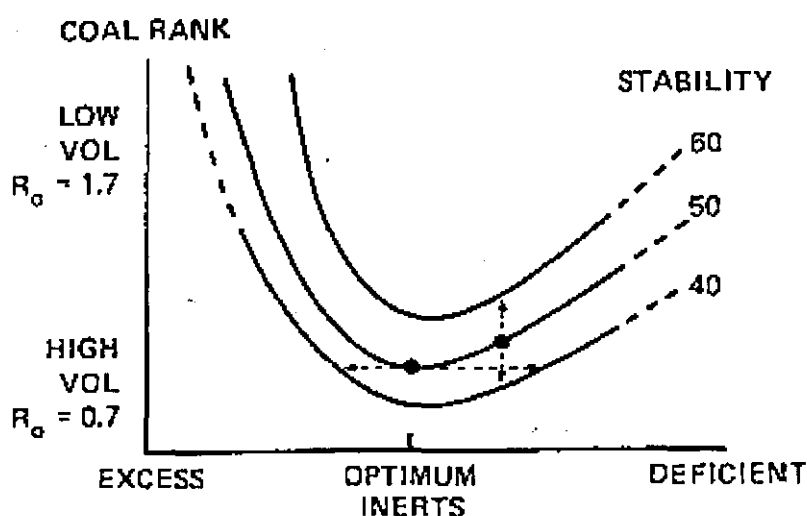


Figure 2.3 Simplified Representation of Coke Strength in Relation to Coal Rank and Inert Content [7]

A method based on the plastic properties of the coals was developed by Miyazu et al [41] and is currently widely used in Japan. It is based on the assumption that good fusion occurs on coking if the average vitrinite reflectance and maximum fluidity measured using a Gieseler plastometer fall within a narrow range of values. Blends are thus formulated to have an average reflectance of 1.2 to 1.3 % and a maximum fluidity between 200 and 1000 dial divisions per minute. A graphical representation of this is known as an MOF diagram, an example of which is shown in figure 2.4. This method

has been criticized for its restrictiveness, meaning that whereas blends within these limits will certainly produce good cokes, it excludes many blends falling outside them which might do so as well [42].

A method based on dilatometry rather than Giesler fluidity is described by Gibson [43]. From the dilatometer parameters of softening and resolidification temperature and percent contraction and dilatation, the caking capacity G of the coal or blend is calculated as defined by Simonis [44]. An M40 iso-strength diagram with G and the volatile matter as axes was empirically arrived at, on which the blend proportions to obtain a coke within acceptable strength limits can be predicted. The volatile matter was thought to introduce a measure of the behaviour in the post-plastic stage of carbonisation, having been successfully related to the contraction coefficient of the semi-cake. One of the main contentions against this method is the use of the G factor, which, by Simonis own admission, cannot be applied to high-inertinite Gondwana type coals [42].

An attempt to devise a prediction model based on both, petrographic analysis and plastic properties, was made by Poos [42], who empirically devised a caking index for different vitrinite classes classified by reflectance. This is in fact similar to Shapiros strength index, but excludes high reflectance vitrinite (> 1.8 %).

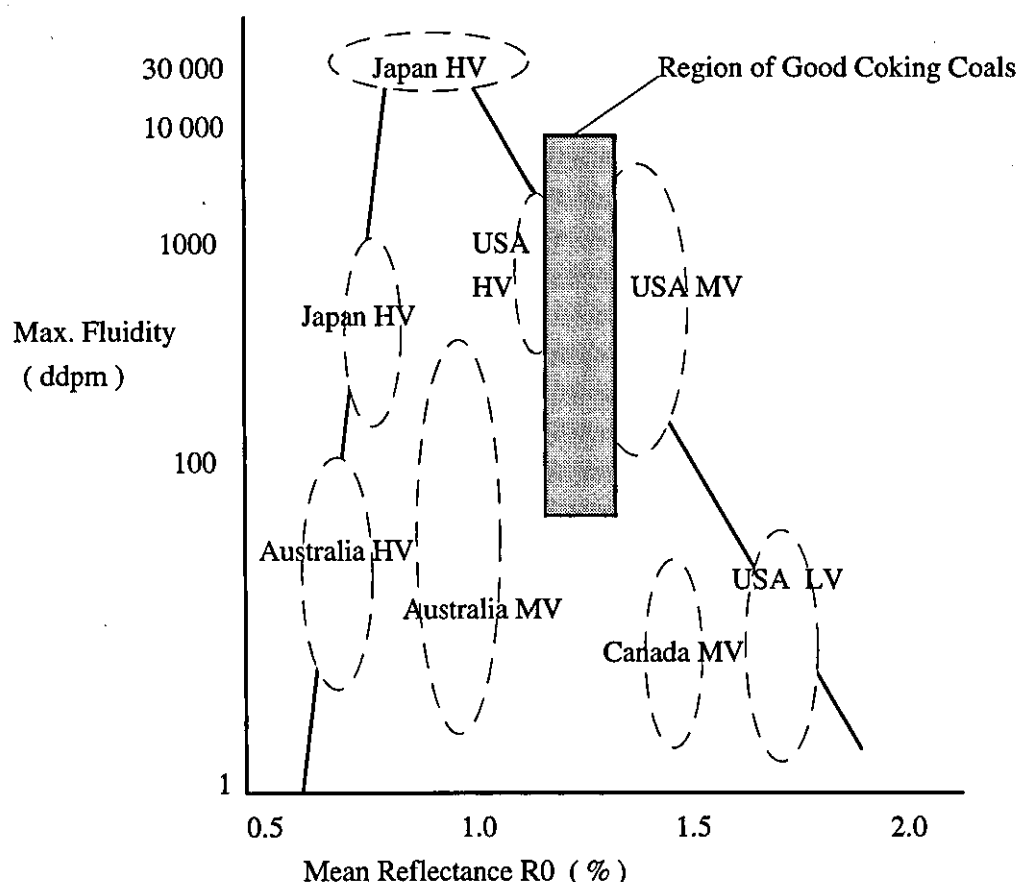


Figure 2.4 Reflectance and Dilatation Limits for Coal Blending (MOF Diagram)

2.2.4 Coal Blending and Coking Additives

Coals of the NCB Rank Code Number 301 make excellent coke, but the depletion of these prime coking coals has led to the increased use of more marginal coking coals [45]. Resources are being extended by blending coals of different coking properties and by the use of selected additives, either coal or petroleum based [46]. Low volatile coals or additives such as coke breeze, semi-cokes or petroleum cokes are usually added to high volatile coals in order to reduce fissuring [22] and are therefore sometimes referred to as antifissurants. As fissuring is mainly associated with differential contraction in the semi-coke stage, they act by modifying the contraction curve. Additives which do not contract appreciably themselves, such as breeze or anthracite, tend to reduce the order of magnitude of the contraction by dilution and by offering resistance to contraction. Carefully chosen contracting additives can act in such a way as to smooth the contraction curve by offsetting the maxima and minima which occur at certain temperatures.

Economic reasons, rather than coke quality improvement, may prompt the use of coking additives, in which case the maximum amount that can be tolerated without deterioration in coke properties becomes of interest. The advantage of petroleum coke, for example, is that it introduces additional carbon associated with very little ash ($< 1\%$) into the coking blend [22]. Extensive commercial trials [47] showed that the addition of suitably selected and prepared delayed petroleum coke to coal blends can significantly reduce specific coke consumption in the blast furnace due to lower ash and higher effective carbon content. Triska and Schubert [47] thought that the amount of petroleum coke that can be incorporated is limited by the fluidity of the blend available to coat the surface of the petroleum coke particles. They suggested that added petroleum coke may improve coke strength by acting as an aggregate, but that it will not improve coke properties if the blend used produces a weak (excessively cracked) coke when carbonised additive-free. It was later pointed out that the requirement of high blend fluidity does not hold true for higher volatile petroleum cokes (about VM=12 %wt daf), which were found to bond well into the coke matrix of low fluidity coal blends [48].

The overall effect of additives is complex and depends on the properties of both, the base coal or blend and the additive. Apart from the amount added and the particle size distribution of the additive the main criterium appears to be the extent to which it remains inert during carbonisation, which is widely seen to depend on its volatile matter content. As a general rule, the lower the volatile matter, the more inert behaves the additive and the less of it can be tolerated before the coke becomes incohesive. Patrick and Stacey [49] compared the effect of coke breeze (VM = 2.3 / 0.5 %) and petroleum coke (VM=14.7 %wt daf) on coke tensile strength as measured by the

diametral compression test. They found that maximum strength for coke breeze addition was achieved at low concentrations ($< 5\%$), whereas strength increased into the 30 - 50 % range for petroleum coke addition. They commented that the petroleum coke appeared to be well bonded into the coke matrix and did not behave like an inert. The effect of coke breeze on the other hand was likened to that of silica sand, i.e. of a true inert, which weakens the coke structure by introducing micro-cracks at its interfaces with the coke matrix. Apparent strengthening at low concentrations was explained by the possibility that its action as a filler outweighs the weakening effect. This was further elaborated on by Hartwell et al [47], who investigated the effect of blending high / medium volatile coals with low volatile ones. They found that the structural effect of the added coals with 12-13 % volatile matter was quite distinct from that of lower volatile ones. Additives which do soften and decompose to some extent tend to reduce pore sizes, whereas lower volatile ones act as wall thickeners. Their work also illustrates well the dependence of the effect of the added coal on the properties of the base coal, having established that there are individual coke strength maxima occurring at different percentages of addition of the same low volatile coal for each base coal.

The importance of particle size has been stressed by Loison et al [22] for the case of coke breeze addition. They found that there is an optimum size for coke strength improvement as measured by the M40 index, which they described as moderately sized (0.1 - 0.5 mm). Above this size fissuring increases and below it, it becomes less effective. Conversely the M10 index, i.e. cohesion or abrasion resistance, is least impaired by the addition of fine breeze (< 0.1 mm) and deteriorates progressively with coarser particle sizes.

2.3 The Fundamentals of Coal Carbonisation

Some coals when heated pass through a transient plastic stage, where they soften, swell and resolidify into a somewhat distended coke [51]. Not all coals that soften on being heated will produce a good coke [52]. If the plastic properties are such that this conversion can yield a high strength metallurgical coke, they are referred to as coking coals. The best coking coals tend to be medium-volatile bituminous coals at about 88 wt% carbon with about 29 wt% volatile matter [51]. The existence of a plastic or fluid stage, associated with the evolution of a large amount of volatile products [53], during carbonisation has long been recognised as vital for coke formation [52], and most carbonisation theories are in some way concerned with it. The phenomena involved in carbonisation, pyrolysis, volatile matter release, softening, swelling, caking, fusion, pore formation and finally resolidification, contraction and fissuring, are all strongly interrelated. Loisons attempt to present them as a causal chain against increasing carbonisation time and temperature illustrates this well [22] and is therefore reproduced as figure 2.5. But it is probably still more expedient to treat the phenomena divided into three stages in accordance with the division made by Patrick [52], who distinguishes between the pre-plastic, the plastic and the post-plastic stage.

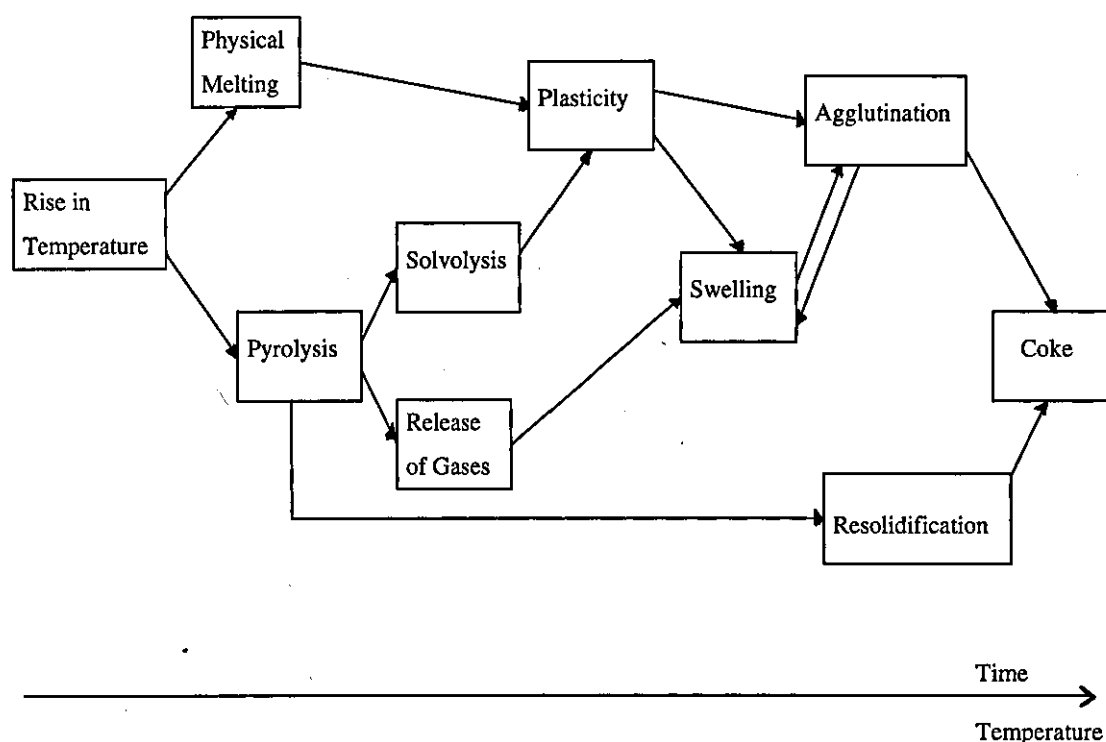


Figure 2.5 Causal Chain of the Phenomena in Coke Formation [22]

2.3.1.1 The Pre-Plastic Stage

Carbonisation up to about 350 °C is described as the pre-plastic stage [52]. During this temperature interval no substantial changes in the coal structure take place, although some slight depolymerization may occur. Some volatile matter is released, but the rate of weight loss is small compared to that in the plastic stage. A small peak in the 100 - 150 °C range is associated with moisture release. Apart from water, CO₂ and some light hydrocarbons, such as CH₄, are evolved. They are thought to originate from the removal of various surface groups from the condensed aromatic coal structures [52] or are described as readily formed gases occluded in the micro-pores of the coal [22].

2.3.1.2 The Plastic Stage

In the plastic stage, between about 350 and 500 °C, extensive molecular disruption and considerable evolution of volatile matter, both aromatic and aliphatic in nature, takes place. The extent of the plastic temperature range and the viscosity within it is strongly rank dependent [22]. Very low rank coals (with carbon contents below 81 wt% and oxygen contents above 10 wt%) do not soften at all. Plasticity reaches a maximum around 87 wt% carbon or 32 - 34 wt% volatile matter content and decreases thereafter, ceasing at about 15 wt% volatile matter content. In prime coking coals the main release of volatile matter follows the onset of plasticity, whereas in lower rank coals active decomposition precedes plasticity [39, 52]. This characteristic of coking coals is illustrated by figure 2.6, where they are located in the region where the decomposition curve lies to the right of the softening curve.

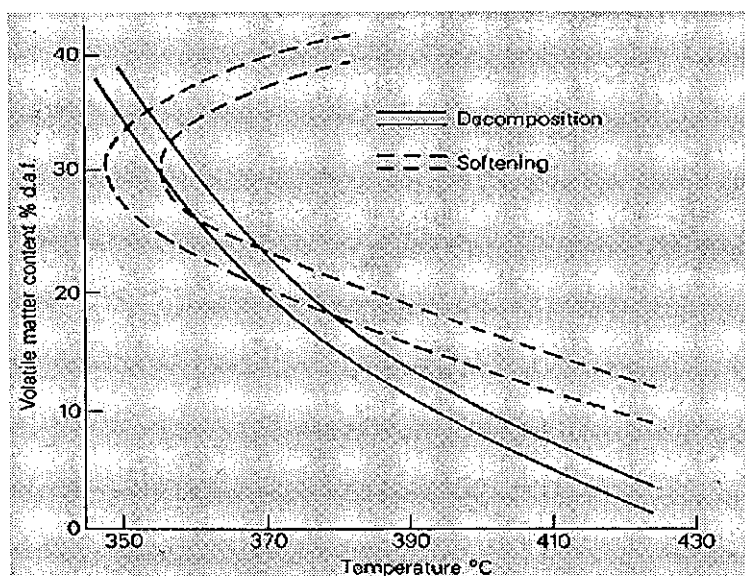


Figure 2.6 Volatile Matter of Coal in Relation to Softening and Decomposition Temperatures [39]

It appears that high plasticity is associated with decomposition and probably a result of those reactions. In its initial phase decomposition can be considered to be depolymerization, giving rise to smaller molecules which have sufficient mobility to produce the overall plasticity of the system [52]. It is thought that coal produces fluid products originating from the aromatic networks, the breakage of linkages [52] or cracking [22] leading to the liberation of free radicals which take part in a wide range of different reactions. The lower molecular weight products are released as gaseous volatile matter, the medium weight ones form tar products and the high molecular weight products remain to form the semi-coke. The residual matter becomes increasingly aromatic, probably by dehydrogenation mechanisms [22] or recombination by condensation reactions [22, 52]. Both imply the formation of additional C-C bonds and of larger, more rigid molecules, layers of which consequently arrange themselves in an ordered three dimensional structure. The hydrogen content is progressively reduced during the plastic stage [52], which is thought to shift the equilibrium from the hydrogen consuming decomposition to the aromatisation reactions [22] thereby limiting the duration of the plastic stage. It has been shown that the formation of tars and volatile matter can be enhanced by increasing the H/O and H/C ratio, i.e. the availability of hydrogen for cracking reactions [22].

The combination of softening and volatiles formation gives rise to swelling of the coal mass, if the suitable carbonisation conditions in terms of particle size, charge density and heating rate are chosen [22]. A plausible explanation of the swelling phenomena based on the pore structure of the coal has been given by Berkowitz [55]. He states that where pore access is constricted, diffusion to the exterior will be slow, or not occur at all for molecules larger than the constriction. As temperature increases, the rate of decomposition will increase disproportionately to the rate of diffusion given by existing pore structure, so that gas pressure will build up, particularly in coking coals where pore constrictions are most marked. The intrinsic strength of the coal weakens as thermal oscillations of atomic groups or molecules increase with temperature. When the yield strength of the coal structure has been reduced below the internal pressure the coal will distend. The softened particles move closer together and will agglomerate readily, which is usually referred to as caking [22]. A strong, mutually reinforcing relationship exists between swelling and caking. Caking leads to the closure of intergranular pores and thus enhances swelling, which in turn causes the build-up of localized pressure thereby aiding further agglomeration.

Coarse ($> 10 \mu\text{m}$) and macro-pores (10 nm to $10 - 20 \mu\text{m}$) develop in the plastic temperature range as gas is trapped on resolidification. The pore system in the coke is the residual effect of the bubbling action which effectively redistributes the void space

in the original charge [53]. Apart from modifications caused by shrinkage the pore structure remains unchanged on further heating.

2.3.1.3 The Post-Plastic Stage

Beyond 500 °C virtually all condensable products will have left and the coal mass will have solidified into semi-coke, with most of the coke characteristics having been determined in the 350 - 500 °C plastic temperature range. The exact temperature of resolidification is rank dependent and rises continuously with rank [22]. Devolatilisation continues, but the rate of weight loss begins to decrease, stabilising at about 1000 °C. The composition of the evolved gas differs from that in the plastic stage, CH₄ being virtually the only hydrocarbon which is given off at above 500 °C. CO continues to be released up to about 800 °C and the rate of H₂ evolution peaks at about 750 °C. The hydrogen is thought to be removed from the the periphery of the aromatic layers, possibly by condensation [52]. Micropores form as a result of the loss of these small molecules [22]. Their pore size of about 0.5 nm corresponds to the size of the evolved molecules. Contraction occurs as the formation of a more ordered structure proceeds. The rate of contraction is temperature dependent, so that the temperature gradient across the charge introduces differential stresses, which lead to the formation of macro-fissures. Those macro-fissures originate near the oven wall and extend into the coke mass [53]. Micro-fissures arise from local stresses. Particularly where inerts are included in the charge, small fissures may form at the interfaces and travel through the surrounding coke matrix. These micro-fissures need not necessarily be a source of weakness, but may provide controlled relief for residual stresses present in the coke [53].

2.3.2 Theories of Coal Plasticity

As coal plasticity has been recognized as vital for coke formation, its exact nature has attracted much research effort and a number of theories concerning it have been put forward. The plastic stage phenomena are interrelated with decomposition and devolatilisation, which occur roughly in the same temperature interval [51]. The system known as coal in its plastic stage is complicated by the fact that various chemical and physical processes overlap, so that undecomposed coal, fluid state coal, primary gas and solid semi-coke all exist simultaneously. It is not known whether the material that causes softening exists in the coal or whether it is a pyrolysis product [51]. Moreover it is not certain whether the plastic fraction acts as a dispersion agent or as a lubricant for the still solid fraction of the coal.

In the early days of coal research it was attributed to a specific fraction of the coal. Bone, Fisher and many other researchers extracted coal with solvents at elevated pressures and temperatures and ascribed specific properties to the fractions thus separated [54]. When certain fractions were removed the coals would not form adherent cokes, so those fractions were said to contain a 'coking principle', i.e. the constituents responsible for coking. They were found to be contained in the solid benzene insoluble part of the fractions and in the petroleum ether and benzene soluble fractions. This chemistry based view was challenged by Berkowitz [55, 56], who conceived coking as a physical process in which the plastic flow of the coal is regarded as analogous to the flow of granular solids. From the fact that X-ray diffraction patterns do not change significantly below 450 °C and that heats of wetting (a measure of total, i.e. internal and external, surface) only fall slightly when the coal is allowed to attain maximum fluidity before measurement he deduces that the collapse of the pore structure of a coal in the plastic range is only very limited and that the structural units of the coal retain their identity. He points out that coal possesses many features of macro-molecular polymeric substances, which do not melt at a definite temperature to form a homogeneous liquid, but acquire molecular mobility in stages, as various atomic groups attain additional degrees of freedom with increasing temperature. The mobility of such molecules would be restricted to the two dimensions parallel to any supporting surface to which they happen to adhere, i.e. function as a two dimensional liquid layer much in the same way as a boundary lubricant between two solid surfaces. It would undergo certain internal re-arrangements under its own weight, i.e. soften without losing its porosity. Plasticity according to Berkowitz is a fundamental property arising from the re-orientation under external constraint of small units, micelles, against surface forces functioning between them. Berkowitz's 'boundary lubrication' theory was criticized by Lahiri [54] for not being able to account for the production of coke from a blends of coals, nor for the effects of oxidation and hydrogenation. Lahiri proposed that coal is a system made up from a lyophobic part (micelles), a lyophilic part (protective colloids similar to resins and asphaltenes) and a medium composed of low molecular weight fractions, which becomes free and mobile as the temperature is raised above the gel point T_g . For coking this proposed coal structure translates into a 'dispersion-coagulation' mechanism. Lahiri defined coking as "a phenomenon of coagulation of the surface active micelles in the dispersed state due to loss of and / or change in the nature of the dispersing medium during heating, followed by the development and strengthening of the primary bonds at the expense of secondary bonding forces". He maintained that there is strong experimental evidence that the softening of coking coals is due to a truly plastic state, in which it is likely that a uniform geometrical redistribution of the

structural constituents in the dispersion takes place prior to coagulation. Lahiri's theory does not conflict with the relation between internal surface and coking properties, as coagulation depends on the distance of particles from one another, i.e. their concentration.

A systematic study of the plastic behaviour of coal on heating was undertaken by van Krevelen, Huntjens and Dormans [57] using Gieseler plastometry, the Audibert-Arnudilatometer and a thermobalance. In formulating a model substance for the plastic behaviour of coal they showed that softening, degassing and condensation must all occur within the same temperature range to obtain the desired characteristics. They interpreted softening as a depolymerization process, i.e. the rupture of bonds between the coal units. They named the primary pyrolysis or depolymerization products 'metaplast', as they are unstable intermediates subject to further conversions. One has to bear in mind though that metaplast is only a useful mathematical concept that represents no real chemical knowledge [51]. A strong relationship between the concentration and viscosity of the metaplast and the apparent viscosity of the softened coal is expected [57]. Carbonisation has been shown to result in an increase of aromaticity and the liberation of non-aromatic groups, which are taken to account for the mechanisms of degassing and condensation. Radicals formed by the decomposition of the metaplast react rapidly with one another and condense to semi-coke, liberated groups escape as gases. On continued heating the semi-coke further decomposes, in particular demethanation and dehydrogenation take place, leading to secondary degassing and the growing together of the aromatic clusters.

New impetus was given to the understanding of coal plasticity with the awakening research interest in coal liquefaction. Brown and Waters [58] first suggested that low molecular weight, hydrogen-rich bitumens indigenous to coal probably serve as solvating and hydrogen donating agents during pyrolysis. Following this Neavel [59] proposed that the development of plasticity is essentially a transient, hydrogen-donor liquefaction process in which the 'vehicle' is supplied by the coal itself and where the depletion of transferable hydrogen leads to the decay of fluidity even under isothermal conditions. He set three conditions for the development of plasticity. Firstly the presence of lamellae bridging structures that can be thermally ruptured, secondly, a supply of hydroaromatic hydrogen and finally an initial intrinsic potential for micellar and lamellar mobility other than by rupture of bonds. The importance of hydrogen content was confirmed by the experiments conducted by Sakurovs et al [60]. They examined the thermoplasticity of 33 Australian bituminous coals by proton nuclear magnetic resonance thermal analysis, which gives a reasonable approximation of the fraction of the molecular structure that is mobile during heating of a coal specimen through the thermoplastic stage. This can be taken as a measure of coal

thermoplasticity and hence reactivity in the sense of the pyrolysis behaviour of coals. They found that even below 600 K (327 °C) a significant fraction of the coal structure is mobile. Below 650 K (377 °C) the increase in mobile hydrogen with temperature is attributed to the thermal activation of mobility in mainly aliphatic parts of the structure. Above 650 K the mobile hydrogen rapidly increases as the coal enters the thermoplastic state, reaches a maximum and then decreases to zero as volatile matter loss and coking occur. They found that the hydrogen content of the coal is the most important variable in determining the maximum extent of molecular mobility during heating and pyrolysis. At the heating rate used (4 K/min) no molecular mobility was observed in coals containing less than 4 wt% hydrogen, which corresponds to the approximate dividing line between bituminous coals and anthracites as defined by equally abrupt changes in aromatic cluster size and solvent extraction yields.

A more recent model of coal fluidity is again derived from polymer science, but in contrast to Lahiris three phase system a two phase one is suggested. Solomon et al [61] attempted to develop an empirical model based on macromolecular network pyrolysis. This was devised applying the theories of cross-linked polymers forming inhomogeneous reacting melts. They thought that the theories describing the viscosity of a suspension of a solid in a liquid are the most appropriate ones for coal. They pursued the two phase approach with a gel point, i.e. the point at which viscosity goes to infinity, at a concentration of solid phase greater than zero, as opposed to the homogeneous gel point which coincides with the first occurrence of a solid phase. To improve upon the prediction of the liquid fraction they employed polymer concepts to describe the molecular weight distribution during pyrolysis, from which the solid and liquid fractions can be determined. Using first linear chain, and subsequently network statistics, they arrived at their DVC macromolecular decomposition model. DVC stand for the processes of depolymerisation (bond breaking), vaporisation (mass transport) and cross-linking. They combined this with their functional group (FG) model for gas evolution, to arrive at the FG-DVC model. In the combined model the cross-linking process is related to the evolution of CO₂ and CH₄. Monte Carlo methods were employed to compute the network properties. The molecular weight distribution of the decomposing network is predicted by the model, from which the solid and liquid fractions are defined. Using the concepts of inhomogeneous mixtures the fluidity is predicted from the solid fraction, the liquid viscosity and the temperature. Good agreement between the predicted and tested fluidities were observed. A sensitivity analysis suggested that the model is most sensitive to changes in the cross-linking density, the amount of donatable hydrogen and the oligomer length.

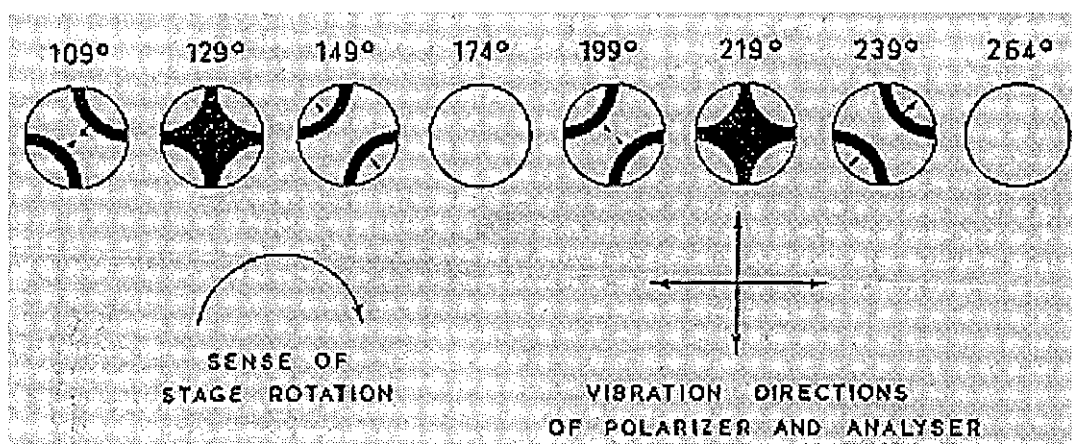
2.3.3 The Development of Coke Texture

Optical, or micro-, texture refers to the nature of the carbon in the coke, its crystalline development, its degree of optical anisotropy and the shape and size of anisotropic areas [62]. Although often used synonymously, it should not be confused with microstructure, which refers to physical parameters such as porosity, pore size distribution and pore wall thickness.

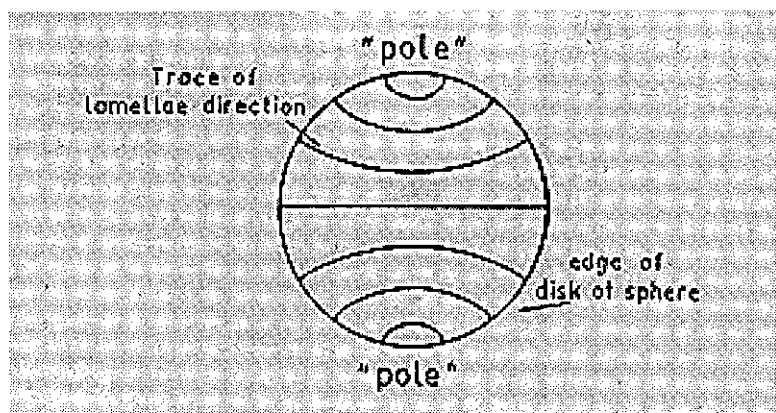
One of the first comprehensive accounts of coke microtexture and its variation with the rank of the parent coals was given by Abramski and Mackowsky [63]. They explained its formation in terms of densification and progressive ordering of the micelles or crystallites coal was assumed to be composed of, likening it to the processes occurring on a much larger time scale during coalification. They recognized the importance of a plastic stage during coking, finding that coals, or lithotypes, which do not soften appreciably on heating remain isotropic and that the formation of the largest anisotropic areas coincides with the ranks for which fluidity reaches a maximum.

It was however the investigation of natural cokes, which led to the first attempts to elucidate the exact mechanism of microtexture formation. After initial observations of small spherical bodies in the thermally metamorphosed coal of the Wongawilli seam, Taylor [64] carbonised small samples of the same coal in a solder bath accurately recording the end temperatures before rapid quenching. He examined thin sections of the products by transmitted light in oil up to the ones exposed to temperatures in excess of 550 °C, for which he found translucency virtually impossible to obtain. Within a temperature range of 10 °C, situated slightly below the measurable softening temperature, the vitrinite lost its original anisotropy. He attributed this to incipient molecular mobility. He observed that the vitrinite remained isotropic up to about 10 to 15 °C below the onset of resolidification. This made Taylor the first researcher to recognize the importance of the processes occurring in the narrow temperature range prior to resolidification. It is now widely accepted that the relative disposition of the carbon atoms in this interval cannot be profoundly modified at any later stage [22].

During this period Taylor [64] found that spherical bodies developed and grew at the expense of the isotropic vitrinite material. This continued until the isotropic material was entirely consumed and the spheres coalesced giving a mosaic appearance. He found these spheres to be highly pleochroic, but of a more complex pleochroism than that of simple crystals. This complexity he attributed to the shrinkage stresses due to contraction on cooling. The optical behaviour and inferred structure of the spheres is illustrated overleaf in figure 2.7.



a) Phenomena observed when a Mesophase Sphere is rotated between Crossed Nicols [64]



b) Inferred Structure of the Mesophase Sphere [65]
(Sphere sectioned parallel to the Main Axis of Symetry)

Figure 2.7 Optical Appearance and Inferred Structure of Mesophase Spheres

A more detailed study into the origin and nature of these spheres using a wide range of carbon materials was later conducted by Brooks and Taylor [65]. They identified a whole range of materials which carbonise in the manner described above, including various coal and petroleum pitches and a number of organic substances such as naphthalene and polyvinyl chloride. The common feature of these materials was that they went through a plastic or liquid stage on being heated in the temperature range of 400 to 520 °C and on solidification formed readily graphitisable semi-cokes. They ascribed the term 'mesophase', literally meaning intermediate phase, to the substance the spheres are composed of. From the electron diffraction pattern of the spheres in their earliest stages, before deformation due to interference by neighbouring spheres, other phases or non-softening particles occurs, they concluded that their structure must be lamellar. They found that their molecular arrangement resembled most closely that of the nematic phase of substances which form liquid crystals at low temperatures.

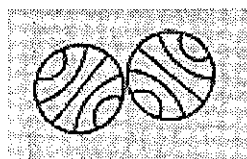
The analogy of mesophase to liquid crystals obviously is limited by the fact that mesophase is not chemically stable, but that reactions, such as polymerization and chain cross-linkage, proceed within it, which will eventually lead to irreversible solidification [66]. Further studies showed that spherical growth, although common, is not an essential feature in the development of anisotropic units in carbons [67]. It is now thought to be due to certain physical conditions, where the viscosities are such that the requirement of minimum surface area dictate the spherical shape. Employing scanning electron microscopy (SEM) on materials carbonised under hydraulic pressures, Marsh et al [67] identified elongated mesophase units, which they described as 'spaghetti'- or 'tadpole'-like in some materials (anthracene), and mixtures of such units and spherical ones in others (anthracene-phenanthrene). They found that a transition from one shape to the other could be achieved by changing the viscosity.

The chemistry of these spheres is very complex. Even for single substance starter materials a mixture of a wide range of pyrolysis products will have been arrived at by the time of mesophase formation. In view of the great differences in chemical composition of substances following the same carbonization pattern, it was later stated by Marsh and Walker [66] that the exact structure and composition of the molecules does not appear to be critical for mesophase formation. They did, however, assume that the average molecular size, planarity of the molecules and an effective concentration of such molecules do play an important role.

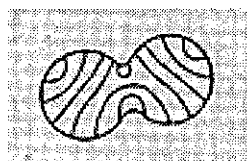
Brooks and Taylor [65] found that insoluble particles, irrespective of whether they were present in the substance being carbonised originally, formed during the plastic stage or were added deliberately, provided preferred sites for the nucleation of mesophase spheres, but were in no way essential for their formation. Marsh [68]

differentiates between the effect of small solids, which he considers as restricting the growth of anisotropic domains, and large ones, which may promote it.

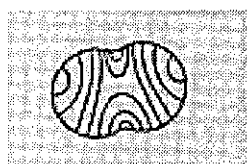
When two mesophase spheres coalesce free from restrictions, they will form a new, larger sphere and reorientation of the lamellae to form a more complex order will occur given sufficient time [65]. This process is illustrated in figure 2.8.



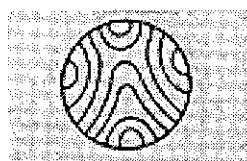
Before contact



Just after contact



Short time after contact



Type of complex internal structure formed when composite of two or more spheres contracts to one large sphere

Figure 2.8 The Reorientation of the Lamellae when two Mesophase Spheres coalesce [65]

As coalescence becomes more general, complete merger can no longer be universally achieved, and various intermediate forms appear. The overall appearance becomes that of a mosaic, even though the texture may not be strictly speaking composed of individual, sharply bonded units. The coalescence having occurred in three dimensions, any cross-section will alternate between areas of fairly uniform orientation of the lamellae and areas where they curve to link up with the next area of uniform orientation. A mosaic type appearance is, however, not the only anisotropic texture formed by carbons. For substances for which the mesophase can be held in a

viscous state for some time before irreversible solidification sets in, much larger areas of uniform orientation (up to 1 mm in size) can be obtained by mechanical deformation, provided the mesophase is locally free from unconverted melt. For petroleum derived precursors White and Price [69] were able to distinguish between two classes of microtexture development according to the temperature of mesophase formation and its reactivity. Small microtextures are formed by fast reacting components for which mesophase spheres precipitate at relatively low temperatures, and large ones, which lend themselves to subsequent deformation, by slow reacting components forming at higher temperatures. No such clear distinction has been observed for coal derived precursors.

The distinction between different appearances of the microtextures may not always be straightforward, White [70] viewing the same section of needle coke in two positions at right angles to one another, found that the typical striated texture appears granular at the second cross section.

Coalescence of the type outlined above may not occur universally. The mosaic of Gilsonite pitch was at a later stage described as "small, irregularly shaped growth units of mesophase simply fusing together without significant deformation" [67]. This description of appearance also fits the even smaller mosaics found in coal cokes.

In attempting to simulate coal coke textures using low temperature and high temperature pitch, Ihnatowicz et al [71] found that the oxygen content of the starter material appears to have a dominant effect on the mechanism of formation of carbon texture, due to material formed at low temperatures in the presence of oxygen groups, which is insoluble in the higher temperature melt. A similar effect has since been ascribed to other hetero-atom, namely nitrogen and sulphur, so that the one likely explanation of the failure of vitrains to form mesophase spheres could be the inhibiting effect of non-carbon atoms present in them [68].

Marsh [68] summarizes the conditions for the development of different sizes and shapes of anisotropic units as the chemical composition of the pyrolysing system, the presence and surface structure of solids, the rate of heating and physical factors such as convection currents and disturbances by gas evolution.

Brooks and Taylor [65] themselves had raised the possibility that with some compounds, of which they identified dibenzanthrone, the crystalline material appears to be converted directly into mesophase without the formation of spheres, though no reasons for this were suggested. Vitrains from British coals may be a class of materials fitting this description. Patrick et al [12] extensively studied the development of anisotropy in vitrains from a wide range of coals, carbonised in open silica boats to temperatures between 400 and 1000 °C. They found no evidence of sphere formation at any stage of the carbonisations. They concluded that either

spheres are formed at a submicroscopic level (of a size smaller than $0.1\text{ }\mu\text{m}$) or that the mechanism for the development of anisotropy differs fundamentally from that of pitch-like materials. Marsh et al [72] on the contrary did observe spheres in American coals ranging from 25 to 34 wt% in volatile matter content (daf) examined under SEM. This might well be due to the different carbonisation process used, as those coals were carbonised under pressure in a closed system without the release of volatiles. The importance of volatile matter release was later commented on by Patrick, Reynolds and Shaw [13], who suspected that a delicate balance needs to be achieved between sufficient volatile matter loss to enable molecular rearrangements and sufficient retention to achieve a degree of fluidity.

2.3.3.1 Rank Dependence of Optical Coke Components

The dependence of the type of anisotropy developed during carbonisation on the rank of the parent coal has been recognised for quite some time [63, 65] and has been thought to reflect the chemical and physical variations of coals with the extent of coalification they have undergone. This view is supported by the work of Patrick et al [14] who successfully correlated the reflectance of the parent coals to an anisotropy index, which they calculated by assigning increasing values to the optical coke components in ascending order of the assumed degree of structural ordering. In the same paper it was, however, pointed out that there are limitations to the linkage of coal rank to coke component distribution, as the classification of coals by NCB Code Numbers is a rather broad one and coals of the same code number may exhibit significant variations in chemical properties such as oxygen contents, which has previously been shown to strongly affect the formation of anisotropy types. Nevertheless, there is a clear trend of coke component types with coal rank as originally outlined by Patrick et al [12], who investigated the development of the different anisotropy types with temperature. High rank, low volatile coals (NCB Code No 200) develop basic or flow type anisotropy. Cokes from medium volatile, prime coking coals (NCB Code No 300) typically show flow or intermediate types and some larger mosaics. As the volatile matter increases (NCB Code No 400/500) the mosaic sizes decrease from medium to predominantly fine. Finally, on further decreasing the coal rank (NCB Code No 600), isotropic material becomes dominant, until it is the only component present (NCB Code No 800).

2.3.3.2 Development Routes of Optical Coke Components

The data obtained by Patrick et al [12, 14] has later been reappraised to show that the optical coke components differ fundamentally in their development as the carbonisation temperature is increased. Moreland [9] identified seven basic patterns:

1. Basic anisotropy present in the coal remains unchanged on carbonisation
2. Basic anisotropy changes directly into flow type components
3. Basic anisotropy changes into flow type components after first developing fine mosaics
4. Isotropic material changes into fine mosaics from which larger units, medium mosaic, coarse mosaic and granular flow (flow/mosaic intermediate) grow, giving a mixture of the above
5. Isotropic material changes into fine mosaics, a proportion of which subsequently grows to medium mosaic size
6. Isotropic material changes into fine mosaics
7. Isotropic material remains isotropic

2.3.4 The Influence of Petrographic Composition

The importance of petrographic composition in the prediction of coke quality has already been outlined in section 2.2.3. The main division made is that between reactive and inert components. Reactivity, used in the description of the coking behaviour of coal macerals, must not be confused with the chemical meaning of the word, but it signifies the ability of coal components to soften and agglutinate to form a strong, continuous coke matrix. Inerts are thus defined in coke petrography as constituents of the coal which show no evidence of having softened and deformed during carbonisation [15].—

There is strong evidence that the properties of a coal causing swelling, caking, fluidity and dilatation, which are all highly relevant for the coking process, depend not only on the rank of the coal, but also on its petrographic composition. Coals of the same rank can vary widely in plastic properties owing to the different types of vitrinite present or its association in different microlithotypes [21]. One of the main difficulties in investigating the effect of petrographic composition on coking lies in the fact that the behaviour of the maceral groups varies with the rank of the coal they constitute. Loison et al [22] illustrate this for plasticity when they state that the plasticity of vitrinite, being the main constituent of bituminous coals, never deviates much from that of the coal as a whole, although it tends to be slightly more fusible in high rank coals (VM > 30 wt%) and slightly less so in low rank ones (C < 82 wt%). From that it would follow that a truly meaningful comparison is only possible for two coals of a similar degree of coalification. Indeed, many of the controversies over the coking behaviour of the macerals seem to stem from the fact that coals of widely different origins were used by the various researchers concerned with this subject.

2.3.4.1 The Reactivity of Inertinite

The maceral group inertinite actually takes its name from the assumption that it remains inert on coking, although to what extent this holds true is highly debatable. Early studies by Shapiro and Gray, concerned with the prediction of coke strength from coal petrographic data, assumed that a third of the semi-fusinite below a reflectance of 1.4 % and a fifth of that above it were reactive [21]. By contrast Taylor investigated the behaviour of different macerals on carbonization [73] and pronounced virtually all semifusinite inert. He investigated two Australian and two German coals and identified four categories of coke constituents. Of these he attributed highly reflecting, moderately anisotropic material composed of small mosaic areas to vitrinite, large ($> 50 \mu\text{m}$, typically $100\text{--}200 \mu\text{m}$) moderately reflecting, isotropic or strain-type anisotropic grains to semifusinite and fusinite and smaller areas ($< 10 \mu\text{m}$) fitting the same description to micrinite, the fourth category being inorganic material. As no maceral separation was effected, nor direct comparison of the same particle before and after carbonisation, it is not clear how he arrived at that identification. He concluded that semifusinite and fusinite are essentially inert and that, although some semifusinite was distorted and possibly altered in chemical nature, it did not fuse to an appreciable extent.

The assumption that semifusinite, fusinite and micrinite remain inert on coking is maintained by Abramski and Mackowsky [63], but they emphasize the importance of the size distribution of the inertinite maceral for adherence and thus strength of the coke. Also, they point out the influence macerals exert on one another, for example the possible effect of exinite on the coking behaviour of vitrinite. Brown, Taylor and Cook [74], carbonizing a piece of coal containing not only semi-vitrinite, but also transitional material between vitrinite and semi-fusinite, using hot stage microscopy, noted its distinct behaviour, differing from that of both of the pure macerals. As this intermediate material would be classified as vitrinite in petrographic analysis, this did not affect their conclusion that all, or virtually all, inert components normally classified as semi-fusinite and micrinite remain inert on carbonisation. In a further paper Taylor et al [75] reviewed the findings of three different laboratories (CSIRO, CHERCHAR and Bergbau-Forschung) on the behaviour of inertinite during carbonization. Again it was found that, apart from some transitional material, semifusinite remains inert on carbonisation. They were of the opinion that, as that transitional material rarely accounts for more than 2 vol% of a coking coal, it would be expedient to count it into the vitrinite group rather than to add a new sub-group to the classification system. However, they assumed that some sclerotinite might fuse at higher temperatures than those used in the experiments, as it is rarely found in high temperature coke. As another possible exception they cited fine micrinite, as

associated with exinite, which was not observed in the cokes. They concluded that the proportions of fusible and infusible material in a coal can be estimated from a reflectance/frequency histogram.

Bennett [76] supplied a more detailed description of the vitrinite-semifusinite transitional material and its carbonisation behaviour. He observed layers of a mottled, granular appearance, some fifty to several hundred microns in size, which he related to closely packed aggregates of sub-angular or lenticular units set in a matrix of normal vitrinite. On carbonisation he found that they did not become uniformly fluid and that smaller pores were formed and the granular units retained their shape. He attributed areas of abnormally high bireflectance in the coke to this transitional material. In Bennetts opinion granular vitrinite is an early stage in the formation of fusinite from woody material prior to burial and coalification.

Bennett [76] also makes an interesting point concerning the co-carbonisation of different macerals. He observed that pure vitrinite of layers in excess of 200 μm formed very large pores often several hundred microns in diameter with thin walls of a micro-mosaic texture. But in association with about 10 % of isolated fragments of semifusinite in the 5 to 50 μm size range, he found that it produced a much denser coke, with pores 20 to 50 μm in diameter, separated by thick pore walls.

In the same year Benedict et al [77] suggested the creation of an entire new maceral group to account for 'altered' vitrinite, following an investigation of Appalachian coking coals. The term pseudovitrinite was suggested for material which optically resembles vitrinite, but the coking properties of which are more akin to inert macerals. Pseudovitrinite is described as having a higher reflectance than equivalent vitrinite, often containing peculiar slits or remnant cellular structures. They were careful to point out that it is quite different in character and origin from weathered or secondarily oxidized vitrinite and formulated the hypothesis that it is formed by partial oxidation during the earliest stages of the coalification process, i.e. before or during the peat stage. In the coals they investigated they found that pseudovitrinite accounted for typically 15 to 25 vol% of the vitrinitic material, in some cases even up to 50 vol%. The coking behaviour of pseudovitrinite was found to depend on its degree of alteration, highly altered material behaving as an inert, i.e. changing neither optical texture nor shape during carbonisation, moderately altered material behaving as a semi-inert exhibiting minimal changes and developing some internal pores.

Nandi and Montgomery [78] investigated maceral concentrates from four Cretaceous western Canadian coals using hot-stage microscopy and claimed to have identified a type of semifusinite which melts and fuses on heating. They found that there are two types of semi-fusinite, a low and a high reflectance one. The high reflectance semi-fusinite remained inert, but the low reflectance one softened and melted at a

temperature lower than the softening temperature of the vitrinite of the same coal and formed a coke of granular texture, which they suspected might help with the cementation of other inerts into the coke matrix. The case for low reflectance reactive inertinite is supported by Diessel [79] who carbonized a series of Australian coals as solid half-cylinders, retaining the other half to enable direct comparison. He found that inertinite of a pre-carbonisation reflectance of 1 - 1.5 % was highly reactive, developed pores and integrated texturally completely into the coke matrix. Inertinite of 1.5 - 1.8 % reflectance behaved moderately reactive. He concluded that the reflectivity of the inertinite is a good indicator of reactivity, with the cut-off point between reactive and inert behaviour depending on the rank of the coal considered. However, he implied that the difference between his findings and previous ones could be due to the nature of the inertinites present, as up to 20 % of the semifusinites and semifusinite - macrinite transitions, accounting for the low reflectance fraction, were derived from mesophyll tissues of leaves and cuticles, rather than from woody material as in Carboniferous Northern Hemisphere coals. They are therefore likely to have a higher H \ C ratio and fewer cross-linked aromatic clusters restricting molecular mobility. In a later investigation Diessel and Wolff-Fischer [80] examined both, Australian and Carboniferous coals, and applying mass balances to the coal and coke petrographic data concluded that the quantity of fused coke matrix is systematically underestimated if vitrinite and exinite only are assumed to be reactive. They found that on average less than half of the inertinite remained unaffected by carbonisation, but maintained that inertinite in the Permian coals is more fusible than that in equivalent Carboniferous coals.

Coin [81] investigated semi-inertinite in Australian and South African coals. Although no definition is given, it can be assumed that semi-inertinite stands for semifusinite and associated transitional macerals. Conducting mass balances based on petrographic data he found very large variations of the percentage of the semi-inertinite that was fusible. No trend with coal rank in the variation of fusibility was found.

Kaegi et al [82] have recently expressed the opinion that the reactive - inert division may be a gross oversimplification. They devised a microcarbonisation method in which the coal particles are carbonized embedded in a refractory, so that coal and coke petrography could be performed on the same pellet, and applied it to several North American coals. They concluded that particles of the same maceral from the same coal can behave in widely different manners, partly, but by no means necessarily, due to their association with particles of other macerals. Examples of this include two particles of fusinite, both of which retained their morphology, but the higher reflectance one remained isotropic, whereas the lower reflectance material developed

some, probably stress-induced, anisotropy, indicating plastic deformation. Another example is a macrinite particle, which developed fissures at its interface with a vitrinite derived coke particle, but fused well with adjacent semifusinite. They question the division between fusinite and semifusinite, as they found semifusinite particles behaving identically to fusinite particles which developed anisotropy. Furthermore, they found that some pseudo-vitrinite and some micrinite particles cannot be identified in the coke other than by direct comparison as their carbonisation results in coke carbon forms normally attributed to vitrinite. Particular emphasis was put on the effect of exudatinite on vitrinite. Vitrinite containing exudatinite gave coke of a higher reflectance than expected, suggesting that it can act as a catalyst in the conversion of vitrinite to higher carbon forms.

In contrast Kruszewska [83] maintained that a total reflectance scan can be used satisfactorily to predict the reactive - inert ratio of a coal. She found that taking the average reflectance as a cut-off point between reactive and semi-inert and inert components yielded a good estimation of the amount of reactive inertinite on the basis that macerals below average reflectance are reactive, those above are semi-reactive or totally inert.

2.4 Coke Microscopy

2.4.1 Optical Anisotropy

Certain differences in the behaviour of materials towards incident light are described by the terms of optical isotropy and optical anisotropy [84]. In an isotropic material light spreads in the same way in all directions, especially with the same speed and absorption. For all directions all forms of light-wave vibration are permissible and light, ordinary or polarized, traverses such a medium unaltered. In an anisotropic medium the permissible forms of vibration are dictated by the micro-texture of the material, so that in any direction usually two perpendicular polarized vibrations of different speed, refraction and absorption result analogous to the structural differences in those directions. Optical anisotropy in crystalline materials has been known since the 17th century and has been widely used in their analysis. It was later found to also exist in substances which do not possess the three dimensional periodic order characteristic of crystal lattices, such as liquid crystals and gels, where the ordering is one or two dimensional only, and to be possible to be induced in some isotropic media by mechanical deformation or thermal stress.

Optical anisotropy is always an expression of structural anisotropy [84]. It results from a micro-structure which differs in different directions, i.e. which is anisometric, be it on an a-microscopic level (atoms, molecules) or on a sub-microscopic one (macromolecules, aggregates of molecules). Isotropy, on the contrary, can result in two different ways, either from a perfectly isometric structure or from randomly directed anisotropic units. The second case is referred to as statistical isotropy.

As a general rule optical anisotropy only indicates the existence of an anisometric structure without being able to lead to conclusions regarding its nature. Other methods, such as X-ray diffraction, usually are employed for this aim.

2.4.1.1 Optical Anisotropy in Carbon Materials

Carbon forms, with the exception of diamond, are based on the graphite lattice [85]. Graphite is composed of layers or lamellae of carbon atoms arranged parallel to each other. Its physical and chemical properties vary strongly according to the axis selected, as the chemical bonding within the lamellae is strong, but only van der Waals forces exist between them. This structural anisotropy is reflected as optical anisotropy. Graphite is a uniaxial negative crystal which has its optical axis at right angles to its basal layer planes and its slow direction, i.e. the direction of maximum optical properties, along the layer planes perpendicular to the optical axis. This is illustrated in figure 2.9.

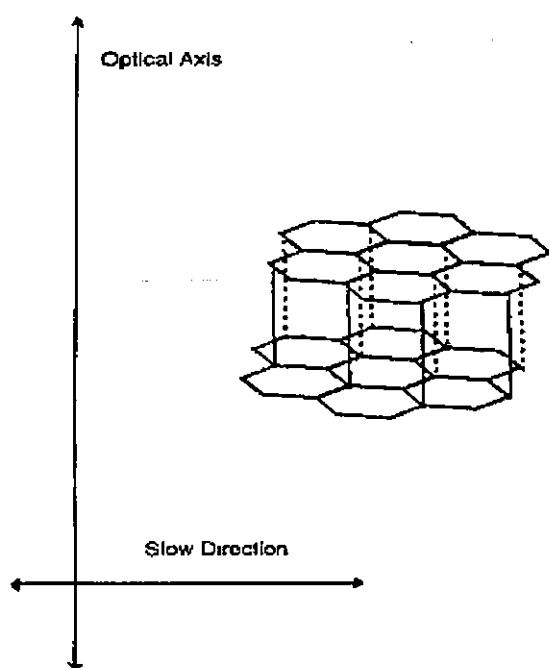


Figure 2.9 Structural and Optical Anisotropy of Graphite

Other carbon forms differ from graphite in that they contain imperfections. Their lamellae are much smaller, not necessarily planar and may include non-carbon atoms. The lamellae are more or less randomly arranged, so that the bulk properties are isotropic. Carbons are usually classified as graphitisable and non-graphitisable depending on whether restructuring occurs on heating which leads to a larger degree of order, approaching that of graphite. Graphitisable carbons will develop some degree of anisotropy as the stacking of their layer planes becomes more regular. Figure 2.10 illustrates the structural differences between graphitisable and non-graphitisable carbons as originally proposed by Franklin [86]. Most coking coals fall into the category of graphitisable carbons. The changes they undergo on heating are dealt with in section 2.3.1, which concentrates on the fundamentals of the carbonisation process.

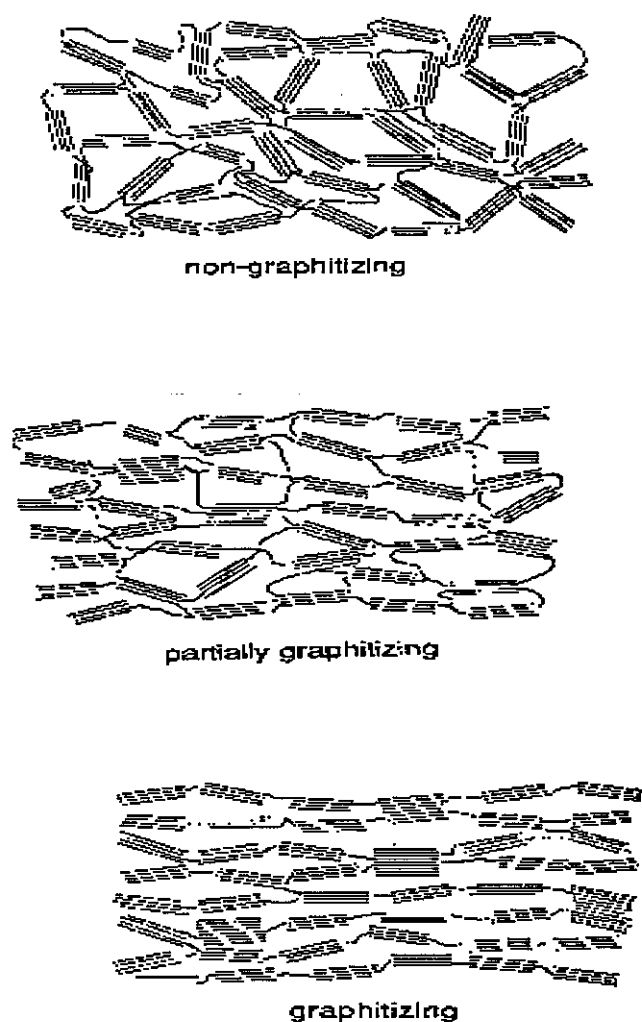


Figure 2.10 Schematic Representation of the Difference of Graphitisable and Non-graphitisable Carbons [86]

2.4.2 The Theory and Application of Polarized Light Microscopy

Light energy is considered to travel by means of transverse wave motion in which the vibration of the particles is usually perpendicular to the direction of travel of the energy [87]. Ordinary unpolarized light vibrates randomly in all directions in the plane perpendicular to the propagation direction of a light ray. With the aid of materials or devices known as polarizers it can be made to vibrate in a single direction only. Light in which the vibration direction of all rays is parallel is called plane polarized.

Materials in which monochromatic light travels with the same speed regardless of its direction of vibration are called optically isotropic media, materials for which this is not the case are known as optically anisotropic [87]. Optically anisotropic media display some symmetry, usually analogous to the geometric symmetry of their crystals. Light travelling along an optical axis of an anisotropic medium behaves as it would in an isotropic medium [88]. Media with a single optical axis are said to be optically uniaxial. This will be the only case considered here. The optical properties of such media vary with their position relative to an incident light ray, i.e. they exhibit bi-reflectance, bi-sorbance and birefringence, which are defined as the difference between maximum and minimum reflectance, absorbance and refraction respectively. Light striking the surface of an isotropic transparent medium at an oblique angle is partly reflected and partly refracted. Both rays are partially polarized in the process, meaning that their vibration takes on a preferred direction. In the special case of the reflected and refracted ray being at right angles to one another, the reflected ray becomes totally polarized [89].

Light entering a birefringent crystal in any direction other than along its optical axis is divided into two rays which are both plane polarized to have vibration planes at right angles to one another [89]. One ray travels with the same velocity in all directions and obeys Snells law, hence it is called the ordinary (O -) ray. The other, direction dependent one, is called the extraordinary (E -) ray [90]. The E - ray vibrates in the plane containing the optical axis and the incident ray [89]. If the ray velocities are represented by vector surfaces for an imaginary light source at the center of a crystal, the O-ray takes on the shape of a sphere, the E-ray that of an ellipsoid. The two surfaces would touch each other at the optical axis. If the E-ray is the slow ray relative to the O-ray, i.e. the ellipsoid lies within the sphere, the crystal is said to be optically positive. If the E-ray is the fast ray, it is called optically negative [88]. The direction of maximum optical properties, which is parallel to the optical axis in positive crystals and perpendicular to it in negative ones, is called the slow direction.

On emerging from the anisotropic medium the light rays re-combine and generally will be elliptically polarized due to their velocity differential within the medium

having introduced a phase difference. In the special case of a phase difference of $n\lambda/2$ (where n is any integer and λ is the wavelength) linear polarization occurs.

Polarizing devices for polarized light microscopy however achieve this effect by isolating one of the polarized rays. Traditionally Nicol prisms were used cemented together with Canada balsam in such a way that the ordinary ray is totally reflected at the interface. Nowadays polarizing filters are more commonly used, often referred to as 'Polaroid filters'. They consist of films of long - chain polymers which have been stretched to orientate the chains and then treated with certain dyes, which will make them strongly pleochroic and thus lead to virtually complete absorption of the ray with the vibration direction parallel to the direction of strong absorption.

If two polarizers are placed on top of one another and one of them is then rotated through 360° , there will be two positions where no light passes through them. At these two positions their vibration directions are perpendicular to one another. A sample placed between two polarizers in such a position in polarized light microscopy is said to be viewed under 'crossed polars' or 'crossed Nicols'. The polarizer situated between the sample and the ocular is referred to as the analyser.

An isotropic sample placed between crossed polars remains unaffected and displays the same shading at any point of a 360° rotation. An anisotropic sample on the contrary will appear dark at 90° intervals when the vibration plane produced by it is at right angles to that of either of the polarizers. From one dark image to the next its brightness will vary reaching a maximum half way between the two.

Anisotropic crystals can display some pleochroism which is often enhanced using phase retarder plates. In polarized light microscopy (PLM) a half-wave retarder plate is inserted before the analyser with its slow direction at 45° to it and the polarizer. It polarizes the incident ray elliptically resulting in two orthogonal polarized rays when the ray is resolved into a single plane by the analyser. The two out-of-phase rays can interfere either destructively or constructively depending on the phase difference. For an isotropic sample the center of the spectrum colours (yellow / green) interfere destructively, whereas the end of spectrum colours (blue / red) interfere constructively, resulting in a purple shading. For an anisotropic sample the phase difference introduced by the sample is added to / subtracted from that caused by the retarder plate. If the anisotropic sample has its slow direction parallel to that of the plate the phase difference is increased, destructive interference now occurs for the red end of the spectrum, so that blue shading is observed. Conversely, the slow direction of the sample at right angles to that of the plate decreases the phase difference, so that interference occurs at the blue end of the spectrum leading to a yellow or orange shading. From an anisotropic crystal with its slow direction parallel or perpendicular to the incident polarized ray, the reflected light is linearly polarized, so that it takes the

purple colour of isotropic samples. The purple colour appears bright when the slow direction is parallel to the incident ray, dark when it is perpendicular to it.

The orientation of the constituent lamellar planes of an anisotropic carbon at the polished sample surface can thus be assessed [67]. Yellows and blues are indicative of the prismatic edges exposed at the surface, one changing to the other during a 180° rotation. Purple is indicative of the basal layer planes lying parallel or perpendicular to the surface and remains unchanged during rotation. The colour changes of an anisotropic sample during rotation are illustrated by figure 2.11. 'Anisotropic purple' is distinguished from the purple of isotropic carbons by its darker shade. The optical microscope can thus be used to determine the presence or absence of anisotropy, the shape and size of the anisotropic areas, and the orientation of the layer planes at the sample surface.

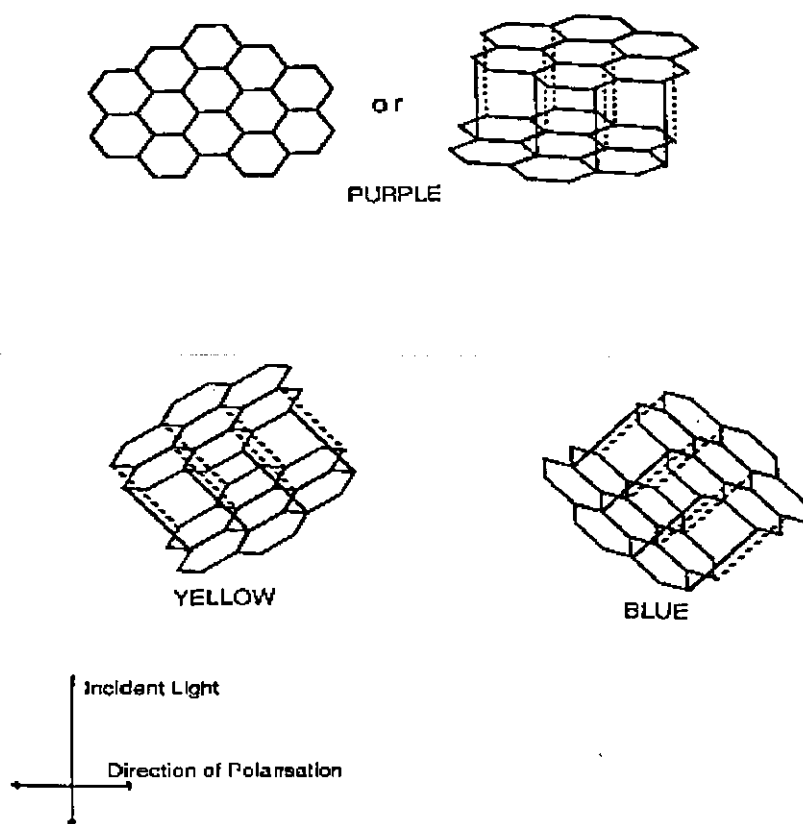


Figure 2.11 Colour Changes on Rotation of an Anisotropic Sample between Crossed Polars using a Half Wave Retarder Plate [85]

2.4.3 The Texture of Cokes

2.4.3.1 Historical

The microscopic appearance of carbon materials was first studied by Ramdohr in 1928 [91], who noted the anisotropy of graphite and graphitising carbons. He referred to the texture of pitch coke as 'mosaic', believing it to be composed of crystalline graphite of variable grain size, even though that view conflicted with its diffuse X-ray pattern.

The optical appearance of natural coke was studied by Marshall [92] on coal altered by igneous intrusions. He described the semi-coke as granular, with a mean grain size in the order of 3 μm , which did not correspond to the dimensions of the crystallites, which he found to be in the order of 25 Å. This distinction between a primary order on the scale of tens of angstrom and of a secondary one large enough to be observable by optical microscopy was later more clearly stated by Dahme and Mackowsky [93]. Mackowsky [94] proceeded to study the variations for cokes derived from different coals and was able to link the size of the anisotropic regions to the fluidity of the coals during their plastic stage. Abramski and Mackowsky [95] later succeeded in relating the size of the anisotropic regions to the rank of the coking coals carbonised. Coke from high volatile bituminous coals appeared isotropic, though submicroscopic ordered domains were suspected to exist. With increasing rank the mosaic units were found to increase up to a maximum in the medium volatile range. Low volatile coals produced fine domains, but exhibited an additional larger scale polarization effect, which was thought to be related to the original preferred orientation in the coals. An important point made by these authors is that the microscopic texture of coke does not alter significantly after solidification, in spite of the increasing degree of anisotropy with increasing temperature.

The same variation with coal rank / volatile matter content for vitrinite texture on carbonisation was described by Brooks and Taylor [65]. They stated that for more than 35 wt% VM the coke appears optically isotropic, but can be shown to possess a submicron mosaic texture by electron microscope techniques. They report an increase in mosaic unit size up to 24 wt% VM, after which it decreases, but the original orientation persists.

An important contribution made by Alpern [96] was to attempt to classify the mosaic textures by grain size and to show that the textures were characteristic for different coals and pitches and could be recognized even when blends were carbonised.

2.4.3.2 Classification of Coke Textural Components

A great number of coke microtexture classification schemes have since been devised, which vary widely in the amount of details taken into account and the nomenclature used. A comprehensive review of them has been undertaken by Coin [62], who found that their differences are partially based on the different analysis methods used. In particular the magnification under which the samples are viewed varies widely. He identified some common criteria, namely the division between fusing and non-fusing components, between coke matrix and inclusions, between optical isotropism and anisotropism, size variation of mosaics and shape, form and size of other textural entities.

The only classification system which will be described here is the one originally developed by Patrick et al [12], which will be used in the experimental part of this work. They carbonised vitrains from British coals ranging from 201 to 802 in NCB Coal Rank Code Number in small silica boats and viewed the embedded and polished samples under polarized light with a total magnification of $\times 1425$ in oil. From this they distinguished between basic anisotropism, isotropism, three different mosaic sizes, a mosaic/flow type intermediate and flow type domains. The mosaic categories were distinguished by grain size into fine ($0.3 \mu\text{m}$), medium ($0.7 \mu\text{m}$) and coarse ($1.3 \mu\text{m}$). The classes are supposed to reflect the degree of order in the carbon matrix, increasing from isotropic, via mosaic to flow and basic anisotropy, a view which was later backed by the measurement of the layer plane spacing by X-ray diffraction [97], which did indeed show a narrower spacing for flow type components than for mosaics.

The classification system was further developed by re-naming and subdividing some of the classes [9]. The mosaic / flow intermediate is now known as granular flow. The original flow type components have been divided into two separate classes according to their appearance, named broad and striated flow. Finally the carbonisation of whole coals rather than vitrains, as in the original work, necessitated the inclusion of non-softening components, which were termed inerts and subdivided according to size into small and large inerts. Table 3.5 summarizes the classification system as it is currently being used. The optical component classes are further illustrated by the micrographs in figure 3.2.

2.5 Interfaces

2.5.1 The Analogy between Cokes and Composites

There are many similarities between metallurgical cokes and carbon composites, well beyond the fact that both are principally comprised of carbon materials, to the extent that where mechanical and physical properties are concerned metallurgical coke can be classed as a composite [98].

There is no all embracing definition of a composite, but three main points for an acceptable composite for use in structural applications have been identified [99]. Firstly, it consists of two or more distinct, mechanically separable materials. Secondly, it can be made by mixing the separate materials in such a way that the dispersion of one material in the other can be done in a controlled way in order to achieve optimum properties. And finally the properties of the product composite will be superior to the properties of the individual components, and possibly unique in some specific respects.

Metallurgical coke comprises two main components, inerts, which do not pass through a fluid stage on carbonisation, and reactivities, which pass through a fluid stage and fuse to form the coke matrix enclosing the inerts. However, on one count it does not fully comply with the above definition of a composite. The precursors for the coke matrix and the inerts, i.e. mainly vitrinites for the former, infusible inertinites and mineral matter for the latter, do occur in a wide variety of associations in the various coal rock types, and can be at best concentrated, but hardly separated. Their proportions can be influenced by blending and selective crushing and grinding, or even by the use of supplementary coking additives, but no accurate, close control over amount, size and distribution of the inerts is possible.

But as no comprehensive study of the interfacial behaviour of metallurgical cokes has as yet been undertaken, it is still expedient to commence by considering suggestions regarding the nature of component bonding derived from research into composites.

2.5.2 Classification of Interfaces in Composites

One of the most important factors determining the nature and properties of a composite is the interfaces between its components. The adhesive forces at the interfaces may be chemical, physical or a combination of both [100]. Considering metal matrix composites Scott et al [101] classified interfaces into three types, mechanical bonds, chemical diffusion bonds and chemical reaction bonds, in terms of bonding mechanisms. Mechanical bonds are produced by differential contraction, but also include interlocking effects promoted by roughened surfaces. Chemical diffusion bonds involve some limited dissolution of one or both components. Chemical reaction

bonds are bonds where linkage between the molecules of the components across the interface occur. They are considered to lead to brittle behaviour, but might be feasible provided the reaction zone thickness does not exceed a certain critical value.

Qian et al [102] describe a similar classification system of interfaces for the description of anode carbons for aluminium manufacture. They distinguish between direct bonding, transitional bonding and interlocking. Direct bonding is adhesion at the carbon - carbon interface without any change in the carbon forms at either side of it. In contrast, in transitional bonding the carbon forms interfacing are modified, so that some intermediate material is observed at the interface. Interlocking occurs where a fluid phase carbon form enters into the surface porosity, fissures or roughness of a solid carbon form. The carbon form entering into the porosity is a continuum of the bulk carbon. There may not be any interaction between the surface carbon forms.

Patrick and Clarke [98] suggest five main bonding mechanisms for fibre - matrix interfaces in carbon-carbon composites, namely adsorption and wetting, interdiffusion, electrostatic attraction, chemical bonding and mechanical adhesion. They do not attempt to evaluate the probability with which any of them or a combination of them occur, nor elaborate on the conditions which may favour them. In contrast, in a paper considering the bonding between coke grist and coal tar binder as employed in electrode manufacture, Marsh and Sherlock [103] identify three factors that potentially determine the interfacial behaviour of carbon-carbon composites. The first is the degree of surface roughness, which would influence the effectiveness of mixing and wetting. Secondly, the presence of chemically bonded surface groups or atoms such as oxygen, hydrogen, sulphur and nitrogen, which presumably would encourage chemical bonding across the interfaces. And thirdly, the perfection of stacking of the lamellae and of the atomic arrangement within them. It has in the past been considered that the degree of adhesion between coal-tar pitch and coke decreases as the coke becomes more graphitic in structure [104]. Marsh and Sherlock [103] employ the argument of more perfect stacking, due to less disturbance during heat treatment, to explain why they found the quality of grist - pitch interfaces to deteriorate as heating rates are lowered from $150 / 300 \text{ K h}^{-1}$ to 5 K h^{-1} . Alternatively they propose that slower rates of heating may influence the free-spin concentrations (radicals) of the carbons, which, if chemical bonding mechanisms apply, would have an impact on them by reducing the 'chemical reactivity' of the surfaces.

2.5.3 Interfaces in Metallurgical Cokes

In spite of the fact that it has long been recognised that cokes from different rank coals form distinct optical components [12, 65, 95] and that they retain their characteristic appearances even when carbonised in blends [96], few efforts have been made to examine the interfaces between them. This may be due to the fact that, unlike for carbon fibre composites, the mechanical properties of metallurgical coke are perceived as being governed by its porosity [98]. It is hardly surprising that most principle flaws and defects are expected to be pores, considering that porosity regularly exceeds 50 %. Nevertheless it can be envisaged that under some circumstances the interfacial behaviour of the pore wall material may become significant. Marsh [105] expects that for a given porosity the strength of a coke will be dependent on the composition of the solid coke wall material. But as texture and porosity are impossible to vary independently, their relative importance cannot easily be estimated.

Textural coke components have received some attention from the point of view of crack propagation through the coke matrix. But interfaces within rather than between the components were focussed on in this case. Mosaic textures have been found to be associated with high strength cokes [22, 98, 106]. Due to the connection between coke texture and the nature of the parent coal it is difficult to demonstrate that any relation of coke texture to macroscopic coke properties is direct and independent [22]. Nevertheless it has been attempted to explain the suspected high strength of mosaics in terms of the interfacial behaviour of the small units they are comprised of. One such explanation is that interlocking between the units occurs at molecular level leading to very firmly bound interfaces and that good resistance to crack propagation is provided by the randomness of the orientation of the units [98]. Interlocking was suggested to be facilitated by a boundary layer of more disordered, even isotropic, material formed at the interfacial positions. This was thought to be the case as compressive forces disturb the stacking sequence of the basal layer planes at the surfaces of the units [106]. This is based on the assumption that mosaics are formed by small irregularly shaped growth units of mesophase, which, by some mechanism, which is not yet fully understood, fuse, rather than coalesce, leaving distinct boundaries between them [67]. This view has been challenged by Walker [8] who found it inconsistent with the optical properties of the mosaics. He regards the boundaries between the isochromatic areas in mosaic textures purely as changes of direction of the alignment of the crystallites, so that their exact positions actually change during rotation of the sample between crossed Nicols. Walker described all textures on the scale considered as continuous. He expects fracture in mosaics to occur as cleavage parallel to the aligned crystallites, rather than along the perceived

grain boundaries. This does not conflict with the view that the randomness of orientation necessitates frequent changes in direction during crack propagation and therefore assists in resisting it.

One of the few references to the interfaces between optical components is by Bernard et al [107], who observed transition textures at the boundaries between the coal grains from the different constituents of binary blends. In contrast, Ragan and Marsh [108], in a paper mainly devoted to the co-carbonisation with petroleum pitch, comment that in a 1 : 1 blend of a 602/702 NCB Rank Code number coal and a 334/434 one that "the interfaces are distinct with no evidence of a common fused state having existed at the interface". This presumably means that they did not observe any transitional material between the characteristic textures of the two cokes.

2.5.4 Interfaces involving Coking Additives

Some research effort has been devoted in the past to the nature of the interfaces between particles of coking additives and the coal coke matrix, though their treatment has been qualitative, rather than a systematic classification and quantification having taken place.

Triska and Schubert [47] examined interfaces with petroleum coke at a magnification of $\times 300$ and reported that the petroleum coke particles appeared to be well bonded into the coke matrix. Patrick and Stacey [49] proposed that coke breeze particles, unlike petroleum coke ones, are likely to introduce micro-cracks into the coke structure originating at their interfaces with the coke matrix.

Qian et al [102], investigating the possible bonding mechanisms between coking additive particles and the coal coke matrix, found that anthracite and green petroleum bonded well into the coal coke matrix and that there was some evidence of softening at their surfaces. They concluded that transitional bonding was the most likely mechanism for their incorporation. Contrarily the interfaces with coke breeze and calcined petroleum coke, which, having been pre-treated to high temperatures, must be considered as true inerts, were found to be poor. They assumed that, where bonding does take place at all, it will be by interlocking. No reasons are given as to why the direct bonding mechanism is thought highly unlikely by the authors.

Forrest and Marsh [109] included microscopic examination into their investigation of the effect of the pre-treatment temperature of pitch coke on coke strength. They found that green pitch coke was firmly bonded into the coke matrix and that fissures inherent in it did not propagate across the interfaces. As the pre-treatment temperature was increased fissures began to appear at the interfaces. Some petroleum coke seemed detached from the coke matrix, possibly forcibly separated by contraction forces. With

increasing pre-treatment temperature detachment from the coke matrix and propagation of fissures into it increased progressively.

Qian et al [102] make a distinction regarding the parent coal of the coke matrix. Bonding into a coke originating from a 401 NCB Code number coke was found to be superior to that into a 301a / 204 one. Into the former anthracite appeared to be well bonded, green petroleum coke was described as excellently bonded and calcined petroleum coke as showing limited bonding. Into the latter, anthracite was only partially or non-bonded, bonding with green petroleum coke lacked continuity and cohesion and calcined petroleum coke showed no adhesion at all.

Ragan and Marsh [108] co-carbonised a binary coal blend with various petroleum pitches. They found that microscopic examination revealed optical textures which could not be clearly assigned to either the coals or the pitches, leading them to the conclusion that they must originate from a fluid phase containing a mixture of coal and pitch substances. In most cokes those new textures occurred at the coal - pitch interfaces, so that they termed them 'intermediate optical textures'. They linked them to an observed improvement of coke micro-strength with pitch addition, stating that crack development at positions of contact between isotropic and anisotropic components was particularly prevalent where such intermediate textures were absent. The intermediate textures were credited with enhancing bonding and inhibiting crack propagation.

2.6 Present Position

It has been known for quite some time that metallurgical cokes are composed of optically distinguishable textural components [12, 65, 95]. Various classification schemes have been devised for them [62] and they have been linked definitively to the rank of the parent coal or coals of the cokes they occur in [12, 14, 63, 65]. Their formation mechanism has been widely debated and is thought to be a special case of the mesophase theory of carbonisation described in section 2.3.3. A few reasonably successful attempts have been made to link textural composition to macroscopic coke properties such as mechanical strength and reactivity [8, 105]. But interfaces between the textural components, inspite of being one of the more obvious possible links to mechanical coke properties in the sense that, when poor, they could provide weak points in the coke matrix, have received surprisingly little attention. Where interfaces have been considered, those involving coking additives are usually focussed on. Concepts for interface descriptions are borrowed from the investigation of other materials and the treatment is qualitative, highlighting individual cases rather than attempting a statistically viable appraisal [47, 102, 108, 109].

This thesis therefore sets out to conduct a fundamental study into the interfacial behaviour of the textural components in metallurgical cokes. Initially a system of classification is to be arrived at and methods of quantitative interface analysis to be devised and evaluated. The data eventually obtained will be used to address the question whether interfacial behaviour is characteristic for individual components or whether a component behaves differently when derived from coals of different rank. It will be tested to ascertain if interface distributions can be predicted from component distributions. Allowing for the division commonly made between reactive and inert components, the interfaces involving inerts, both, coal derived and as coking additives, will receive special attention and the effect of varying inert contents will be investigated.

3 Experimental Studies

Three series of cokes were produced on an experimental scale under conditions resembling those in commercial coke ovens. They have been examined using polarized light microscopy with the view to gain insight into the interfacial behaviour of their optical components.

3.1 The Cokes

3.1.1 Series 1

Series 1 was originally prepared for the work undertaken by Walker on the carbon texture of metallurgical coke [8]. It comprises 6 samples, here labelled A1 to F1, prepared from British coals ranging from 334 to 733 on the International Classification. Details of the coals are given in table 3.1. In addition to the data listed the properties of the cokes have been thoroughly investigated with regard to pore size and distribution and tensile strength [9]. The cokes were prepared in a 0.6 kg oven, which was designed to simulate the temperature regime in a 450 mm width coke oven with gravity charging of the preheated coal [8]. The air-dried coal, sized to 90% < 3 mm, was charged into a 1 m long 60 mm diameter cylindrical retort and compacted to a charge density of about 820 kg/m³. The charge was held in place between silicon spacers by spring loaded rods and the retort was sealed fitting flanges at the ends. The retort was then rotated into a horizontal position and a flow of nitrogen was started across it, for which in- and outlet pipes were positioned at either end. A furnace with a 250 mm constant temperature hot zone, fitted on wheels and mounted on rails, was then drawn along the retort at a constant speed of 20 mm/h, which amounts to a carbonisation time of about 16 h. The furnace temperature was held at 1080 °C throughout the carbonisation aiming at a centre charge temperature of 1040 °C.

	ISO Coal Classf. No	VM %wt (daf)	Ash %wt (db)	Moisture %wt	C %wt (daf)	H %wt (daf)	% Total Dilatation
Series 1							
A1	334	19.7	7.5	0.8	91.5	4.3	85
B1	434	20.2	4.9	0.6	90.6	4.6	98
C1	435	26.4	1.3	0.8	89.5	4.9	241
D1	635	36.4	1.5	0.9	87.2	6.4	285
E1	635	35.0	4.2	2.4	86.0	5.3	188
F1	734	36.6	5.4	2.4	83.4	5.3	73
Series 2							
A2	433	25.1	10.5	2.0	88.9	4.7	23
B2	534	29.0	8.0	0.5	88.2	5.1	128
C2	435	26.5	9.0	1.0	86.6	4.7	213
D2	703	46.7	4.5	4.5	80.1	5.2	0
Series 3							
Coals:							
A3	434	20.4	4.0	0.5	87.6	4.4	80
B3	535	28.7	6.0	0.0	82.7	4.7	229
C3	635	35.4	1.0	0.0	87.7	5.2	n.a.
Additives:							
ADD1	n.a.	10.3	0.3	0.3	93.6	n.a.	n.a.
ADD2	100A	4.8	1.8	1.6	95.2	n.a.	n.a.

Table 3.1 Properties of the Coals

3.1.2 Series 2

Four coals, labelled A2 to D2, were used. A summary of their properties is given in table 3.1 on the previous page.

To facilitate the investigation of varying inertinite contents, maceral concentration was effected¹. The coals, crushed and screened to -1 mm + 75 μ m, were separated in a dense liquid hydrocyclone at two different densities. The underflow of the first separation was used as the feed for the second. The overflow of the first separation is assumed to be vitrinite rich, that of the second, inertinite rich. The results of the maceral analysis (% vol) of the coals and their concentrates is given in table 3.22.

Petrographic Composition (%vol.)			
	Coal	Vitrinite Concentrate	Inertinite Concentrate
A2			
Vitrinite	63.8	70.6	48.2
Exinite	1.8		
Inertinite	34.4	29.4	51.8
B2			
Vitrinite	64.5	84.7	51.1
Exinite	0.4		
Inertinite	35.2	15.3	48.9
C2			
Vitrinite	69.8	88.9	41.8
Exinite	3.9	0.2	0.5
Inertinite	26.3	10.9	57.7
D2			
Vitrinite	77.7	86.1	65.6
Exinite	1.2	3.4	2.7
Inertinite	21.2	10.5	32.7

Table 3.2 Petrographic Composition of the Coals and Maceral Concentrates in Series 2

¹The maceral concentrations and petrographic analysis of the maceral concentrates were carried out by the Coal Technology Research Group based in the Department of Chemical Engineering at Nottingham University.

²Petrographic analysis of the coal was carried out during routine sampling, not on the actual coal used.

The properties of the pure macerals are not known, but an attempt was made to estimate their volatile matter and carbon contents and their densities. The procedure used and results obtained are described in appendix 1.

Carbonisations were undertaken for 30g samples. The scale was necessarily small because of the difficulties in obtaining sufficiently large quantities of the maceral concentrates. The coal particle size used, $-1\text{ mm} + 75\text{ }\mu\text{m}$, was not chosen from any carbonisation related viewpoint, but was dictated by the requirements of the maceral concentration process.

A schematic view of the experimental set-up for the carbonisations of sample series 2 is given in figure 3.1.

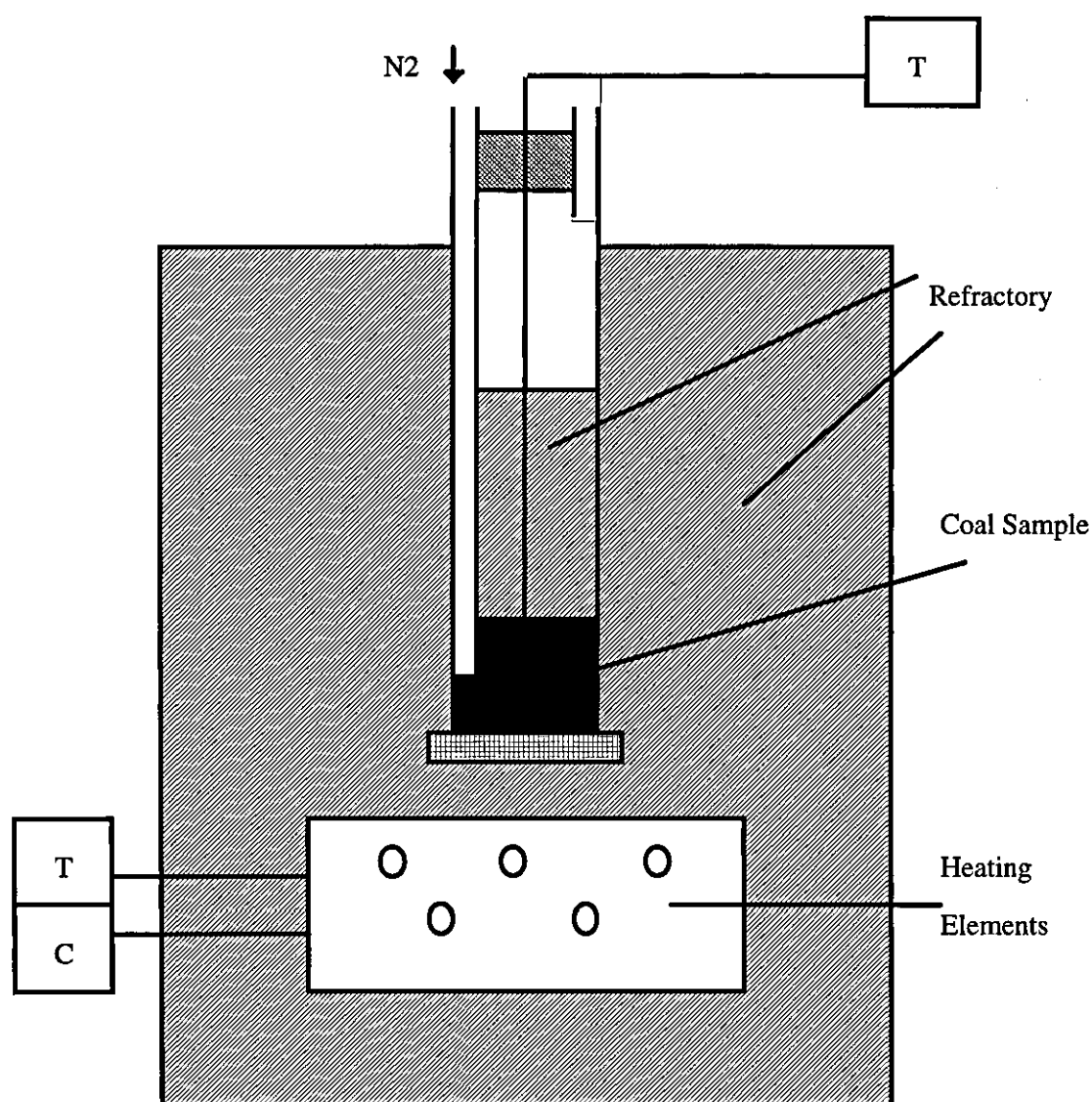


Figure 3.1 Schematic View of the Experimental Carbonisation Set-up

It represents a 33 mm diameter vertical tube, bottom heated furnace. The coals or coal blends were charged from the top and lightly compacted to an average bed height of 44 mm, equivalent to a charge density of about 650 kg/m³. They were then heated under nitrogen to about 600 °C at the charge top surface. Automatic temperature control was used to achieve a heating rate of 5 °C/min up to 400 °C and of 2 °C/min up to 1100 °C, where the wall temperature was kept constant until the desired temperature at the top of the charge was reached. The coke samples were then removed and heat treated at 1000 °C in order to drive off residual volatile matter and harden the cokes produced. Two sub-sets of samples were produced. The first set consists of single coal samples and will hereafter be referred to as series 2.1. In the second set, series 2.2, the samples are composed of binary blends.

3.1.2.1 Formulation of the Maceral Concentrate Blends

The vitrinite weight percentages in the blends are calculated using the fact that the weight of inertinite can be expressed as the product of the total weight and the petrographically determined inertinite fraction (volume percentage / 100). Thus

$$x_{bi} * BL = x_{vi} * VC + x_{ii} * IC \quad (3.1)$$

where x_{bi} - inertinite fraction in the blend

x_{vi} - inertinite fraction in the vitrinite concentrate

x_{ii} - inertinite fraction in the inertinite concentrate

BL - weight of the blend / g

VC - weight of the vitrinite concentrate / g

IC - weight of the inertinite concentrate / g

The weight of the blend is that of the sample, i.e. BL is 30 g, and, as the sum of VC and IC makes up the entire sample, IC can be replaced by (30 - VC) in the above equation, which can then becomes

$$VC = [30 * (x_{bi} - x_{ii})] / (x_{vi} - x_{ii}) \quad (3.2)$$

The vitrinite concentrate weight percentage is then obtained by multiplying VC by (100 / 30).

In series 2.1 for each coal, the coal as received, the vitrinite and inertinite concentrate were carbonised. They are denoted by the suffixes V, C and I. For coals B2 and C2, for which the concentration process proved more successful, additional blends containing 75 and 75 and 50 % (wt) vitrinite were also carbonised as samples B2 75,

C2 75 and C2 50. The weight percentages of the concentrates and coals in these blends are given in table 3.3.

	Vitrinite Conc. (% wt)	Coal (% wt)	Inertinite Conc. (% wt)
B2 75	58.7	41.3	0.0
C2 75	35.3	64.7	0.0
C2 50	0.0	32.0	68.0

Table 3.3 Composition of Blends in Series 2.1

Series 2.2 consists of vitrinite concentrate - inertinite concentrate blends from different coals in every combination possible to obtain 25, 37.5 and 50 %(wt) of inertinite in the blend. Table 3.4 lists the blended samples indicating their composition by the weight percentages of the vitrinite concentrates used. The first letter denotes the vitrinite concentrate, the second the inertinite one and the number the weight percentage of inertinite.

	Vitrinite Concentrate (% wt)
AB37	58.5
AC37	71.4
BA25	73.4
BC25	77.1
BD25	44.3
BA37	39.2
BC37	47.6
BC50	18.2
CA25	65.5
CB25	62.9
CD25	35.3
CA37	35.0
CB37	30.0
DA25	64.9
DB25	62.2
DC25	69.3
DA37	34.6
DB37	29.2

Table 3.4 Weight Percentage of the Vitrinite Concentrates in the Blends in Series 2.2

3.1.3 Series 3

Three different coals were used to prepare the coke samples investigated, two, labelled A3 and B3, of American origin, and one, C3, of British origin. A blend of these three coals, composed of a third of each, was also used. A summary of the available data on these coals is given in table 3.1.

Two carbon materials, which behave in a semi-inert manner on carbonisation, were used as coking additives. One is a petroleum coke, referred to as ADD1, the other, ADD2, a calcined anthracite. Their properties are also summarised in table 3.1. The properties of ADD2 are given as quoted before calcination at 1000 °C.

For each coal seven carbonisations were carried out, one without the addition of semi-inerts, the remaining ones with 10, 30 and 50 % (wt) of each of the two additives. 200 g samples of crushed and sized coal (< 3 mm) and additive (< 212 μm) were heated in a 60 mm diameter vertical tube, bottom heated furnace using the same method as described for series 2 in section 3.1.2. The sample height was identical to that for series 2 and, the same heating rate being used, this should allow for a similar rate of heat transfer and thus progression of the plastic layer through the sample. It is reasonable to assume that that was the case, as the desired final temperature at the sample surface furthest from the heating elements was reached within roughly the same period of time.

3.2 Friability Testing

For samples of series 2 and 3 forming a sufficiently well fused coke, a small scale friability test was performed. For this, small cylinders, 10 mm in diameter by 10 mm in height, were drilled from the cokes, cleaned sonically and dried overnight in a drying oven at 100 °C. They were then charged into a 305 mm long stainless steel tube, 25.4 mm in diameter, together with three 8 mm diameter steel balls. The tube was rotated vertically at 30 rpm for 100 minutes. The friability weight loss is reported as the percentage of the original weight of coke passing through a 1 mm sieve after testing.

3.3 Sample Preparation for Microscopy

For examination under a polarized light microscope the coke was dried, crushed manually and sieved to the size range of 210 - 600 μm . This size range presents a good compromise between achieving a representative sample by avoiding a distortion of the component distribution results by large single component particles and the identification of components, which becomes progressively more difficult with

decreasing particle size. A fraction of the crushed sample was then taken and mixed with epoxy - resin. The paste was formed into thin discs of about 20 mm diameter, which, after hardening, were embedded in blocks of the same epoxy - resin . The blocks were polished on rotating disc polishers applying about 1 bar pressure. Coarse grain emery paper was used to level the block surface, before polishing was put into effect using first 1 μm and then 0.5 μm alumina powder. A highly reflective, scratch - and relief - free surface suitable for reflected light microscopy was thus obtained.

3.4 Polarized Light Microscopy

3.4.1 Coke Component Counts

Coke components were identified using a Leitz Ortholux II reflected light, polarizing microscope. A total magnification of $\times 1000$ in air was used, made up of a $\times 100$ objective and a $\times 10$ eyepiece. The sample was viewed between crossed polars and the image was enhanced by colour induced by a half wave retarder plate placed between the sample and the analyser. A point counting technique was used to quantify the proportions of the different optical components in the coke samples. For this an electronic counter was connected to the microscope stage, which would advance the sample automatically as the component falling under the cross-wire was recorded, or could be advanced without record of the field if the cross-wire fell on the resin in which the coke was embedded.

For each sample two 500-point counts were conducted, the average of which was used in calculations. The raw data from the counts is displayed in appendix 2.

The classification used is that originally devised by Patrick et al [12] in the version modified by A. Moreland [9]. Table 3.5 lists the component classes and gives a brief description of their appearances.

3.4.2 Interface Counts

The same microscope set-up as described for coke component counts in section 3.4.1 was used to count the component interface types. A minor modification of the counting technique was required as it was not realistic to expect any significant number of interfaces to fall exactly under the cross-wire. An additional graticule was therefore placed in the ocular defining a $40\ \mu\text{m} \times 60\ \mu\text{m}$ field of view, within which the interface closest to the cross-wire was counted.

The development and appraisal of an interface classification system and of methods to use it to obtain quantifiable data was in fact one of the objectives of this work and is therefore described in detail in sections 4.1 and 4.2.

Component	Abbr.	Appearance
Anthracitic	A	non - porous, anisotropic, single - coloured, featureless, non - fusing
Flow		anisotropic, composed of elongated isochromatic areas, often curved round pores
broad	BF	$> 20 \mu\text{m} \times > 10 \mu\text{m}$
striated	SF	$> 20 \mu\text{m} \times > 2 \mu\text{m}$
granular	GF	$> 3 \mu\text{m} \times > 1 \mu\text{m}$
Mosaic		anisotropic, composed of small, rounded, isochromatic areas
coarse	CM	mean size $0.91 \mu\text{m}$
medium	MM	$0.63 \mu\text{m}$
fine	FM	$0.50 \mu\text{m}$
Isotropic	ISO	isotropic, well fused
Inerts		isotropic, woody structure (large), sharp, unfused edges; mineral matter
large	INL	$> 50 \mu\text{m}$
small	INS	$< 50 \mu\text{m}$

Table 3.5 Classification of Textural Coke Components

The component classes are further illustrated by the micrographs in figure 3.2.

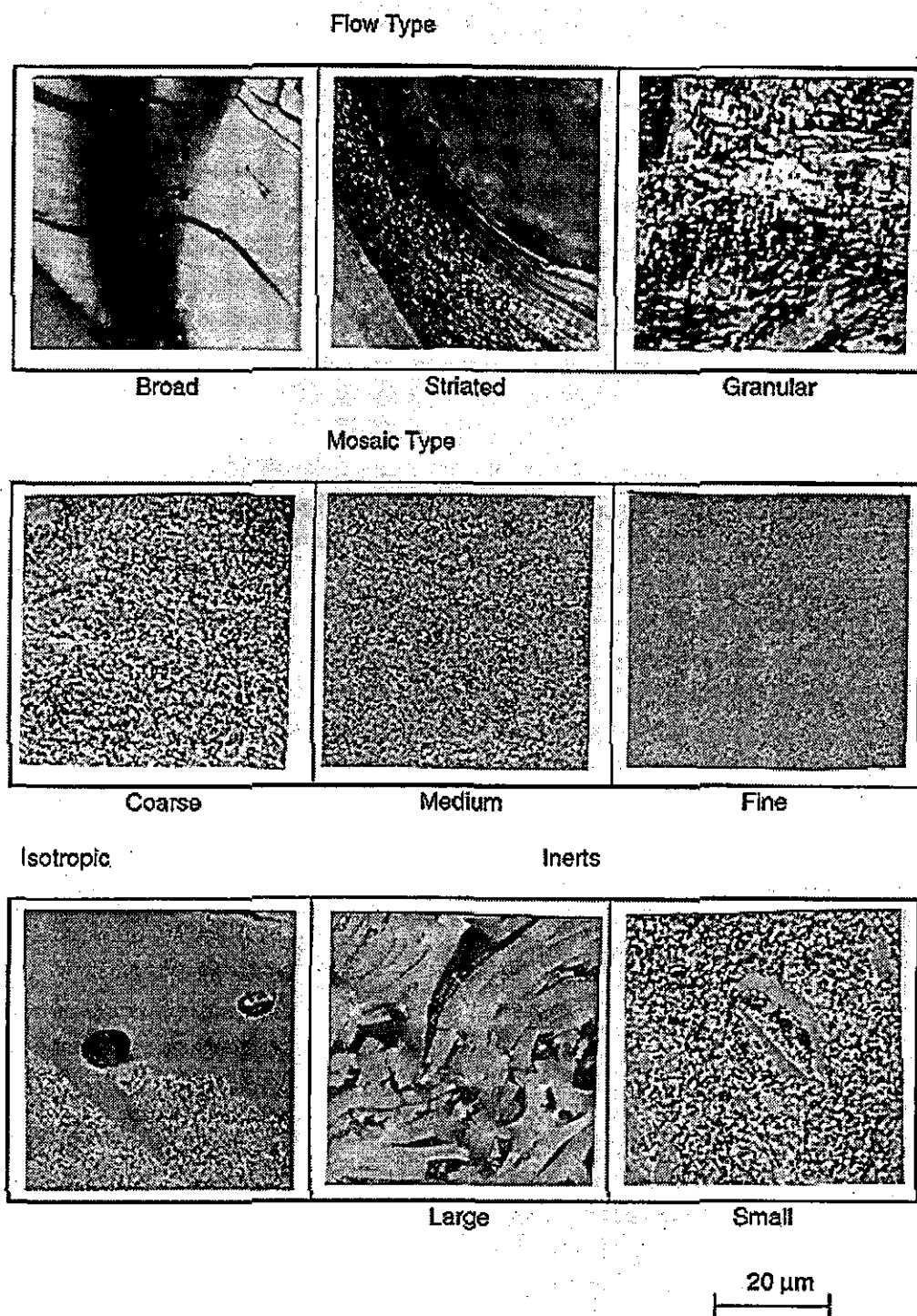


Figure 3.2 Micrographs of the Optical Coke Components

4 Discussion of Results


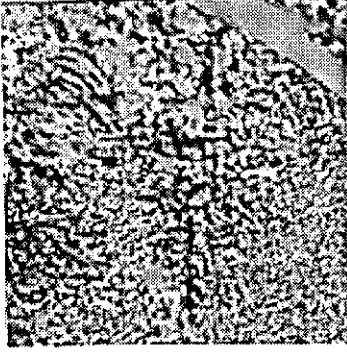
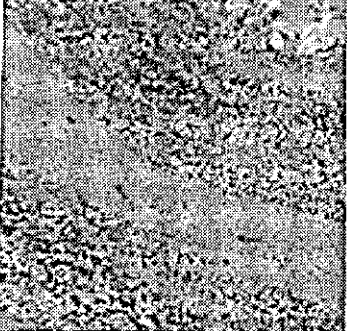
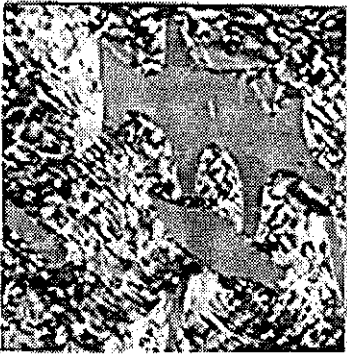
4.1 The Interface Classification System

4.1.1 Interface Classes

To date coke component interfaces in metallurgical cokes have not been looked at in a systematic way, which would enable data to be collected and related to coke properties. The prime objective of this thesis was therefore to attempt to classify coke component interfaces in such a way that their quality can be assessed quantitatively. Careful inspection of the cokes of the first series led to the classification system outlined below in table 4.1 and illustrated by the micrographs in figure 4.1.

Interface Class	Abbr.	Description
Transitional	T	There is no clearly defined boundary between the two interfacing components, but a gradual change in appearance from one to the other. The intermediate material can be quite dissimilar from either of the components and may occupy a large area compared to the size of the components.
Fused	Fu	No intermediate material is present. The boundary between the interfacing components is clearly defined, but the bonding appears flawless.
Fissured	Fi	The interface between the components concerned displays evidence of fissures or cracks, which cover only a small fraction of the interface length.
Unfused	Uf	A substantial gap, along well over half of the interface length, is visible between the components, suggesting that fusion has not occurred.

Table 4.1 Description of the Classification System of Coke Component Interfaces

Interface Type	Components
	Transition Broad Flow Granular Flow
	Transition Granular Flow Medium Mosaic
	Fused Medium Mosaic Fine Mosaic
	Fused Granular Flow Small Inerts

20 μ m

cont. overleaf

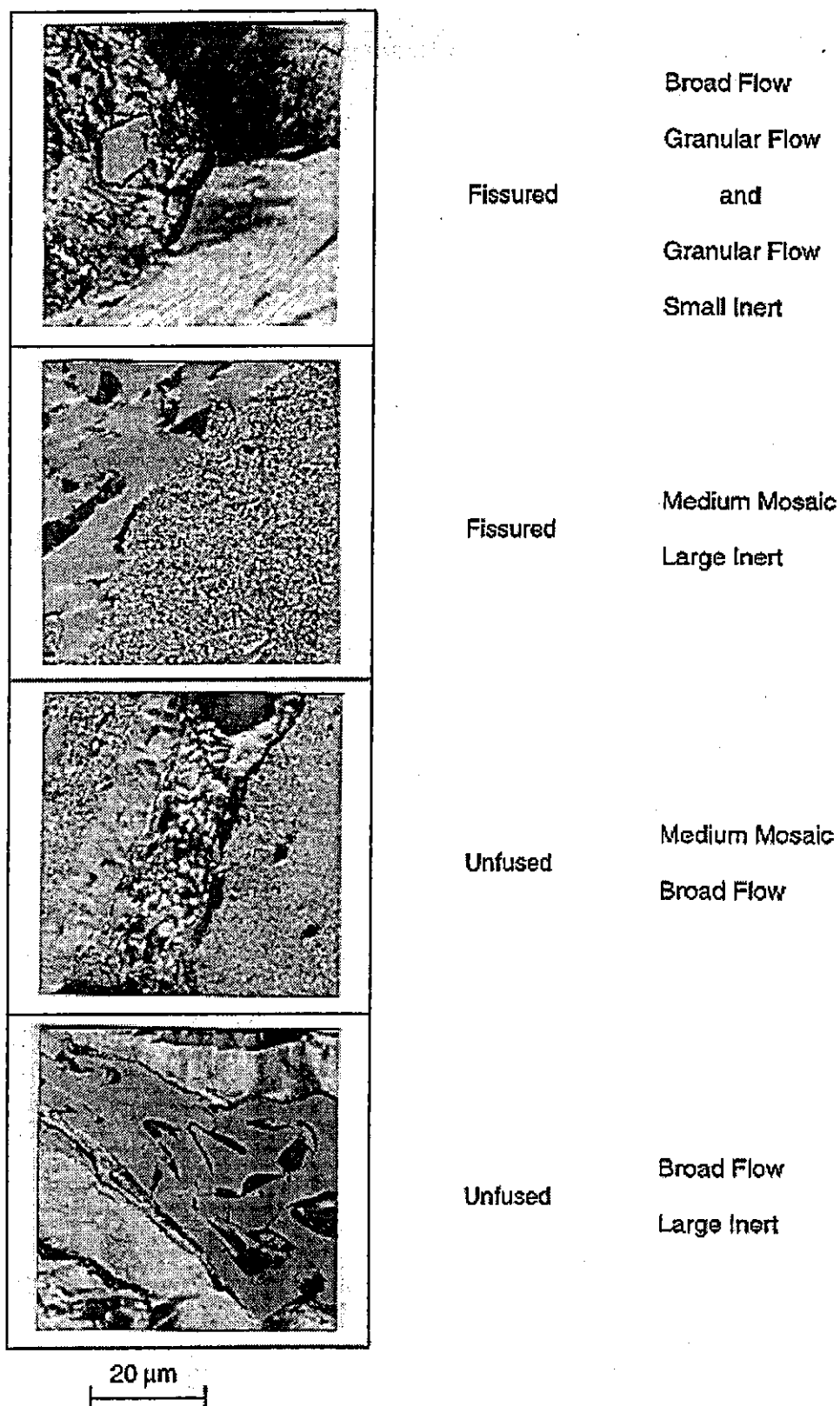


Figure 4.1 Micrographs showing the Interface Types

Interfaces can either be perceived as 'good', i.e. no fissures are present, or 'poor'. Good interfaces can be subdivided into transitional (T) and fused (Fu), depending on whether there appears to be a smooth transition between the components via an intermediate material, or whether a clear boundary between them can be identified. Poor interfaces divide into fissured (Fi) and unfused (Uf) according to the size of the area of no contact between the components relative to the size of the entire interfacial length. This means that, if in excess of one half of the length of an interface the two adjacent components do not touch, they are considered not to have fused, rather than just having fused imperfectly as the expression fissuring implies.

4.1.2 Counting Methods for Quantitative Interface Analysis

Three different types of counts of increasing complexity are used. The first will be referred to as 'simple count' and is confined to noting the type of interface only, irrespective of the nature of the adjacent components. As interfaces between 'reactive' and 'inert' components are of particular interest, a second type of count referred to as 'split count' is also used. It distinguishes between twelve categories by splitting each of the interface types into 3 sets, 'reactive - reactive' (R-R), 'reactive - small inerts' (R-S) and 'reactive - large inerts' (R-L). No 'inert - inert' interfaces were observed during the initial trials of the classification system and such a category was thus deemed unnecessary. In a more complex point count named 'by-component count' not only the interface classes, but also the two components, as identified by their optical anisotropy, adjacent to the interface are noted. This had to be carried out manually using a large worksheet due to the large number of categories. The by-component counts on the samples in the first series were carried out counting the interface closest to the cross-wire only, as for the other two counting methods, but on the samples in the second series a slightly faster procedure counting all interfaces in the field of view defined by a graticule was adopted.

On the samples of the first series four 500 point counts were performed, two simple ones and two by-component counts. To supplement the statistically significant information from the by-component counts some selective counts targeting specific components were also carried out, namely for components making up in excess of 5% of the total volume and only falling marginally short of the 1% of the interfaces taken as the cut-off point for inclusion in the considered data.

On the samples of the second series all three types of interface count were carried out, a 500 point simple one, a 500 point split one and two 500 point by-component ones. On series 3, in addition to a 500 point split interface count, a modified kind of count was conducted, concentrating individually on the interfaces of particular interest in this series. For small and large inerts and small and large particles of the additives

separate 250 point counts were conducted, concentrating on the component in question only. Small and large refer to the inert sizes given in table 3.5. This was primarily carried out because interfaces with large inerts and large additive particles in some samples were so rare that their frequency was insufficient to draw any statistically valid conclusions.

The raw data from the interface counts are given in appendix 3.

4.1.3 Interface Quality Index

In order to appreciate the variation of interface type frequencies more easily an interface quality index (IQI) was defined as the ratio of the percentage of good interfaces counted, transitional P(T) and fused P(Fu), to that of poor ones, fissured P(Fi) and unfused P(Uf) .

$$IQI = \frac{P(T) + P(Fu)}{P(Fi) + P(Uf)} \quad (4.1.1)$$

For the case of the split and by-component counts, where individual component combinations or groups thereof are considered, individual IQI for them can be determined. For any component combination, or group of combinations, x the individual interface quality index IQIx will then be given by

$$IQIx = \frac{P(Tx) + P(Fux)}{P(Fix) + P(Ufx)} \quad (4.1.2)$$

Strictly speaking equation 4.1.1 should therefore be re-written as the overall or total interface quality index IQIt given by

$$IQIt = \frac{\Sigma[P(Tx) + P(Fux)]}{\Sigma[P(Fix) + P(Ufx)]} \quad (4.1.3)$$

The relation between the individual and overall interface quality indices is not as simple as might be expected, as the contributions of the component combinations also depend on their frequencies of occurrence. If the fraction p_x of the total number of interfaces N formed by the component combination x is given by

$$p_x = [P(Tx) + P(Fux) + P(Fix) + P(Ufx)] / N \quad (4.1.4)$$

then combining equations 4.1.2 and 4.1.4 enables $[P(Tx) + P(Fux)]$ and $[P(Fix) + P(Ufx)]$ to be expressed in terms of IQIx and p_x in the following manner

$$p(Tx) + P(Fux) = \frac{IQ_{Ix} * N * px}{IQ_{Ix} + 1} \quad (4.1.5)$$

$$P(Fix) + P(Ufx) = \frac{N * px}{IQ_{Ix} + 1} \quad (4.1.6)$$

In this form they can be substituted into equation 4.1.3 to yield

$$IQ_{It} = \frac{\sum \frac{(IQ_{Ix} * N * px)}{(IQ_{Ix} + 1)}}{\sum \frac{(N * px)}{(IQ_{Ix} + 1)}} \quad (4.1.7)$$

4.1.4 Rank Dependence of the Interface Distribution

The microtextural composition of the cokes A1 to F1 (carbonisation series 1), according to the classification scheme outlined in table 3.5, is shown overleaf in figure 4.2.a. A variation of composition with the rank of the precursor coal can be seen clearly and, in fact, the same cokes have been used in earlier work to demonstrate this [8]. The main components in the cokes from higher rank coals are of the flow types, which change via intermediate types for cokes from medium rank coals to mosaic and isotropic material for cokes from low rank coals. The distribution of the interface types between the components, as described in table 4.1, was also observed to change with coal rank. Their variations are summarized in figure 4.2.b.

It appears that, as the component composition shifts from flow to mosaic, the interface distribution shifts from mainly transitional to predominantly fused type interfaces, suggesting that transitional interfaces are more typical for flow type components. Simultaneously the percentage of fissured and unfused interfaces decreases, which indicates a better interface quality for cokes consisting mainly of mosaic type components. There appears to be a rank dependence of the interface distribution. The question whether this is a genuinely independent property or a secondary effect to the rank dependence of the component distribution will be addressed later.

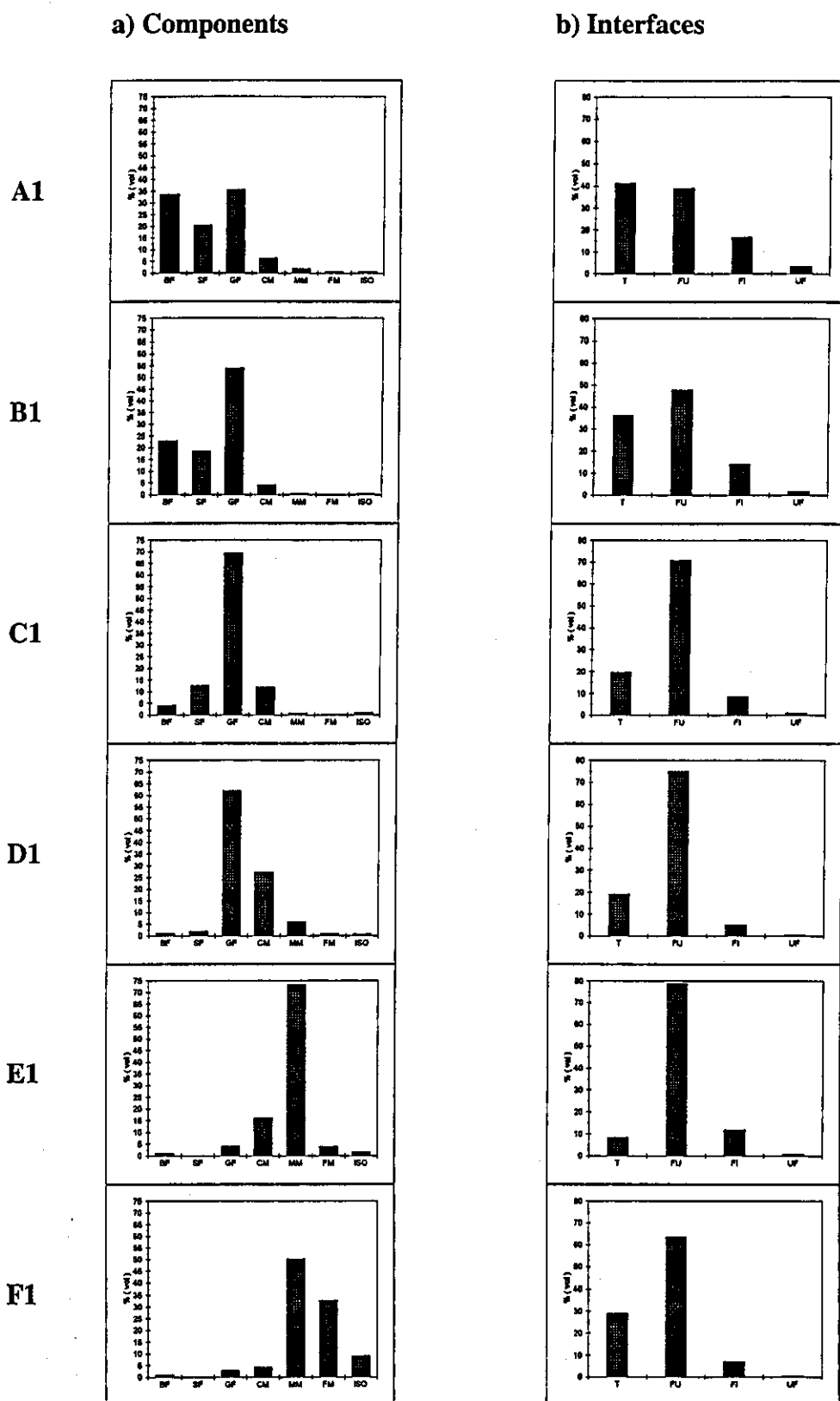


Figure 4.2 Distribution of the Textural Components and their Interfaces in Sample Series 1

The total interface quality index IQIt for each coke was calculated and is displayed in figure 4.3. The interface quality increases with rank initially, but reaches a maximum at coke D1.

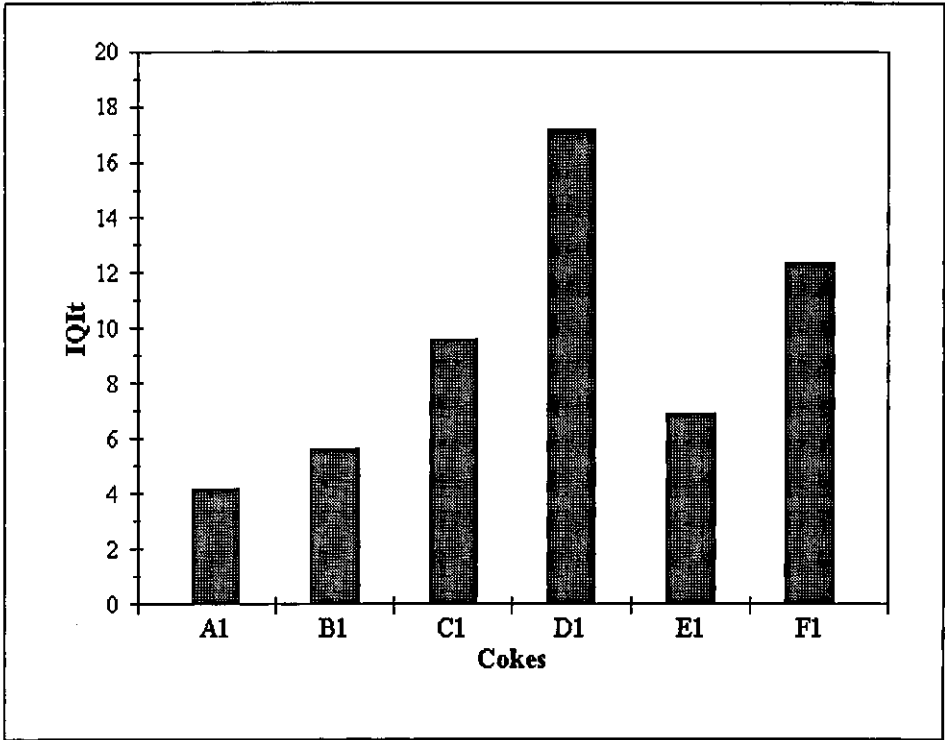


Figure 4.3 Total Interface Quality Indices (IQIt) for the Cokes in Series 1

Figures 4.4 a and b show the relations between IQIt and selected coal rank parameters, namely carbon content and total dilatation. For both of them some weak correlations are evident, although deviations exist and the trends are not unambiguous. With carbon content a parabolic relationship peaking at coke D1 can be argued for, all be it with the exclusion of coke E1. With the exception of coke F1, the IQIt appears to increase in an almost linear fashion with dilatation.

Hence the interface type distribution, as simplified by the interface quality index, shows a systematic variation with both component distribution and parent coal rank. The exact nature of these relations does therefore need to be investigated This is complicated by the fact that, as figure 4.2 a shows, component distribution and rank are themselves interdependent.

The total interface quality index IQIt for each coke was calculated and is displayed in figure 4.3. The interface quality increases with rank initially, but reaches a maximum at coke D1.

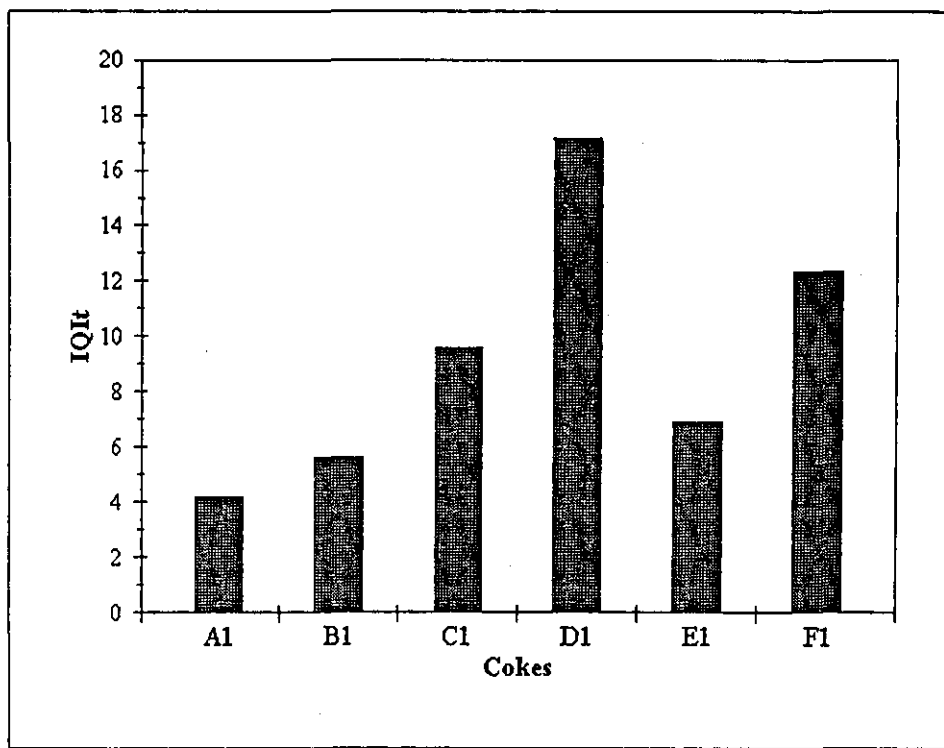


Figure 4.3 Total Interface Quality Indices (IQIt) for the Cokes in Series 1

Figures 4.4 a and b show the relations between IQIt and selected coal rank parameters, namely carbon content and total dilatation. For both of them some weak correlations are evident, although deviations exist and the trends are not unambiguous. With carbon content a parabolic relationship peaking at coke D1 can be argued for, all be it with the exclusion of coke E1. With the exception of coke F1, the IQIt appears to increase in an almost linear fashion with dilatation.

Hence the interface type distribution, as simplified by the interface quality index, shows a systematic variation with both component distribution and parent coal rank. The exact nature of these relations does therefore need to be investigated This is complicated by the fact that, as figure 4.2 a shows, component distribution and rank are themselves interdependent.

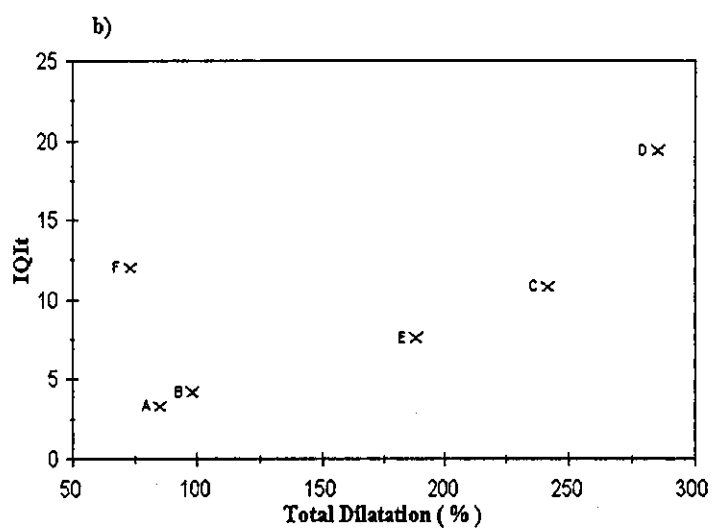
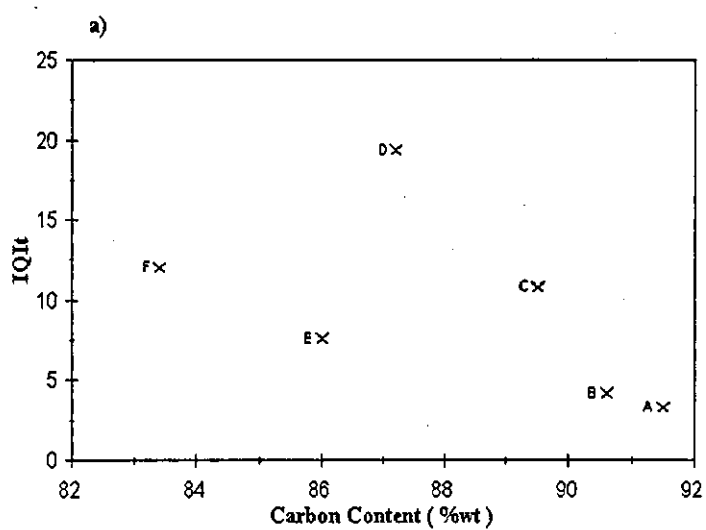


Figure 4.4 Overall Interface Quality versus Selected Coal Rank Parameters for the Cokes in Series 1

4.1.5 Textural Component Dependence of the Interface Distribution

The alternative to seeing the coke component interface distribution as a function of coal rank, is to regard interfacial behaviour as a characteristic property of the components. This would imply that the same individual component combinations should have the same interface quality indices in all cokes they occur in and differences in the overall interface quality arise solely from variations in their frequencies.

The individual interface quality indices from the by-component counts on the cokes of series 1 were examined in this light. Firstly the IQI of the reactive components with the two inert sizes, IQIs and IQII, were considered. If the inerts behaved in a truly inert manner, their interfacial behaviour should be identical in all cokes and interface qualities should reflect the ability of the reactive components to incorporate them. The results are shown in table 4.2. The numbers marked by * include data from selected counts targeting the individual components. The entry 'max'" stands for maximum IQI, meaning that all interfaces are of the transitional and fused types.

Cokes:	A 1	B 1	C 1	D 1	E 1	F 1
IQIs						
BF	0.7	2.3	2.2	4.0*	6.0*	
SF	0.8	1.4	3.7			
GF	2.8	4.5	12.1	17.5	11.0*	23.0
CM	2.3*		25.0	17.1	9.5	28.0
MM				max	6.3	12.9
FM					10.5	5.4
ISO						
IQII						
BF	1.5	1.2				
SF	1.3	0.9	2.0			
GF	3.3	2.5	8.0	15.0	3.6*	5.0
CM	5.0*		7.1	9.0	7.3	5.0
MM				14.0	4.9	4.6
FM						14.5
ISO						

Table 4.2 Interface Quality Indices for Reactive-Inert Interfaces in Series 1

Comparing the interfaces between the reactive components and inerts within each coke, there is an almost universal trend of the best interface quality being achieved by granular flow and coarse mosaic, followed by the smaller mosaics, with the larger domain flow components performing worst. But comparing the actual IQIs and IQII values for the same component in the different cokes shows a wide scatter around the averages. At its most extreme, for the interface between coarse mosaic and small inerts, a tenfold difference between the highest and lowest IQIs was recorded. However, the variations do not appear to follow any identifiable trend in general, as the one that has been shown for the total IQI for the cokes. All three possible patterns, an increase with falling rank of the precursor coal (INS-BF), a decrease with falling rank of the precursor coal (INL-MM) and values peaking at medium rank parent coals (INS-GF and CM for both inert sizes), occur.

Table 4.3 shows the interface quality indices calculated for all reactive-reactive component interface combination occurring at a frequency greater than 1 % or for selected counts of an equivalent number.

Cokes:	A 1	B 1	C 1	D 1	E 1	F 1
IQI						
BF-SF	66.0	53.0				
BF-GF	26.0	48.7	max	max		
BF-CM	max*	max*		max*		
BF-MM	max*	max*		max*	21.5*	
BF-FM						
BF-ISO						
SF-GF	26.8	43.7	110.0	42.0*		
SF-CM	max*	max*		6.0*		
SF-MM						
SF-FM						
SF-ISO						
GF-CM	max*	max*	max	max	max*	max*
GF-MM				max		max*
GF-FM						
GF-ISO			max*	16.0*		
CM-MM				max	max	max
CM-FM				max*		
CM-ISO				max*		
MM-FM				max*	max	97.0
MM-ISO					20.5	20.0
FM-ISO				max*	max*	max

Table 4.3 Interface Quality Indices for Reactive-Reactive Interfaces in Series 1

It can be easily appreciated that in comparison with the IQI of reactive - inert interfaces shown in table 4.2, all reactive - reactive interfaces are very good. Nevertheless some differences between them can be detected. For about half of the interfaces between flow type components some fissuring has been observed, whereas the vast majority of flow-mosaic and mosaic-mosaic interfaces attained the maximum possible IQI. Unfortunately only four combinations, BF-GF, BF-MM, SF-GF and GF-CM, occur at sufficiently high frequencies in enough cokes to enable a comparison between them to be made. Again no clear trend can be detected. The interface quality of the BF-GF combination appears to improve progressively from coke A1 to coke D1. That for BF-MM and SF-GF increases initially, peaks at coke C1 and D1 respectively, and then decreases again. The GF-CM interface quality is constant at the maximum possible IQI in all cokes.

From the IQI listed in table 4.3 there is no evidence of optically similar components interfacing better than optically dissimilar ones. In fact, most of the worst reactive-reactive interfaces are found between the three flow type components and between medium mosaic and isotropic. Unfortunately the single coal cokes of the first carbonisation series do not yield any data of the most dissimilar combinations possible, such as broad and striated flow with fine mosaics or isotropic material.

One of the deficiencies of the IQI as a means to compare interface quality is that it does not differentiate between transitional and fused interfaces, which make up the vast majority of reactive-reactive interfaces. Table 4.4 therefore lists the ratio of transitional to fused interfaces $P(T) / P(Fu)$ for the same component combinations as considered in table 4.3. A component that occurs at a volume percentage greater than 10 % (counted including inerts) is arbitrarily called a 'major' component (M), one accounting for less than 10 % a 'minor' component (m). The letters preceding the ratios in table 4.4 indicate whether the combination is derived from two major or a major and a minor component. The overall impression obtained is that M-M combinations tend to have higher values, but this is not consistently so. The M-m combination of GF-CM in cokes B1 and E1 for example forms transitional type interfaces only. Also, the effect is overshadowed by the fact that the majority of M-M interfaces are flow type ones, for which transitions have been found to be more typical already from figure 4.2.b, whereas among the M-m ones flow-mosaic and mosaic-mosaic combinations dominate.

Viewing table 4.4 from the aspect of optical similarity of the components interfacing shows quite a significant trend. Combinations of components listed adjacent to one another in the classification scheme, for instance broad and striated flow, have an average transitional to fused interfaces ratio of 10 : 1, those once removed, for example broad and granular flow, one of 3 : 1 and those further removed, excluding

two exceptions, BF-CM in coke D1 and BF-MM in coke A1, have a ratio of 1 : 1. From this it may be concluded that well fusing components will form good interfaces with all other reactive components, but are influenced by the nature of that other components regarding the likeliness of formation of an interface of the transitional or fused type. Optically similar textural components appear to form transitional interfaces more readily, which may indicate that structurally similar carbon forms are to a greater extent capable of 'dissolving' into one another, whereas the interaction between dissimilar ones is confined to a narrow border region between the two components.

Cokes:	A 1	B 1	C 1	D 1	E 1	F 1
P(T) / P(Fu)						
BF-SF	MM 9.2	MM 7.2				
BF-GF	MM 4.4	MM 7.1	mM 4.6	mM 8.3*		
BF-CM	Mm 2.3*	Mm 1.3*		mM 14*		
BF-MM	Mm 8.0*	Mm 1.0*		mm 0.8*	mM 0.5*	
BF-FM						
BF-ISO						
SF-GF	MM 6.6	MM 7.2	MM 14.7	mM 13*		
SF-CM	Mm 2.3*	Mm 3.3*		mM 1.6*		
SF-MM						
SF-FM						
SF-ISO						
GF-CM	Mm 17*	Mm max*	MM 21.0	MM 11.7	mM max*	mm max*
GF-MM				Mm 1.8		mM 1.4*
GF-FM						
GF-ISO			Mm 0.2*	Mm 0.3*		
CM-MM				Mm 2.8	MM max	mM 6.0
CM-FM				Mm 1.4*		
CM-ISO				Mm 0.8*		
MM-FM				mm 5.3*	Mm 11.2	MM 12.9
MM-ISO					Mm 0.2*	Mm 0.5
FM-ISO				mm max*	Mm 1.4*	Mm 11.8

Table 4.4 Ratio of Transitional and Fused Interfaces between Reactive Components in Series 1

4.1.6 The Influence of Carbonisation Method

Tables 4.5 and 4.6 list the interface quality indices derived from the by-component counts on the series 2 samples. Comparing these to the interface indices obtained for the same component combinations from the first carbonisation series (tables 4.2 and 4.3) they are seen to be much lower. This is undoubtedly due to the difference in carbonisation methods used. As described in chapter 3, series 1 was carbonised simulating industrial conditions with the aim of producing a dense, strong coke comparable in physical properties to that used in blast furnaces. For series 2 restrictions in the amounts of maceral concentrates obtainable dictated a smaller scale process.

Nevertheless, considering the averages of all cokes of the IQI for reactive-reactive interfaces in the two series, a common ranking of component combinations can be arrived at. This is shown in table 4.7. There is only one exception to the common pattern, that of the fine mosaic - isotropic interface, which takes a very different place in the ranking for the two series. As it only occurs in significant amounts in one of the samples of the first series, whereas it is fairly common in the samples of the second series, it can be assumed that its ranking for the second series reflects its true position more accurately.

The interface qualities with isotropic material are worth commenting on from the point of view that for series 1 on the whole it was concluded that there is no evidence of optically similar components interfacing better than optically dissimilar ones. At first sight interfaces with isotropic material appear to contradict this, as the order of interface quality clearly follows that of component similarity.

The comparison in table 4.7 shows that the absolute values of the IQI strongly depend on the carbonisation conditions, but that nevertheless the differences between the individual textural components persist. Their relative contributions to the IQI appear to be independent of the carbonisation conditions, so that the variation of IQI between coals or coal blends of different textural compositions can be anticipated, even if the absolute numerical values cannot be estimated. To achieve a comprehensive model for the prediction of interface quality, factors accounting for carbonisation conditions, such as particle size, charge density, heating rate etc would have to be introduced. This would require the systematic investigation of the effect on interface quality of all variables involved in the carbonisation process.

Coke:	A2V	A2	A2I	B2V	B275	B2	B2I	C2V	C275	C2	C250	C2I
IQI _r												
GF-CM	14.00	32.00	max	33.00	max	50.00	max	max	max	39.00	39.00	max
GF-MM	max	17.00	max	24.00	max	max	max	24.00	max	6.00	max	5.50
GF-FM	0.79	(2.33)	5.00		0.83		1.43	1.22			1.07	(2)
GF-ISO	2.02	1.72	1.42	1.58	1.00	1.04	0.83	1.61	1.68	1.67	2.40	1.47
CM-MM									max			(max)
CM-FM					0.71			1.00			0.60	
CM-ISO		4.33		1.91	1.18	1.94	3.20	2.11	2.62	1.55	1.33	0.80
MM-FM	max	max	6.00	17.00	2.29	(max)	5.60	3.67	(max)	max	2.22	5.75
MM-ISO	3.33	4.67	1.17	1.45	1.17	2.86	1.17	1.28	1.36	0.87	0.77	1.56
FM-ISO	2.27	(6)	14.00		(1.5)		0.86	3.25			2.67	
Average	2.32	2.92	2.18	2.43	1.53	2.49	1.42	2.10	3.08	2.43	2.11	1.94
IQI _s												
GF	1.64	2.12	1.22	1.85	1.34	2.41	1.12	1.96	2.37	1.75	2.17	1.13
CM	2.78	1.64	2.00	1.46	1.57	2.25	1.81	1.98	3.05	2.10	2.14	1.21
MM	2.21	2.00	2.63	1.29	1.59	1.41	1.67	1.80	1.88	1.23	2.12	1.17
FM	1.20						0.75					(2)
ISO			(0.75)				0.00					(0.75)
Average	1.71	2.02	1.25	1.62	1.44	2.22	1.25	1.90	2.48	1.72	2.13	1.17
IQI _{II}												
GF	1.00	1.33	0.40	0.86	0.29	2.29	0.62	1.17	1.57	1.09	2.33	0.47
CM				(2.5)	(2)	1.83		(3)	3.75	1.00	0.89	(0.75)
MM		(0.8)		0.62	1.20	1.00	0.67	1.33	0.86	0.75	1.13	1.57
FM												
ISO												(0)
Average	0.55	1.23	0.45	0.81	0.73	1.64	0.65	1.50	1.74	0.86	1.29	0.63

Table 4.5 Interface Quality Indices from by-component Counts of Series 2.1

Coke:	AC37	BA25	BA37	BC25	BC37	BC50	CA25	CA37	CB25	CB37
IQI _r										
GF-CM	max	27.50	max	max	37.00	max	max	max	46.00	31.00
GF-MM	max	30.00	max	28.00	max	max	max	20.00	22.00	max
GF-FM	3.67		4.50	1.50	(3)	(max)	(7)	6.50	max	2.67
GF-ISO	1.54	0.94	1.40	1.34	0.94	1.68	1.79	1.67	1.19	1.08
CM-MM		(max)		(max)	max		(max)		(max)	
CM-FM				(7)			(3)		(2.5)	2.33
CM-ISO	2.60	1.19	0.89	3.92	2.07	1.27	1.76	3.83	1.36	1.44
MM-FM	max	max	19.00	6.50	14.00	18.00	8.50	16.00	5.00	4.50
MM-ISO	(1.33)	2.22	3.22	3.27	1.45	1.75	2.78	1.70	1.38	3.33
FM-ISO				0.40						
Average	2.20	2.08	2.74	2.87	2.20	2.92	2.75	2.81	2.20	1.97
IQI _s										
GF	1.78	1.35	1.69	2.02	1.75	2.16	2.12	1.83	1.68	1.75
CM	2.37	2.45	2.07	3.77	2.59	2.08	2.38	1.66	2.19	2.26
MM	1.47	2.37	1.96	5.08	2.28	1.60	2.20	1.46	2.04	1.90
FM						(0.14)		(2)		(2.5)
ISO	0.00									
Average	1.68	1.69	1.77	2.69	2.07	1.92	2.12	1.71	1.81	1.88
IQI _{II}										
GF	0.96	0.36	0.47	0.73	1.38	0.75	1.08	1.25	0.92	0.89
CM		1.17	2.40	1.75	1.67	2.00	2.33	(2.5)	1.37	1.33
MM	(1)	(1)	(2)	2.50	1.89	1.60				1.40
FM										
ISO	(0)									
Average	0.81	0.68	1.00	0.96	1.59	0.97	1.47	1.16	0.96	0.94

Table 4.6 Interface Quality Indices from by-component Counts of Series 2.2

Grouping	Component Combination	Average Interface Quality Index	
		S1	S2
Mosaic-Mosaic Mosaic-Flow (excl. FM)	CM-MM	max	max
	GF-CM	max	63.4
	GF-MM	max	31.9
	BF-CM	max	-
	BF-MM	max	-
	(FM-ISO	max	1.9)
R - FM	MM-FM	147.0	8.7
	GF-FM	-	2.8
	CM-FM	-	2.6
Flow-Flow	BF-SF	62.0	-
	SF-GF	46.1	-
	BF-GF	40.1	-
R-ISO	FM-ISO	max	1.9
	MM-ISO	15.7	1.8
	CM-ISO	-	1.8
	GF-ISO	2.0	1.4

Table 4.7 Ranking of the Average Interface Quality Indices for Reactive-Reactive Interfaces in Series S1 and S2

4.2 Statistical Appraisal of the Counting Methods

As the identification of coke components and interfaces was perceived as being very subjective, it was thought necessary to conduct an investigation into the reliability of the point counting method used. This should prove useful in judging whether a variation in component or interface distribution can be attributed to an actual difference between two samples or whether it may be within the limits of repeatability of the analysis method.

4.2.1 Mathematical Background

For the overall component and interface distribution, a binomial distribution is assumed in line with the work undertaken by Chandra [110] on evaluating the point counting method used for maceral analysis in coal petrography. The following mathematical treatment is taken from a statistical handbook by Chatfield [111]. The assumption of a binomial distribution is reasonable since the occurrence of components / interfaces can be described as a discrete random variable X of values x_1, x_2, \dots, x_n with probabilities p_1, p_2, \dots, p_n , the sum of which is 1 and none of which falls below 0. Also, with respect to any individual component / interface, two successive trials, i.e. the inspection of two successive points on the sample analysed, are independent and have two mutually exclusive possible outcomes, success, i.e. occurrence at that point, denoted by p and failure, i.e. non-occurrence, denoted by $(1-p)$. The probability of encountering r occurrences of a component \ interface $P(r)$ in n trials (i.e. points counted) is then given by

$$P(r) = {}^nC_r * p^r * (1-p)^{n-r} \quad (4.2.1)$$

$$\text{with } \sum_{r=0}^n {}^nC_r * p^r * (1-p)^{n-r} = 1$$

If n trials are made (points are counted) the true or theoretical mean μ will be given by

$$\mu = n * p \quad (4.2.2)$$

for which the observed mean \bar{x} will be an estimate of increasing accuracy as the number of trials increases.

In the general case the variance s^2 of any variable X is defined as

$$s^2 = \sum_{i=1}^N (x_i - \mu)^2 \cdot p_i \quad (4.2.3)$$

Substituting equations (4.2.1) and (4.2.2) into (4.2.3) gives

$$s^2 = \sum_{r=0}^n (r - n \cdot p)^2 \cdot {}^n C_r \cdot p^r \cdot (1-p)^{n-r}$$

which, after lengthy calculations, reduces to

$$s^2 = n \cdot p \cdot (1-p)$$

Thus the standard deviation is given by

$$s = [n \cdot p \cdot (1-p)]^{(1/2)} \quad (4.2.4)$$

Obviously the exact probability or proportion of p cannot be known, and the results of the analysis gives an approximation for p in the form of x / n , so that a confidence interval for p becomes of interest. This would be very tedious to calculate for the binomial distribution, but as n is large, it is reasonable to assume that the central limit theorem applies and that the normal distribution is a good approximation for values of p which are not too close to 0 or 1.

For the normal distribution the 95% confidence limit is given by

$$P (-1.96 < \{ (x' - \mu) / (s / (n)^{(1/2)}) \} < +1.96) = 0.95 \quad (4.2.5)$$

Substituting the theoretical mean and the standard deviation for the binomial distribution, equations (4.2.2) and (4.2.4), into the expression gives

$$p = x/n \pm 1.96 \cdot [(p \cdot (1-p) / n)]^{(1/2)} \quad (4.2.6)$$

This means that 95 % of the expected absolute errors (in %) should lie within $1.96 \cdot [(P \cdot (100 - P) / N)]^{(1/2)}$ of the counted percentage of the component or interface (P) for N points counted, if the errors were purely random fluctuations in

the component \ interface distribution. Obviously this is not the case, as the method offers much scope for operator error, and an estimate of the true 95 % confidence limit is to be arrived at by replacing 1.96 by a multiplication factor a . The expected absolute error (EAE) is then given as

$$\text{EAE} = a * [(P * (100 - P) / N)]^{(1/2)} \quad (4.2.7)$$

The actual absolute error (AAE) is calculated as the difference in percentage counted in two successive counts of the same magnitude C_1 and C_2

$$\text{AAE} = \text{ABS} (P_{C_1} - P_{C_2}) \quad (4.2.8)$$

To obtain an estimate of the true 95 % confidence limit the factor a is increased until less than 5 % of the actual errors exceed the expected errors. This estimates to what extent the results of the point counts are repeatable on the basis of half of the points counted, so that the a -value arrived at is used in equation (4.2.7) to calculate the errors expected for the entire count.

4.2.2 Errors in Component and Interface Counts

The calculations outlined above were used to estimate the factor a by which the standard deviations of the component and interface counts undertaken for this study need to be multiplied for 95 % of the data to fall within their limits.

The results for the component counts are given in table 4.8. As the ease with which different components can be identified is perceived as varying according to the number of other components which appear sufficiently similar to cause confusion, the above calculation was performed separately for each component as well for their entirety. There are indeed significant differences in the magnitude of errors between two counts for the different components. From the results in table 4.8 it seems that small inerts are least likely to be mistaken for any other component, followed by the larger domain flow types and large inerts. The counting data appears to be least reliable for fine mosaic and isotropic material, which in practise are perceived as very similar to one another.

Results for the interface counts are given in table 4.9. Regarding the interface counts, the added difficulty arises that three different counting methods were employed. Where data from different counting methods are compared the errors may therefore be not purely a measure of repeatability, but may also contain possible systematic variations due the differences in these methods. The results shown in table 4.9 support this insofar as the errors between sets arrived at by the same method and those between the

simple and split method are significantly smaller than those comparing them with the by-component method. This point is further investigated in the following section.

Component	Average Error (%)	a $(a*[P*(100-P)/N] (1/2))$
BF	1.5	4.5
SF	0.8	5.0
GF	4.9	7.5
CM	2.9	7.5
MM	3.7	7.5
FM	4.4	11.5
ISO	4.4	10.5
INS	1.5	3.5
INL	2.7	6.0
Total	2.7	7.5

Table 4.8 Average Errors and Multiplication Factor for 95 % Confidence Limit for Component Counts

Counting Method	Sample Series	Av. Error (%)	a $(a*[P*(100-P)/N] (1/2))$
Simple	S1	4.0	6.0
Simple / Split	S21	3.5	5.5
	S22	5.1	6.5
Split	S3	2.8	5.0
	Total	3.1	6.0
Simple /			
By-Component	S1	4.4	12.0
Av Simple Split /	S21	6.2	10.0
	S22	5.6	10.0
By-Component	Total	5.6	10.5

Table 4.9 Average Errors and Multiplication Factor for 95 % Confidence Limit for Interface Counts

Table 4.10 shows the 95 % confidence limits for the a-values listed in tables 4.8 and 4.9. They are further illustrated by figure 4.5 overleaf. The limits indicate a rather wide spread around the percentages counted, which must be taken into account when drawing conclusions from the results. Whereas the inaccuracy of the method should be of no great importance where clear trends are displayed by the data collected, care must be taken not to overestimate seemingly abnormal results. When the method of textural component analysis was first devised by Patrick et al [13] an error of 5 to 10 % was envisaged working with a magnification of $\times 1425$ and it was stressed that the emphasis should be placed on trends rather than absolute values. That error margin does in fact correspond well to the errors shown in table 4.10 for any component occurring with moderate frequency.

95 % Confidence Limit					
a =					
%	3.5	4.75	6	7.5	11
observed					
0-5	1.2	1.6	2.1	2.6	3.8
5-10	2.9	3.9	4.9	6.1	9.0
10-15	3.6	4.9	6.2	7.8	11.4
15-20	4.2	5.7	7.2	9.0	13.2
20-25	4.6	6.3	7.9	9.9	14.5
25-30	4.9	6.7	8.5	10.6	15.5
30-35	5.2	7.0	8.9	11.1	16.3
35-40	5.4	7.3	9.2	11.5	16.8
40-45	5.5	7.4	9.4	11.7	17.2
45-50	5.5	7.5	9.5	11.8	17.3
50-55	5.5	7.5	9.5	11.8	17.3
55-60	5.5	7.4	9.4	11.7	17.2
60-65	5.4	7.3	9.2	11.5	16.8
65-70	5.2	7.0	8.9	11.1	16.3
70-75	4.9	6.7	8.5	10.6	15.5
75-80	4.6	6.3	7.9	9.9	14.5

Table 4.10 95 % Confidence Limit for Component and Interface Counts

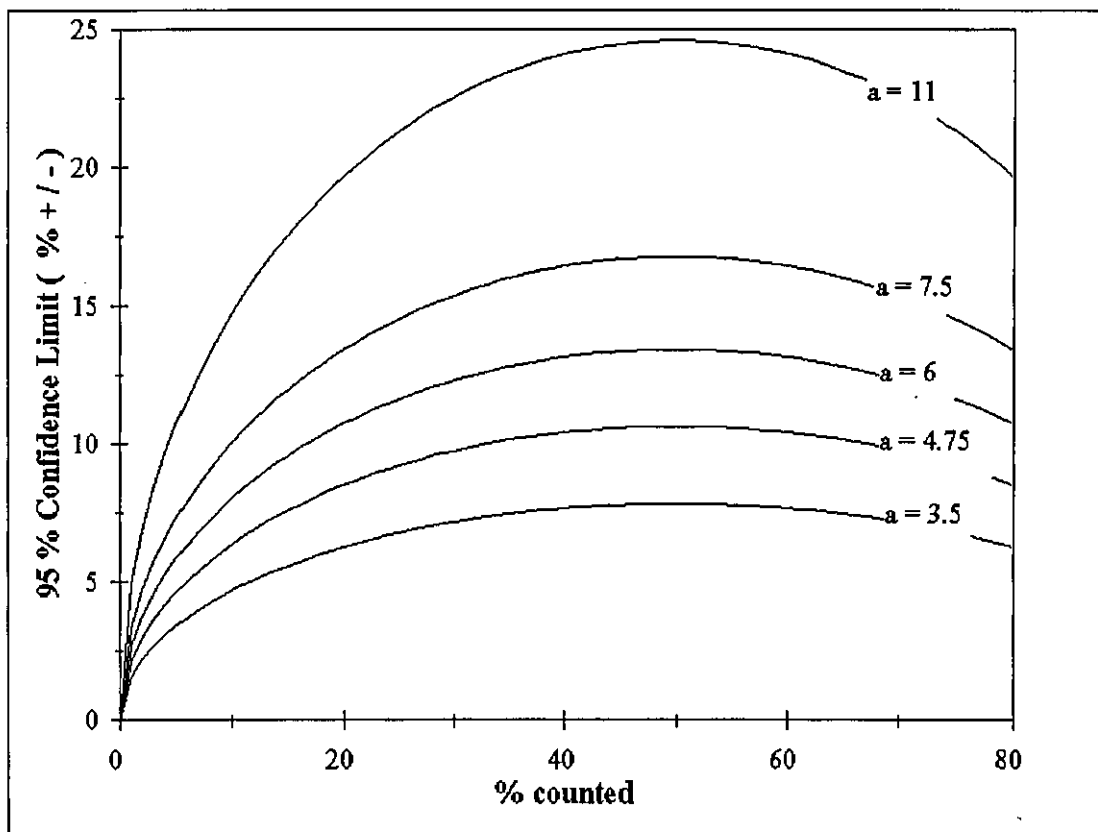


Figure 4.5 Illustration of the 95% Confidence Limits for Component and Interface Counts

4.2.3 Systematic Interface Distribution Errors due to Variations in the Counting Method

Table 4.11 compares the results from the simple and the by-component interface counts on sample series 1. It shows that, although the trend is not universal, the by-component count tends to give lower transitional and higher fused interface type percentages. Fissured and fused interfaces are equally counted lower and higher by the by-component method, so that in their case no systematic error appears to exist. From the first series it seems reasonable to assume that the overall interface quality, i.e. the ratio of 'good' to 'poor' interfaces, is repeatable using the two different counting methods, all be it with errors exceeding those incurred when the count is repeated using the same method.

		Simple	By-Component
A1	T	46.7	35.6
	FU	36.9	41.0
	FI	13.0	20.4
	UF	3.5	3.0
B1	T	37.5	34.7
	FU	50.1	45.6
	FI	10.9	17.2
	UF	1.5	1.9
C1	T	19.8	19.3
	FU	69.6	72.2
	FI	9.6	7.6
	UF	1.0	0.9
D1	T	23.7	14.8
	FU	70.0	80.3
	FI	5.8	4.4
	UF	0.5	0.5
E1	T	8.4	8.1
	FU	77.8	79.7
	FI	12.9	10.7
	UF	1.0	0.9
F1	T	38.1	19.9
	FU	54.6	72.4
	FI	6.6	7.7
	UF	0.7	0.0

Table 4.11 Comparison of the Interface Distributions in Series 1 counted by Simple and by By-Component Counts

There is however a shift from transitional to fused interfaces, the by-component count favouring the latter. It is difficult to find an explanation for this other than operator error. If the by-component count is assumed to be the more accurate method, by merit of the fact that it is a slow manual process and careful consideration has to be given to each interface regarding the identity of the adjacent components, transitional interfaces would be said to be overestimated by simple, and probably also split, counts. This can then only be explained by hasty, inaccurate decisions being made, judging by the overall impression of a change in the appearance of the reactive component, even though the transition is not the nearest interface to the cross-wire or is not actually taking place between two distinct identifiable components.

Table 4.12 shows the interface distributions for both sample sets of the second carbonisation series as the averages between the simple and split count and as the results from the by-component counts.

It can be seen that the percentage of transitional interfaces is universally counted lower for the by-component counts and that of fused interfaces higher. The effect is much more marked than for the first series, for a number of samples the percent of transitional interfaces counted by components is only about half that counted by the other methods. For the fissured interface type the picture is less clear, but particularly in sub-series S2.2 a slight tendency towards less fissured interfaces being counted using the by-component method was observed. The percentage of unfused interfaces observed in the by-component counts is universally lower.

Table 4.13 comparing the percentages of R-R, R-S and R-L type interfaces arrived at by the split and by the by-component count methods confirms the shift from transitional to fused interfaces by showing a corresponding difference in R-R and R-S type interfaces, the former being lower, the latter higher for the by-component counts for all samples. If the same transitional to fused interface type shift had not also been observed on Series 1, this would indicate that counting all interfaces in a given field of view favours interfaces with small inerts, which are more evenly distributed throughout the coke and of which, due to their small size, the possibility of observing more than one in any field of view must be much larger. Obviously this is not the sole explanation, but counting all interfaces in a field of view certainly exacerbates the existing systematic error between the counting methods.

Care must therefore be taken when interface distributions arrived at by different counting methods are considered. Ideally, only the specific aspects targeted by the method used should be considered and comparisons of absolute values, rather than trends in interfacial behaviour, should be avoided.

	Average of Simple and Split Count				By-Component Count			
	%				%			
	T	FU	FI	Uf	T	FU	FI	Uf
A2V	31.4	42.5	24.4	1.7	12.9	51.6	34.6	0.9
A2	26.5	45.3	26.9	1.3	13.6	54.9	31.1	0.4
A2I	23.5	31.7	42.5	2.3	17.5	39.8	41.2	1.4
B2V	24.6	33.4	40.8	1.2	15.8	48.3	35.7	0.3
B2 75	22.2	42.3	34.5	1.0	11.4	47.5	40.9	0.2
B2	21.0	44.4	33.4	1.2	10.1	58.5	30.9	0.4
B2I	21.6	28.7	47.0	2.7	12.9	42.3	44.4	0.3
C2V	22.0	46.7	30.2	1.1	13.4	53.0	33.3	0.3
C2 75	22.8	47.4	28.9	0.9	15.3	57.3	27.2	0.2
C2	21.2	45.1	32.4	1.3	9.7	54.8	34.9	0.6
C2 50	7.4	23.7	17.5	1.4	10.2	57.3	31.7	0.9
C2I	23.6	36.7	37.3	2.4	12.8	43.3	43.5	0.3
AB37	21.7	44.3	32.4	1.6	11.7	56.8	30.8	0.7
AC37	18.5	42.6	37.5	1.4	13.4	50.2	35.8	0.5
BA25	25.7	27.1	45.2	2.0	18.0	45.4	36.1	0.4
BA37	23.9	39.6	34.5	2.0	11.8	54.0	33.7	0.5
BC25	25.2	42.8	30.9	1.1	18.7	53.3	27.5	0.5
BC37	20.2	45.7	32.4	1.7	13.1	54.3	32.3	0.3
BC50	18.0	45.5	34.6	1.9	12.5	54.1	32.4	1.0
CA25	25.7	46.8	26.3	1.2	14.4	55.6	29.6	0.4
CA37	22.5	41.4	33.6	2.5	16.1	50.3	33.3	0.3
CB25	21.6	42.6	33.6	2.2	15.7	49.3	34.3	0.7
CB37	21.8	43.5	32.6	2.1	10.2	54.5	34.9	0.4

Table 4.12 Comparison of the Interface Distributions in Series 2 counted by Simple / Split Counts and by By-Component Counts

	Split Count			By-Component Count		
	%			%		
	R-R	R-S	R-L	R-R	R-S	R-L
S 2.1						
A2V	51.4	42.4	6.2	32.8	65.4	1.8
A2	51.6	42.2	6.2	29.3	66.0	4.6
A2I	45.4	45.0	9.6	29.1	67.5	3.3
B2V	52.6	43.6	3.8	31.9	63.1	5.0
B2 75	51.6	43.0	5.4	31.4	64.5	4.0
B2	37.6	50.8	11.6	25.4	68.6	6.0
B2I	45.4	48.2	6.4	34.5	59.6	5.9
C2V	56.6	37.2	6.2	43.1	53.3	3.6
C2 75	52.8	40.2	7.0	33.0	61.5	5.5
C2	43.2	47.6	9.2	24.3	68.7	7.0
C2 50	41.4	47.8	10.8	30.2	64.0	5.8
C2I	48.8	41.6	9.6	30.3	62.0	7.7
S 2.2						
AB37	46.2	42.8	11.0	28.1	65.7	6.2
AC37	44.6	46.8	8.6	30.0	63.0	7.0
BA25	48.2	45.6	6.2	37.1	59.0	3.9
BA37	42.8	45.6	11.6	26.5	68.2	5.3
BC25	53.4	37.6	9.0	42.1	52.6	5.3
BC37	46.8	40.8	12.4	31.6	60.7	7.7
BC50	40.8	45.2	14.0	27.1	65.3	7.6
CA25	52.2	34.0	13.8	38.6	56.9	4.5
CA37	45.2	42.0	12.8	33.8	60.5	5.6
CB25	49.4	40.2	10.4	38.0	56.7	5.4
CB37	47.0	41.2	11.8	29.6	63.6	6.8

Table 4.13 Comparison of the Percentage of Reactive -Reactive, Reactive - Small - Inerts and Reactive -Large Inerts counted by Split and by By-Component Counts

4.3 Binding Power Hypothesis

Having established a relation between coke component interfaces and coal rank in section 4.1, one of the objectives of this work becomes to elucidate the nature of that relationship. At the extremes two possibilities can be envisaged. There may be direct link between component and interface distribution such that the interfacial behaviour of each component is an invariable characteristic of the same and the overall interface distribution can be predicted from the component distribution. Alternatively, the interfacial behaviour of a component could vary according to its origin and frequency of occurrence, so that it would be a function of some bulk property of the coal or blend carbonised and could be predicted from this.

4.3.1 Formulation of the Binding Power Hypothesis

The hypothesis to be tested here is based on the assumption that the interface type distribution is a function of the textural component distribution. It is proposed that there is a characteristic property of each component which shall be referred to as 'binding power' (BP) and defined as the theoretical, imaginary interface quality index (IQI), given by equation 4.1.1, based on the probabilities of the component forming each of the interface types irrespective of which other component it interfaces with and independent of the origin of the coke. For any component C it would thus be defined as

$$BP_c = \frac{P(T_c) + P(Fuc)}{P(Fic) + P(Ufc)} \quad (4.3.1)$$

where $P(T_c)$, $P(Fuc)$, $P(Fic)$, $P(Ufc)$ are the probabilities with which the component C participates in the respective interface type

The BP would take on a value of zero for a truly inert component and tend to infinity for a highly fusible one.

Considering any component C and any interface type I (where $I = T, Fu, Fi$ or Uf) the probability of it interfacing with itself and forming the interface type I is given by

$$I_c = P(I_c) * P(I_c) = [P(I_c)]^2$$

so that

$$P(I_c) = \sqrt{I_c} \quad (4.3.2)$$

In a single component system the square roots of the interface type frequencies would thus enable the binding power of that one component to be calculated by simple substitution into equation 4.3.1. But in a real coke the majority of interfaces occur between different components.

Considering now two distinct components A and B, the probability of A and B interfacing with the interface type *I* is

$$I_{ab} = P(I_a) * P(I_b)$$

which, substituting equation (4.3.2), gives

$$I_{ab} = \sqrt{I_a * I_b} \quad (4.3.3)$$

This leads to a rather complex system of equations, when considering nine different components interfacing with one another. Thus the hypothesis can only be tested indirectly or binding powers be approximated by making further, simplifying assumptions.

4.3.2 Testing of the Binding Power Hypothesis

To test the binding power hypothesis it is assumed that inerts are least likely to vary in their fusibility. The probabilities with which they participate in specific interface types, *I_s* and *I_l*, are thus chosen to be constant.

Considering any reactive component *R* interfacing with small inerts *S* and large inerts *L*, the probabilities of the interfaces taking any interface type *I* in accordance with equation 4.3.3 is given by

$$I_{rs} = \sqrt{I_r * I_s} \quad (4.3.5)$$

$$I_{rl} = \sqrt{I_r * I_l} \quad (4.3.6)$$

Equations (4.3.5) and (4.3.6) can be re-arranged to read

$$I_s = (I_{rs})^2 / I_r \quad (4.3.5.a)$$

$$I_l = (I_{rl})^2 / I_r \quad (4.3.6.a)$$

As *I_s* and *I_l* were assumed to be constant their ratio *R* = *I_s* / *I_l* should also be constant, so that the ratios of the squares of the percentages of each interface type, *T*, *Fu*, *Fi* and

Uf, for each reactive component R, from BF to ISO, should also be constant, if the hypothesis of characteristic binding powers holds true. Mathematically this is expressed as

$$\frac{(T \text{ BF } s)^2}{(T \text{ BF } l)^2} = \frac{(T \text{ SF } s)^2}{(T \text{ SF } l)^2} = \dots\dots\dots = \frac{(T \text{ ISO } s)^2}{(T \text{ ISO } l)^2} \quad (4.3.7)$$

for the example of transitional interfaces.

The results from calculating the ratios for series 1 in accordance with equation 4.3.7 are shown in table 4.14.

Due to the rarity of interfaces involving minor components, data is only available for a few component combinations per coke. Only interface combinations occurring at a number greater than 10, equivalent to 1% of the total counted, or those that could be made up to that number by selective individual counts (indicated by * in table 4.14), were considered to be statistically significant enough to be taken into account. Even for the remaining combinations little data is available for transitional and unfused interfaces, which are uncommon for reactive - inert interfaces, so that in most cases none of them were observed for either of the inert sizes. With some exceptions, such as coarse mosaic in coke A1, granular flow in D1 and fine mosaic in F1, the interface ratios for the components considered in each coke show little variation. Thus, although the data obtained must be considered insufficient to conclusively prove the binding power hypothesis, it certainly does not contradict the it .

		$(I_{cs})^2 / (I_{cl})^2$			
		T	FU	FI	UF
A 1	BF	-	0.4	1.3	-
	SF	-	0.6	1.4	-
	GF	-	1.0	1.3	0.6
	CM *	-	0.7	3.2	-
	MM *	-	0.6	1.3	-
B 1	BF	0.0	2.0	0.4	0.6
	SF	-	1.6	0.5	-
	GF	-	1.4	0.4	-
C 1	GF	0.0	1.2	0.4	0.4
	CM	-	1.0	-	-
D 1	GF	0.0	1.1	3.0	-
	CM	-	1.2	1.2	-
	MM	-	1.1	-	-
E 1	BF *	0.5	0.9	-	-
	GF *	0.2	1.5	0.3	-
	CM	-	1.3	0.6	-
	MM	0.0	1.3	0.7	0.2
F 1	GF *	0.2	2.0	0.0	-
	CM	-	1.3	0.0	-
	MM	-	1.5	0.2	-
	FM	-	1.4	5.9	-

Table 4.14 Ratio of the Squares of the Interface Types formed with Small and Large Inerts in Series 1

4.3.3 Estimation of the Component Binding Powers

As some evidence to support the binding power hypothesis could be gathered in the previous section, it was attempted to estimate the binding powers of the components from the interface distributions obtained by the by-component counts on the first series.

Taking the any interface type between two components A and B, I_{ab} , and the same interface type for each component interfacing with small and large inerts, I_{as} , I_{al} , I_{bs} and I_{bl} , a set of five equations is obtained from equations 4.3.3, 4.3.5 and 4.3.6.

These can be related in such a way as to enable I_s and I_l to be calculated from any two components which form the interface type concerned in sufficiently great numbers from

$$I_s = \sqrt{[(I_{as}^2 * I_{bs}^2) / I_{ab}^2]} \quad (4.3.8)$$

$$I_l = \sqrt{[(I_{al}^2 * I_{bl}^2) / I_{ab}^2]} \quad (4.3.9)$$

For any reactive component averages of I_s and I_l for all component combinations it occurs in can then be back-substituted into equations 4.3.5 and 4.3.6 to obtain two estimates for any interface, one based on I_s , the other on I_l . The averages of the two estimates, which are shown in table 4.15, are then taken and their square roots are substituted into equation 4.3.1 to obtain estimates of the component binding powers, also given in table 4.15.

It appears that the binding powers vary substantially between the components with a clear division between larger domain flow types (broad and striated) and mosaics, excluding fine mosaic. Granular flow, in keeping with its intermediate optical appearance between flow and mosaic type components, has a binding power intermediate between the two. The magnitude of the differences in binding power between the components is appreciated better by the graphical depiction in figure 4.6. For isotropic material it is impossible to calculate its binding power, as the values for fissured and unfused interfaces are too close to zero to be used.

	P (T)	P (Fu)	P (Fi)	P (Uf)	Binding Power
S	2.98*E-4	6.85	219.8	0.24	0.17
L	16.05*E-4	5.21	901.2	6.55	0.07
BF	0.52	0.05	3.33*E-4	0.0013	7.15
SF	0.85	0.06	3.93*E-4	0.003	15.66
GF	0.80	0.12	0.40*E-4	0.69*E-4	84.46
CM	0.95	0.13	0.12*E-4	0.15*E-4	174.90
MM	1.26	0.13	0.20*E-4	0.07*E-4	194.26
FM	0.67	0.08	0.68*E-4	0	40.11
ISO	0.33	5.77	0	0	-

Table 4.15 Estimated Component Binding Powers

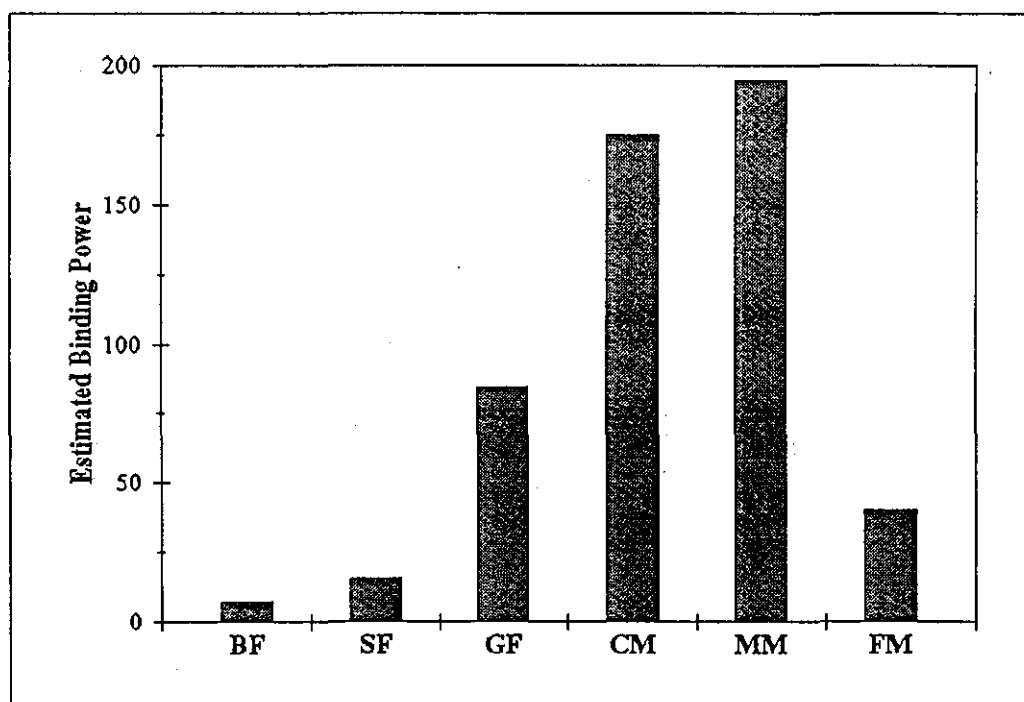


Figure 4.6 Estimated Component Binding Powers

4.3.4 Prediction of the Interface Quality Indices for Series 2

For the purpose of testing the binding power theory, the estimates for the component binding powers shown in table 4.15 were used to predict the interface quality indices for reactive-inert interfaces in series 2. Reactive-inert interfaces were chosen because they occur with greater frequency and more reliable averages than can be obtained for the interfaces of reactive-reactive component combinations. Interface quality indices for the individual component combinations were calculated from the sums of each interface types for all samples listed in tables 4.5 and 4.6. Table 4.16 compares the average counted IQI for both inert sizes with the corresponding predicted IQI. It shows that in spite of the differences in absolute values the trends expected from the binding power theory are met for interfaces with inerts. The similarity of the trends between the predicted and counted interface qualities is more easily appreciated from figures 4.7 and 4.8. The difference in absolute values is very much in line with the observations made regarding the influence of carbonisation method in section 4.1.6. Thus binding power, like the interface quality index it is derived from, is only a useful concept in comparing cokes produced under the same conditions. This means that the hypothesis of a characteristic binding power for each component does not hold true insofar as it appears to be influenced by variables appertaining to the carbonisation method used.

	Predicted	Counted
IQIs		
CM	17.8	2.14
MM	14.1	1.81
GF	9.1	1.76
FM	6.1	0.80
IQII		
CM	7.3	1.71
MM	5.9	1.21
GF	3.8	0.88
FM	2.7	0.66

Table 4.16 Predicted and Counted Interface Quality Indices for Inerts in Series 2

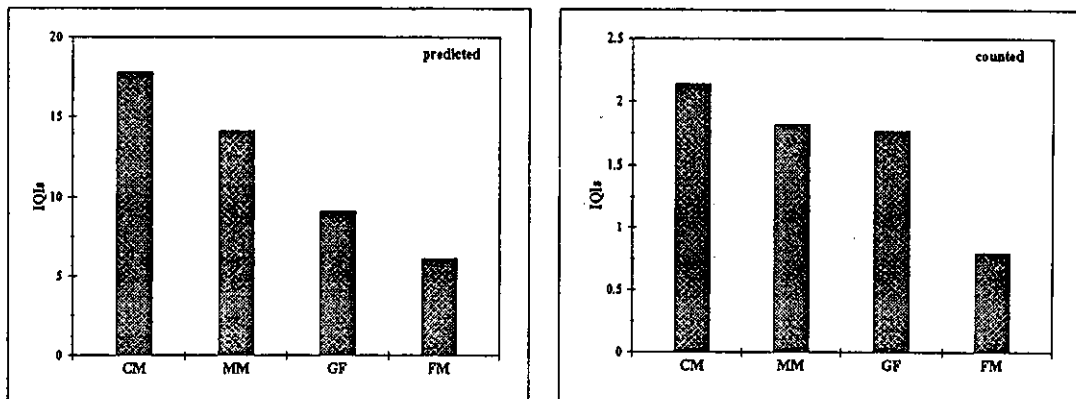


Figure 4.7 Predicted and Counted Interface Quality with Small Inerts in Series 2

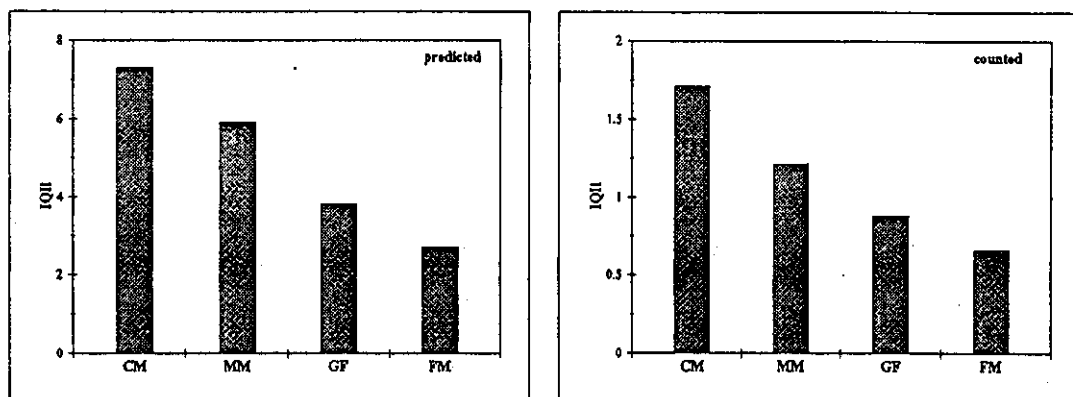


Figure 4.8 Predicted and Counted Interface Quality with Large Inerts in Series 2

4.4 Component Size Modelling

The impact of a component on the interface quality of the coke as a whole will depend on the number of interfaces it is involved in, as well as its actual ability to fuse with other components. The number of interfaces formed by a component will be a function of its surface area available for interfacing. Only if it is thought that there is a characteristic unit size and shape for each component identical in all cokes will this be directly proportional to the volume percent of the component counted. Otherwise it could be argued that the contribution of a component to the IQIt will also depend on the variation of its surface area to volume ratio, introducing an additional variable, which would complicate any model devised to predict interface quality. The size of reactive components has not been assessed experimentally, as it is complicated by several difficulties, particularly by their irregular shapes. This section describes an attempt to estimate the sizes of the textural components from the data obtained from the first carbonisation series.

4.4.1 Interface Participation and Component Size

If all components occur with equal unit sizes and shapes, are randomly distributed throughout the coke matrix and equally likely to interface with one another, then there should be a relation between the combined volume percent of two components and the number of interfaces they share. The most likely physical parameter determining the number of interfaces between two components under these conditions would be the combined surface area of the two components available for interfacing. This will be a function of their combined volumes. The ratio of the number of interfaces to the sum of the volumes of the participating components has therefore been calculated for the first series of cokes. The results are listed in table 4.17. In spite of large variations between the values for certain combinations in different cokes, the averages of all cokes do yield some interesting information. The most striking difference is found between the average number of interfaces per unit volume for small and large inerts. The ratios for small inerts mostly range between 2 and 5, whereas those for large inerts all lie below 1. As the two categories of inerts in any one coke can be assumed to resemble one another in all aspects other than size, this clearly proves the importance of the surface area to volume ratio, which obviously decreases with increasing unit size. Or, more precisely, for a given volume percentage for a smaller unit size a larger surface area is available for interfacing, so that a small component would be expected to participate in more interfaces.

	Number of Interfaces / Sum of Components (% vol)						Average
	A 1	B 1	C 1	D 1	E 1	F 1	
R-R							
BF-SF	3.1	3.2	0.7			1.3	2.1
BF-GF	2.9	2.3	0.8	0.2	0.2	0.6	1.2
BF-CM	0.2	0.1		0.0	0.1		0.1
BF-MM	0.0				0.2	0.1	0.1
BF-FM		0.1					0.1
BF-ISO							-
SF-GF	2.4	2.2	1.7	0.4			1.7
SF-CM	0.1	0.1		0.1			0.1
SF-MM		0.1		0.1			0.1
SF-FM	0.1						0.1
SF-ISO							-
GF-CM	0.1	0.0	0.3	1.2	0.2	0.3	0.4
GF-MM			0.1	0.2	0.0	0.1	0.1
GF-FM			0.0	0.1			0.1
GF-ISO	0.0			0.0			0.0
CM-MM			0.1	0.8	0.2	0.5	0.4
CM-FM			0.1	0.0			0.1
CM-ISO							-
MM-FM				0.2	0.8	1.5	0.8
MM-ISO					0.1	0.9	0.5
FM-ISO					1.8	1.5	1.7
R-S							
BF	4.0	7.5	3.6	0.3		0.1	3.1
SF	2.7	3.7	4.0	0.8			2.8
GF	7.3	3.6	8.0	7.7	1.6	2.4	5.1
CM	0.5		1.7	7.3	5.2	5.1	4.8
MM			0.4	1.9	9.2	9.2	5.2
FM					2.2	1.5	1.9
R-L							
BF	0.9	2.3	0.2			0.1	0.9
SF	0.3	1.0	0.4	0.1			0.5
GF	1.5	1.1	2.2	1.1	0.4	0.4	1.1
CM	0.5	0.1	0.8	1.3	1.0	1.2	0.8
MM	0.1		0.2	1.2	1.3	2.7	1.1
FM				0.2	0.4	0.8	0.5

Table 4.17 Ratio of the Number of Interfaces to the Sum of the Volume Percent of the Interfacing Components (Series 1)

It is also worth noting that the variation of the interface to volume ratios amongst the different reactive components is analogous for the two inert sizes, i.e. they follow the same pattern, but with the absolute values differing by a factor of roughly 4.5. This indicates that either there also is a specific unit size for each reactive component or a characteristic ability or inclination to incorporate inerts.

Contemplating the reactive - reactive interface combinations, the first impression is that of much higher interface to volume ratios for flow type interfaces than for flow-mosaic and mosaic type ones, with the exceptions of MM-FM, MM-ISO and FM-ISO. If this was attributed to size only, it would indicate that mosaic components are at least equivalent in size to large inerts, whereas flow type components would fall into the size range between the two inert sizes. The fact that mosaic components only combinations take higher values than flow-mosaic ones contradicts this. The opposite would be expected if size was the only determining factor.

Viewing the results under the aspect of component similarity shows that all of the higher ratios (> 0.4) occur for components which are adjacent or once removed on the classification scheme. A tendency of similar components favouring interfaces with one another can therefore be concluded. This would, for example, mean that the probability of an area of broad flow interfacing with an area of striated flow would be larger than that of it interfacing with one of fine mosaic, even if the two offered identical surface areas available for interfacing. Obviously it is difficult, if not impossible, to prove such a tendency, as the components are not randomly distributed, but are subject to prior associations.

4.4.2 Mathematics of the Component Size Model

Since the size of the component units is likely to be one of the factors, though by no means the only one, governing the frequency of interfaces involving different component combinations, a more thorough investigation of the variation of unit size between the components was undertaken. The component sizes cannot easily be measured. They have therefore been estimated using a simple mathematical model. The model is based on the assumption that the probability of an interface occurring between two components is directly proportional to their combined surface areas available for interfacing. It is assumed that all components and pores, C_n , are cubic units of characteristic side lengths a_n . The component volume V_n , which can be obtained from the component counts, can then be used to calculate the component surface area S_n from :

$$V_n = N_n * a_n^3 \quad (4.4.1)$$

$$S_n = 6 * N_n * a_n^2 \quad (4.4.2)$$

where N_n = number of units of the component C_n

Hence,

$$S_n = 6 * V_n / a_n \quad (4.4.3)$$

The total surface area of components in a coke, ST , is given by

$$ST = \sum S_n \quad (4.4.4)$$

and the area fraction, A_n , for each component can be calculated as

$$A_n = S_n / ST \quad (4.4.5)$$

It is also useful to define the total area fraction of 'reactive' components A_r

$$A_r = \sum A_n \quad \text{for } n = BF \dots ISO \quad (4.4.6)$$

Using the area fractions, interface probabilities can now be calculated.

The probability of any two different components A and B interfacing, assuming that no preferential association of certain components occurs, is given by

$$P_{AB} = 2 * A_A * A_B \quad (4.4.7)$$

A special case of equation 4.4.7 is the probability of a unit of a component A interfacing with a unit of the same component, which is given by

$$P_{AA} = A_A^2 \quad (4.4.8)$$

The probability of single component interfaces for reactive components P_c is therefore

$$P_c = \sum (A_n^2) \quad \text{for } n = BF \dots ISO \quad (4.4.9)$$

Inert - inert interfaces, although supposed to be non-existent on the basis of empirical observations, have a theoretical total probability P_{ii} given by

$$P_{ii} = A_s^2 + 2 * A_s * A_l + A_l^2 \quad (4.4.10)$$

From equation 4.4.7 the probability P_{cr} of a reactive component C interfacing with any other dissimilar reactive components R is

$$P_{cr} = 2 * A_c * (A_r - A_c) \quad (4.4.11)$$

The sum of P_{cr} for all reactive components gives the total probability for reactive - reactive interfaces P_r

$$P_r = 2 * [A_r^2 - \sum (A_n^2)] \quad \text{for } n = BF \dots ISO \quad (4.4.12)$$

The probabilities of interfaces between a reactive component C and a small or large inert, S or L, are

$$P_{cs} = 2 * A_c * A_s \quad (4.4.13)$$

$$P_{cl} = 2 * A_c * A_l \quad (4.4.14)$$

The sums of equations 4.4.13 and 4.4.14 for all reactive components again yield the probability of reactive - small inert interfaces P_s and of reactive - large inert interfaces P_l , i.e.

$$P_s = 2 * A_r * A_s \quad (4.4.15)$$

$$P_l = 2 * A_r * A_l \quad (4.4.16)$$

The probability of any component C being bordered by a pore P is

$$P_{cp} = 2 * A_c * A_p \quad (4.4.17)$$

and hence the total probability of interfaces with pores P_p is

$$P_p = 2 * (A_r + A_s + A_l) * A_p \quad (4.4.18)$$

4.4.3 Calculation of Component Sizes for Series 1

From the by-component interface counts, the relative proportions of interfaces with dissimilar reactive components and with inerts are known for each reactive component in the cokes of series 1. Their ratios can be equated to those from the probability model in order to estimate the component unit side length.

This is done using the side length of units of the small inerts as a universal basic unit, assuming that it is most likely to be constant for all cokes and the easiest to measure in practice.

For each coke the proportions of interfaces with small and large inerts are selected for all reactive components for which they occur for both inert sizes. They are then equated to P_{cs} and P_{cl} as defined by equations 4.4.13 and 4.4.14. From the ratio of interfaces of each component C with small and large inerts, the unit side length ratio of small and large inert sizes, a_s / a_l , can then be calculated:

$$a_s / a_l = (V_s / V_l) * (P_{cl} / P_{cs}) \quad (4.4.19)$$

The average ratio is then calculated for all components of each coke.

Choosing any value for a_s , a_s and a_l can then be substituted back into the formulae for P_{cs} and P_{cl} to obtain two estimates for the reactive component side length a_c , a_{cs} and a_{cl} , based on small and large inert side length

$$a_{cs} / X = (V_c * V_s) / (P_{cs} * a_s) \quad (4.4.20.a)$$

$$a_{cl} / X = (V_c * V_l) / (P_{cl} * a_l) \quad (4.4.20.b)$$

$$\text{where } X = 72 / (ST)^2$$

Substituting these estimates into all expressions for individual reactive-reactive interfaces between any two components, A and B , occurring in the coke considered yields

$$a_{Bs} = (X / a_{As}) * ((V_A * V_B) / P_{AB}) \quad (4.4.21.a)$$

$$a_{Bl} = (X / a_{Al}) * ((V_A * V_B) / P_{AB}) \quad (4.4.21.b)$$

The average of all these estimates has been calculated for each component occurring in the coke considered taking the small inert side length as 10 μm , which seems a realistic estimate from the observations made during counting. The results are summarized in table 4.18.a.

Estimated Component Side Length (μm)							
	A 1	B 1	C 1	D 1	E 1	F 1	Average
BF	39	33	26	-	82	27	41
SF	84	38	69	129	-	-	80
GF	69	55	74	123	1631	162	352
CM	215	450	180	132	300	39	219
MM	270	230	50	146	752	118	261
FM	36	70	39	144	112	116	86
ISO	274	-	-	225	74	43	154
Average	141	146	73	150	492	84	
INL	50	50	73	40	66	24	51

Table 4.18.a First Estimates for Component Unit Side Length

From table 4.18.a it can be seen that the component side length estimates vary widely for the different components in each coke as well as for any one component between the cokes. But with a few exceptions it would be fair to say though that the variations between the components, rather than between the cokes, are more marked and more systematic, so that it can be considered more likely that there is a characteristic size for each component, rather than a coke specific component size. A clearer picture of this emerges on discounting the results for components which occur with a small volume percentage only ($< 5\%$), which would be statistically unreliable, and for coke E1, the unexpected behaviour of which has already been shown in figure 4.3. Table 4.18.b shows the results thus edited.

Flow type components and isotropic material appear to occur in rather smaller units than mosaic ones. The average component size increases from broad flow to coarse mosaic, where it peaks and then falls.

	Estimated Component Side Length (μm)					Average
	A 1	B 1	C 1	D 1	F 1	
BF	39	33				36
SF	84	38	69			64
GF	69	55	74	123		80
CM			180	132		156
MM				146	118	132
FM					116	116
ISO					43	43

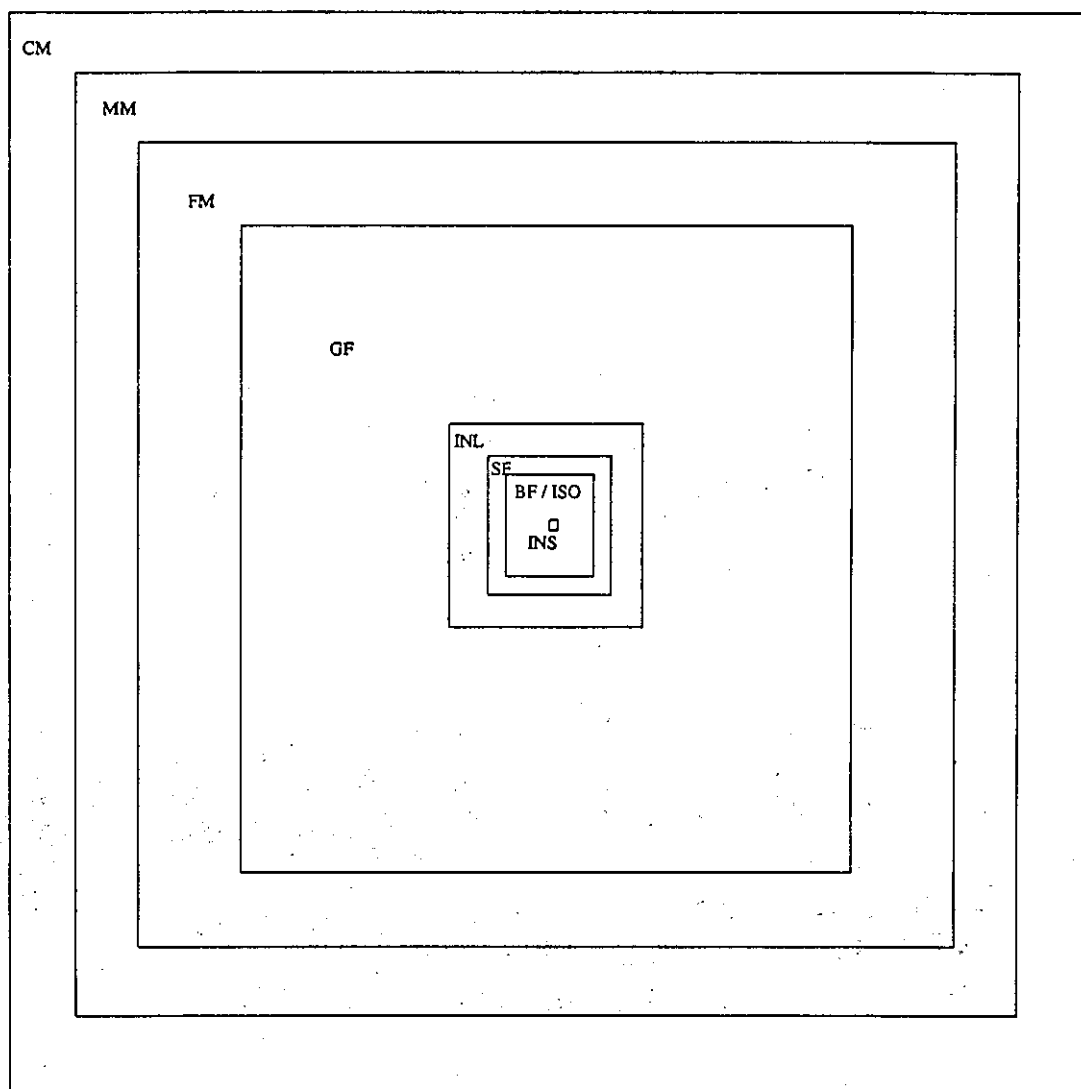
Table 4.18.b Edited Estimates for Component Unit Side Length

The average component side length from table 4.18.b were then used as the first estimates for an iterative process attempting to minimize the errors between the counted and calculated data. The ratios of the number of interfaces between dissimilar reactive-reactive components, reactive components and small inerts and between reactive components and large inerts were calculated from the side length estimates. The input was modified until the closest possible match to the counted data was achieved. The final estimates from this process are shown in table 4.18.c.

Final Estimates for Component Side Length (μm)	
BF	25
SF	30
GF	130
CM	230
MM	210
FM	180
ISO	25
INS	5
INL	40

Table 4.18.c Final Estimates for Component Unit Side Length

It was found that inert sizes needed to be decreased to account for the large numbers of reactive-inert interfaces. Also, in balancing the errors for the percentages of reactive-reactive interfaces between the cokes, the size difference between two sets of components needed to be accentuated. It appears there is a 'small size' group comprising broad and striated flow and isotropic material and a 'large size' one comprising granular flow and mosaics. This division, as well as the scale of unit size difference between the individual components, is more clearly illustrated by the squares drawn in figure 4.9 representing the estimated component units.



1 cm : 15 μ m

Figure 4.9 Illustration of the Estimated Component Unit Sizes

4.4.4 Estimation of Pore- and Single Component Interfaces

The final estimates for the component unit side length as shown in table 4.18.c are substituted back into equations for single component interfaces P_c (4.4.9), inert-inert interfaces P_{ii} (4.4.10), dissimilar reactive component interfaces P_r (4.4.12), interfaces with small inerts P_s (4.4.15), large inerts P_l (4.4.16) and pores P_p (4.4.18). The percentages of the different interface combinations are then calculated and shown in table 4.19.a.

	Calculated Interface Combination Percentages					
	P_c	P_r	P_s	P_l	P_{ii}	P_p
A1	3	10	9	4	5	68
B1	3	9	13	3	8	66
C1	1	4	9	3	10	72
D1	1	3	8	1	9	78
E1	1	2	9	2	12	75
F1	1	2	8	1	15	74

Table 4.19.a All Interface Combination Percentages Calculated from the Final Component Side Length Estimates

Two points are worth noting about the estimates in table 4.19.a. The first is the dominance of pore interfaces, which make up between roughly 65 and 80 % of all interfaces. They are obviously irrelevant for interface quality assessment, but due to being so dominant in numbers will make any model predicting interface frequency difficult to achieve. The largest part of the surface area of any component will be taken up by bordering pores, so that a model will be highly sensitive to variations in pore volume and pore size distribution. Furthermore, the possibility that some components may be more porous than others, or include pores of different sizes, will become highly significant and lead to large distortions. The second point is that of the high theoretical frequency of inert-inert interfaces. The failure of inerts to interface with one another, be it due to an inability to adhere to one another or due to their pre-existing distribution in the coke matrix forming material, can be envisaged at the extreme of a behaviour in which certain combinations are naturally favoured over other, equally probable, ones. The large percentage of theoretically occurring inert-

inert interfaces is then an indication of the scope such behaviour may have of interfering with the task of predicting interface combinations.

Discounting interfaces between inerts and with pores as in table 4.19.b allows an indication of the percentage of 'invisible' interfaces between units of the same reactive component to be obtained.

	Calculated Interface Combination Percentages			
	Pc	Pr	Ps	Pl
A1	11	39	36	14
B1	9	34	46	10
C1	7	25	53	16
D1	6	23	62	9
E1	7	18	63	11
F1	4	16	72	8

Table 4.19.b Interface Combination Percentages Calculated from the Final Component Side Length Estimates Excepting Inert-Inert and Pore Interfaces

The percentage of single component interfaces Pc varies in proportion to the interfaces between dissimilar reactive components Pr. In other words, if Pc and Pr were considered as the total of reactive-reactive interfaces, Pc would consistently account for 20 - 30 % of them. Assuming Pc interfaces to be good, in line with dissimilar reactive-reactive interfaces, the failure to include interfaces between identical component units underestimates the coke IQIt. But provided the reactive-inert component ratio does not vary excessively, the errors are comparable for all cokes and the overall trends are unaffected.

4.4.5 Prediction of Interface Combinations in Series 2 from the Component Size Model

As a test of the model and the component side length estimates an attempt was made to calculate the percentages of R-R, R-S and R-L interfaces of the samples in both sets of the second carbonisation series from their component compositions. The predicted and counted percentages are compared in table 4.20.

	Predicted			Counted		
	R-R	R-S	R-L	R-R	R-S	R-L
S 2.1						
A2V	22	60	18	33	65	2
A2	22	66	12	29	66	5
A2I	16	69	15	29	68	3
B2V	21	69	10	32	63	5
B2 75	20	71	9	31	65	4
B2	17	74	9	25	67	6
B2I	18	68	14	35	60	6
C2V	21	65	14	43	53	4
C2 75	20	68	12	33	62	5
C2	14	74	11	24	69	7
C2 50	18	70	12	30	64	6
C2I	17	68	15	30	62	8
S 2.2						
AB37	21	59	20	28	66	6
AC37	22	60	18	30	63	7
BA25	28	61	11	37	59	4
BA37	23	61	16	27	68	5
BC25	24	66	10	42	53	5
BC37	20	64	16	32	61	8
BC50	19	61	20	27	65	8
CA25	22	66	12	39	57	5
CA37	18	68	14	34	61	6
CB25	18	71	11	38	57	5
CB37	19	68	13	30	64	7

Table 4.20 Comparison of the Predicted and Counted Percentages of Reactive-Reactive, Reactive-Small Inerts and Reactive-Large Inerts Interfaces for Series 2

The prediction clearly underestimates the number of R-R interfaces, mostly by about a third. R-S interfaces tend to be overestimated by the model. R-L interfaces for all samples are grossly overestimated. The discrepancy between the predicted and counted values are in line with the difference in particle size between the two series. The size range of the particles carbonised in series 2 (75 μm to 1 mm) is such that the component side length for granular flow and the mosaics estimated from series 1 fall above the minimum size. It could be assumed that severe comminution as undertaken for the purposes of maceral concentrations might destroy the characteristic reactive component sizes by fracturing the vitrinite particles they originate from prior to carbonisation. This would then lead to smaller, more uniform component sizes and hence a larger proportion of reactive-reactive interfaces. This was tested by re-running the iteration used to obtain the component side length giving the best fit for the counted R-R, R-S and R-L percentages for series 1 with the component composition data of six samples selected from series 2. The best results were indeed obtained using a uniform side length for all reactive components just below the particle size range (55 to 75 μm). A further modification was however necessary, namely a drastic increase in the estimated side length of the large inerts to about 100 μm . This indicates another possible difference between the two carbonisation series. It appears that the inerts in series 2 are substantially larger and are more resistant to size degradation than the reactive components in that series. The nature and size distribution of inerts is thereby stressed as an important factor for the interfacial behaviour of cokes, and it may well be that the model is oversimplified by working on the assumption that inerts do not vary significantly between different cokes. Whereas this assumption holds true for the cokes in series 1, from which the data to devise the model was derived, it may not do so for cokes from dissimilar precursor coals.

The textural components of the cokes were shown to vary significantly with regard to the number of interfaces they participate in per unit volume occurrence. A simple mathematical model was therefore devised for estimating their relative sizes, approximating them as squares. It strongly suggests that there are indeed significant differences in the sizes of the components, but these might be superceded by particle size, when very small sizes are used.

4.5 Effect of the Maceral Separation Process

The second carbonisation series was aimed at investigating the role of the maceral composition of the coal or coal blend in interface formation. In order to be able to vary the maceral composition more widely, the cokes were carbonised from maceral concentrates rather than coals. For this, the maceral separation process briefly described in chapter 3 was used on the coals. The possibility that some of the carbonisation properties of the coals were altered due that process must be taken into account. It does therefore seem expedient to investigate the effect of the maceral separation process on component and interface distribution, before the results of this series are considered in detail.

4.5.1 Component Distribution

In order to check the effect of maceral concentration and blending on the component and interface distributions, an additional set of blends of the vitrinite and inertinite concentrates containing the same weight percentage of vitrinite as the original coal was carbonised. The component compositions, counted as described in section 3.4.1, for the coal samples and the equivalent vitrinite-inertinite (V-I) blends are compared in table 4.21. Also, the theoretical component composition for the blends is calculated from the individually carbonised vitrinite and inertinite concentrates. For this the maceral concentrate volume fractions, calculated from the estimated densities in appendix 1, are multiplied by the component percent counted for the respective pure concentrate samples and added. The values for component percentages, of the coal sample or calculated, for which the difference to the V-I blend exceeds the error permissible within the 95 % confidence limit, as determined in section 4.2, are highlighted. It appears from table 4.21 that the component compositions of the V-I blends correspond more closely to those calculated from the compositions of the individually carbonised concentrates than to those of the cokes carbonised from the untreated coals. It must therefore be assumed that some the properties appertaining to the formation of textural components have been altered during the maceral separation process. Particularly in the case of coal B2, where the deviations are largest, this must be borne in mind when the cokes of the untreated coal samples are compared with those from the concentrates in series 2.1.

		Coal	V-I.BI	BI calc.
A2	BF	1.3	1.5	1.6
	SF	0.2	0.3	0.2
	GF	30.1	28.7	30.4
	CM	8.7	2.8	3.7
	MM	10.7	6.2	6.0
	FM	14.6	14.3	11.0
	ISO	12.8	25.6	17.8
	INS	8.8	5.8	9.3
	INL	12.7	14.8	20.0
B2	BF	0.8	1.0	2.0
	SF	0.1	0.0	0.0
	GF	22.8	20.1	21.7
	CM	22.0	7.7	10.0
	MM	12.5	15.4	14.2
	FM	9.7	12.5	13.2
	ISO	11.7	27.0	13.7
	INS	10.2	6.2	10.0
	INL	10.2	10.1	15.0
C2	BF	1.8	2.2	2.2
	SF	0.1	0.0	0.2
	GF	21.0	13.9	17.4
	CM	19.9	13.1	12.7
	MM	10.9	15.1	10.4
	FM	6.9	11.1	11.8
	ISO	12.1	23.7	19.3
	INS	12.1	6.9	9.5
	INL	15.0	14.0	16.3
D2	BF	0.0	0.0	0.0
	SF	0.0	0.0	0.0
	GF	0.0	0.0	0.0
	CM	0.0	0.0	0.0
	MM	0.0	0.6	0.1
	FM	20.1	37.0	26.2
	ISO	71.9	45.7	59.7
	INS	1.6	1.0	2.3
	INL	6.3	15.7	11.7

Table 4.21 Comparison of the Component Distributions for the Cokes from the Coals in Series 2 and their equivalent Vitrinite-Inertinite Concentrate Blends

4.5.2 Interface Distribution

The same procedure as for the component distributions is repeated for the interface distributions determined as the averages from the simple and split counts described in section 4.1. The results are shown in table 4.22. None of the errors between the V-I blends and their calculated interface percentages fall outside the 95 % confidence limit, whereas some of those with the untreated coal do. This leads to the same conclusion as for the component distribution, namely that the possibility of some alteration in interfacial behaviour due to the maceral concentration process cannot be excluded. As component and interface distributions are not independent this may however be a secondary effect following from the alteration of the component distribution. This view is supported by the fact that for both, components and interfaces, the largest deviations are found for the same coal (B2).

		Coal	V-I.BI	BI calc.
A2	T	26.5	22.4	29.0
	FU	45.3	36.5	39.2
	FI	26.9	39.2	30.0
	UF	1.3	1.9	1.9
B2	T	21	20.6	22.8
	FU	44.4	32.6	30.5
	FI	33.4	45.1	44.6
	UF	1.2	1.7	2.1
C2	T	21.2	22	22.7
	FU	45.1	45.1	42.6
	FI	32.4	31.7	33.1
	UF	1.3	1.2	1.6

Table 4.22 Comparison of the Interface Distributions for the Cokes from the Coals in Series 2 and their equivalent Vitrinite-Inertinite Concentrate Blends

4.6 Relation between Coal Inertinite and Coke Inerts

One of the questions raised by the concept of characteristic binding powers is what happens to inert material when components of poor binding power or inert incorporation ability predominate in a coke or when inerts themselves become one of the major components. It is possible that in those cases large fractions of inert coal constituents fail to be included into the coke. This was investigated by estimating the inertinite derived fraction of the solid coke residue and comparing it to the total inerts counted in the cokes of series 2.1.

4.6.1 Conversion of Maceral Group Weight Percentage to Volume Percentage

Before it can be attempted to relate the inertinite content in a coal blend to the amount of inerts counted on the coke produced from it, an adjustment for the fact that blends are formulated by weight percentages, but coke component counts supply volume percentages must be made. Or, in other words, the assumption that the densities of the different macerals in each coal are sufficiently similar to be considered equal must be tested. This assumption, which has in fact been made when the blends of series 2 were formulated, was necessary as the maceral densities were not known.

To test it the densities were estimated from data available in the literature [25, 28] as described in appendix 1. The weight percent of inertinite in the blends was re-calculated using the estimated densities and the deviation from the desired weight percent was determined. The re-calculated percentages and the errors incurred are listed in table 4.23. Taking these errors as an indication of those likely to be caused by the above assumption, it can be said that, averaging at about 1.3 %, they stay within the limits of acceptability.

Sample	Inertinite calculated using Density Estimates (%wt)	Absolute Error (%wt)
B2 75	24.8	0.2
C2 75	21.9	3.1
C2 50	49.1	0.9
V-I A2	37.7	1.5
V-I B2	37.0	1.5
V-I C2	30.9	0.7
V-I D2	20.4	1.9
AB37	39.1	1.6
AC37	38.9	1.4
BA25	26.2	1.2
BC25	26.1	1.1
BD25	26.0	1.0
BA37	38.9	1.4
BC37	38.8	1.3
BC50	51.4	1.4
CA25	26.0	1.0
CB25	26.1	1.1
CD25	25.9	0.9
CA37	38.8	1.3
CB37	39.0	1.5
DA25	26.0	1.0
DB25	26.1	1.1
DC25	25.9	0.9
DA37	38.8	1.3
DB37	39.2	1.7
Average Error		1.3

Table 4.23 Potential Errors in Blend Inertinite Weight Percentage

4.6.2 Relation between Inerts and the Inertinite Derived Coke Fraction

The amount of inertinite derived material in the cokes of series 2.1 was estimated using the weight percentages of the maceral groups in the samples and their estimated volatile matter contents given in appendix 1. For the calculation it is assumed that the volatile matter content of all macerals tends to zero when carbonisation temperatures around 1000 °C are reached. This is a reasonable assumption in view of the data reported by Loison et al [22] showing that the overall volatile matter content of cokes carbonised to that temperature is very close to zero for a wide range of precursor coal ranks. The weight loss from the vitrinite and inertinite fractions of the samples are thus calculated for complete loss of volatile matter and the weight fractions of vitrinite and inertinite derived coke are deduced. Unfortunately it is not possible to convert them to volume percentages, as the density changes on carbonisation are not known. It appears reasonable to assume though that the differences in densities between the maceral groups diminish on carbonisation, as the loss of volatile matter and the structural ordering occurring in the process lead to greater chemical and physical similarity between the maceral groups.

Hence, taking the densities of the vitrinite and inertinite derived fractions of the cokes as equal, the weight percent of the cokes derived from inertinite was estimated. For simplicity it is hereafter referred to as calculated or theoretical inerts, in spite of this implying the not necessarily true assumption that inertinite exclusively converts to what is counted as inerts. The calculated and the counted percent of inerts are compared in table 4.24. The results are shown in two ways. Firstly as the percent of calculated inerts appearing as counted inerts and secondly as the absolute numerical difference between the calculated and counted percent. It can be clearly seen that there is almost a linear decrease of the percent of calculated inerts showing as counted inerts with the total amount of inertinite derived coke (calculated inerts). Or in other words, the part of calculated inertinite derived coke not accounted for by appearing as recognizable inerts increases with the size of the inertinite fraction in the blend. This is further illustrated by figure 4.10, in which a linear fit is attempted. Although there is quite a large amount of scatter, the trend of a increasing discrepancy between calculated and counted inerts with increasing inertinite fraction is clearly shown to exist.

The difference between calculated and counted inerts can not, however, be related to the combined percentage of fine mosaics and isotropic material. This is most evident from the fact that the discrepancy between the calculated and counted inerts in the samples from coke D2, where those two reactive components are virtually the only ones present, is no worse than that in most other samples. This leads to the conclusion that fine mosaic and isotropic components will in fact incorporate inerts in the

	% vol Inerts counted	% wt Inerts calculated	% calc. Inerts counted	% calc. - % counted	%FM+ISO
A2V	27.4	33.5	81.8	6.1	31.2
A2	21.5	40.1	53.6	18.6	27.4
A2I	33.7	56.4	59.8	22.7	23.5
B2V	19.7	18.8	+100	-0.9	27.6
B275	18.9	28.1	67.2	9.2	24.9
B2	20.4	41.1	49.6	20.7	21.4
B2I	28.5	55.0	51.8	26.5	26.6
C2V	23.3	13.4	+100	-9.9	29.7
C275	22.1	24.9	88.8	2.8	21.3
C2	27.1	31.4	86.3	4.3	19.0
C250	24.0	53.2	45.1	29.2	27.1
C2I	29.6	62.7	47.2	33.1	33.2
D2V	8.4	14.3	58.7	5.9	91.6
D2	8.0	27.2	29.4	19.2	92.0
D2I	22.1	40.5	54.6	18.4	77.7

Table 4.24 Calculated and Counted Inerts in Sample Series 2.1

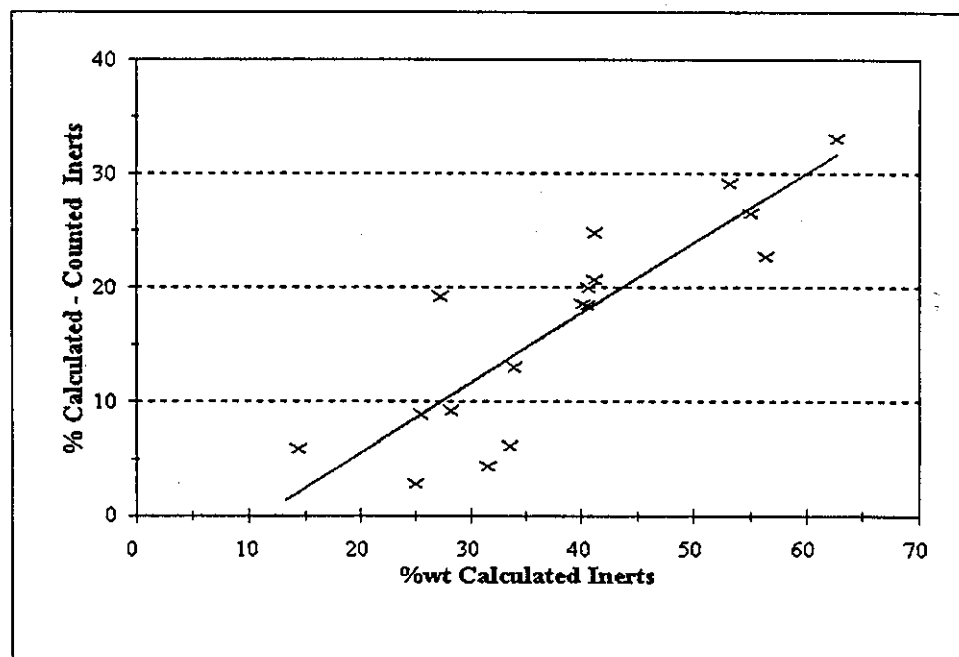


Figure 4.10 Percentage of Calculated Inerts versus the Difference between Calculated and Counted Inerts in Series 2.1

absence of other reactive components, but are more reluctant to do so. Given the presence of more 'reactive' components, these will preferentially interface with the inerts. This contradicts the theory of characteristic binding powers, as fine mosaic and isotropic material appear to be influenced by the presence of other components. It may suggest that it might be more accurate to talk about variations in the readiness of components to incorporate inerts, rather than absolute abilities to do so.

The above observations leave the question unanswered of what becomes of the coke fraction derived from inertinite which does not appear as inerts. Either the vitrinite derived coke matrix must have failed to incorporate it, or it must be unrecognisable as inert, i.e. take on the appearance of the reactive material in the cokes. It would then form part of what is widely cited as 'reactive inertinite' [16, 76, 78, 79, 80, 82]. If a certain proportion of the inertinite in each coal behaved as a reactive, then it would be expected that this proportion would not change with the amount of inertinite in the sample. The ratio of calculated to observed inerts would be expected to be constant. This is shown not to be the case in table 4.24. Although the trend is not universal, there is a tendency of an increasing unaccounted for fraction relative to the total inertinite derived coke. This implies that the effect is enhanced by increasing the total inertinite fraction, which would be more in line with a progressive failure of the reactive components to incorporate all of the inerts added. Also, if a proportion of the inertinite was reactive, its most likely appearance would be that of isotropic material. Inerts and the isotropic component have the same colour viewed by PLM. In the absence of a residual woody structure and with evidence of softening at the unit boundaries, inerts would appear identical to isotropic material. There should then be a relation between the unaccounted for inertinite derived material and the variation of the amount of isotropic material in the coke matrix. There is no evidence to support this. It is therefore more likely that the unaccounted for fraction of inertinite derived coke has failed to be incorporated and was lost, e.g. as fine breeze, rather than that it was converted to take the appearance of a reactive component.

4.7 The Effect of Coke Inerts on Interfaces

A number of models predicting coke strength assume that for every vitrinite type, i.e. the material the reactive components originate from, there is an optimum level of inerts, below and above which coke properties deteriorate [16, 35]. If there is a connection between textural component interfaces and those properties, it is possible that the quality of interfaces formed with inerts will depend not only on the absolute binding power of a reactive component, but also on the amount of inerts in a coke. It is therefore of interest to investigate the effect of variations in the amount of inerts in the cokes on the quality of interfaces between the components.

4.7.1 Relative Importance of Interfaces with Inerts

One of the aspects concerning interface frequency revealed by studying the first carbonisation series is the large number of interfaces involving inerts. This is illustrated by the data in table 4.25.

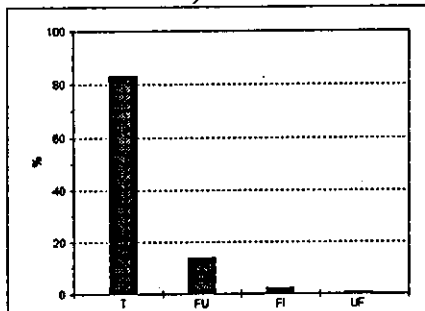
	Inerts (%vol)	Interfaces involving Inerts (%vol)
A 1	19.0	57
B 1	16.6	60
C 1	22.1	80
D 1	13.3	83
E 1	17.8	89
F 1	18.9	78

Table 4.25 Comparison of Inert Component Percentages and their Percentage Participation in Interfaces in Series 1

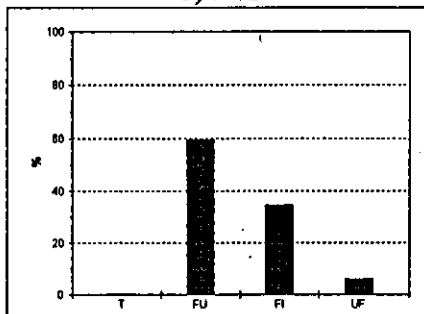
Inerts typically make up 15 to 20 % of the volume of the solid coke residue in that series, but participate in up to 89 % of the interfaces. In conjunction with the fact that interfaces between any two reactive components, with the possible exception of the larger flow types and isotropic material, tend to be very good, it must be expected that the quality of interfaces in a coke is strongly dependent on the ability of the reactive components to incorporate inerts.

A1

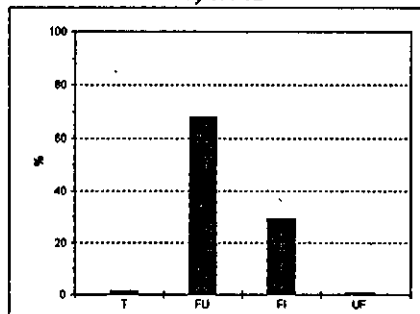
a) R-R



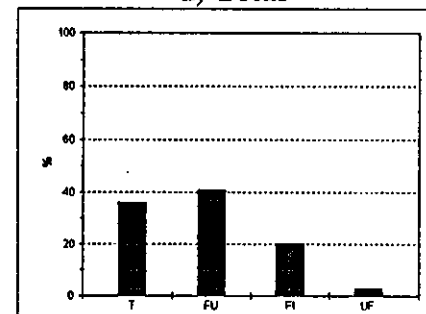
b) R-S



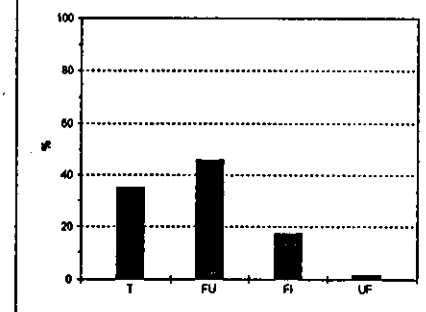
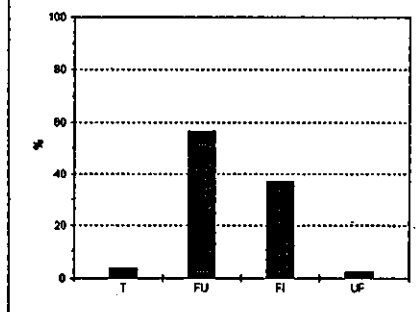
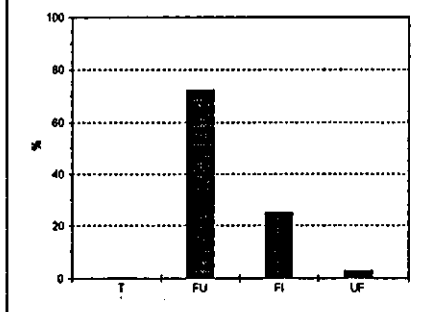
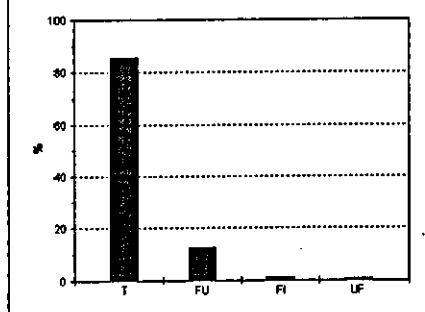
c) R-L



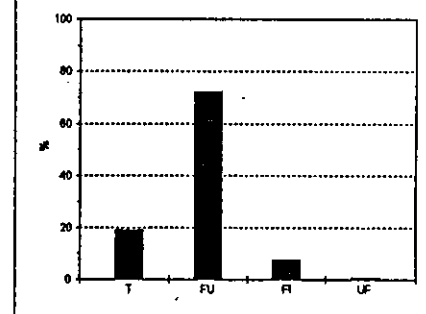
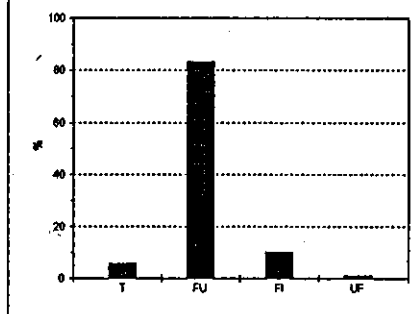
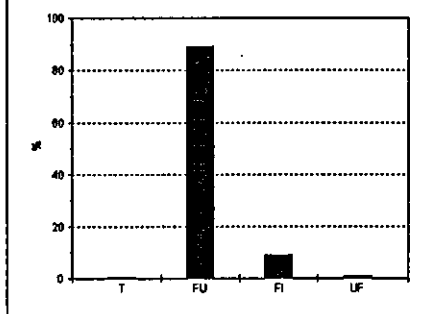
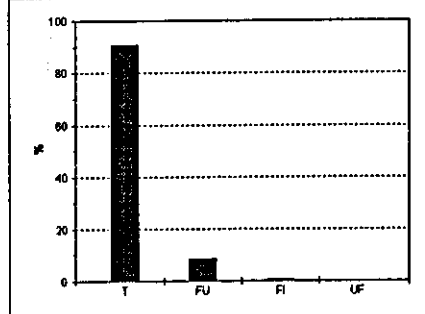
d) Total



B1



C1



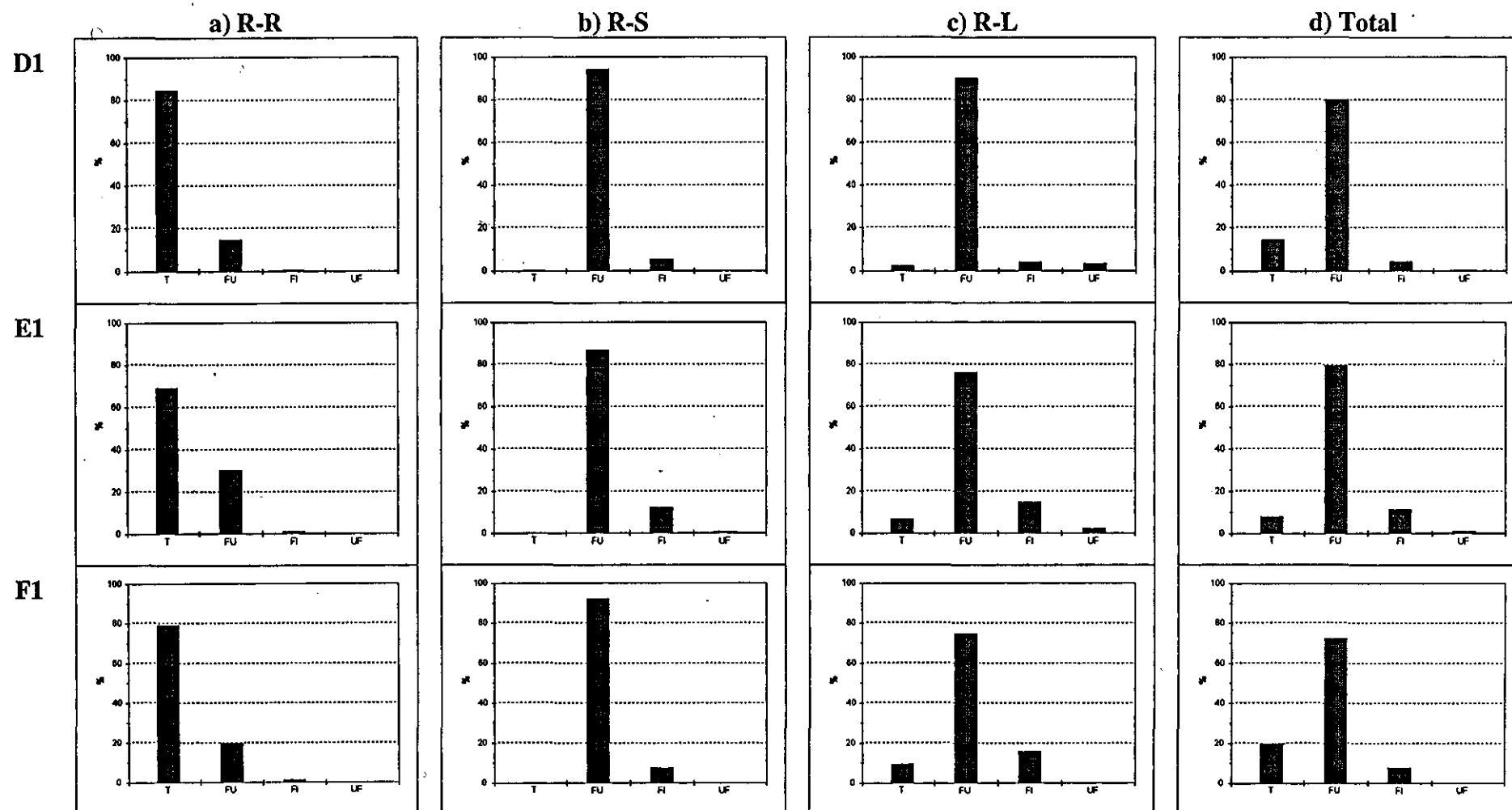


Figure 4.11 Interface Distributions Split by Interface Types in Series 1

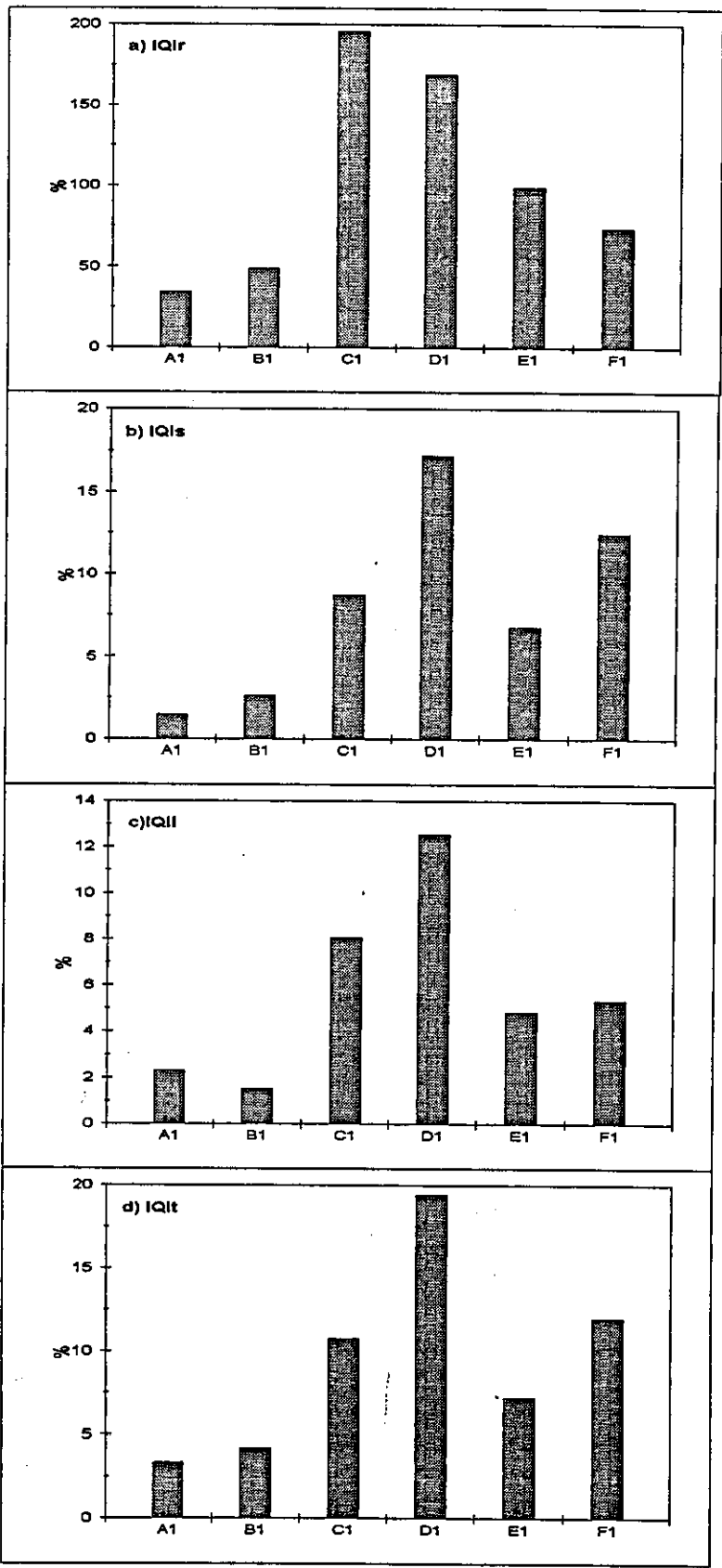


Figure 4.12 Comparison of Average Interface Type Quality Indices with the Overall Interface Quality Index in Series 1

This view is supported by plotting the interface type distributions for reactive - reactive (R-R), reactive - small inerts (R-S) and reactive - large inerts (R-L) interfaces separately and comparing them with the overall coke interface distributions (figure 4.11 a) to d)). The distribution profiles for interfaces with inerts are more similar to those of the cokes as a whole. They peak at the fused interface type and exhibit an appreciable amount of fissuring. In contrast, R-R interface profiles decrease from transitional to unfused.

Referring to figures 4.12 a) to d) it can also be seen that the order of magnitude of the interface quality indices of interfaces involving inerts (IQIs and IQIl) are more akin to that of the overall indices for the cokes (IQIt), whereas those for R-R interfaces (IQIr) exceed them by a factor of about 10. Also, the trend for variation of the IQI with the rank of the precursor coals is identical for the cokes as a whole and the interfaces with inerts of both sizes. The IQI for R-R interfaces, however, peaks at coke C1, rather than at D1, and decreases smoothly from C1 to F1 without the irregularity displayed by coke E1 for inert interfaces.

Thus it appears that there are fundamental differences in the interfacial behaviour of reactive components with one another and with inerts, which require additional explanation. It is likely that the total inert volume content of the coke strongly influences interface quality. The ability of reactive components to incorporate inerts might be limited and deteriorate if a certain amount is exceeded. This would explain why coke C1, which has the best R-R interfaces, performs worse for inerts, as, at 22.1 %, it has the largest inert content of the samples in series 1. Series 2.1. was therefore produced with the main objective to compare cokes derived from the same vitrinite material containing varying amounts of inerts.

4.7.2 Variation of Interface Frequencies with Inert Levels

The question addressed in this section is whether there is a limit to the proportionality of inert volume and the number of interfaces involving inerts. At the extreme, there may be a limit to the incorporation ability of any component, which beyond this limit may become 'saturated'. If this is the case there will be a frequency of interfaces between a component and inerts, possibly characteristic to that component, above which no increase will be observed on the addition of further inerts.

Figures 4.13 a) to e) consider the variations of the ratio of the number of interfaces to the sum of the volume percentage of the interfacing components for interfaces involving small and large inerts for the carbonisation series 2.1. The ratios are plotted against the percentages of the inerts counted on the respective samples. The broad and striated flow components did not occur in sufficient amounts in the samples to be included.

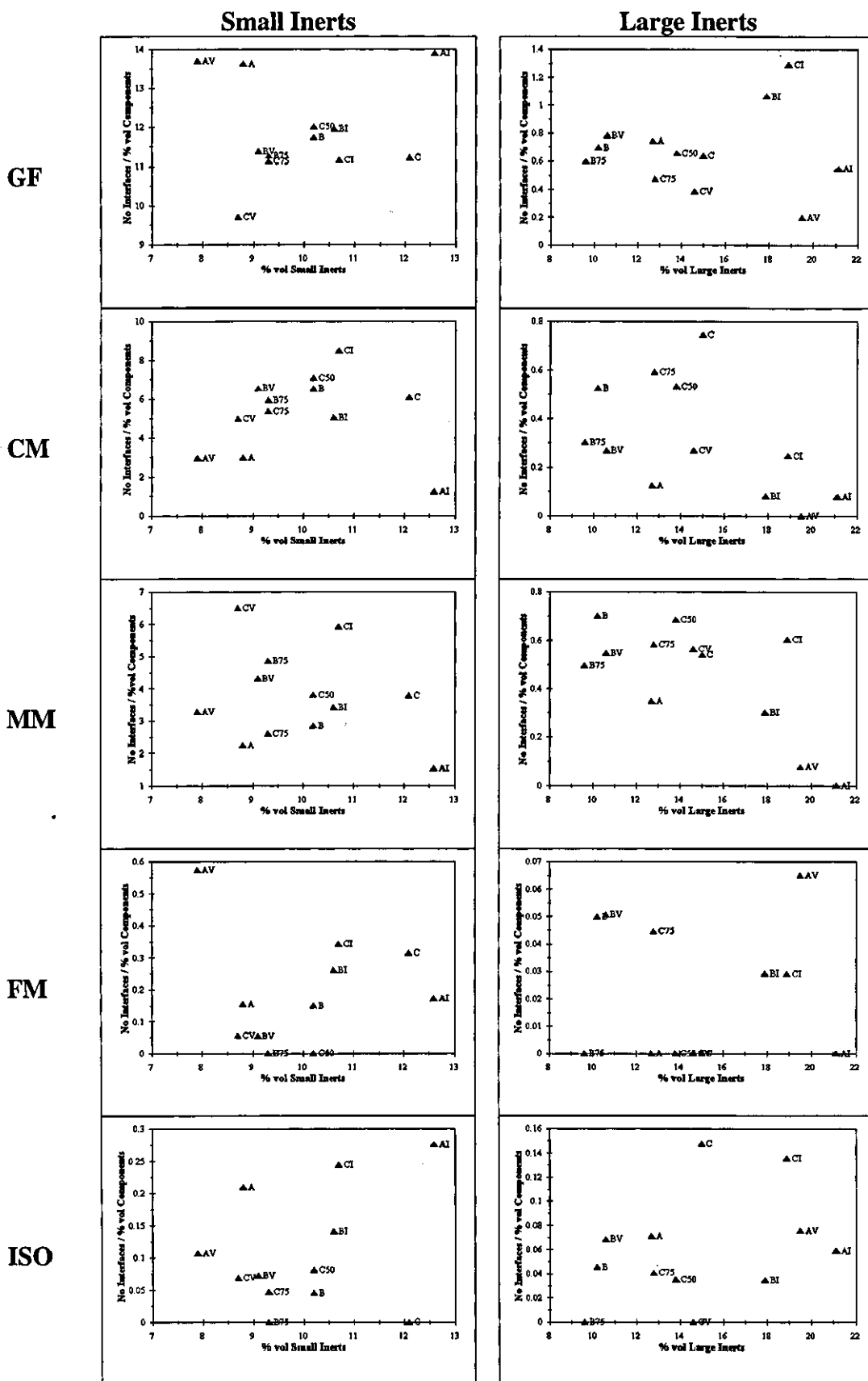


Figure 4.13 Variation of the Interface Frequency to Component Volume Ratio for Reactive-Inert Interfaces with Inerts Content in Series 2.1

No consistent trend could be detected either for the samples originating from the same coal or for any individual component. Although the interface frequency - volume percent ratio does vary to some extent with the amount of inerts counted in the coke, it appears to do so in a rather random fashion, showing about equal numbers of increasing, decreasing and inflecting curves of various shapes. The absence of a detectable trend discounts the hypothesis of an incorporation limit or saturation effect for inerts in the range of inert concentrations that could be achieved for the coals used. However, as the largest percentage of total inerts amounts to 33.7 % of the solid coke volume, the possibility that such a limit exists, but lies above the inert levels considered, persists.

A summary of the interface to volume ratios is given in table 4.26. It shows that the differences between the reactive components irrespective of the coal of origin and the level of inerts in the cokes. This corresponds well with the hypothesis of interface frequencies being a characteristic property of the components derived from their binding powers and typical unit sizes. For small inerts the averages of the ratios indicate that there is a decreasing ability to incorporate them from granular flow to isotropic material. For large inerts the trend is less pronounced, firstly by the absolute differences between the components being much smaller and secondly by medium mosaic appearing to incorporate more large inerts than coarse mosaic.

	No of Interfaces / %vol Component +Inert				
	GF	CM	MM	FM	ISO
Ins					
A2V	13.7	3.0	3.3	0.6	0.1
A2	13.6	3.0	2.2	0.2	0.2
A2I	13.9	1.3	1.5	0.2	0.3
B2V	11.4	6.6	4.3	0.1	0.1
B275	11.3	6.0	4.9	0.0	0.0
B2	11.7	6.5	2.9	0.2	0.0
B2I	12.0	5.1	3.4	0.3	0.1
C2V	9.7	5.0	6.5	0.1	0.1
C275	11.1	5.4	2.6	0.0	0.0
C2	11.2	6.1	3.8	0.3	0.0
C250	12.0	7.1	3.8	0.0	0.1
C2I	11.2	8.5	5.9	0.3	0.2
Average	11.9	5.3	3.8	0.2	0.1
Inl					
A2V	0.2	0.0	0.1	0.1	0.1
A2	0.7	0.1	0.3	0.0	0.1
A2I	0.6	0.1	0.0	0.0	0.1
B2V	0.8	0.3	0.5	0.1	0.1
B275	0.6	0.3	0.5	0.0	0.0
B2	0.7	0.5	0.7	0.1	0.0
B2I	1.1	0.1	0.3	0.0	0.0
C2V	0.4	0.3	0.6	0.0	0.0
C275	0.5	0.6	0.6	0.0	0.0
C2	0.6	0.7	0.5	0.0	0.1
C250	0.7	0.5	0.7	0.0	0.0
C2I	1.3	0.2	0.6	0.0	0.1
Average	0.7	0.3	0.5	0.0	0.1

Table 4.26 Ratio of Number of Interfaces of the Reactive Components with Inerts and their combined Volume Percent for Series 2.1

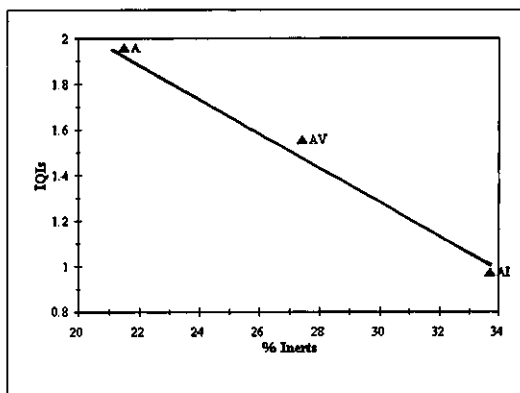
4.7.3 Variation of IQI with Inert Levels

If individual components, like the vitrinite types they originate from, also have characteristic optimum inert levels, the quality of interfaces involving inerts should peak in the vicinity of this optimum inert level for the major components in a coke. Plotting inert content against interface quality should then give a parabolic curve analogous to that used for strength prediction [7].

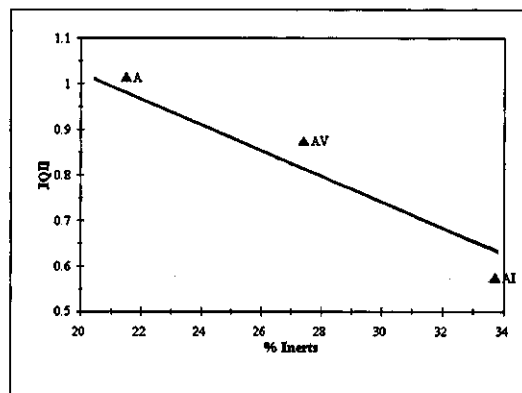
Figures 4.14, 4.15 and 4.16 show the variation of IQI with the total amount of inerts for cokes A2, B2 and C2 respectively, split into interfaces with small inerts (IQIs), large inerts (IQII), total inerts (IQIi) and between reactive components (IQIr). For coals A2 and C2 there is a clear trend of deterioration in interface quality with increasing inert levels. For coal B2 the inert levels for all samples but the inertinite concentrate one are very similar. The interface quality is markedly lower for the coke prepared from the inertinite concentrate, corresponding to the trend for the other two coals, but the IQI of the remaining samples also vary substantially without significant differences in inert levels. The appearance is more in line with a curve which steeply increases in the 20 %(vol) inert range, into which those three samples fall, peaks for the untreated coal sample and then tails off. This would actually correspond to the shape of a curve indicating an optimum inert level at that of the untreated coal. The trend for A2 and C2 does not completely contradict the optimum inert level theory. It is possible that only the right hand side of such a curve is represented for them, the peak lying somewhere below the 20 %(vol) inerts mark at which their curves start.

For coals A2 and C2 the trend, although at different orders of magnitude, is almost identical for all three types of interfaces. This clearly shows that the fall in interface quality, even though it can be attributed to the increased amount of inerts, does not merely arise from poor interfaces with 'excess' inerts, but that it reflects on the ability of reactive components to interface with one another. It could be said that, assuming a limited binding power, the use of it to incorporate more inerts depletes the capacity of reactive components to adhere to one another. Coal B2 again fails to deliver a clear picture. For R-S interfaces the vitrinite concentrate sample shows an unexpectedly low IQI, whereas for R-R interfaces the 75 %wt vitrinite sample does so.

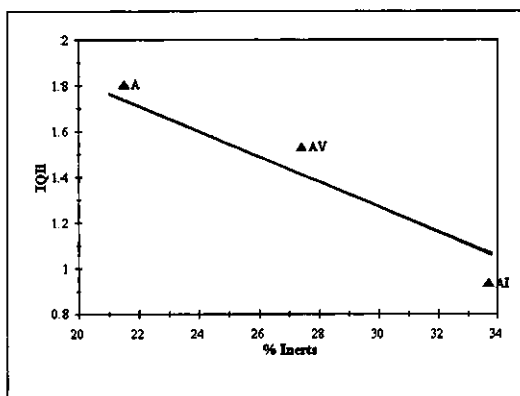
a)



b)



c)



d)

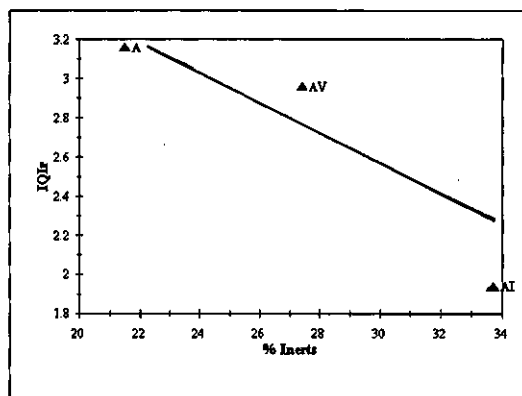
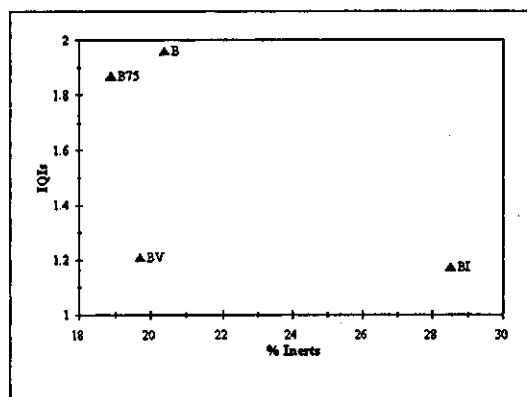
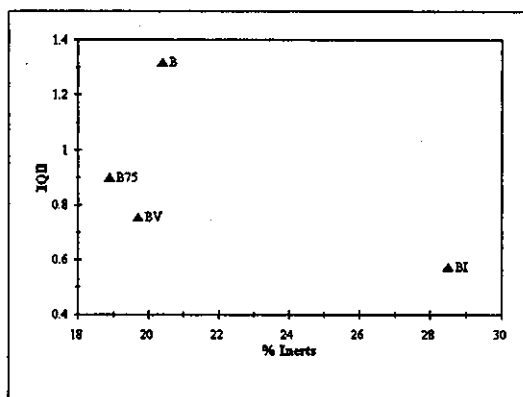


Figure 4.14 Variation of the Interface Type Quality Indices with the Inerts Content for Coal A2

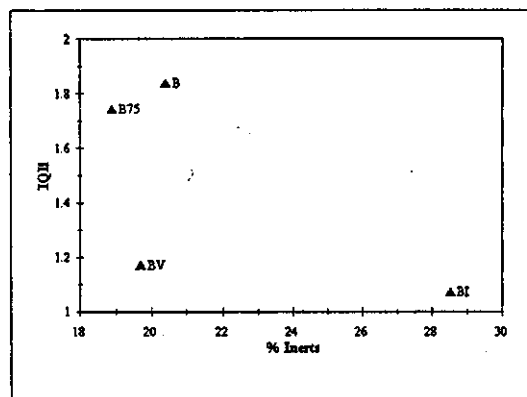
a)



b)



c)



d)

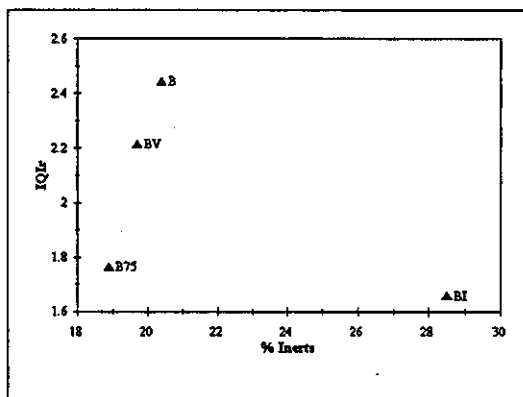
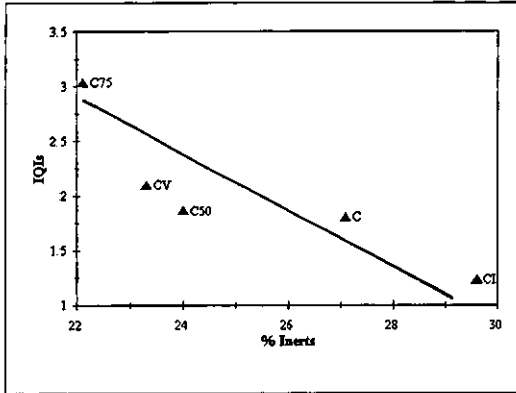
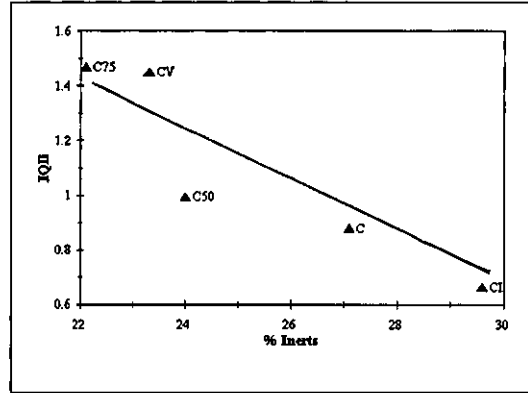


Figure 4.15 Variation of the Interface Type Quality Indices with the Inerts Content for Coal B2

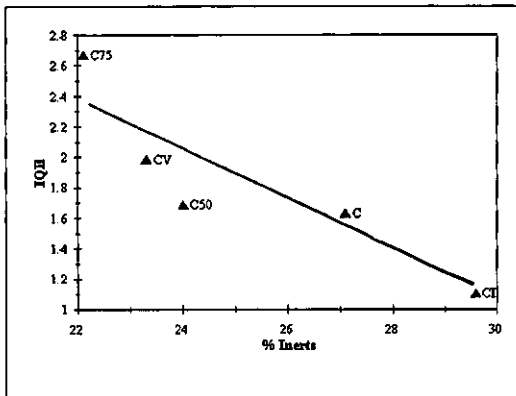
a)



b)



c)



d)

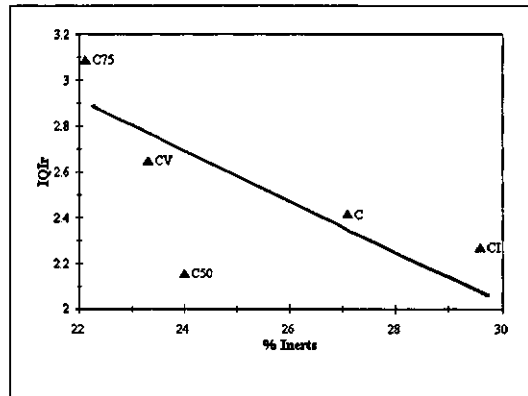


Figure 4.16 Variation of the Interface Type Quality Indices with the Inerts Content for Coal C2

4.8 The Effects of the Blending of Maceral Concentrates

One of the assumptions implicitly made in formulating the binding power and component size hypotheses in section 4.3 and 4.4 is that component and interface distributions are additive. That means that a specific coal constituent will form a characteristic textural component with a characteristic interfacial behaviour, irrespective of the other constituents with which it is carbonised. In order to investigate the validity of this assumption the vitrinite concentrates of each of the coals in series 2 were carbonised with the inertinite concentrates from the other coals in the series. If the component distributions and interfacial properties are additive, it should be possible to predict the component composition and the interface frequency and quality with reasonable accuracy from the data of the individually carbonised concentrates.

4.8.1 Component Composition

To investigate the effect of blending on the textural composition, the counted results from series 2.2 were compared with the textural composition calculated from the composition of the individually carbonised concentrates, which formed part of series 2.1. This was done by multiplying the component compositions of the individually carbonised concentrates (as listed in appendix 2 table A2.2) by their estimated volume fractions in the blends and adding these. In order to convert the known weight percentages of the concentrates in each blend into volume fractions, the maceral concentrate densities were estimated by combining the pure maceral densities given in appendix 1 with the petrographic composition (table 3.2). Table 4.27 compares the results from the component counts with the calculated component compositions. The calculated values where the difference to the counted component percent falls outside the 95 % confidence limit determined in section 4.2 are highlighted. In fact, very few values fall outside this limit. With the exception of broad and striated flow, of which there are only small amounts found in the samples, large discrepancies are found exclusively for medium mosaics. Closer inspection shows that for all samples composed from concentrates from coals A2, B2 and C2, less medium and fine mosaics are found than expected, with a shift towards both, larger mosaics and isotropic material. The trend towards larger than expected amounts of isotropic material is less universal, two exceptions having been found.

	Counted							Calculated						
	BF	SF	GF	CM	MM	FM	ISO	BF	SF	GF	CM	MM	FM	ISO
AB37	2.1	0.1	42.0	9.2	4.4	12.5	29.6	2.3	0.1	36.9	6.6	13.5	18.3	22.2
AC37	2.8	0.4	42.1	8.3	6.0	9.3	31.0	2.2	0.2	36.1	7.2	10.1	17.3	26.9
BA25	2.1	0.0	37.9	20.4	6.8	5.4	27.3	2.6	0.2	32.5	15.6	14.5	12.6	22.0
BC25	1.5	0.0	31.2	23.3	7.5	8.3	28.2	2.5	0.1	26.4	17.7	16.1	13.7	23.5
BD25	1.1	0.0	19.6	4.4	6.4	23.3	45.2	1.1	0.0	12.4	8.5	7.4	24.0	46.7
BA37	2.7	0.4	48.3	13.4	4.6	12.2	18.3	2.9	0.4	38.4	11.2	12.1	14.3	20.7
BC37	2.1	0.0	31.9	23.7	8.7	11.3	23.3	2.6	0.2	24.4	15.9	15.8	16.9	24.2
BC50	2.4	0.1	31.8	21	8.9	9.5	26.2	2.7	0.2	22.5	14.2	15.5	20.0	24.9
CA25	1.8	0.4	28.2	16.7	9.2	15.7	27.9	3.1	0.4	31.9	15.0	12.0	13.5	24.0
CB25	1.4	0.0	34.6	21.3	6.4	8.0	28.3	3.0	0.2	26.7	15.7	16.2	16.0	22.1
CD25	2.0	0.1	15.0	9.6	6.1	16.4	50.8	1.1	0.1	8.8	7.0	4.9	26.3	51.8
CA37	2.8	0.1	42.0	12.4	7.4	9.2	26.0	3.1	0.5	38.0	10.9	10.8	14.7	21.8
CB37	1.7	0.1	31.7	17.9	6.7	10.4	31.5	2.9	0.1	28.3	12.2	18.7	19.4	18.3
DA25	0.2	0.1	17.2	1.8	1.4	31.7	47.5	1.2	0.2	16.2	2.3	3.4	23.9	52.8
DB25	0.7	0.0	12.1	3.1	3.8	34.7	45.6	1.1	0.0	11.6	3.5	8.1	26.0	49.6
DC25	0.4	0.0	8.2	2.4	2.1	31.1	55.9	0.9	0.1	6.7	4.1	4.8	26.3	57.1
DA37	0.8	0.1	30.5	1.8	2.8	20.1	44.0	2.1	0.4	29.8	4.2	6.3	20.2	36.9
DB37	1.0	0.1	21.6	3.7	4.3	25.8	43.4	2.1	0.0	21.4	6.5	15.1	24.1	30.9

Table 4.27 Counted and Calculated Component Distribution (Inert-Free Basis) for Series 2.2

Blends including either of the concentrates from coal D2 behave less consistently, but coarse and medium mosaics can be said to feature less prominently than expected, whereas granular flow is underestimated by the calculation. Fine mosaics and isotropic material are virtually equally under- and overestimated.

It is probably true to say that the component distribution behaves additively and can be estimated for a blend from that of its constituents. Nevertheless, some minor alterations due to co-carbonisation effects cannot be excluded.

4.8.2 Interface Distribution

The overall interface distribution data for the cokes, as averages between the simple and split counts, are summarised in table 4.28. As for the textural components the expected distributions are calculated from the results for the individually carbonised concentrates (given in appendix 3 tables A3.3 and A3.4). Again the number of calculated values falling outside the 95 % confidence limit is relatively small. It does appear though that for the majority of samples the interface quality improves with blending, i.e. the percentage of fused interfaces is higher, that of fissured ones lower, than that calculated from the blend constituents. This is reflected in better than calculated IQIt for all but two samples.

The variation in interface distribution does not appear to be related in any obvious way to that in component distribution. In some samples both, component and interface distribution, fall outside their respective 95 % confidence limits, but there are as many cases where only one of them does. This does not necessarily, as it may superficially seem, contradict the theory of interfacial behaviour, or binding power, being a characteristic of each textural component, as blending offers different interface combinations not available in the individually carbonised concentrates.

%	counted					calculated				
	T	FU	FI	UF	IQI	T	FU	FI	UF	IQI
AB37	21.7	44.3	32.4	1.6	1.94	27.3	36.7	33.9	2.1	1.78
AC37	18.5	42.6	37.5	1.4	1.57	29.2	40.8	28.1	1.9	2.33
BA25	25.7	27.1	45.2	2	1.12	24.3	32.9	41.3	1.5	1.34
BC25	25.2	42.8	30.9	1.1	2.13	24.4	34.2	40.0	1.5	1.41
BA37	23.9	39.6	34.5	2	1.74	23.9	32.4	41.8	1.9	1.29
BC37	20.2	45.7	32.4	1.7	1.93	24.1	35.1	38.9	1.8	1.45
BC50	18	45.5	34.6	1.9	1.74	23.8	36.1	37.9	2.2	1.49
CA25	25.7	46.8	26.3	1.2	2.64	22.5	41.4	34.5	1.5	1.77
CB25	21.6	42.6	33.6	2.2	1.79	21.8	39.9	36.6	1.7	1.61
CA37	22.5	41.4	33.6	2.5	1.77	23.0	36.8	38.3	1.9	1.49
CB37	21.8	43.5	32.6	2.1	1.88	21.7	34.0	42.1	2.2	1.26

Table 4.28 Counted and Calculated Interface Distributions for Series 2.2

4.8.3 Interface Quality Indices

Table 4.29 shows the average total interface quality indices (IQIt) of the maceral concentrate blends from the simple and split interface counts on series 2.2. Table 4.30 summarizes the results from the split counting method giving the interface qualities for interfaces between reactive components (IQIr) and for interfaces with small and large inerts (IQIs and IQIl). In both tables the first letter stands for the origin of the vitrinite concentrate, the second for that of the inertinite concentrate, e.g. AB is the blend of the vitrinite concentrate of coal A2 with the inertinite concentrate from coal B2. The results are presented ordered in two different ways, firstly by vitrinite concentrate in the blend and secondly in matching pairs (e.g. AB and BA, the blends of the vitrinite concentrate from A2 with the inertinite concentrate from B2 and the vitrinite concentrate from B2 with the inertinite concentrate from A2 containing the same percentage of inertinite).

4.8.3.1 Vitrinite Concentrates from Coal A2

Carbonising the vitrinite concentrate of coal A2 with the inertinite concentrates of coals B2 and C2 improves its total interface quality index relative to being carbonised with its own inertinite concentrate from 1.4 to 1.9 and 1.6 respectively. The most likely explanation for this is the introduction of 'more reactive' vitrinite from the more fluid coals B2 and C2 in the process. The inertinite concentrates, the maceral composition of which was given in table 3.2, contain substantial amounts of vitrinite. The larger quantity of its vitrinite in the blend would also explain the greater effect of coal B2, even though it is less fluid than C2. It appears from table 4.30 that the carbonisation of vitrinites from coals A2 with those from B2 and C2 leads to a marked improvement of the reactive-reactive interfaces from 2.0 to 3.9 and 2.6 respectively. The effect on reactive-inert interfaces is less marked and inconsistent insofar as a slight deterioration for the AB blend relative to the V/I blend of coal A2 occurred.

4.8.3.2 Vitrinite Concentrates from Coal B2

For 25% (wt) inertinite the IQIt of the blends from the vitrinite concentrate of coal B2 improves with the addition of inertinite concentrate derived from coal C2 from 1.8 to 2.1. But it deteriorates with the addition of inertinite concentrates from coals A2 and D2 to 1.1 and 1.6 respectively. From the results of the split counts shown in table 4.30 it appears that this deterioration is due to the inerts from coals A2 and D2, as the reactive-reactive interfaces are unaffected in the case of A2 and even quite substantially improved for D2.

	<u>IQIt</u>	
	<u>25 %(wt) Inertinite</u>	<u>37 %(wt) Inertinite</u>
AA		1.4
AB		1.9
AC		1.6
BB	1.8	1.1
BA	1.1	1.7
BC	2.1	1.9
BD	1.6	
CC	2.4	2.0
CA	2.6	1.8
CB	1.8	1.9
CD	2.7	
DA	1.5	1.1
DB	1.0	1.2
DC	1.3	

	<u>IQIt</u>	
	<u>25 %(wt) Inertinite</u>	<u>37 %(wt) Inertinite</u>
AB		1.9
BA		1.7
AC		1.6
CA		1.8
BC	2.1	1.9
CB	1.8	1.9
BD	1.6	
DB	1.0	
CD	2.7	
DC	1.3	

Table 4.29 Average Total Interface Quality Indices in Series 2.2

	25 %(wt) Inertinite			37 %(wt) Inertinite		
	IQIr	IQIs	IQII	IQIr	IQIs	IQII
AA				2.0	1.1	1.0
AB				3.9	1.7	0.9
AC				2.6	1.3	1.2
BB	2.0	2.3	1.1	1.6	1.1	0.7
BA	2.1	1.0	0.7	6.6	1.5	0.9
BC	2.9	2.3	1.1	2.7	2.9	0.8
BD	3.5	1.0	0.9			
CC	3.1	3.6	1.2	1.8	2.1	0.9
CA	5.7	2.3	1.8	3.6	1.6	0.8
CB	3.3	1.9	1.1	3.3	2.0	1.8
CD	5.6	1.6	1.5			
DA	2.9	1.4	0.4	2.6	0.6	0.4
DB	1.6	1.0	0.6	1.8	0.7	0.5
DC	2.7	0.7	0.6			

	25 %(wt) Inertinite			37 %(wt) Inertinite		
	IQIr	IQIs	IQII	IQIr	IQIs	IQII
AB				3.9	1.7	0.9
BA				6.6	1.5	0.9
AC				2.6	1.3	1.2
CA				3.6	1.6	0.8
BC	2.9	2.3	1.1	2.7	2.9	0.8
CB	3.3	1.9	1.1	3.3	2.0	1.8
BD	3.5	1.0	0.9			
DB	1.6	1.0	0.6			
CD	5.6	1.6	1.5			
DC	2.7	0.7	0.6			

Table 4.30 Interface Quality Indices of Series 2.2 determined by Split Counts

The total interface quality for the 37 %(wt) inertinite BA sample improves to 1.7, not only relative to the V/I blend of B2 of the same inertinite percentage (1.1), but also compared to the 25 %(wt) inertinite BA blend (also 1.1). It is in fact better than that of either concentrate carbonised singly due to the exceptionally good reactive - reactive interface quality (6.6) a blend of these proportions of the two vitrinites achieves. No similar effect was found for the 37%(wt) inertinite BC blend, possibly because blending the vitrinites of two higher fluidity coals, even though it seems to positively affect the incorporation of small inerts, does not sufficiently improve reactive-reactive interfaces.

4.8.3.3 Vitrinite Concentrates from Coal C2

The addition of inertinite concentrates of coals A2 and D2 to make up 25 %(wt) inertinite blends improves the total interface quality in blends based on the vitrinite concentrate of coal C2 relative to the V/I blend of C2 from 2.4 to 2.6 and 2.7, whereas addition of the inertinite concentrate of coal B2 causes a deterioration (to 1.8). Table 4.30 shows that the main improvement for the CA and CD blends lies again with the reactive-reactive interfaces, but some improvement is also observed for interfaces with large inerts. There is obviously a beneficial effect in blending the highly fluid vitrinite of coal C2 with the inertinite concentrates from less fluid coals A2 and D2. The effect is more marked for coal D2, which shows no fluidity or dilatation.

The beneficial effect of the inertinite concentrate of coal A2 observed for the 25 %(wt) inertinite sample does not persist when the inertinite contents is increased to 37 %(wt). It causes a small deterioration in IQIt relative to the V/I blend of C2, almost identical to that caused by the inertinite concentrate from B2, from 2.0 to 1.8 and 1.9. Their effects differ though, the blend with the inertinite concentrate from coal A2 having better reactive-reactive interfaces (3.6 as opposed to 3.3) and that with the blend from coal B2 better interfaces with inerts (2.0 to 1.6 for small inerts and 1.8 to 0.8 for large inerts).

It is of some interest that CB blends of both inertinite percentages have rather similar total interface quality indices. The IQIt of the 37 %(wt) inertinite blend at 1.9 is even slightly higher than that of the 25% blend at 1.8. In contrast, the decrease in IQIt on increasing the total inertinite is very substantial for the CA blends, from 2.6 for 25 to 1.8 for 37 %(wt). This might be an indication of the different location of optimum inert levels for the blends, be it for different combinations of vitrinites or due to the difference in the nature of the inerts.

4.8.3.4 Vitrinite Concentrates from Coal D2

The remarkable result for the blends of the vitrinite concentrate of coal D2 is that the best IQIt is achieved by the 25 %(wt) inertinite blend with the inertinite concentrate from coal A2, which is also a low fluidity coal and would thus expected to be not very reactive. As for the blends with the vitrinite concentrates of coal C2, the total interface quality deteriorates for the blend with the inertinite concentrate from A2 (from 1.5 to 1.1), but increases for the inertinite concentrate from B2 (from 1.0 to 1.2), as the inertinite level is raised from 25 to 37 %(wt).

Comparing the blends as matching pairs, e.g. BA with AB, it is most striking that quite large difference exist for the interface qualities amongst the pairs at 25 %(wt) inertinite, whereas they tend to be rather similar at 37 %(wt) inertinite. At 25 %(wt) inertinite the vitrinite is predominately derived from the vitrinite concentrate, while at 37 %(wt) there is a much more even split between vitrinite and inertinite concentrate derived vitrinite. Assuming that the inertinites differ to a lesser extent than the vitrinites between the different coals, as seems reasonable from the estimated pure maceral properties in appendix 1, this may offer a possible explanation. Inspection of table 4.30 supports this view. It shows that the variation in interface quality for the reactive-reactive, i.e. vitrinite derived, components is large within the pairs, whereas for the most part it is relatively small for the inerts of both sizes.

This leads to suspect that the total interface quality is dominantly influenced by the reactivity or bonding ability of the vitrinites in a blend. The total interface quality in a blend would thus strongly depend on the proportions of the vitrinite originating from the different coals in it. With regard to inerts, their origin appears to be of lesser importance, whereas the total amount of them in the blend obviously plays a vital role.

4.9 The Effect of Coking Additives on Coke Component Interfaces

Having investigated the effects of the inerts derived from material occurring naturally in coal in part 4.7, this section attempts to explore the effect of adding supplementary inerts and semi-inerts. Apart from the interaction of the reactive coke components with these additives, it is of some interest whether their addition influences the interfacial behaviour between the reactivities themselves and with the coal derived inerts, and, if this is the case, in what manner. For this purpose the third series of cokes was prepared using two additives, a petroleum coke (ADD1) and a calcined anthracite (ADD2).

4.9.1 Additive Incorporation

Analogous to the process of estimating the theoretical amount of solid coke residue derived from the inertinite fraction in series 2.1 as outlined in section 4.6, the theoretical percentage of coke derived from the additives, assuming complete loss of volatile matter for both, coals and additives, and a negligible difference in densities between them, is calculated. A correction had to be made for the calcined anthracite (ADD2), as a 500 point component count on the pure additive showed that 22.7 %(vol) of it is composed of components other than the anthracitic one, mainly inerts and isotropic material.

Figures 4.17 a) and b) show that for all single coal samples of the third series there is a linear increase in the difference between the calculated and counted amount of additive in the coke with the weight percent added to the coal prior to carbonisation. There does not appear to be a limit beyond which no further additive particles can be taken in, as would be indicated by a disproportionate increase in the difference between the calculated and the counted additive content with increasing addition levels. But for some of the samples coherence was very poor. Illustrating this, for all samples of coal A3, but the additive-free one, and the for the samples of coal B3 with 50 %(wt) additive, friability testing was impossible. For another two samples the friability weight loss approached 100%. To what extent incorporation of the additive into the coke matrix can be talked of in these cases is questionable, as there is obviously only a loose association rather than cohesion between the coke components and the additives.

Figures 4.17 a and b show that there are significant differences in the proportion of the calculated additive which is actually perceived in the sample by counting between the two additives and between the different precursor coals

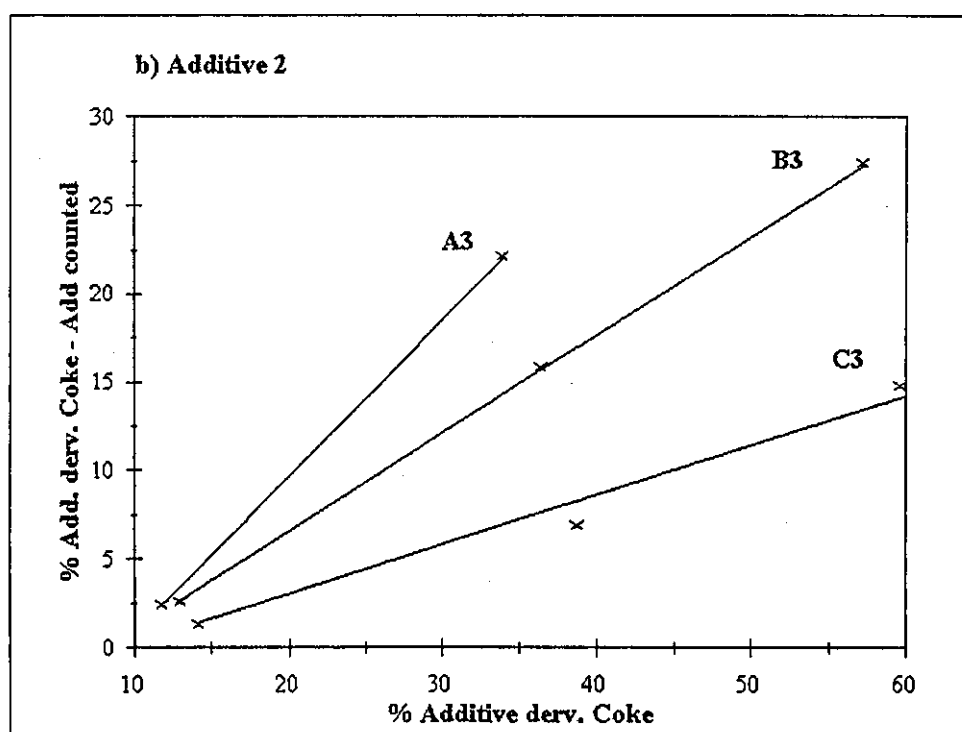
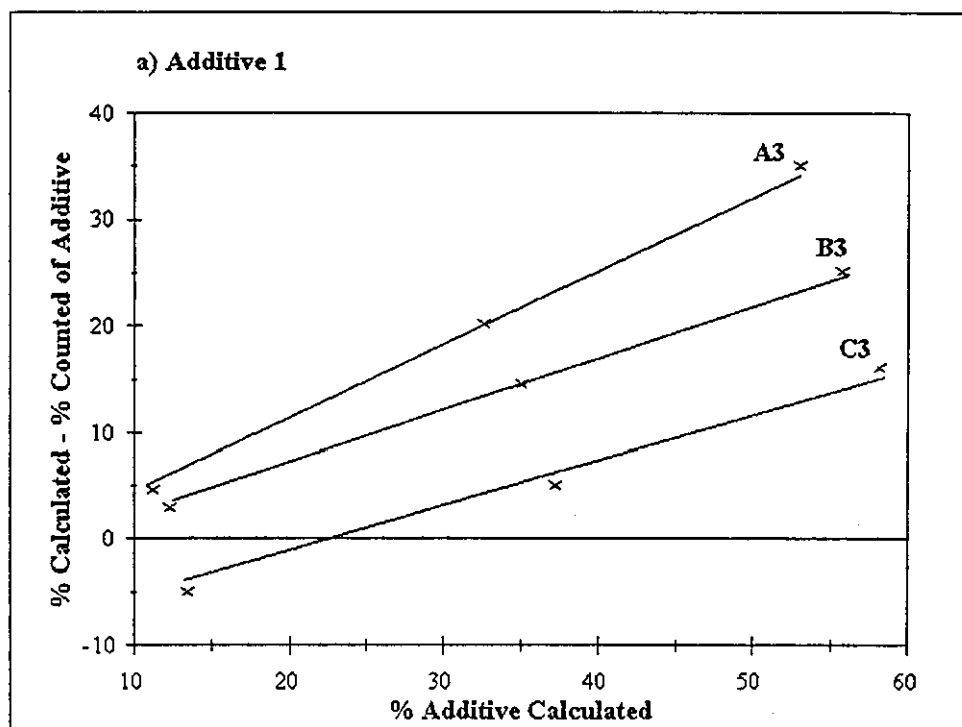


Figure 4.17 Additive Derived Coke Fraction not Counted as Additive Component in Series 3

Referring to the coal properties given in table 3.1, for the samples investigated here the amount of additive a coal appears to be able to incorporate into its coke on carbonisation increases with decreasing rank and with increasing dilatation, i.e. increasing plasticity.

Another possible relation is that of additive incorporation with the level of natural, or coal derived, inerts in the sample. Assuming a limited ability of the reactive components to incorporate inerts, a high level of coal derived inerts may take up too much of this ability for additives to be incorporated effectively. The progression of the amount of inerts counted in the additive-free samples is indeed the same as for decreasing additive incorporation. But it is doubtful if differences of that magnitude, 17.9 % for coal A3 to 14.2 % for coal C3, could have a sufficiently large impact.

4.9.2 Relative Participation in Interfaces

Table 4.31 compares the ratios of the percentage participation in interfaces to the combined volume of the components in question. For small inert and additive particles the ratio is consistently higher for the coal derived inerts, indicating either their greater readiness to interface or their smaller average unit size, i.e. greater surface area available for interfacing relative to their volume. For the large inert and additive particles there is no clear trend. In the samples from coal A3 the ratios for the coals inerts are higher, in those from coal C3 the ratios for the additive particles and in those from coal B3 a cross-over from one to the other occurs for both additives. This could be an indication that the average unit sizes of large inerts vary between the coals, as their interface frequency to volume ratio varies relative to the additives, which have been prepared in the same way for all samples and are likely to have identical size distributions. By that argument, given the same size distribution, the ratios should be constant for the additives for all coals. Whereas the ratios for any one coal are fairly consistent, independent of which additive is considered and at which level of addition, the differences between the coals are quite marked. There must therefore be a property of the reactive components that varies correspondingly, which is either their unit sizes (surface area to volume ratios) or a difference in some inherent inclination or readiness to interface with inerts. The reactive components vary in both, size and binding power, but the trends are so similar that it is not possible to distinguish between their effects. The only observation indicating that, where participation in interfaces is concerned, irrespective of the quality of the interfaces formed, component unit sizes are more likely to be the dominant factor, is that the ratios between the two additives for the same coal do not differ significantly. Whereas the size distribution of the additives are expected to be fairly similar, their reactivities or fusibilities were expected to differ to some extent.

Patrick and Stacey [49] have linked volatile matter contents to the reactivity of additives, according to which the petroleum coke at 10.3 % (daf) volatile matter should be more reactive than the anthracite, which, even before calcination, only contained 4.8 %. This might lead to the conclusion that given sufficient overall binding power of the coke matrix forming components to incorporate additives, the number of interfaces formed per unit volume of additive depends on the average unit sizes of the reactive components and additive particles.

		%vol Interfaces / %vol interfacing Components						
		ADD1			ADD2			
		10	30	50	10	30	50	
A3	R-R	0.25	0.31	0.27	0.30	0.25	0.25	
	R-S	0.58	0.47	0.43	0.40	0.43	0.42	
	R-L	0.09	0.06	0.08	0.05	0.07	0.10	
	R-ADDS	-	0.09	0.17	0.25	0.20	0.21	
	R-ADDL	-	0.00	0.04	0.03	0.03	0.02	
B3	R-R	0.22	0.19	0.18	0.21	0.15	0.14	0.16
	R-S	0.62	0.48	0.49	0.44	0.48	0.43	0.48
	R-L	0.10	0.08	0.10	0.10	0.09	0.09	0.09
	R-ADDS	-	0.22	0.35	0.39	0.30	0.37	0.45
	R-ADDL	-	0.07	0.11	0.14	0.05	0.13	0.12
C3	R-R	0.15	0.14	0.10	0.15	0.11	0.10	0.14
	R-S	0.72	0.74	0.61	0.71	0.57	0.61	0.62
	R-L	0.06	0.03	0.06	0.05	0.05	0.07	0.08
	R-ADDS	-	0.24	0.51	0.56	0.29	0.40	0.46
	R-ADDL	-	0.07	0.16	0.15	0.09	0.11	0.16
BL3	R-R	0.27	0.20	0.20	0.25	0.23	0.19	0.21
	R-S	0.53	0.53	0.40	0.37	0.45	0.49	0.52
	R-L	0.09	0.07	0.09	0.08	0.06	0.09	0.09
	R-ADDS	-	0.18	0.49	0.44	0.20	0.25	0.38
	R-ADDL	-	0.08	0.10	0.09	0.06	0.08	0.12

Table 4.31 Ratio of Interface Frequency to Combined Volume Percentage of the Interfacing Components for Series 3

4.9.3 Variation of Total Interface Quality Index with Additive Levels

4.9.3.1 Additive 1

Table 4.32 summarises the total interface quality indices for the samples in the third series. It can be seen that the three coals and their blend react in different manners to the addition of the petroleum coke (ADD1). For coal A3 an improvement of the total interface quality index at all three levels of addition is achieved, which is highest for the 10 %(wt) addition, rising from 1.78 to 2.64. It then slumps to 1.83 at 30 %(wt) and recovers to 2.08 at 50 %(wt). The behaviour of the blend is similar to that of coal A3 insofar as the interface quality is better for all samples containing additive 1 than for the additive-free sample. It peaks at the 10 %(wt) addition level with an IQIt of 3.43, but falls thereafter to 2.75 at 30 %(wt) and 2.74 at 50 %(wt), which is only slightly above the additive-free value.

Addition of the petroleum coke to coal B3 causes a deterioration in IQIt. This is most marked for the initial addition of 10% of the additive, which causes a fall from 2.86 to 2.20. It remains virtually constant on increasing the amount of additive to 30 % and then further falls to 2.10 for the 50 % addition level.

The variations in IQIt are largest for coal C3. On addition of 10% of petroleum coke its IQIt increases steeply from 4.73 to 7.21. This is followed by an even more drastic decline to 2.75 for the 30 % addition, which acutally falls below the additive-free value. The IQIt further deteriorates to 2.74, about half the value of the additive-free sample.

IQIt		0	10	30	50
	%(wt) Additive				
ADD1	A3	1.78	2.64	1.83	2.08
	B3	2.86	2.20	2.21	2.10
	C3	4.73	7.21	4.65	2.35
	BL3	2.68	3.43	2.75	2.74
ADD2	A3	1.78	1.79	2.00	-
	B3	2.86	1.93	1.60	1.42
	C3	4.73	5.47	2.23	2.10
	BL3	2.68	2.33	1.71	1.66

Table 4.32 Total Interface Quality Indices for Series 3

4.9.3.2 Additive 2

The effect of the calcined anthracite (ADD2) is almost universally adverse on the total interface quality index. The only exceptions are coal A3, where the addition leads to a slight improvement (from 1.78 to 1.79 at 30 % and 2.00 at 50 %) and the 10 % addition to coal C3, which has a markedly beneficial effect raising the IQIt from 4.73 to 5.47. In the samples of coal B3 and the blend there is a clear trend of progressive worsening of the total interface quality index with increasing additive levels.

4.9.3.3 Comparison of the Additives

Comparing the effects of the two additives it can be seen from table 4.32 that at all addition levels for all coals and the blend the effect of the calcined anthracite (ADD2) is either less beneficial or more detrimental on the overall interface quality index than that of the petroleum coke (ADD1). This difference was expected from the perceived reactivities of the additives in terms of softening ability and fusibility. Reactivity has been linked to the volatile matter contents of additives in previous work [36], and at 10.3 % VM (daf) the petroleum coke would clearly be expected to be more reactive than the anthracite, which, even before calcination, only contained 4.8 %.

4.9.3.4 Influence of Changes in Component Composition

As the component composition depends on the overall properties of the carbonisation system, such as plasticity, it may well be changed by the use of additives. It should therefore be investigated if there are variations in component composition which correspond to or even could explain the variations found for interface quality with increasing amounts of additives.

Table 4.33 displays the deviation in the textural component composition of the reactive material of the additive containing samples (on an inert- and additive-free basis) from the additive-free samples. Although certain variations seem to be predominant in each single coal sample set, they rarely follow a progressive trend with increasing additive levels.

The almost universal trend in coal A3 is from granular flow to broad flow. From their relative binding powers estimated in section 4.3 this should be accompanied by a deterioration in interface quality, if the reactive component binding powers were the main determining factor for total interface quality. In reality the reverse occurred.

The reactive component composition may however offer an explanation as to why the interface quality for A3 improves as the amount of ADD1 is increased from 30 to 50 % (wt).

% Add.	ADD1				ADD2		
	0	10	30	50	10	30	50
A3							
BF	38.0	53.3	56.1	52.8	41.1	52.4	
SF	8.5	7.1	5.9	6.3	6.9	5.3	
GF	43.0	30.8	29.1	29.3	46.4	35.2	
CM	4.1	3.0	4.6	4.7	3.5	4.1	
MM	1.9	1.8	1.6	3.0	1.0	1.4	
FM	0.3	0.1	0.3	0.0	0.0	0.0	
ISO	2.1	1.0	1.4	1.5	1.0	1.4	
B3							
BF	2.5	2.0	2.0	2.0	4.6	4.4	2.4
SF	1.3	1.0	1.2	0.8	0.8	1.6	1.1
GF	44.2	40.2	31.1	31.4	42.4	32.8	38.8
CM	25.0	23.0	27.5	30.6	24.9	35.2	34.5
MM	20.4	25.5	29.4	23.3	22.2	20.7	16.3
FM	2.8	5.4	4.3	6.9	3.8	3.7	2.7
ISO	3.8	2.8	4.5	5.0	1.4	1.5	4.2
C3							
BF	2.0	1.2	0.7	0.4	2.0	1.1	1.8
SF	0.1	0.7	0.4	0.0	0.1	0.3	0.2
GF	49.9	51.3	42.9	33.0	46.5	41.0	40.8
CM	32.5	25.9	29.1	33.6	33.6	27.1	29.1
MM	10.3	17.4	24.2	23.6	12.2	21.6	15.9
FM	1.0	1.3	0.5	2.1	1.0	3.5	3.8
ISO	4.2	2.2	2.3	7.3	4.6	5.4	8.2
BL3							
BF	17.4	11.7	12.9	19.5	14.6	14.3	18.5
SF	2.2	2.4	2.9	2.3	1.5	1.0	2.5
GF	36.8	48.5	40.2	26.1	39.6	33.5	42.7
CM	22.3	17.5	18.7	21.0	21.4	26.2	20.5
MM	16.2	14.7	17.6	20.6	16.5	17.3	10.0
FM	2.5	1.4	3.2	5.2	2.5	3.4	1.5
ISO	1.9	3.5	4.4	4.5	3.8	4.2	4.3

Table 4.33 Deviation of the Textural Component Composition (%vol)from the Additive-free Samples in Series 3

Firstly, the granular to broad flow shift is largest for the 30 %(wt) sample, so that it could be argued that the interface quality at 30 %(wt) is unexpectedly low because of that, rather than that of the 50 %(wt) one being unexpectedly high. Secondly, for the 50 % sample there is a minor shift towards medium mosaic not present in any of the other samples of coal A3. The binding power associated with medium mosaic is far above that of the dominant components and may suffice to counteract the effect of additional additive particles. A good argument for the importance of the textural component composition for interface quality is found in the 10 %(wt) ADD2 sample of coal A3. Its composition resembles most closely that of the additive-free sample and they have virtually identical total interface quality indices. The predominant trend for the component composition in coal B3 is from granular flow to mosaics, in the case of ADD1 mainly medium mosaics. This should theoretically have a beneficial effect on interface quality, which in reality has not been observed. It could be that, even though the shift seems minor in comparison, this is due to the increase in fine mosaic and in the case of the 50 %(wt) sample isotropic material, which both have worse binding powers than granular flow. Viewed as a contributing factor in conjunction with the effect of the additive, the component shifts are consistent with the interface qualities observed. The 10 and 30 %(wt) samples having almost identical interface quality indices could be explained by the stronger shift towards medium mosaic counteracting the effect of additional additive particles in the 30 %(wt) sample. The ensuing deterioration for the 50 %(wt) sample may partially arise from the shift towards medium mosaic being weakened in favour of that towards coarse and fine mosaics, which are associated with lower binding powers. The interface qualities for the B3 samples with ADD2 being worse than those for ADD1 is consistent with the absence of the trend towards medium mosaic. An exception to this is the 10 %(wt) sample, where the deviation from the additive-free sample is again comparatively small and the shift towards medium mosaic is superseded by the one to broad flow. For the 30 and 50 %(wt) ADD2 samples of coal B3 the main shift is from granular flow to coarse mosaic, which again fails to yield the theoretical improvement in interface quality probably by a combination of being too weak to balance the extra inerts and by being opposed by smaller shifts to components of poorer binding power, namely broad flow and isotropic.

In the ADD1 samples of coal C3 there is a strong trend towards medium mosaics, which should improve interface quality. However, even though it is much more marked for the 30 and 50 %(wt) samples, particularly as for them it is from mainly granular flow rather than from coarse mosaic as in the 10 %(wt) sample, the expected improvement only takes place for the 10 %(wt) sample. In this case the explanation clearly has to be that component shifts of the order observed here are

secondary to the effect of added inert or semi-inert material. This, in fact, is in line with the binding power theory, if it is assumed that the binding powers of the additives are of the same order of magnitude as those of the coal derived inerts. Referring to table 4.15 it is envisaged that any variation in the amount of inerts would have a far greater impact than a shift from one reactive component to another. The difference in binding power was estimated to be much larger between reactives and inerts than between any two reactive components.

For the addition of ADD2 to coal C3 the component shifts and interface qualities correspond reasonably well. The shift from granular flow to coarse and medium mosaic for the 10 %(wt) sample is likely to contribute to its improved interface quality relative to the additive-free sample. Although a shift towards medium mosaic persists for the 30 %(wt) sample, it is opposed by shifts from coarse mosaic and towards fine mosaic and isotropic. Further deterioration in interface quality would be duly expected for the 50 %(wt) sample, where the shift is actually from medium mosaic and very markedly towards isotropic.

For the blend no clear trends can be identified. The variations, with few exceptions, seem more random than those for the single coals. This is undoubtedly because the trends for the different coals to some extent oppose and cancel one another. The most striking example for this is that for the 10 %(wt) addition of ADD1, for which there is a strong shift towards granular flow composed almost equally from a decrease in broad flow and in mosaics.

4.9.4. Individual Interface Quality Indices for Inerts and Additives

4.9.4.1 Inerts

Table 4.34 compares the individual interface quality indices for small and large coal derived inerts, IQIs and IQIL, for samples containing different amounts of the additives. Although they appear to be affected to some extent, the variations do not follow any identifiable trend. Most significantly, the interface quality of the coal derived inerts improves as often as it deteriorates with the addition of the petroleum coke or anthracite. This is not completely random. The cases where an improvement was observed concentrate at the 10 and 30 %(wt) addition levels, with only three such cases being observed at 50 %(wt) addition, opposed to 10 and 7 respectively for 10 and 30 %(wt). This could be taken as evidence that the interface quality index of the coal derived inerts is more likely to fall below its value in the additive-free sample at higher levels of addition. Also, more of the cases of improving interface quality are found in the samples with petroleum coke (ADD1), accounting for 15 of the 20 cases in total. This implies that interface quality is more likely to improve due to the

addition of a less inert additive. But the above observations are purely statistical and do not correspond to any trend for any of the coals.

		ADD-free	10 % ADD	30 % ADD	50 % ADD
IQIs					
A3	ADD1	1.21	1.40	1.07	1.07
	ADD2		1.12	1.13	-
B3	ADD1	1.98	1.79	2.11	1.66
	ADD2		2.27	2.17	1.83
C3	ADD1	4.87	7.80	8.53	2.93
	ADD2		9.05	4.33	3.81
BL	ADD1	1.97	2.70	3.81	2.50
	ADD2		2.40	1.80	1.62
IQII					
A3	ADD1	0.65	1.10	0.86	1.24
	ADD2		0.49	0.61	-
B3	ADD1	1.16	0.80	0.94	0.74
	ADD2		0.89	0.92	0.95
C3	ADD1	1.36	2.39	2.46	1.33
	ADD2		5.70	1.32	1.27
BL	ADD1	1.14	1.52	1.50	1.63
	ADD2		1.00	0.99	1.05

Table 4.34 Individual Interface Quality Indices for Small and Large Coal Derived Inerts

4.9.4.2 Additives

Table 4.35 shows the variations in the individual interface quality indices for small and large additive particles, IQIas and IQIal. It would be expected that the reactive components would experience increasing difficulties in incorporating additional non- or weakly reactive particles, given a limited ability of them to incorporate inerts. This would be reflected by a deterioration of the quality of the interfaces formed at higher levels of addition. On the whole this holds true insofar as, with the exception of the samples from coal A3 and large particles of ADD1 in coal B3, the interface qualities are worse at 50 % (wt) than at 10 % (wt) addition. But there is no clear trend of decreasing interface quality with increasing addition levels, as for quite a significant number of samples interface quality for reactive - additive interfaces increases from the 30 to 50 % (wt) addition level.

		10 % ADD	30 % ADD	50 % ADD
IQIas				
A3	ADD1	0.42	0.73	0.80
	ADD2	1.00	1.18	-
B3	ADD1	1.48	1.31	1.28
	ADD2	0.81	0.73	0.76
C3	ADD1	5.75	3.85	1.97
	ADD2	3.41	1.28	1.37
BL	ADD1	3.05	1.82	1.85
	ADD2	1.21	0.74	1.03
IQIal				
A3	ADD1	0.07	0.59	0.42
	ADD2	0.50	0.57	-
B3	ADD1	0.66	1.15	1.30
	ADD2	0.41	0.49	0.23
C3	ADD1	2.03	1.39	0.91
	ADD2	0.75	0.32	0.39
BL	ADD1	1.50	1.11	1.07
	ADD2	0.52	0.40	0.25

Table 4.35 Individual Interface Quality Indices for Small and Large Additive Particles

4.9.4.3 Variation between Coals

Figures 4.18 a-h depict the individual interface quality indices for inerts and additives for each of the three coals. They show that the differences between the coals are more systematic and consistent than those between the different percentages of additives used. With only two exceptions the interface quality increases in the order A3 - B3 - C3. This supports the view that the reactivity of a coal, in terms of its ability to soften, fuse and incorporate inerts, is in some way linked to its volatile matter content and plastic properties. The order of the individual interface qualities is identical to that of increasing volatile matter content and dilatation for the coals considered here. From the component binding power theory formulated in section 4.3 a less certain prediction could be made. The worst interface qualities would be expected for coal A3, as its main textural components are all of the flow type. In most samples broad flow, which has the poorest binding power of the three flow type components, occurs with the greatest frequency. But the difference between coals B3 and C3 would be expected to be less marked, as they share the same main components, namely granular flow and coarse and medium mosaic. This must be taken as evidence that factors other than binding power play an equally important role in determining the quality of the interfaces with inerts and additives. In the case of the coal derived inerts it could be argued that, as the volatile matter content of the maceral groups varies analogous to the overall volatile matter content [112], the inertinite of coal C3 has a larger volatile matter content and its reactive components are thus likely to deal with 'more reactive inerts'. But this would not explain why the difference persists for almost all of the interfaces with the additives.

The two exceptions to the A3 - B3 - C3 order of increasing interface quality are the particles of ADD2 of both sizes. Small particles of ADD2 appear to be incorporated better into coal A3 than coal B3. The large particles of ADD2 are very poorly incorporated into all three of the coals. Their interface quality indices centre around 0.5 irrespective of the coal they were added to. This may indicate that, although for most cases encountered here the reactivity of the coal appears to be the dominant factor in determining the interface quality, the situation could be reversed by choosing an additive that is sufficiently difficult to incorporate. It could well be envisaged that for a truly inert material interface quality would deteriorate rapidly with the amount of larger particles added. This may become particularly significant when particles in the millimetre size range are considered, rather than particles reduced to below 212 μm as used for this investigation. Such an effect corresponds well with the findings of previous investigations into the effects of additive particle size [22].

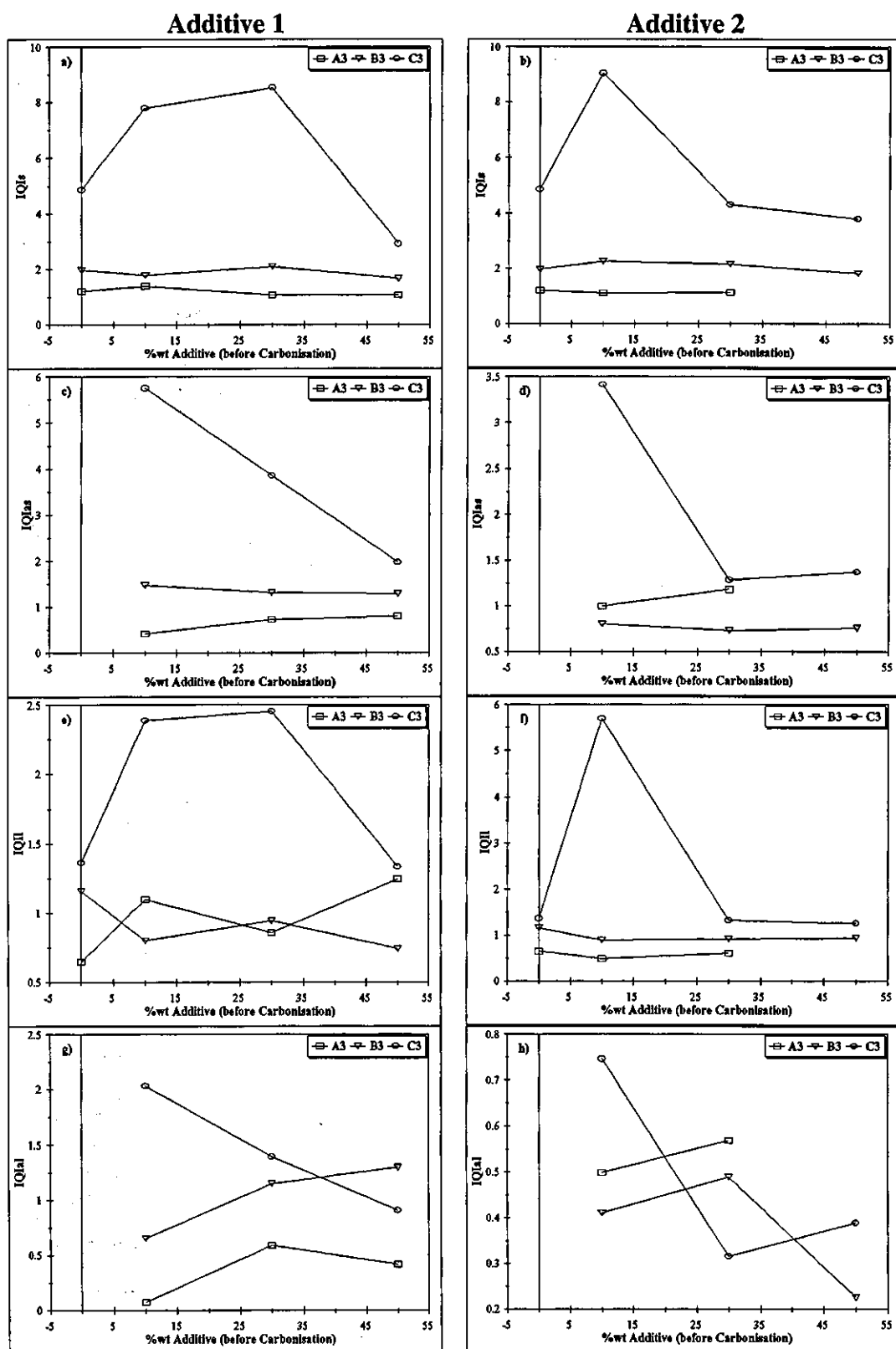


Figure 4.18 Variation of the Individual Interface Quality Indices in Series 3

4.9.4.4 Relation of Total to Individual Interface Quality Indices

The mathematical relation between the individual and the total interface quality indices has been shown in section 4.1.3 by equation 4.1.7. It is not as simple as might have been expected, as the frequencies of the individual interface combinations have to be taken into account. Each combination in the equation 4.1.7 is represented by a term in the nominator (N_t) and a term in the denominator (D_t).

$$N_t = \frac{IQ_{Ix} * N * p_x}{IQ_{Ix} + 1} \quad (4.9.1)$$

$$D_t = \frac{IQ_{Ix} * p_x}{IQ_{Ix} + 1} \quad (4.9.2)$$

Calculating the terms of the nominator and denominator derived from each of the individual interface type indices can be used to gain some idea of their relative contributions to the total amount of good and poor interfaces and hence estimate their influence on the overall interface index. This was necessary as the data obtained from the interface counts shows that the individual interface quality indices follow only in very few cases the same trend as the total one.

The terms in the nominator (N_t) and denominator (D_t) appertaining to the individual interface types, reactive-reactive (R-R), reactive-small inerts (R-S), reactive-large inerts (R-L), reactive-small additive particles (R-AS) and reactive-large additive particles (R-AL), were calculated. Their terms in the nominator represent their relative contributions to the sum of good interfaces, their terms in the denominator those to the sum of poor interfaces. The results are compiled in tables 4.36 a and b. The first insight that can be derived from this treatment of the data is that the contributions of large particles of inerts and additives are very small throughout and very rarely seem to exercise any significant influence on the total interface quality index. This point is worth mentioning as there is the temptation to overestimate their importance, as they persistently form the worst interfaces. The importance given to them may be appropriate when the physical properties of the cokes are considered, but not for interface quality indices.

The relative contributions of the remaining interface types to the total interface quality index varies between the coals. The improvement in interface quality in coal A3 can clearly be attributed to the effect of reactive - reactive interfaces. The trend is strong enough to counterbalance slight decreases in the quality of interfaces with small inerts and negative contributions by small additive particles. No explanation can be offered for this improvement in reactive-reactive interfaces, as the textural component shift outlined in section 4.9.3.4 would lead to expecting the opposite effect.

a) Nt								IQIt
ADD1	% ADD		R-R	R-S	R-L	R-AS	R-AL	
A3	0	N	0.33	0.28	0.03			1.78
		D	0.08	0.23	0.05			
	10	N	0.45	0.22	0.03	0.02	0.00	2.64
		D	0.03	0.16	0.03	0.05	0.00	
	30	N	0.37	0.18	0.03	0.06	0.01	1.83
		D	0.05	0.17	0.04	0.08	0.02	
	50	N	0.41	0.16	0.02	0.09	0.01	2.08
		D	0.03	0.15	0.02	0.11	0.02	
B3	0	N	0.33	0.36	0.05			2.86
		D	0.03	0.18	0.04			
	10	N	0.27	0.26	0.03	0.11	0.02	2.20
		D	0.02	0.15	0.04	0.07	0.03	
	30	N	0.23	0.23	0.04	0.15	0.04	2.21
		D	0.01	0.11	0.04	0.11	0.04	
	50	N	0.25	0.18	0.03	0.16	0.06	2.10
		D	0.01	0.11	0.04	0.12	0.05	
C3	0	N	0.22	0.57	0.03			4.73
		D	0.03	0.12	0.02			
	10	N	0.18	0.50	0.02	0.15	0.04	7.21
		D	0.01	0.06	0.01	0.03	0.02	
	30	N	0.11	0.34	0.02	0.28	0.07	4.65
		D	0.01	0.04	0.01	0.07	0.05	
	50	N	0.12	0.28	0.02	0.23	0.05	2.35
		D	0.02	0.09	0.01	0.12	0.06	
BL	0	N	0.37	0.31	0.05			2.68
		D	0.07	0.16	0.04			
	10	N	0.27	0.32	0.04	0.11	0.04	3.43
		D	0.02	0.12	0.02	0.04	0.03	
	30	N	0.22	0.21	0.04	0.23	0.04	2.75
		D	0.03	0.05	0.02	0.13	0.04	
	50	N	0.28	0.18	0.04	0.21	0.03	2.74
		D	0.03	0.07	0.02	0.11	0.03	

b)Dt								IQIt
ADD2	% ADD		R-R	R-S	R-L	R-AS	R-AL	
A3	0	N	0.33	0.28	0.03			1.78
		D	0.08	0.23	0.05			
	10	N	0.34	0.19	0.02	0.08	0.01	1.79
		D	0.05	0.17	0.04	0.08	0.02	
	30	N	0.35	0.18	0.03	0.09	0.01	2.00
		D	0.03	0.16	0.06	0.08	0.01	
B3	0	N	0.33	0.36	0.05			2.86
		D	0.03	0.18	0.04			
	10	N	0.22	0.28	0.04	0.11	0.01	1.93
		D	0.01	0.12	0.04	0.14	0.03	
	30	N	0.20	0.23	0.03	0.12	0.03	1.60
		D	0.01	0.11	0.04	0.17	0.07	
C3	0	N	0.22	0.57	0.03			4.73
		D	0.03	0.12	0.02			
	10	N	0.17	0.43	0.04	0.18	0.03	5.47
		D	0.01	0.05	0.01	0.05	0.04	
	30	N	0.12	0.35	0.03	0.17	0.02	2.23
		D	0.01	0.08	0.02	0.13	0.07	
BL	0	N	0.15	0.30	0.03	0.17	0.03	2.10
		D	0.01	0.08	0.02	0.13	0.09	
	10	N	0.37	0.31	0.05			2.68
		D	0.07	0.16	0.04			
	30	N	0.30	0.27	0.03	0.09	0.02	2.33
		D	0.06	0.11	0.03	0.07	0.03	
	50	N	0.25	0.24	0.04	0.08	0.02	1.71
		D	0.03	0.14	0.04	0.11	0.05	
		N	0.24	0.20	0.03	0.13	0.02	1.66
		D	0.01	0.13	0.03	0.13	0.08	
		N						
		D						

Table 4.36 Relative Contributions of the Interface Types to the Total Interface Quality Index

No simple trend could be found for coal B3, where the relative importance of the interface types appears to vary with the amount of additive incorporated. The initial deterioration due to a 10 %(wt) addition of either additive can be attributed to a fall in interface quality for reactive-reactive interfaces and for interfaces with small inerts. On further addition the two additives produce different effects. For ADD1 the total interface quality remains almost constant on increased addition to 30 %(wt) due to an improvement in the interfaces with small additive particles balancing out the fall in quality of interfaces with small inerts. Increasing the amount of additive to 50 %(wt) a further fall in interface quality for small inerts is supplemented by a negative contribution by large additive particles. For ADD2 moving from 10 to 30 %(wt) addition produces a fall in total interface quality, reflected by interfaces of both small particles and already receiving a noticeable negative contribution by large additive particle. The further deterioration in IQIt for a 50 %(wt) addition appears to be followed by all interface types.

For coal C3 all interface types more or less follow the same trend. Nevertheless their relative contributions to the IQIt differ between the different levels of additive content. For ADD1, although there is a strong contribution of the small additive particles, at 10 and 30 %(wt) the variation in quality for reactive-reactive interfaces and for those involving small inerts appear dominant, whereas at 50 %(wt) the variation for small and large additive particles is more marked. For ADD2 the contribution of small additive particles is quite significant at 30 %(wt), but does not change on the further increase of addition to 50 %(wt), for which large additive particles show the greatest variation.

For the blend there is a much less consistent picture. For ADD1 reactive-reactive interfaces and interfaces with small inerts mainly account for the fall in total interface quality at 10 %(wt), whereas the main contributor to the continuing deterioration at 30 %(wt) are small additive particles. At 50 %(wt) an improvement in the quality of reactive-reactive interfaces partially balances the fall in that for small inerts. For ADD2 the initial fall in total interface quality is mainly due to worse interfaces between the reactive components, which then at 30 %(wt) actually improve again. This is not reflected by the IQIt as it is superseded by a deterioration of the interfaces involving both types of small particles. The further decrease in interface quality at 50 %(wt) addition can be mainly attributed to small inerts, with a significant contribution by large additive particles, but opposition from an improvement in IQI for small additive particles.

4.10 Interface Quality and Coke Properties

A first speculative attempt was made to relate the total interface quality indices of the cokes to the few available data on the mechanical properties of the cokes. The obvious difficulty with this is the same that has previously been pointed out for the textural components [22], namely that they cannot be varied independently. Therefore no proof can be undertaken to determine whether any relation is direct, secondary or even dependent on other factors which coincidentally vary analogous to interface quality. If the interface quality of the textural components of the samples is a truly independent parameter, which has a significant bearing on the macro-properties of the cokes, then there should be a general relationships irrespective of the nature of the precursor coals and additives used.

4.10.1 Tensile Strength (Series 1)

For the cokes of series 1 tensile strength results obtained by diametral compression testing were available [9]. These have been plotted against the total interface quality indices of the cokes in figure 4.19. Superficially it would be expected that if there is a relation between interface quality and coke strength it should be such that an increase in interface quality would result in an increase in coke strength. This trend is mostly followed by the plot obtained. Coke F1 however deviates strongly from it, its interface quality being such that a much greater tensile strength would be expected.

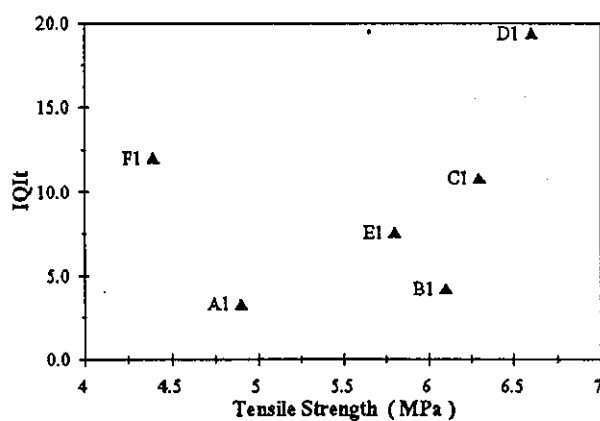


Figure 4.19 Total Interface Quality versus Tensile Strength for the Cokes in Series 1

The interface quality - coke strength relation might in fact not be straightforward [98]. The effect of an interface on total strength does not depend on the absolute strength of the bonding across it, but on its bonding strength relative to the cohesive strength of the adjacent material. Above a certain difference an interface will withstand crack propagation along it and a crack will cross it propagating into the material on the other side, which makes the solid behave in a brittle manner. Below a certain difference the interface will be pulled apart and the crack will change direction propagating along the interface, which may lead to crack arrestment. To a certain extent weak bonding, relative to the inherent strength of the components, may actually be beneficial.

As the quality of the interfaces is judged by their optical appearance and no method has as yet been developed to investigate their individual strength, nor that of the components, the difference in strength between components and their interfaces cannot be tested. Interfaces of the same optical appearance may differ significantly in strength, depending, for example, on the extent of chemical bonding across them. Equally, interfaces of identical quality may have opposing effects on the coke strength depending on the components between which they occur. This may account for the deviations of cokes B1 and F1 from the simple trend expected.

4.10.2 Friability (Series 2 and 3)

It is attempted to relate the percentage weight loss on friability testing by the method described in section 3.2 to the total interface quality index of the cokes in series 2 and 3. Friability data is only available for part of the samples, as in most cases in series 2 and some cases in series 3 the cokes were so incoherent that they would crumble on touch. It would be expected that, if there is a relation between friability and interface quality, the friability weight loss would increase with deteriorating interface quality. Poor interfaces would be expected to introduce weak points into the coke structure, encouraging breakage.

4.10.2.1 Series 2

In figure 4.20 the total interface quality index is plotted against friability weight loss for the few cokes of series 2, which were coherent enough to be tested. There appears to be a general tendency for friability weight loss to increase with decreasing interface quality. But this trend is very weak and it is more than likely from this that interface quality may well be one of the factors affecting friability weight loss, but that there are other influences diluting the trend sought for.

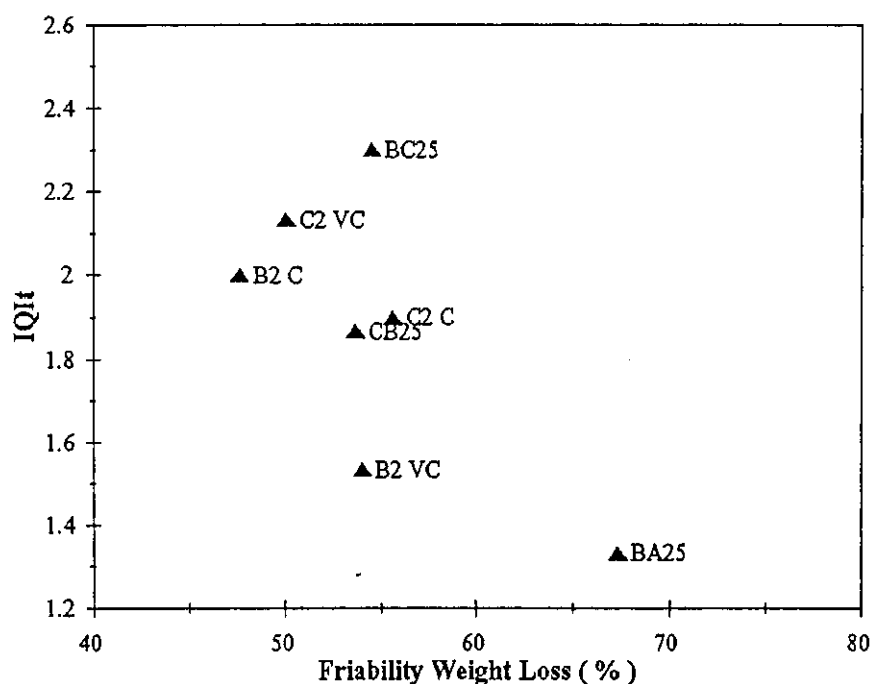


Figure 4.20 Total Interface Quality versus Friability Test Weight Loss for the Cokes in Series 2

4.10.2.2 Series 3

Figure 4.21 shows the relationship between the total interface quality indices for the coke samples in series 3 and their friability weight losses. The additives are indicated by the numbers 1 (for the petroleum coke) and 2 (for the calcined anthracite), the additive-free samples by 0. Although the trend is not very clear, there appears to exist a general relationship holding true for the samples from different coals and with the different additives. Similar IQIt are found in samples incurring similar friability weight losses, implying that interface quality can be regarded as an independent parameter influencing coke properties. Again, as the trend is very weak, it is more than likely that interface quality is one of the contributing factors affecting friability weight loss, rather than the sole responsible one.

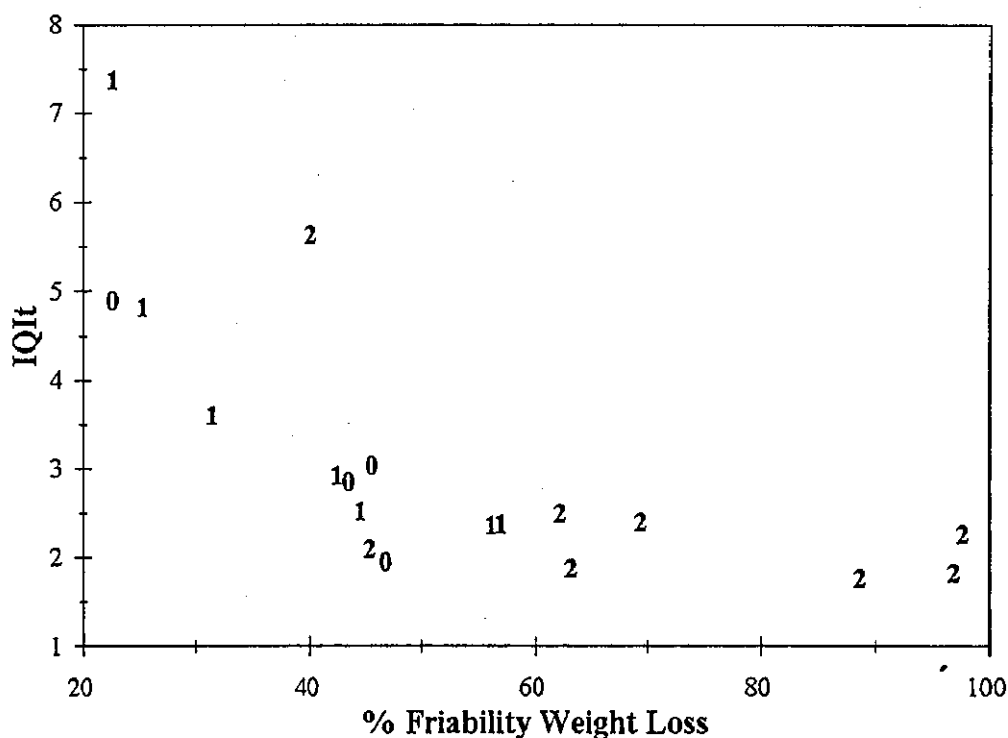


Figure 4.21 The Relation between Friability Weight Loss and Total Interface Quality Index for Samples in Series 3

5 Discussion

5.1 The Nature and Origin of the Interfaces

Part 4.1 of this thesis describes the optical appearances of the interfaces between the micro-textural components of metallurgical cokes, according to which they have been classified. Optical microscopy however does not yield any information on the nature of the interfaces at molecular level, so that the bonding associated with the different types of interfaces is not known. In part 2.5 the literature on bonding mechanisms at interfaces in other (composite) materials was reviewed, which pointed towards the gaps in knowledge concerning the coke component interfaces. Definitions, or at least good estimates, for bonding mechanisms for materials such as metal matrix composites [101] and anode carbons for aluminium manufacture [102] have been attempted. This was possible because the atomic or molecular structures at the surfaces of those materials were known to some extent. For the coke components no such information is available.

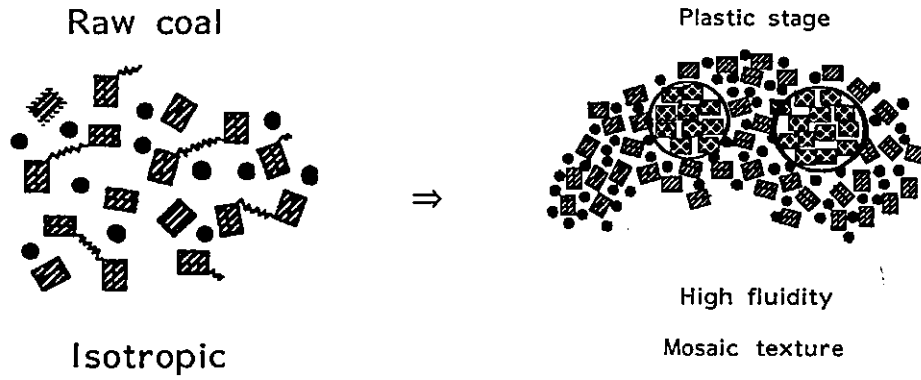
It is hoped though that some clues as to the nature of the interfaces can be derived from the way in which the components, and hence their interfaces, are formed. But the formation of the coke components is an area of considerable controversy. Whereas the theory of carbonisation via mesophase formation is well established, there still is some doubt to what extent it applies to the carbonisation of coal. Some researchers have observed mesophase spheres during coal carbonisation [72], whereas others consider this formation route unlikely [12]. Electron microscope studies [113, 114] do however strongly suggest that mesophase spherules, not necessarily of the structure described by Brooks and Taylor [65], do play a role in the carbonisation of some ranks of coal. There is the strong possibility that different components form via different development routes, which would suggest a difference in the nature of interfaces between components forming in similar and dissimilar ways. One of the most comprehensive studies of microtexture formation to date is that recently undertaken by Fortin and Rouzaud [114]. They use a model of coal and coke structure which assumes them to consist of polyaromatic structural units (PSU), which can arrange themselves to form clusters in which they are aligned in parallel. These clusters are named molecular orientation domains (MOD) and range from a few nanometer to tens of microns in size. They found that coals that develop anisotropy on carbonisation can essentially be divided into two categories, lower rank coals with well developed plasticity and high rank coals which remain essentially solid on carbonisation. The former carbonise with a mechanism

rather like pitch and go through a stage during which spherules are visible. But these spherules only grow to 0.1 to 1.5 μm in diameter, have irregular shapes and do not develop the optical appearance, and hence structure, suggested by Brooks and Taylor [65], which was illustrated in figure 2.7. Nevertheless the spherules coalesce to form mosaic textures, whereas in coals of the second category a pre-existing ordering of the basic units in the coal is directly converted to what they refer to as massive textures [114]. The two carbonisation mechanisms are illustrated in figure 5.1. In coals of intermediate rank they found that the two mechanisms superimpose, so that mosaics are formed in which the entities are not randomly orientated, but show some preferential alignment. Mesophase spherules were observed in only a very narrow temperature band and mosaic textural units were found to continue to grow after the coalescence and disappearance of the spherules until the samples reached their resolidification temperatures.

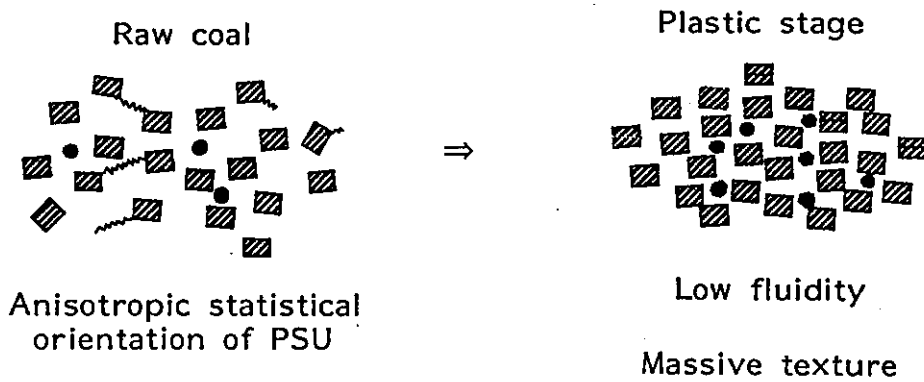
The two category model described above does actually correspond fairly well to earlier work relying on optical microscopy only and using the same classification as employed in this thesis, in which seven development routes for optical textures were identified [9]. Four of them are based on isotropic material being present in the plastic range, which either remains isotropic or changes into anisotropic units starting with fine mosaics and growing into progressively larger units up to granular flow. The remaining three start from the basic anisotropy present in the coal, which remains unchanged on carbonisation or changes into flow type components, either directly or after first developing fine mosaics. Discounting the coke from very low rank coals remaining isotropic, there is only one development route which does not clearly fit one of the two categories: the development of flow type components via fine mosaics. Fine mosaics would imply a high degree of plasticity and growth from mesophase spherules, whereas flow type components imply a large scale order associated with pre-orientation in the coal. This could be a case of superposition of the mechanisms, with the optical microscope failing to recognise the preferred orientation in the entities of the fine mosaic.

Fortin and Rouzaud [114] found their carbonisation model consistent with the general frame of a colloidal model for coal structure, as some sort of plasticising component must provide the PSU with a suspensive medium in which they gain sufficient mobility to re-arrange themselves. This would be referring to carbonisation models such as that suggested by Lahiri [53] and more recently by Solomon [61], which are described in some detail in section 2.3.2. The shortcoming of all of these carbonisation models is that they do not attempt to tackle the differences within one coal, i.e. no thought is given to the question of what happens when two adjacent areas of different plasticity and different degrees of pre-orientation are carbonised.

a)



b)






-  polyaromatic structural unit (PSU)
-  molecular component
-  aliphatic compounds

Figure 5.1 Sketches of the two Basic Mechanisms of the Development of Coke Microtexture [114]

- a) medium Rank, softening Coal
- b) high Rank, non-softening Coal

Coal and coke are both treated as homogenous systems and the fact that coals are composed of different constituents [21] and cokes even from single coals comprise dissimilar textural components [12, 65, 95], which interface with one another, is completely ignored. Interfaces can be formed in two ways. They either correspond to the original coal particle boundaries, which may remain visible unless the system becomes fluid enough to form a continuous melt, or they arise from chemically and structurally different areas already 'interfacing' in the coal, which will be referred to as pre-association. It is likely that some of the interfaces correspond to particle boundaries, as the fluidities achieved even by the most plastic coals are much lower than those of true liquids. The viscosity at maximum fluidity of the most plastic coal used by Fortin and Rouzaud [114] was 1000 poises ($100 \text{ Nm}^{-2}\text{s}$), whereas the viscosity of true liquids tends to lie in the region of 100 poises. But particle boundaries do not suffice to account for the number of interfaces in cokes. This is clearly illustrated by the results of the component size estimation for the first carbonisation series in part 4.4. The coal particle size in that series was 90% < 3 mm, which would amount to a much larger average size than the sizes implied by the unit side length estimated for the components, which ranged from $5\mu\text{m}$ for small inerts to $230\mu\text{m}$ for coarse mosaic. By the same argument, if the fluidity is insufficient to eliminate pre-existing particle boundaries, it is likely also to be insufficient to homogenise the system, so that chemically and structurally dissimilar areas in the coal will form corresponding chemically and structurally different areas in the coke. In this case interfaces are not so much formed, but maintained throughout the coal to coke transformation.

Without observing interfaces being formed in situ it is difficult to make any judgement as to whether the majority of them are pre-existing in the coal or whether they are formed on carbonisation. As hot stage transmission electron microscope studies observing the formation of the optical textures have in fact been undertaken [113], there is no reason why this should not be carried out, although it would be a very lengthy, tedious procedure to acquire sufficient data for any quantitative assessment of interface origin in this way.

Some interfaces obviously must exist in the coal, as it is a multi-constituent system, and some interfaces must be formed on carbonisation, as otherwise there would not be a transition from individual coal particles to a coherent coke matrix. The relative importance of the two possible origins of interfaces can only be guessed at this stage. But the dominance of interfaces with inerts illustrated previously (part 4.7), where for the first carbonisation series between 57% and 89% of the interfaces were found to involve inerts, suggests that pre-association is more common. The link between inertinite in coals and inerts in coke has been widely reviewed [73 - 83] and has

further been elaborated on in part 4.7. Obviously the inertinite in the coal is enclosed by vitrinitic material, which forms the 'reactive' components on carbonisation, so that interfaces between the precursors of reactive and inert coke material exist prior to carbonisation. Exactly what happens at these interfaces as the vitrinitic material undergoes the chemical changes and structural re-orientation required for the formation of optical textures, cannot be deduced from the data available.

It would, for instance, be of interest to ascertain whether the interfaces between the different coal constituents can be identified and classified in a similar way to those of the textural coke components. If it was possible, a suggestion for future work might be an undertaking to compare and possibly relate interfaces in coals to those in the cokes derived from them. It could for instance be assumed that the interfaces between the coal constituents are very good, having been welded together under the influence of heat and pressure during the coalification process. It is likely that some cross-linking at molecular level has occurred across the coal constituent interfaces. On carbonisation these interfaces may well be weakened by the disturbance caused by the evolution of volatile matter, the breaking of some of the cross-link bonds as mobile, reactive chemical species become available and by differential expansion and contraction of the interfacing constituents. On the other hand, whereas an initial weakening would be thought inevitable, at the later stages of carbonisation molecular re-arrangement could be thought to actually improve interface quality by allowing the structural units or micelles to align themselves more neatly along the interface, maybe introducing an element of interlocking or even interdiffusion at the interface, or at least orientating themselves in such a way as to partially overcome the difference in orientation between the interfacing domains. As the resolidification stage of the carbonisation is associated with the formation of chemical bonds, there is no reason to exclude the possibility that some of the dehydrogenation [22] or condensation reactions [22, 52] assumed to take place involve molecules at opposite sites of an interface, provided the interface is flawless and offers close contact right down to molecular scale.

On the grounds of pre-association, it is questionable whether transitional interfaces are interfaces in the traditional sense at all, i.e. in the sense of representing a boundary region between two distinct, dissimilar components which have been brought together and are held together by adhesive forces. They may merely reflect a gradual change in the coal from one vitrinite type to another, which translates itself into an equally gradual change from one optical component to another.

5.1.1 The Formation of Transitional and Fused Interfaces

Working essentially on the assumption of the two main development routes outlined above, there should then be a fundamental difference in the interfaces between components following the same and components following a different route. The most obvious division would be between flow type and mosaic type components, but regarding the development routes [9] granular flow would fall into the mosaic category, as it is formed by coalescence and growth from fine mosaic. On the simplest basis it would be expected that two components which both become plastic simultaneously would 'flow into' one another, so that a mixing or diffusion zone would form in the interfacial region between them. If one of them remains essentially solid, no such process is likely and a sharp boundary along the original outline of the non-softening component would remain visible, resulting in the appearance of a fused interface. A second possibility for the origin of the transitional appearance must, however, be considered. Coals themselves are heterogeneous materials, comprising a number of different vitrinite types, which are thought to be the precursors of the different optical coke components. The precursor coal constituents of two components may already have been placed adjacent to one another in the coal with a gradual transition from one to the other and this existing association might have been left largely undisturbed during carbonisation.

The idea of interdiffusion and mixing is more consistent with the idea of both participants in a transitional interface simultaneously developing a considerable degree of plasticity. Thus if this was to be the main origin of transitional interfaces, they should be largely limited to interfaces between reactive components typically formed in high fluidity coals. Table 5.1, relating the percentage of mosaic type components, which for this purpose include granular flow, to the interface distributions for reactive-reactive component combinations, clearly shows that this is not the case. Cokes A1 and B1, in which a considerable amount of flow type components was found, have in fact larger percentages of transitional interfaces for their reactive components than cokes E1 and F1, which, on an inert-free basis, are essentially composed of mosaics only. This could be a strong indication that transitional interfaces reflect gradual variations in vitrinite type present in the precursor coals. If this is the case it is doubtful if it is strictly speaking correct to refer to transitions as interfaces at all, because their formation would not comprise any adhesive process between previously separate elements.

The mosaic percentages in the cokes from series 2 are comparable to those of coke C1 in series 1. Nevertheless, their reactive-reactive interfaces form less than half of the percentage of transitions as coke C1. This is consistent with the argument that pre-existing gradual transitions are responsible for transitional type interfaces, rather than

the plasticity associated with mosaic type components. In series 2 a much smaller particle size was used, so that more of the constituent associations in the coal were broken and a larger number of interfaces needed to be formed from particle boundaries.

	Mosaic Comp. (%vol inert-free)	P(T) (%)	P(Fu) (%)	P(Fi) (%)	P(Uf) (%)	P(T) +P(Fu) (%)
A 1	44.6	83.3	13.9	2.4	0.5	97.2
B 1	58.3	85.5	12.5	1.3	0.8	98.0
C 1	82.3	90.9	8.6	0.5	0.0	99.5
D 1	96.3	84.7	14.7	0.6	0.0	99.4
E 1	97.3	69.0	30.0	1.0	0.0	99.0
F 1	90.0	79.0	19.6	1.3	0.0	98.7
A 2	81.7	43.2	31.3	25.5	0.0	74.5
B 2	84.2	38.3	33.1	27.8	0.8	71.4
C 2	80.5	37.8	33.0	29.2	0.0	70.8

Table 5.1 Relation of Interface Distributions for Reactive-Reactive Components with the Percentage of Mosaic Type Components in Series 1 and 2

5.1.2 Formation of Poor Interfaces (Micro-Cracks)

Poor interfaces can be thought to originate in two ways, they can either represent a failure of the two adjacent components to form good interfaces or they can arise from interfaces being pulled apart due to forces acting on them at a later stage. In the case of existing interfaces in the coal, cracks would be expected to arise due to their disruption during carbonisation. The former case is only applicable when two surfaces are originally separated and would arise in a situation where local pressure build-up due to the release of volatile matter and swelling [22] is insufficient to bring them into close enough contact.

One of the most common reason cited for crack formation is the differential rates of contraction of different components, in particular reactive and inert material, during the contraction stage. Close to the resolidification temperature the coke matrix can still be thought of as being elastic. But as the temperature increases, the plasticity and hence elasticity of the matrix decreases, so that its yield stress may eventually exceed its fracture strength. For inerts less loss of residual volatile matter and structural re-

ordering is thought to occur at this stage, so that they contract to a lesser extent than the coke matrix. Contraction stresses on such a particle will thus build up, balanced by corresponding tensile stresses in the surrounding matrix. If these tensile stresses locally exceed the fracture stress in the matrix, micro-cracks will occur to relieve them. On theoretical grounds therefore micro-cracks due to differential contraction are more likely to occur in the matrix material than at the interface, as compression is not conducive to pulling apart components at an interface. But this case considers a system containing a single inert particle in a comparatively large amount of matrix. If the inert particles are large and / or closely spaced the tensile stresses imposed on the matrix by one particle may well influence the force distribution at the interface of its neighbour, even to the extent of creating a resulting net tensile stress. Also, considering two large inert particles in close proximity, the contracting matrix material between them does not have the option of compensating for the contraction by shifting external surfaces, so that it either has to create compensating cracks in the middle between the particles, or detach itself from one or both of them. If the adhesive forces at the interfaces are smaller than the cohesive forces of the matrix then it is plausible that cracks preferentially appear at the interfaces. If this is thought to be the case there should be a strong relation between the amount of inerts in the coke and the interface quality, on the basis that the larger the amount of inerts, the closer they are situated to one another and the greater the probability of them influencing each other in the manner described above. The relation between interface quality and inert level was investigated in part 4.7. It was found that for two out of the three coals considered there is a clear trend of increase in poor interfaces with inert level, but this trend applied equally for reactive-reactive interfaces. It was therefore thought to be in line with a characteristic and limited ability of reactive components to form good interfaces as formulated by the binding power hypothesis in part 4.3. It could however be argued that if a reactive-reactive interface is situated close to an inert the tensile stress build-up due to the differential contraction may act to pull apart the interface, if it is comparatively weak. Also, differential contraction, although probably most marked between reactives and inerts, is not necessarily confined to them. The different reactive components may well contract at different rates and/or temperatures. It has been pointed out previously [115] that even within an area containing only a single anisotropic component, stresses will build up, as the coefficient of thermal expansion varies parallel and normal to the graphitic layers. This would imply that two similar or even identical components interfacing would have different rates of contraction if the preferred orientation of the graphitic layers within them differs.

5.1.3 Estimated Percentage of Particle Boundary derived Interfaces

In the previous sections a distinction was made between interfaces originating from particle boundaries and interfaces corresponding to those of the precursor materials in the coal. It would therefore be interesting to have an estimate of the relative proportions of the two, and how these are affected by particle size and component distribution.

In part 4.4 the sizes of the textural components were estimated from the interface data obtained for the first carbonisation series. It was then attempted to predict the interface distribution of the second carbonisation series in terms of the percentages of interfaces involving reactive components only and those involving inerts. The poor agreement of the predicted and counted results was partially attributed to the much smaller particle size used for the second series. A larger than predicted proportion of reactive components only interfaces corresponds well to a larger number of particle boundary derived interfaces, as the reactive components are on average much larger than the inerts (table 4.18.c) and are therefore likely make a larger contribution to the additional surface area created by size reduction.

A larger particle boundary derived proportion of the interfaces, particularly those between reactive components, could be thought to explain the worse interface quality for the second series, as particle boundary derived interfaces would imply a greater scope for interfaces to fail to develop perfect continuity. It could be assumed that the probability of two component areas on originally separate particles failing to bond perfectly is greater than that for two previously joined precursors, as the extra step of bringing them into sufficiently close contact is involved. Also, it is more than likely that the changes between vitrinite types in coals are gradual, so that the precursor materials for optically and structurally similar components are likely to be adjacent to one another for pre-associated interfaces. For particle boundary derived interfaces the mixing is random and optically and structurally quite dissimilar components might be brought into contact. However from the IQI of the reactive components in series 1 listed in table 4.3 there is no evidence of optically similar components interfacing better than optically dissimilar ones. But the ratio of transitional to fused interfaces appears to vary for similar and dissimilar component combinations (table 4.4). Optically similar textural components appear to form transitional interfaces more readily. This could substantiate the expectation that optically similar components are pre-associated, but it could equally well indicate that structurally similar carbon forms are to a greater extent capable of 'dissolving' into one another, whereas the interaction between dissimilar ones is confined to a narrow border region between the two components.

An estimation of the proportion of particle boundary derived interfaces was undertaken. Assuming cubic particles and components, their volumes and surface areas can easily be calculated. A total coke volume is then chosen and the number of particles and components required to fill it is calculated. The numbers are then multiplied by the surface area of an individual particle/component to give the total surface area available for interfacing. Taking the total surface area of the components as 100% (as the component sizes were arrived at without taking particle boundaries into account), the proportion of the particle boundary derived surface area was then calculated. The results are shown in figure 5.2. The calculation was conducted three times, firstly varying the particle size from 3 mm to 100 μm (a), secondly varying the average reactive component size from 40 to 300 μm (b.) and finally increasing the percentage of inerts in the coke from 10 to 60 % (c.). The average reactive component side length was taken to be 140 μm , which includes a weighting towards the larger components, which appear to be more frequent in most cokes considered in this thesis. It can clearly be seen that particle size is by far the most influential parameter of those considered, increasingly so the closer the particle size approaches that of the average reactive component. For a particle side length much greater than that of the components (in excess of 7 times their size), the percentage of particle boundary derived interfaces is low and its variation with particle size is very gradual. But as the particle side length approach those of the components (less than 4 times their size), the percentage increases rapidly. This supports the claim that the percentage of particle boundary derived interfaces is likely to be much larger for the second carbonisation series than for the first one. At a rough guess, for particle sizes below 3 mm the bulk of the particles probably have side length between 1 and 2 mm, which would amount to a percentage of about 10 % particle boundary derived interfaces. For particle sizes between 1 mm and 75 μm a realistic side length estimate could be 750 to 250 μm , which would correspond to about 40 % particle boundary derived interfaces.

Graph 5.2.b shows that the variation of the particle boundary derived interface percentage is less sensitive to component size than to particle size. Nevertheless, notable differences can be expected between cokes in which the smaller or the larger size components are dominant. For the example considered here a particle unit side of 1.5 mm was taken. For this particle size a coke containing significant amounts of broad and striated flow averaging, say, a component unit side length of 100 μm , would have about 5 % of its interfaces derived from particle boundaries, whereas a coke in which coarse and medium mosaic predominate, estimated to average a component unit size of 200 μm , would have about 15 %.

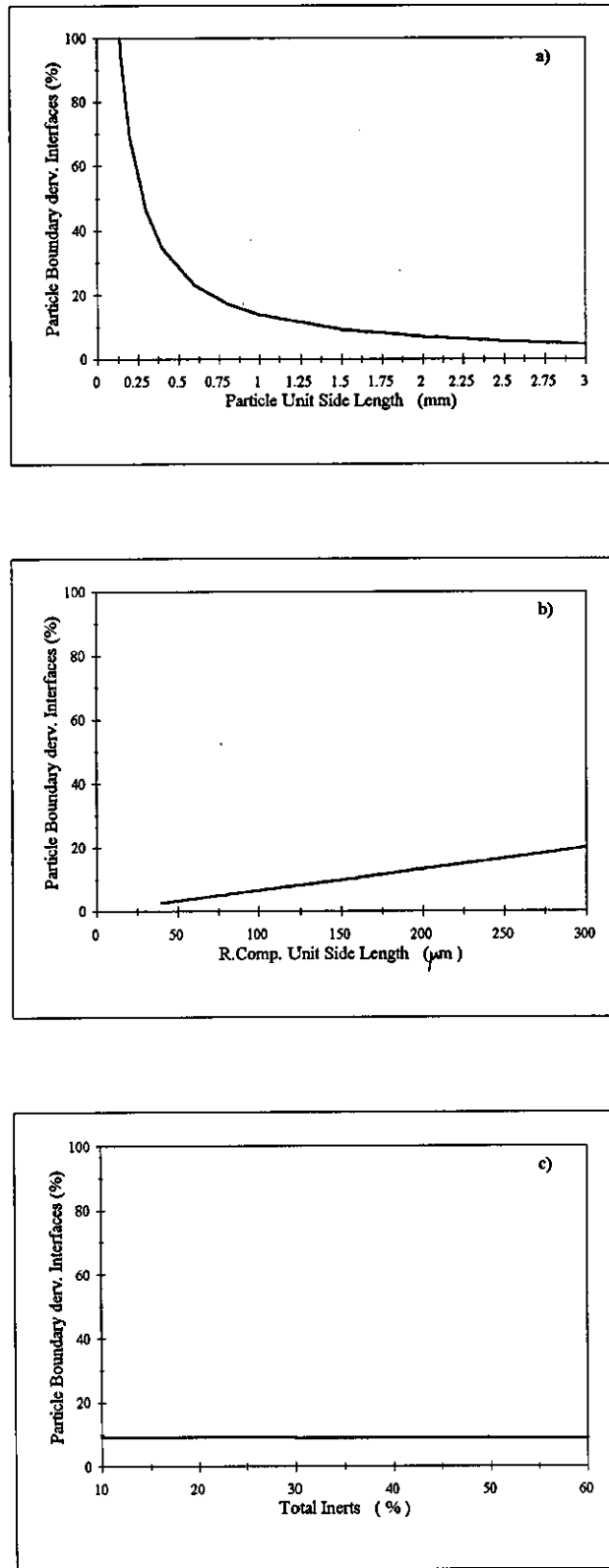


Figure 5.2 Variation of the Percentage of Particle Boundary Derived Interfaces with Particle Size (a), Average Reactive Component Size (b) and Inert Content (c)

The amount of inerts (graph 5.2.c) seems to have little bearing on the percentage of particle boundary derived interfaces. This is somewhat surprising considering the number of interfaces they take part in (table 4.25) and probably is an indication of the limits of the modelling approach of equating available surface area and the number of interfaces, as, during the point counting of interfaces no account was taken of the interface length. Small inerts thus present the anomaly of forming a large number of short interfaces, the total length of which is relatively small in line with their small contribution to the total surface area available for interfacing.

5.2 Theoretical Relation between Interfaces and Strength

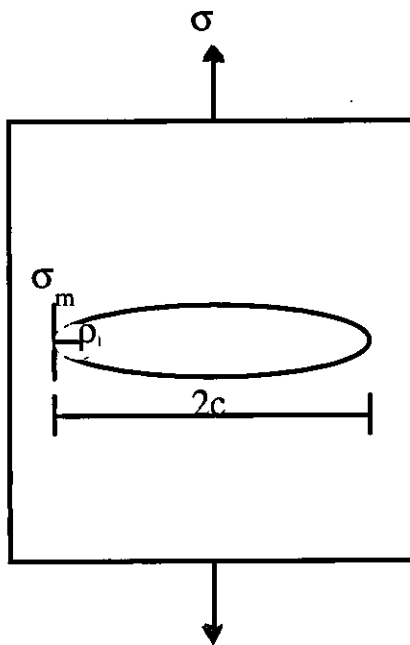
5.2.1 Theory of Fracture and Stress Propagation

Strength is obviously the resistance of a body of material against separation under stress into two or more parts, i.e. fracture [116]. Fracture can either proceed in a ductile or a brittle manner, that is with or without appreciable plastic deformation prior to failure. Fracture occurs by the propagation of cracks through the material. In brittle solids, once the conditions for crack propagation are given, cracks spread spontaneously, picking up speed from zero to the limiting velocity (about a third of that of a longitudinal sound wave travelling in the material in question). When the yield stress depends strongly on the strain rate, i.e. the material has some ductility, the velocity of crack propagation increases to the extent that plastic deformation can no longer accommodate the stress concentration at the tip of the crack.

Cracks can propagate through a material along two preferred path. Either they run along characteristic crystallographic planes, known as cleavage planes, which is the typical behaviour of crystalline substances and is also referred to as transgranular crack propagation. Alternatively, in polycrystalline materials, they can also proceed along the grain boundaries, which is described as intergranular crack propagation. Transgranular crack propagation is the more common type, but intergranular propagation often occurs when the interfaces are weakened by substances segregating from the bulk material and collecting at the boundaries. Grain boundaries to some extent inhibit crack propagation due to the change in orientation they are associated with. Cracks propagating transgranularly 'jump' boundaries by nucleating a new crack in the adjoining grain and the two cracks then joining by tearing action across the boundary.

The two types of crack propagation are also referred to as cohesive and adhesive failure. In general both, cohesion between the crystallographic planes within a

material and adhesion at grain boundaries are good and the theoretical strength of materials is very high, compared to the strength encountered in reality [116]. This was explained in terms of imperfections in materials, for which the shape of small elliptical cracks was assumed. Stress would concentrate at the crack tip, much like the stress in structures concentrates around holes in them as first described by Inglis. Under certain conditions therefore a relatively small stress applied to the bulk sample can be amplified to a critical level at the crack tip. The relation between the stress applied and the stress concentrated at a crack tip is given below.



$$\sigma_m \approx 2 \sigma \sqrt{\frac{c}{\rho}} \quad (5.1)$$

where

σ_m Maximum Stress Concentration at Crack Tip

σ Applied Stress

c Half Crack Length

ρ Curvature at the Crack Tip

Figure 5.3 Griffith Estimate for the Relation between the Stress applied and the Stress concentrated at a Crack Tip [116]

The extent to which stress is concentrated at a crack tip is thus dependent on the size of the crack and its sharpness, i.e. it is inversely proportional to the radius of the crack tip.

When a crack propagates, the elastic strain energy which has build up at the crack tip is released and the energy required to form two new surfaces is absorbed. If the balance between them is such that the creation of the two new surfaces does not alter or decrease the total energy of the system, the conditions for crack propagation are given.

For the simplest case, plane stress applied across a thin plate, this condition is given by

$$\sigma = \sqrt{\frac{2\gamma E}{\pi c}} \quad (5.2)$$

where γ Shear Strain

E Youngs Modulus

As very few materials are truly brittle, some plastic deformation occurs and the work of plastic deformation therefore needs to be taken into account. Orowan has shown that the work plastic deformation p may be treated as a contribution to the effective surface energy which needs to be supplied for a crack to propagate, provided that the deformation is confined to a region the thickness of which is small compared to the crack size. The above equation is thus modified to the Griffith-Orowan criterion for crack propagation. As the shear strain is much smaller then the work of plastic deformation it is neglected in the approximation.

$$\sigma \approx \sqrt{\frac{E p}{c}} \quad (5.3)$$

The relation of the applied stress necessary to induce crack propagation being inversely proportional to the crack size remains intact. For a not truly brittle material though, the critical crack length becomes much larger. The critical crack length in an amorphous (truly brittle) material is of the order of a few microns, whereas crystalline materials which show some degree of ductility have critical crack lengths in the millimetre range.

5.2.2 Application of the Fracture Theory to Metallurgical Cokes

The interfaces between the textural components in metallurgical cokes, with the possible exception of transitional interfaces, can in many respects be likened to the grain boundaries in polycrystalline materials. Their contribution to the coke strength would then depend on whether crack propagation proceeds in a trans- or intergranular manner. In this case, whether the components are more likely to fracture by cohesive failure or to be pulled apart at the interfaces (adhesive failure). As neither the cohesion of individual components, nor the strength of individual interfaces, has been tested, and are unlikely to be tested, as the experimental difficulties of such an undertaking would be foreboding, this question is difficult to solve. In a previous thesis [8] this question has been tentatively addressed. Walker, in statistically

relating coke strength and textural composition, expected the structures of all anisotropic components to be continuous and did not anticipate intergranular breakage between them. Whereas this view of a continuous coke matrix, in which merely the size of the domains of equal lamellar orientation varies, is perfectly compatible with transitional interfaces occurring between two reactive components, it does not allow for the other interface types. Even for the first carbonisation series, which has the best interface quality of the series considered, only 4 of the 35 observed interface combinations between anisotropic components have transitional interfaces only (table 4.4) and 11 of them show evidence of some fissuring at the interfaces (table 4.3). Sharply defined boundaries between reactive components (fused interfaces), and even more so fissuring, suggests that interfaces are structural parameters and should be considered as possible influences on coke strength. They obviously represent a discontinuity in the coke matrix, and there is no reason to exclude them as sites for crack initiation and propagation, unless concrete data of their adhesive strength can be obtained showing it to greatly exceed the cohesive strength of the components.

Although few materials fracture in a purely brittle or ductile manner, most can be assigned to one or the other as the dominant failure mechanism. Metallurgical coke is considered to fail by brittle fracture. This means that its material properties are such that relatively small imperfections can lead to critical stress levels for crack propagation locally. To what extent the interfaces between the textural components influence the overall coke strength would by this argument depend on whether and to what extent they are superseded by other structural features as stress concentrators. On the largest scale, coke obviously fractures along the lines of macrofissures, several millimetres in size, induced during the contraction stage of carbonisation [22]. Once its size has degraded to the extent of eliminating these large fissures, pores and flawed interfaces can be thought to compete as sites to initiate crack propagation and failure. On first sight pores appear more likely to influence mechanical behaviour. This was expressed by Patrick and Stacey [117] who stated that pores become the significant structural features in high porosity materials where they constitute the larger defects. Pores typically make up about 50 % of the coke volume [9], which makes them a far more prominent feature than interfacial imperfections. Also the average pore size can be quite large compared to the fissures encountered at the component interfaces. In terms of size and quantity pores are therefore much more likely to concentrate stress sufficiently to initiate crack propagation. This corresponds to the view that pores effectively control the critical flaw size [117]. Pore structure has in fact been successfully linked to the tensile strength of metallurgical cokes [8, 9]. But the

proven relation between pore structure and strength need not necessarily exclude textural component interfaces as a contributing factor. Their quantitatively much smaller contribution would explain why the relations found in part 4.10 are so weak, being overshadowed by the more significant influence of the pore structure. As equation 5.1 shows, there is a shape factor influencing stress concentration. Pores as a general rule tend to be rather rounded, so that, as far as a 'crack tip' can be thought of, the curvature at the tip is very large. Fissures, by their very definition, tend to be narrow with sharp crack tips, i.e. small curvatures. This means that larger stress concentrations could be thought of developing at fissures at interfaces, even though they are much smaller than the pores associated with the coke.

In the above argument it was assumed that the same magnitude of critical stress is required to propagate cracks originating from pores and from fissures at interfaces. It is likely that for a crack to connect two pores transgranular propagation needs to proceed, i.e. the cohesive forces of the components need to be overcome. A crack propagating from an interfacial fissure has the option to do so along the interface, thereby overcoming the adhesive forces between two components, which may well be much smaller than the cohesive forces, depending on the bonding mechanism. As already pointed out, neither the cohesive nor the adhesive strength of the components is known, which prevents any definite conclusion being drawn.

The interdependence of the parameters under investigation makes it very difficult to establish any clear relationships. Coke strength has been linked to the micro-textural composition and the pore structure, both of which depend on the rank of the precursor coal and the carbonisation conditions and cannot be varied independently. A weak link between coke strength and the quality of interfaces between the components has been shown in part 4.10 of this thesis. But the interface quality does obviously strongly depend on the micro-textural composition, meaning it cannot be varied independently of it nor of precursor coal rank and pore structure.

With the techniques available, and in view of the interconnectedness of the parameters under investigation, it will be very difficult to establish why coke, once stabilised on a macroscopic scale, fails. Weaknesses in the matrix material, cohesive failure due to the separation of poorly bonded lamellae, maybe due to residual side chains or hetero-atoms, poor adhesion at interfaces encouraging the propagation of cracks along them, and stress concentration by pores of a certain size and form are all equally valid possibilities and are likely to contribute to determining coke strength.

6 Conclusions

1. It was found possible to devise a classification system for the interfaces between the textural components in metallurgical cokes, which is suitable for quantitative microscopic analysis. The system is based on the distinction between 'good' and 'poor' interfaces. 'Good' interfaces are subdivided into transitional (T) and fused (Fu), depending on whether there appears to be a smooth transition between the components via an intermediate material, or whether a clear boundary between them can be identified. 'Poor' interfaces divide into fissured (Fi) and unfused (Uf) according to the size of the area of no contact between the components relative to the size of the entire interfacial area.

2. An interface quality index (IQI) defined as the ratio of 'good' interfaces, transitional and fused , to 'poor' ones, fissured and unfused, was found to be a suitable working construct for the purpose of comparing the quality of interfaces formed by individual components, groups of components and for cokes as a whole.

3. The distribution of the interface types between the textural components of cokes was observed to change with the rank of the precursor coal. As the component composition shifted from flow to mosaic type components with decreasing rank, the interface distribution shifted from the transitional to the fused interface type, suggesting that transitional interfaces are more typical for flow type components. Simultaneously the percentage of fissured and unfused interfaces decreased, which indicates a better interface quality for cokes consisting mainly of mosaic type components.

4. The rank dependence of the interface distribution was thought to be a secondary one arising from the variation in component composition. It was proposed that interfacial behaviour is a characteristic property of each component referred to as 'binding power' (BP) and defined as the theoretical, imaginary IQI, based on the probabilities of the component forming each of the interface types irrespective of which other component it interfaces with and independent of the origin of the coke.

5. The binding powers vary substantially between the components with a clear division between larger domain flow types (broad and striated) and mosaics, excluding fine mosaic. Granular flow, in keeping with its intermediate optical appearance between flow and mosaic type components, has a binding power intermediate between the two.

Even though the hypothesis of binding power as a fundamental component property could be substantiated, it was shown to be insufficient to explain the interfacial behaviour of the components in any coke completely or to definitively predict the overall coke interface quality.

6. The isotropic, and to some extent the fine mosaic, component forms an exception to the binding power theory. For isotropic material occurring in conjunction with other reactive components the values for fissured and unfused interfaces are too close to zero to calculate its binding power. This does not reflect an exceptionally good binding power, but on the contrary, a virtually complete failure to interface with inerts. Conversely, fine mosaics and isotropic material, when they are virtually the only reactive components present, will form sufficient interfaces with inerts to incorporate them into the coke matrix. Their reluctance to do so in the presence of 'more reactive' components suggests that, in the case of interfaces with inerts, it might be more accurate to talk about variations in the readiness of components to incorporate inerts, rather than absolute abilities to do so.

7. The quality of the interfaces formed between two components depends on their reactivities or binding powers, but the impact of a component combination on the total coke interface quality depends also on its frequency of occurrence. The most likely physical parameter determining the number of interfaces between two components is their combined surface area available for interfacing, which is a function of their combined volumes and their unit sizes. Thus, given sufficient binding power to fuse with other components, the number of interfaces a component forms per unit volume depends on its average unit size.

8. An attempt to devise a model to estimate component unit size and predict interface frequencies showed that the largest part of the surface area of any component is taken up by bordering pores. It is therefore suspected that interface frequency will be highly sensitive to variations in pore volume and pore size distribution.

9. Interface frequency modelling gives an indication of the percentage of 'invisible' interfaces between units of the same reactive component. It was found to vary in proportion to the interfaces between dissimilar reactive components. The failure to include the, presumably transitional, interfaces between identical component units underestimates the total coke IQI. But, provided the reactive-inert component ratio does not vary excessively between the cokes considered, the errors are comparable for all samples and do not affect the overall trend.

10. Comparing the absolute values of the IQI in sample series 1 and 2 shows that they strongly depend on the carbonisation conditions, but that the differences between the individual textural components persist irrespectively. Their relative contributions to the IQI appear to be independent and the variation of IQI between coals or coal blends of different textural compositions can be anticipated, even if the absolute numerical values cannot be estimated. To achieve a model for the prediction of interface quality, factors accounting for carbonisation conditions, such as particle size, charge density and heating rate would have to be introduced.

11. Relative to the volume percent of the cokes made up by inerts they are involved in a disproportionately large number of interfaces. In conjunction with the fact that interfaces between any two reactive components, with the possible exception of the larger flow types and isotropic material, tend to be very good, it can be concluded that the overall quality of interfaces in a coke is strongly dependent on the quality of the interfaces with inerts.

12. No evidence was found to support the view that part of the inertinite maceral group behaves as a reactive component on carbonisation. The trend towards an increasing discrepancy between inertinite derived coke and the coke fraction counted as inerts with total inertinite content is more in line with a progressive failure of the reactive components to incorporate all of the inerts added than with the existence of reactive inertinite. It is therefore more likely that the unaccounted for fraction of inertinite derived coke is 'lost' rather than converted to take the appearance of a reactive component.

13. The effect of coking additives on interface quality cannot be described by a simple universal trend. It appears to depend on both, the nature of the coal and that of the additive used. Their addition does influence the interfacial behaviour of the reactive coke components and of the coal derived inerts, but in such a manner that it varies for different coals, additives and the quantities added. Variations in the textural component composition of the reactive material due the additives can be used as a contributing factor to explain some of the deviations in interface quality observed.

14. Using tensile strength for the cokes of series 1 and friability testing for those of series 2 and 3 it was not possible to unambiguously determine if the interface quality of the textural components is a truly independent parameter, which has a bearing on the macro-properties of the cokes. Some weak trends could however be established providing evidence that interface quality is one of the contributing factors governing the mechanical properties of cokes.

References

- [1] Gray, R.J., ed Marsh,H., Introduction to Carbon Science, Butterworths, 1989, ch 9, p.285
- [2] Gibson, J., Gregory, D.H., Carbonisation of Coal, Mills and Boon ltd, London, 1971
- [3] BCRA News, 18 , Nov. 1992
- [4] Bertling, H., Schonau, H., Erdol, Kohle, Erdgas 106 (4), 1990, p. 217
- [5] Nashan, G., 2nd Int. Cokemaking Congress, London, 1992, p. 3
- [6] Walker, R. D., Modern Ironmaking Methods, The Institute of Metals, 1986
- [7] Paxton, H. W., COMA Yearbook, 1983, p. 246
- [8] Walker, A., The Carbon Texture of Metallurgical Coke, PhD Thesis, Loughborough University of Technology, 1988
- [9] Moreland, A , The Structure and Strength of Metallurgical Coke, PhD Thesis , Loughborough University, 1990
- [10] Vandezande, J. A, AIME Ironmaking Proc. 44, 1985, p. 189
- [11] Hays, D., Patrick, J.W. and Walker, A., (in print), in 'Handbook of Material Testing' , Marcel Dekker Publications
- [12] Patrick, J.W., Reynolds, M.J., Shaw, F.H., Fuel 52, 1973, p.198
- [13] Patrick, J.W., Reynolds, M.J., Shaw, F.H., Carbon 13, 1975, p.509
- [14] Patrick, J.W., Reynolds, M.J., Shaw, F.H., Fuel 58, 1979, p.501
- [15] BCRA Quaterly, No 27, April 1990, p.41
- [16] Shapiro, N., Gray, R.J., Journal of the Institute of Fuel, June 1964, p.234
- [17] McVeigh, J.C., Energy around the World, Pergamon Press, 1984
- [18] van Krevelen, D.W., Coal, Elsevier, 1961
- [19] Bend, S.L., Fuel 71, 1992, p.851
- [20] Kershaw, J.R., Fuel Processing Technology 31, 1992, p.127

- [21] Neavel, R.C. , The Chemistry of Coal Utilisation, ed. Lowry, H.H., 2nd Supp. Vol., 1981, Ch. 3
- [22] Loison, R., Foch, P., Boyer, A. Coke - Quality and Production, Butterworth, 1989
- [23] Stach, E., Coal and Coal bearing Strata, ed. Murchinson, D., Westoll, T.S., Oliver and Boyd, 1969, pt 1.1., p. 3
- [24] Murchison, D.G.Cook, A.C., Raymond, A.C., Phil.Trans.R.Soc., London, 1985, 315A, 157
- [25] Dormans, H.N.M., Huntjens, F.J., van Krevelen, D.W., Fuel 36, 1957, p.321
- [26] Kroger, C., Gluckauf Forschungshefte 93, 1957, 5/6, p.122
- [27] Dyrcaz, G.R., Bloomquist, C.A.A., Ruscic, L., Fuel 63 ,1984, p.1166
- [28] Kroger, C., Pohl, A., Kuthe, Fr., Hovestadt, H., Burger, H., Brennstoff-Chemie 38, 1957, 3/4, p.33
- [29] Kroger, C., Pohl, A., Brennstoff-Chemie 38, 1957, 7/8, p.102
- [30] Gray, R.J., Champagne, P.E., Proc. Ironmaking Conf., 1988, p.313
- [31] Monson, J.R., COMA Yearbook 1979, p.267
- [32] Street,A., Alexander, W., Metals in the Service of Man, Penguin Books, 8th ed., 1982
- [33] Higgin, R.A., Engineering Metallurgy, Part 1, Hodder and Stroughton, 5th ed, 1983
- [34] Peacey, J.G., Davenport, W.G., The Iron Blast Furnace, Pergamon Press, 1979
- [35] Marshall, R.J., COMA Yearbook 1979, p. 135
- [36] Patrick, J.W., Wilkinson, H.C., Analytical Methods for Coal and Coal Products, Vol.2, Ch.29
- [37] Perch, M., The Chemistry of Coal Utilisation, ed. Lowry, H.H., 2nd Supp. Vol., 1981,Ch. 15, p.919
- [38] McNeil, D., Coal Carbonization Products, Pergamon Press, 1966
- [39] Grainger, L. , Gibson, J., Coal Utilisation, Graham and Trotman, 1981

- [40] Eisenhut, W., The Chemistry of Coal Utilisation, ed. Lowry, H.H., 2nd Supp. Vol., 1981, Ch. 14
- [41] Miyazu, T., Okuyama, Y., Fukuyama, T., Suzuki, N., Mori, T., Int. Iron Steel Congr., Dusseldorf, Paper 1.2.2.1., 1974, p.1
- [42] Poos, A., COMA 1987, p.223
- [43] Gibson, J., COMA 1972, p.182
- [44] Simonis, W., Proc. Int. Congr. in Iron and Steelmaking, Charleroi, 1966, p.160
- [45] Dainton, A.D. , COMA 1988, p.214
- [46] Ruiz, O., Romero-Palazon, E., Diez, M.A., Marsh, H., Fuel 69, 1990, p.456
- [47] Triska, A.A., Schubert, C.D., Congres International de Charleroi 1966, C9, p.1
- [48] Valia, H.S., AIME Ironmaking Proc. 1992, p. 435
- [49] Patrick, J.W., Stacey, A.E., Fuel 57, 1978, p.258
- [50] Hartwell, R.R., Stacey, A.E., Wilkinson, H.C., Fuel 61, 1982, p. 329
- [51] Grimes, W.R., Coal Science, ed. Gorbaty, L.M., Larson, J.W., Wender, I., Vol.1, Academic Press, 1982, p.21
- [52] Patrick, J.W., COMA 1976, p. 201
- [53] Grainger, L., COMA 1975, p.282
- [54] Lahiri, A. , Fuel 30, 1951, p.241
- [55] Berkowitz, N., Fuel 28, 1949, p.97
- [56] Berkowitz, N. Fuel 29, 1950, p.138
- [57] van Krevelen, D.W., Huntjens, F.J., Dormans, H.N.M., Fuel 35, 1956, p.462
- [58] Brown, H.R., Waters, P.L., Fuel 45, 1966, p.17
- [59] Neavel, R.C., Coal Science, ed. Gorbaty, L.M., Larson, J.W., Wender, I., Vol.1, Academic Press, 1982, p.1
- [60] Sakurovs, R., Lynch, L.J., Maher, T. P., Banerjee, R.N., Energy & Fuels, 1987, 1, p.167

- [61] Solomon, P.R., Best, P. E., Yu, Z. Z., Charpenay, S., Energy & Fuels, 1992, 6, p.143
- [62] Coin, C.D.A., Fuel 66, 1987, p. 702
- [63] Abramski, C., Mackowsky, M.Th., ed. Freund, H. , Handbuch der Mikroskopie in der Technik, Bd 2, Teil 1, Umschau Verlag, Frankfurt, 1952, pp311-410
- [64] Taylor, G.H., Fuel 40, 1961, p.465
- [65] Brooks,J.D., Taylor, G.H., Chemistry and Physics of Carbon, Vol.4, 1968, p.243
- [66] Marsh, H., Walker, P.L., Chemistry and Physics of Carbon, Vol.15, 1979, p.229
- [67] Marsh, H., Schmidt, J., Analytical Methods for Coal and Coal Products, Vol.2, Ch.30
- [68] Marsh, H., Fuel 52, 1973, p.205
- [69] White, J.L., Price, R. J., Carbon 12, 1974, p.321
- [70] White, J.L., ACS Symposium Series No 21, American Chemical Society, 1976
- [71] Ihnatowicz,M., Chiche, P., Deduit, J.,Pregermain, S., Tournant, R. , Carbon 41, 1966, 4
- [72] Marsh, H., Dachille, F., Iley, M., Walker,P.L., Whang, P.W., Fuel 52, 1973, p.253
- [73] Taylor, G.H., Fuel 36, 1957, p.221
- [74] Brown, H.R., Taylor, G.H., Cook, A.C., Fuel 43, 1964, p.43
- [75] Taylor, G.H., Mackowsky, M.Th., Alpern, B., Fuel 46, 1967, p.431
- [76] Bennett, A.J.R., Fuel 47, 1968, p.51
- [77] Benedict, L.G., Thompson, R.R., Shigo III, J.J., Aikman, R.P., Fuel 47, 1968, p.125
- [78] Nandi, B.N., Montgomery, D.S., Fuel 54, 1975, p.193
- [79] Diessel, C.F.K., Fuel 62, 1983, p.883
- [80] Diessel, C.F.K., Wolff-Fischer, E., Gluckauf-Forschungshefte 47, 1986, Nr. 4, p. 203

- [81] Coin, C.D.A., 20th Newcastle Symposium on Advance in the Study of the Sydney Basin, University of Newcastle (NSW), 246, 1986, p. 77
- [82] Kaegi, D.D., Valia, H.S., Harrison, C.H., Proc. Ironmaking Conf., 1988, p.339
- [83] Kruszewska, K., Fuel 68, 1989, p.753
- [84] Freund, H. (ed.), Handbuch der Mikroskopie in der Technik, Bd 1, Teil 1,Umschau Verlag, Frankfurt, 1957
- [85] Edwards, I.A.S., ed Marsh,H., Introduction to Carbon Science, Butterworths, 1989, ch 1, p.1
- [86] Franklin, R.E., Acta Cryst., 4, 1951, p.253
- [87] Bloss, F.D., An Introduction to the Methods of Optical Crystallography, Holt, Rinehart and Winston, New York, 1961
- [88] Wood, E.A., Crystals and Light, D.van Nostrand Company inc., 1964
- [89] Hartshorne, N.H., Stuart, A., Practical Optical Crystallography, Edward Arnold ltd, 1969
- [90] Haynes, R., Optical Microscopy of Materials, International Textbook Company, Blackie & Son ltd, 1984
- [91] Ramdohr,P., Eisenhüttenwesen, 1, 1928, p.669
- [92] Marshall,C.E., Fuel 24, 1945, p.120)
- [93] Dahme,A., Mackowsky, M.Th., Brennstoffchemie
30, 1949, p.141/218
31, 1950, p.129
32, 1951, p.175
- [94] Mackowsky, M.Th., Fortschr.Mineral., 29/30, 1951, p.10
- [95] Freund, H. (ed.), Handbuch der Mikroskopie in der Technik, Bd 2, Teil 1,Umschau Verlag, Frankfurt, 1952, pp311-410
- [96] Alpern,B., Brennstoffchemie, 37(13/14), 1956, p.194
- [97] Patrick, J.W., Walker,A., Fuel 70, 1991, p.465
- [98] Patrick, J.W., Clarke, D.E., Introduction to Carbon Science, ed Marsh,H., Butterworths, 1989, ch 7, p.229

- [99] Hull, D. "An Introduction to Composite Materials", Cambridge University Press, GB, 1981
- [100] Savage, G., Carbon-Carbon Composites, Chapman and Hall, 1993
- [101] Scott, V.D., Trumper, R.L., Ming Yang, "Interfaces in Composites", Pigot, M.R. (ed)
- [102] Qian, Z., Marsh, H., Clarke, D.E., Fuel 64, 1988, p. 125
- [103] Marsh, H. , Sherlock, J., Fuel 60, 1981, p.434
- [104] Sukhorukov, I.F., Babenko, E.M., Gavrina, M.V., Tovetnye Metally, 39, 1966, p.59
- [105] Marsh, H., AIME Ironmaking Proc., 41, 1982, p.2
- [106] Marsh, H., Forrest, M., Pacheco, L.A., Fuel 60, 1981, p.423
- [107] Bernard, Duchene, Vogt, Jeulin, Steiler, Bourrat, Rouzaud, Ironmaking Proc., 45, 1986 , p.211
- [108] Ragan, S., Marsh, H., Fuel 60, 1981, p.522
- [109] Forrest, M., Marsh, H., Fuel 60, 1981, p.429
- [110] Chandra, D., Fuel 42, 1963, p.457
- [111] Chatfield, C., Statistics for Technology, 3rd ed., Chapman and Hall, 1983
- [112] BCRA, Coke Research Report 73, July 1972
- [113] Friel, J.J., Metha, S., Mitchell, G.D., Karpinski, J.M., Fuel 59, 1980, p.610
- [114] Fortin, F., Rouzaud, J.-N., Fuel 73, 1994, p.795
- [115] Patrick, J.W., Stacey, A.E., Fuel 51, 1972, p.81
- [116] Hayden, H.W., Moffatt, W. G., Wulff, J., The Structure and Properties of Materials, Vol III, John Wiley & Sons inc, 1965
- [117] Patrick, J.W., Stacey, A.E., COMA 1984, p.90

Appendix 1

The Estimation of the Properties of the Pure Macerals

The volatile matter, VM (%wt, daf), carbon content, C (%wt), and densities, d (g/cm³) of the pure macerals of the coals in sample series 2 were estimated, primarily to obtain a comparison of the tested properties of the maceral concentrates with the predictions from the maceral property estimates.

From data obtained by BCRA [112] a plot of volatile matter (% wt daf) against mean random refraction (Rmo) of the coal is drawn and the Rmo of the coals taken from it is used to obtain a first estimate of the pure maceral VM from a table in the same work listing maceral VM variation with Rmo in small intervals. From the data available from the work of Dormans et al [25] two graphs are drawn, one of pure maceral VM versus C, the other of C versus d. From these the preliminary estimates of C and d are obtained. The estimate for d is used to convert the maceral composition (table 3.2) from volume to weight percent. The weight percentages are then used in an interpolation based on the below equation to obtain a second estimate for C, such that the calculation would yield the coal C actually tested.

$$C = (C_v * \% \text{ Vitrinite}/100) + (C_e * \% \text{ Exinite}/100) + (C_i * \% \text{ Inertinite}/100) \quad [A1]$$

where C = C of the coal as tested
 C_v = C of vitrinite
 C_e = C of exinite
 C_i = C of inertinite

The same graph as previously is then used to obtain a second estimate of d, the maceral weight percentages are re-calculated and using them and the new C values as input the interpolation is repeated. After 2 repeats (3 in the case of coke D2), the estimates for C and d do not show any more significant changes, so that the values are taken as the final estimates.

The same interpolation is then performed for VM using the initial pure maceral estimates as starting values.

Using the above equation and its equivalent for VM, C and VM are calculated for the maceral concentrates based on the pure maceral property estimates obtained for the coals. These are compared with the tested values on the graphs in figure A1. The calculated properties obviously reflect those to be expected from the literature on

maceral properties [25, 28]. As inertinite is generally perceived as being rich in C and poor in VM relative to the vitrinite of the same coal, C would be expected to rise with increasing inertinite content and VM to fall. This is not the case for the properties of the coals and their concentrates as tested. In some cases (A2 for VM or C2 for C, for example) the trend is exactly opposite to that expected. Experimental error is highly unlikely as the same tests were conducted simultaneously for the coals in series 3, where the results correspond well to those of the coals suppliers.

A step by step summary of the estimation process, including the data, is given below. In the tables V stands for vitrinite, E for exinite and I for inertinite.

Step 1 The VM (% wt) of the coal as tested is used to estimate the mean random reflectance Rmo and the pure maceral VM (% wt) using data from [112]

	%wt VM (coal)	Rmo	% wt VM		
			V	E	I
A2	25.1	1.33	25.7	27.4	17.1
B2	29.0	1.18	30.4	35.3	18.7
C2	28.5	1.28	27.3	29.6	17.6
D2	46.7	0.43	35.4	95.8	24.8

Step 2 First estimates of pure maceral Carbon contents (% wt) and densities are obtained from graphs of data from [25]

	% wt C			Density 1 (g/m ³)		
	V	E	I	V	E	I
A2	88.9	96.5	91.9	1.30	1.24	1.38
B2	86.0	93.0	90.1	1.30	1.22	1.38
C2	87.8	94.6	90.9	1.31	1.20	1.37
D2	83.4	76.5	86.5	1.37	1.26	1.42

Step 3 The density estimates are used to convert the petrographic composition from volume to weight percent. These are used in an interpolation to fit C (% wt) to the ultimate analysis test result. The second estimate of the densities are taken from the same graph as above

	% wt C 2			Density 2 (g/m ³)		
	V	E	I	V	E	I
A2	87.7	95.2	90.7	1.30	1.26	1.39
B2	86.7	93.7	90.8	1.30	1.26	1.40
C2	85.5	92.2	88.6	1.29	1.22	1.37
D2	79.5	73.0	82.5	1.35	1.25	1.43

	% wt C 3			Density 3 (g/m ³)		
	V	E	I	V	E	I
A2	87.6	95.1	90.6	1.30	1.26	1.39
B2	86.6	93.6	90.7	1.30	1.26	1.39
C2	85.4	92.1	88.5	1.29	1.22	1.37
D2	80.2	73.6	83.2	1.34	1.24	1.41

	% wt C 4			Density 4 (g/m ³)		
	V	E	I	V	E	I
D2	80.3	73.6	82.2	1.35	1.25	1.43

Step 4 An interpolation is performed to fit the pure maceral VM (% wt) to the VM (% wt) of the coal as tested

	% wt VM		
	V	E	I
A2	28.5	30.4	18.9
B2	33.7	39.2	20.8
C2	29.3	31.7	18.9
D2	49.2	133.0	34.4

Step 5 The VM (%wt) and C (%wt) for the vitrinite and inertinite concentrates are calculated from the pure maceral estimates and compared to the results as tested.

	% wt VM		% wt C	
	tested	calc.	tested	calc.
Vitrinite Concentrate				
A2	23.4	25.5	86.7	88.6
B2	28.3	31.6	87.6	87.2
C2	25.6	28.1	87.7	85.8
D2	46.5	50.2	82.4	80.4

Inertinite Concentrate				
A2	31.7	23.4	78.5	89.2
B2	29.4	27.1	80.8	88.7
C2	21.9	23.1	81.1	87.3
D2	46.0	46.2	85.8	81.1

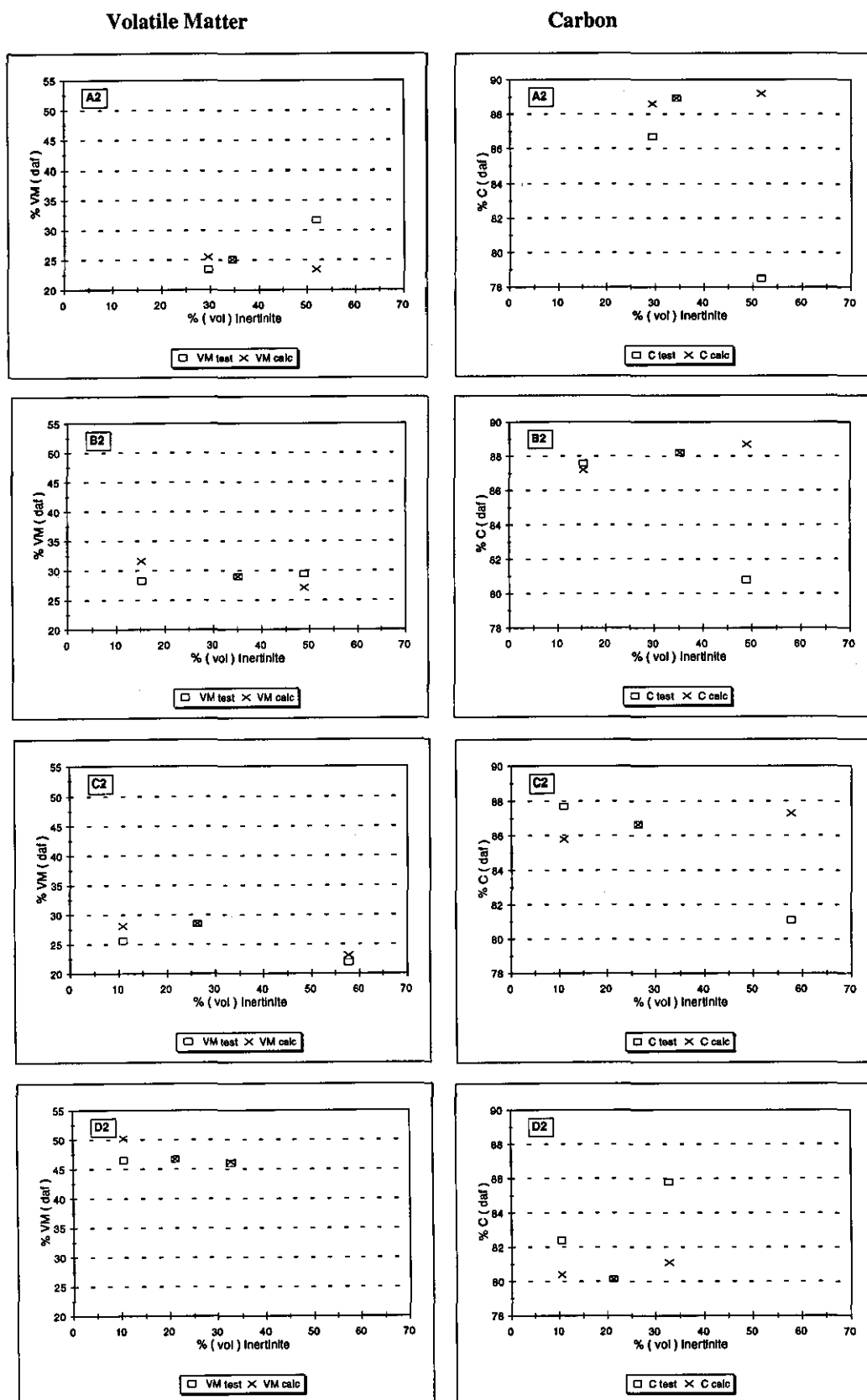


Figure A1

Comparison of Tested and Calculated Volatile Matter and Carbon Content for Series 2

Appendix 2

Component Count Data

List of Tables

- T A2.1 Results from 500 Point Component Counts on Sample Series 1
- T A2.2 Results from 500 Point Component Counts on Sample Series 2.1
- T A2.3 Results from 500 Point Component Counts on the V/I Blends of Sample Series 2
- T A2.4 Results from 500 Point Component Counts on Sample Series 2.2
- T A2.5 Results from 500 Point Component Counts on Sample Series 3

		Observer 1		Observer 2	
		Count 1	Count 2	Count 1	Count 2
A1	A	1	0	2	1
	BF	184	90	134	137
	SF	74	123	47	87
	GF	99	143	215	121
	CM	23	28	14	39
	MM	6	4	9	16
	FM	4	2	1	2
	ISO	6	6	0	0
	INL	80	82	52	65
	INS	23	22	26	32
B1	A	0	0	2	0
	BF	47	78	160	95
	SF	60	84	85	76
	GF	248	236	173	241
	CM	47	7	8	6
	MM	1	1	4	0
	FM	0	0	1	0
	ISO	4	0	2	0
	INL	65	61	45	54
	INS	28	33	20	28
C1	A	0	0	0	0
	BF	11	4	18	34
	SF	55	58	28	57
	GF	285	266	246	278
	CM	36	47	86	18
	MM	0	1	7	4
	FM	1	0	1	1
	ISO	5	7	1	2
	INL	78	85	75	77
	INS	29	32	38	29
D1	A	0	0		
	BF	2	2	6	7
	SF	11	8	3	11
	GF	313	242	280	240
	CM	73	146	107	145
	MM	10	19	35	42
	FM	4	7	6	0
	ISO	7	1	3	4
	INL	38	42	34	30
	INS	42	33	26	21

cont. overleaf

E1	A	0	0	0	0
	BF	5	3	4	7
	SF	0	0	0	0
	GF	5	4	31	26
	CM	38	25	82	118
	MM	344	325	289	245
	FM	15	48	0	2
	ISO	8	13	0	6
	INL	52	42	60	61
	INS	33	40	34	35
F1	A	0	0	0	0
	BF	1	2	8	4
	SF	0	0	0	0
	GF	1	7	17	23
	CM	30	17	13	10
	MM	186	191	227	208
	FM	146	161	102	121
	ISO	84	35	6	21
	INL	49	32	78	63
	INS	3	55	49	50

Table A2.1 Results from 500 Point Component Counts on Sample Series 1

			C1	C2
a) A2	VC	A	0	0
		BF	6	8
		SF	1	0
		GF	139	167
		CM	15	20
		MM	45	13
		FM	88	24
		ISO	57	143
		INS	47	32
		INL	102	93
	C	A	0	1
		BF	6	7
		SF	2	0
		GF	149	152
		CM	44	43
		MM	58	49
		FM	103	43
		ISO	36	92
		INS	43	45
		INL	59	68
	IC	A	0	0
		BF	6	15
		SF	3	1
		GF	129	169
		CM	26	16
		MM	47	16
		FM	79	28
		ISO	30	98
		INS	69	57
		INL	111	100
b) B2	VC	A	0	0
		BF	7	12
		SF	0	0
		GF	100	124
		CM	75	78
		MM	77	54
		FM	72	19
		ISO	73	112
		INS	48	43
		INL	48	58
	75V	A	0	0
		BF	5	13
		SF	0	0
		GF	97	112
		CM	108	98
		MM	74	55
		FM	98	22
		ISO	29	100
		INS	49	44
		INL	40	56

c) C2	C	A	0	0
		BF	1	7
		SF	1	0
		GF	109	119
		CM	117	103
		MM	63	62
		FM	83	14
		ISO	48	69
		INS	41	61
		INL	37	65
	IC	A	0	0
		BF	10	11
		SF	0	0
		GF	90	123
		CM	28	37
		MM	85	65
		FM	128	32
		ISO	28	78
		INS	53	53
		INL	78	101
c) C2	VC	A	0	2
		BF	7	16
		SF	1	1
		GF	98	92
		CM	73	78
		MM	51	51
		FM	71	22
		ISO	67	137
		INS	53	34
		INL	79	67
	75V	A	0	0
		BF	13	16
		SF	0	0
		GF	126	123
		CM	97	96
		MM	47	48
		FM	80	16
		ISO	21	96
		INS	54	39
		INL	62	66
	C	A	1	1
		BF	4	14
		SF	0	1
		GF	95	115
		CM	97	102
		MM	60	49
		FM	56	13
		ISO	39	82
		INS	74	47
		INL	74	76

d) D2	50 V	A	0	2
		BF	7	15
		SF	0	0
		GF	89	80
		CM	98	86
		MM	67	45
		FM	106	18
		ISO	33	114
		INS	43	59
		INL	57	81
	IC	A	0	0
		BF	6	14
		SF	0	2
		GF	71	79
		CM	37	55
		MM	74	34
		FM	129	25
		ISO	46	132
		INS	49	58
		INL	88	101
	VC	A	0	0
		BF	0	0
		SF	0	0
		GF	0	0
		CM	0	0
		MM	0	0
		FM	149	129
		ISO	300	328
		INS	11	9
		INL	40	33
	C	A	0	0
		BF	0	0
		SF	0	0
		GF	0	0
		CM	0	0
		MM	0	0
		FM	122	101
		ISO	340	360
		INS	5	8
		INL	33	32
	IC	A	0	0
		BF	0	0
		SF	0	0
		GF	0	0
		CM	0	0
		MM	3	0
		FM	173	131
		ISO	203	260
		INS	15	14
		INL	106	95

Table A2.2. Results from 500 Point Component Counts on Sample Series 2.1

		C1	C2
A2	A	0	0
	BF	7	8
	SF	2	1
	GF	163	124
	CM	9	19
	MM	37	25
	FM	82	61
	ISO	134	122
	INS	23	35
	INL	43	105
B2	A	0	0
	BF	6	4
	SF	0	0
	GF	98	103
	CM	32	45
	MM	96	58
	FM	76	49
	ISO	129	141
	INS	32	30
	INL	31	70
C2	A	0	0
	BF	8	14
	SF	0	0
	GF	61	78
	CM	47	84
	MM	104	47
	FM	61	50
	ISO	132	105
	INS	37	32
	INL	50	90
D2	A	0	0
	BF	0	0
	SF	0	0
	GF	0	0
	CM	0	0
	MM	0	4
	FM	244	252
	ISO	214	209
	INS	4	0
	INL	38	34

Table A2.3. Results from 500 Point Component Counts on the V/I Blends of Sample Series 2

A2	B2 37		C2 37	
	C1	C2	C1	C2
A	0	0	0	0
BF	10	5	14	6
SF	0	1	0	3
GF	154	142	150	153
CM	32	33	33	27
MM	13	18	23	20
FM	54	34	32	35
ISO	116	93	98	125
INS	41	39	48	33
INL	80	135	102	98

B2	A2 25		A2 37		C2 25		C2 37		C2 50		D2 25	
	C1	C2	C1	C2	C1	C2	C1	C2	C1	C2	C1	C2
A	0	0	0	0	0	0	0	0	0	0	0	0
BF	5	13	10	10	7	6	5	11	10	7	5	4
SF	0	0	1	2	0	0	0	0	0	1	0	0
GF	166	156	180	184	144	119	133	109	119	105	75	81
CM	97	76	52	49	101	96	85	87	60	88	17	18
MM	20	38	14	21	16	47	20	46	28	35	24	27
FM	25	21	41	51	29	41	35	51	33	34	80	105
ISO	115	117	69	69	126	112	98	79	80	105	179	180
INS	31	32	44	34	37	34	46	35	55	26	28	21
INL	41	47	89	80	40	45	78	82	115	99	92	64

cont.
overleaf

C2	A2 25		A2 37		B2 25		B2 37		D2 25	
	C1	C2	C1	C2	C1	C2	C1	C2	C1	C2
A	1	0	0	0	0	0	0	0	0	0
BF	7	7	10	10	5	6	5	8	10	6
SF	3	0	0	1	0	0	0	1	1	0
GF	110	114	151	146	141	128	123	122	44	75
CM	78	55	43	45	72	94	65	73	40	36
MM	35	38	26	26	23	27	34	18	28	20
FM	64	61	28	37	24	38	47	33	65	65
ISO	116	106	94	90	118	102	125	118	207	195
INS	43	40	62	47	55	45	46	45	50	39
INL	43	79	86	98	62	60	55	82	55	64
D2	A2 25		A2 37		B2 25		B2 37		C2 25	
	C1	C2	C1	C2	C1	C2	C1	C2	C1	C2
A	0	0	0	0	0	0	0	0	0	0
BF	0	2	2	4	3	3	1	7	2	1
SF	1	0	1	0	0	0	1	0	0	0
GF	77	66	111	126	42	56	92	79	29	40
CM	10	5	4	10	13	12	14	15	7	13
MM	6	6	16	6	17	14	16	18	12	6
FM	162	101	66	90	129	153	90	114	132	131
ISO	166	228	191	151	203	168	182	161	244	229
INS	29	26	40	32	23	28	41	34	27	14
INL	49	66	69	81	70	66	63	72	47	66

Table A2.4. Results from 500 Point Component Counts on Sample Series 2.2

a) A3		Add1		Add2	
		C1	C2	C1	C2
0% Add	A	7	9		
	BF	151	160		
	SF	51	22		
	GF	143	202		
	CM	14	19		
	MM	12	5		
	FM	3	0		
	ISO	4	12		
	INS	26	21		
	INL	89	49		
10 % Add	A	9	14	0	0
	BF	204	211	171	155
	SF	32	23	29	26
	GF	118	123	171	198
	CM	13	10	11	17
	MM	9	6	3	5
	FM	0	1	0	0
	ISO	2	6	1	7
	INS	17	19	21	14
	INL	68	54	51	50
	ADD	30	35	43	29
30 % Add	A	5	3	1	0
	BF	217	214	181	219
	SF	31	15	24	17
	GF	107	117	142	126
	CM	14	22	16	16
	MM	9	4	9	2
	FM	1	1	0	0
	ISO	3	8	3	9
	INS	18	22	20	19
	INL	39	33	57	54
	ADD	60	65	50	41
50 % Add	A	8	9		
	BF	205	179		
	SF	32	15		
	GF	116	98		
	CM	15	20		
	MM	8	15		
	FM	0	0		
	ISO	5	7		
	INS	12	10		
	INL	39	33		
	ADD	63	117		

b) B3		Add1		Add2	
		C1	C2	C1	C2
0% Add	A	0	0		
	BF	12	9		
	SF	4	7		
	GF	156	212		
	CM	99	109		
	MM	113	57		
	FM	14	9		
	ISO	8	24		
	INS	32	20		
	INL	63	53		
10 % Add	A	0	0	0	0
	BF	8	8	26	10
	SF	4	4	4	2
	GF	140	174	255	79
	CM	87	93	130	66
	MM	120	79	131	44
	FM	28	14	28	2
	ISO	5	17	8	3
	INS	31	34	37	11
	INL	31	30	66	18
	ADD	46	47	29	15
30 % Add	A	0	0	0	0
	BF	5	8	27	5
	SF	6	2	9	3
	GF	79	123	187	52
	CM	82	97	186	70
	MM	113	78	113	38
	FM	17	11	23	4
	ISO	18	11	7	4
	INS	22	27	31	14
	INL	49	47	49	19
	ADD	109	96	43	41
50 % Add	A	0	0	0	0
	BF	7	5	11	4
	SF	3	2	4	3
	GF	68	122	191	52
	CM	87	98	156	60
	MM	87	54	76	26
	FM	26	16	14	3
	ISO	20	10	20	6
	INS	23	20	29	9
	INL	28	19	78	25
	ADD	151	154	58	62

c) C3		Add1		Add2	
		C1	C2	C1	C2
0% Add	A	0	0		
	BF	10	7		
	SF	1	0		
	GF	172	256		
	CM	152	127		
	MM	56	32		
	FM	6	3		
	ISO	17	19		
	INS	54	44		
	INL	32	12		
10 % Add	A	0	0	0	0
	BF	6	2	3.5	11.5
	SF	3	2	0	1
	GF	173	180	162.5	192.5
	CM	93	85	132.5	123.5
	MM	95	25	63	30
	FM	6	3	4	4
	ISO	5	10	17.5	17.5
	INS	39	48	34	35
	INL	37	27	42	27
	ADD	70	118	41	58
30 % Add	A	0	0	0	0
	BF	3	1	3.5	3.5
	SF	2	0	1.5	0.5
	GF	85	160	122.5	136.5
	CM	75	91	73.5	97.5
	MM	111	27	85.5	50.5
	FM	1	2	12	10
	ISO	4	9	13	21
	INS	41	34	42.5	36.5
	INL	26	23	26	18
	ADD	178	153	120	126
50 % Add	A	0	0	0	0
	BF	0	2	5	5
	SF	0	0	1	0
	GF	52	106	110	113
	CM	60	101	66.5	92.5
	MM	88	25	51	36
	FM	8	2	11	10
	ISO	14	21	14.5	30.5
	INS	35	25	25.5	29.5
	INL	29	29	27.5	25.5
	ADD	243	189	188	158

d) Blend		Add1		Add2	
		C1	C2	C1	C2
0% Add	A	2	4		
	BF	73	70		
	SF	13	5		
	GF	143	160		
	CM	76	109		
	MM	83	49		
	FM	11	9		
	ISO	7	9		
	INS	36	32		
	INL	56	53		
10 % Add	A	2	0	0	0
	BF	48	41	58	57
	SF	10	9	7	5
	GF	150	219	143	169
	CM	69	64	81	88
	MM	70	41	76	54
	FM	9	2	11	9
	ISO	16	10	15	15
	INS	33	29	21	28
	INL	36	33	37	37
	ADD	57	52	51	38
30 % Add	A	0	1	0	0
	BF	35	44	51	53
	SF	12	5	1	6
	GF	93	156	116	126
	CM	56	59	84	106
	MM	79	28	74	51
	FM	10	10	15	10
	ISO	14	13	23	18
	INS	31	20	26	20
	INL	52	44	32	62
	ADD	118	120	76	48
50 % Add	A	3	2	0	0
	BF	53	70	56	54
	SF	8	5	5	11
	GF	67	100	128	123
	CM	50	86	68	65
	MM	71	51	25	29
	FM	22	7	6	4
	ISO	18	8	17	11
	INS	31	24	20	17
	INL	44	50	34	38
	ADD	135	97	141	148

Table A2.5. Results from 500 Point Component Counts on Sample Series 3

Appendix 3

Interface Count Data

List of Tables

- T A3.1 Results from the 500 Point Simple Interface Counts on Sample Series 1
- T A3.2 Results from the 1000 Point by Component Interface Counts on Sample Series 1
- T A3.2.S Results from the Supplementary 50 Point by Component Interface Counts on Sample Series 1 targeting Specific Components
- T A3.3 Results from the 500 Point Simple Interface Count on Sample Series 2.1
- T A3.4 Results from the 500 Point Split Interface Count on Sample Series 2.1
- T A3.5 Results from the 500 Point Simple and Split Interface Counts on the V/I Blends of Sample Series 2
- T A3.6 Results from the 1000 Point by Components Interface Count on Sample Series 2.1
- T A3.7 Results from the 500 Point Simple Interface Count on Sample Series 2.2
- T A3.8 Results from the 500 Point Split Interface Count on Sample Series 2.2
- T A3.9 Results from the 1000 Point by Components Interface Count on Sample Series 2.2
- T A3.10 Results from the 500 Point Split Interface Count on Sample Series 3
- T A3.11 Results from the 250 Point Interface Count targeting Large Inerts, Small Inerts, Large Additive Particles and Small Additive Particles on Sample Series 3

		Observer 1		Observer 2	
		Count 1	Count 2	Count 1	Count 2
A1	T	241	237	252	203.5
	FU	198	162	172	205
	FI	49	80	60	71.5
	UF	12	21	16	20
B1	T	146	155	236	213
	FU	279	276	218	229
	FI	70	64	44	39
	UF	5	5	2	19
C1	T	74	83	76	162
	FU	353	348	391	300
	FI	72	64	30	27
	UF	1	5	3	11
D1	T	85	129	150	111
	FU	363	333	333	370
	FI	52	37	13	15
	UF	0	1	4	4
E1	T	53	38	33	43
	FU	396	392	380	389
	FI	48	64	84	61
	UF	3	6	3	7
F1	T	222	197	210	133
	FU	257	248	257	330
	FI	21	54	23	34
	UF	0	1	10	3

Table A3.1 Results from the 500 Point Simple Interface Counts on Sample Series 1

a) A 1	T	FU	FI	UF
R-R				
BF-SF	119	13	1	1
BF-GF	127	29	6	
BF-CM	6	2		
BF-MM	1			
BF-FM				
BF-ISO				
SF-GF	93	14	3	1
SF-CM	2	1		
SF-MM				
SF-FM	1			
SF-ISO				
GF-CM	4			
GF-MM				
GF-FM				
GF-ISO	1			
CM-MM				
CM-FM				
CM-ISO				
MM-FM				
MM-ISO				
FM-ISO				
R-S				
BF	1	51	58	21
SF	0	25	31	2
GF	0	184	62	3
CM	0	3	2	0
MM				
FM				
ISO				
R-L				
BF	0	23	15	0
SF	0	5	4	0
GF	2	48	14	1
CM	0	7	2	0
MM	0	1	1	0
FM				
ISO				
b) B 1				
R-R				
BF-SF	93	13	2	
BF-GF	128	18	2	1
BF-CM		2		
BF-MM				
BF-FM	1	1		
BF-ISO				
SF-GF	115	16	1	2
SF-CM	1			
SF-MM	1			
SF-FM				

SF-ISO				
GF-CM	2			
GF-MM				
GF-FM				
GF-ISO				
CM-MM				
CM-FM				
CM-ISO				
MM-FM				
MM-ISO				
FM-ISO				
R-S				
BF	1	126	48	8
SF		44	30	2
GF		148	31	2
CM				
MM				
FM				
ISO				
	1	318	109	12
R-L				
BF	4	34	27	4
SF		12	14	
GF	2	41	17	
CM		1		
MM				
FM				
ISO				
c) C 1				
R-R				
BF-SF	8	1		
BF-GF	37	8		
BF-CM				
BF-MM				
BF-FM				
BF-ISO				
SF-GF	103	7	1	
SF-CM				
SF-MM				
SF-FM				
SF-ISO				
GF-CM	21	1		
GF-MM	7			
GF-FM	1			
GF-ISO				
CM-MM	1			
CM-FM	1			
CM-ISO				
MM-FM				
MM-ISO				
FM-ISO				
R-S				
BF	1	23	10	1
SF		52	13	1

GF	2	444	33	4
CM		25		1
MM		3		
FM				
ISO				
R-L				
BF		2	1	
SF	1	7	1	
GF	8	127	17	2
CM	1	19		
MM	1	3		
FM				
ISO				
d) D 1				
R-R				
BF-SF				
BF-GF	9	2		
BF-CM	1			
BF-MM				
BF-FM				
BF-ISO				
SF-GF	21			
SF-CM	3			
SF-MM	1			
SF-FM				
SF-ISO				
GF-CM	82	7		
GF-MM	9	5		
GF-FM		3		
GF-ISO		1	1	
CM-MM	17	6		
CM-FM	1			
CM-ISO				
MM-FM		1		
MM-ISO				
FM-ISO				
R-S				
BF		2		
SF		4	2	
GF	1	437	25	
CM		205	12	
MM		22		
FM				
ISO				
R-L				
BF				
SF		1		
GF	2	58	2	2
CM	1	35	2	2
MM		14	1	
FM		2		
ISO				

e) E 1	T	FU	FI	UF
R-R				
BF-SF				
BF-GF		1		
BF-CM		1		
BF-MM	1	11		
BF-FM				
BF-ISO				
SF-GF				
SF-CM				
SF-MM				
SF-FM				
SF-ISO				
GF-CM	4			
GF-MM		1		
GF-FM				
GF-ISO				
CM-MM	16			
CM-FM				
CM-ISO				
MM-FM	45	4		
MM-ISO		7	1	
FM-ISO	3	5		
R-S				
BF				
SF				
GF		16	1	
CM		95	10	
MM	2	530	79	6
FM		21	2	
ISO				
R-L				
BF				
SF				
GF	1	2	1	1
CM	2	20	3	
MM	6	72	14	2
FM		4	1	
ISO				
f) F 1				
R-R				
BF-SF	1			
BF-GF	2			
BF-CM				
BF-MM	1	3		
BF-FM				
BF-ISO				
GF-CM	2			
GF-MM	2	1		
GF-FM				
GF-ISO				
CM-MM	18	3		

CM-FM			
CM-ISO			
MM-FM	90	7	1
MM-ISO	14	26	2
FM-ISO	47	4	
R-S			
BF		1	
SF			
GF	2	21	1
CM		56	2
MM		412	32
FM		43	8
ISO			
R-L			
BF		1	
SF			
GF	1	4	1
CM		15	3
MM	10	105	25
FM	7	22	2
ISO	1		

Table A3.2 Results from the 1000 Point by Component Interface Counts on Sample Series 1

	T	Fu	Fi	Uf
a) D1-BF				
BF				
SF				
GF	16	1	0	0
CM	13	1	0	0
MM	4	5	0	0
FM				
ISO				
INS	0	6	2	0
INL	1	1	0	0
b) E1-BF				
BF				
SF				
GF	1	0	0	0
CM	2	2	0	0
MM	12	18	2	0
FM				
ISO				
INS	2	4	1	0
INL	2	3	0	0
c) D1-SF				
BF	0	1	0	0
SF				
GF	18	3	0	1
CM	8	7	2	1
MM	3	2	0	2
FM	1	0	0	0
ISO				
INS	0	1	0	0
INL				
d) F1-GF				
BF	1	0	0	0
SF				
GF				
CM	6	0	0	0
MM	13	10	0	0
FM	0	1	0	0
ISO				
INS	1	13	0	0
INL	1	3	1	0
e) E1-GF				
BF	2	1	0	0
SF				
GF				
CM	16	0	0	0
MM	3	0	0	0
FM				
ISO				
INS	1	16	2	0
INL	0	8	1	0

	T	Fu	Fi	Uf
f) A1-CM				
BF	10	5	0	0
SF	5	2	0	0
GF	13	1	0	0
CM				
MM	6	0	0	0
FM				
ISO				
INS	0	4	1	0
INL	0	3	0	0
g) B1-CM				
BF	12	7	0	0
SF	10	2	0	0
GF	16	0	0	0
CM				
MM				
FM				
ISO				
INS	0	3	0	0
INL				
h) A1-MM				
BF	23	3	0	0
SF	2	0	0	0
GF	4	2	0	0
CM	6	1	0	0
MM				
FM				
ISO				
INS	0	4	2	1
INL	0	2	0	0
i) B1-MM				
BF	16	16	0	0
SF	2	1	0	0
GF	6	1	0	0
CM				
MM				
FM				
ISO				
INS	0	6	0	0
INL	1	5	1	0
j) D1-FM				
BF	1	0	0	0
SF				
GF	1	3	0	0
CM	6	5	0	0
MM	16	2	0	0
FM				
ISO	7	1	0	0
INS	0	5	0	0
INL	0	5	0	0

	T	Fu	Fi	Uf
k) C1-ISO				
BF	1	2	1	0
SF				
GF	5	28	0	0
CM	2	5	0	0
MM	0	3	0	0
FM	3	0	0	0
ISO				
INS				
INL				
l) D1-ISO				
BF	0	1	0	0
SF				
GF	4	11	0	0
CM	8	10	0	0
MM	4	3	0	0
FM	9	0	0	0
ISO				
INS				
INL				
m) E1-ISO				
BF				
SF				
GF				
CM	0	6	0	0
MM	6	28	1	0
FM	7	2	0	0
ISO				
INS				
INL				

Table A3.2.S Results from the Supplementary 50 Point by Component Interface Counts on Sample Series 1 targeting Specific Components

A2	VC	T	174
		FU	222
		FI	97
		UF	7
	C	T	121
		FU	247
		FI	127
		UF	5
	IC	T	124
		FU	175
		FI	189
		UF	12
B2	VC	T	129
		FU	169
		FI	196
		UF	6
	75V	T	110
		FU	199
		FI	185
		UF	6
	C	T	115
		FU	218
		FI	162
		UF	5
	IC	T	107
		FU	114
		FI	268
		UF	11
C2	VC	T	100
		FU	224
		FI	170
		UF	6
	75V	T	117
		FU	210
		FI	166
		UF	7
	C	T	116
		FU	217
		FI	161
		UF	6
	50V	T	57
		FU	243
		FI	194
		UF	6
	IC	T	106
		FU	186
		FI	195
		UF	13

Table A3.3 Results from the 500 Point Simple Interface Count on Sample Series 2.1

	R-R				R-S				R-L			
	T	FU	FI	UF	T	FU	FI	UF	T	FU	FI	UF
A2												
VC	137	64	54	2	0	125	80	7	3	14	13	1
C	143	56	58	1	0	137	69	5	1	13	15	2
IC	103	40	82	2	0	91	127	7	8	11	27	2
B2												
VC	116	60	84	3	0	98	117	3	1	7	11	0
75V	111	61	84	2	0	150	63	2	1	13	13	0
C	91	42	53	2	0	159	91	4	4	25	28	1
IC	105	43	77	2	0	124	105	12	4	6	20	2
C2												
VC	119	97	65	2	0	129	55	2	1	17	12	1
75V	110	89	64	1	0	157	43	1	1	18	16	0
C	94	59	60	3	1	154	79	4	1	21	24	0
50V	74	69	60	4	0	146	85	8	0	22	30	2
IC	129	47	67	1	0	116	86	6	1	18	25	4

Table A3.4 Results from the 500 Point Split Interface Count on Sample Series 2.1

a) Simple			
A2	T	102	
	FU	189	
	FI	200	
	UF	9	
B2	T	96	
	FU	153	
	FI	239	
	UF	12	
C2	T	117	
	FU	234	
	FI	143	
	UF	6	

b) Split		R-R	R-S	R-L
A2	T	120	1	1
	FU	56	105	15
	FI	87	92	13
	UF	1	6	3
B2	T	109	0	1
	FU	53	108	12
	FI	103	92	17
	UF	1	3	1
C2	T	102	0	1
	FU	70	127	20
	FI	91	59	24
	UF	4	2	0

Table A3.5 Results from the 500 Point Simple and Split Interface Counts on the V/I Blends of Sample Series 2

a) A2 VC	T	FU	FI	UF
GF-CM	14	0	1	0
GF-MM	17	1	0	0
GF-FM	10	13	27	2
GF-ISO	46	55	50	0
CM-MM	3	0	0	0
CM-FM	2	2	0	0
CM-ISO	1	3	0	0
MM-FM	11	5	0	0
MM-ISO	7	3	3	0
FM-ISO	2	23	11	0
INS-				
GF	0	328	197	3
CM	0	25	9	0
MM	0	31	14	0
FM	0	6	4	1
ISO	0	2	1	0
INL-				
GF	0	5	5	0
CM	0	0	0	0
MM	0	1	1	0
FM	0	0	2	0
ISO	0	0	2	1
Other	16	14	19	2
b) A2 C				
GF-CM	31	1	1	0
GF-MM	15	2	1	0
GF-FM	5	2	3	0
GF-ISO	44	71	67	0
CM-MM	0	1	0	0
CM-FM	2	2	0	0
CM-ISO	4	9	3	0
MM-FM	22	0	0	0
MM-ISO	8	6	3	0
FM-ISO	3	3	1	0
INS-				
GF	1	395	185	2
CM	0	36	22	0
MM	0	32	14	2
FM	0	2	2	0
ISO	0	1	4	0
INL-				
GF	1	19	15	0
CM	0	3	0	0
MM	0	4	5	0
FM	0	0	0	0
ISO	0	0	2	0
Other	14	14	14	0

e) A2 IC	T	FU	FI	UF
GF-CM	13	0	0	0
GF-MM	11	1	0	0
GF-FM	7	3	2	0
GF-ISO	73	31	73	0
CM-MM	2	0	0	0
CM-FM	2	0	0	0
CM-ISO	4	0	2	0
MM-FM	22	2	4	0
MM-ISO	6	1	6	0
FM-ISO	12	2	1	0
INS-				
GF	0	323	258	7
CM	0	14	7	0
MM	0	21	8	0
FM	0	0	3	1
ISO	0	3	4	0
INL-				
GF	1	7	19	1
CM	0	1	1	0
MM	0	0	0	0
FM	0	0	0	0
ISO	0	1	0	1
Other	9	13	13	1
d) B2 VC				
GF-CM	32	1	0	1
GF-MM	21	3	1	0
GF-FM	1	1	0	0
GF-ISO	49	38	55	0
CM-MM	2	0	0	0
CM-FM	2	1	1	0
CM-ISO	9	12	11	0
MM-FM	16	1	1	0
MM-ISO	16	13	20	0
FM-ISO	3	0	1	0
INS-				
GF	0	233	126	0
CM	0	95	64	1
MM	0	54	42	0
FM	0	0	1	0
ISO	0	0	2	0
INL-				
GF	1	11	14	0
CM	0	5	2	0
MM	0	5	7	1
FM	0	0	1	0
ISO	0	0	2	0
Other	6	10	6	0

e) B2 75V	T	FU	FI	UF
GF-CM	27	4	0	0
GF-MM	17	3	0	0
GF-FM	3	12	17	1
GF-ISO	26	22	48	0
CM-MM	4	0	0	0
CM-FM	4	6	14	0
CM-ISO	6	14	17	0
MM-FM	9	7	7	0
MM-ISO	5	9	12	0
FM-ISO	1	2	2	0
INS-				
GF	0	191	143	0
CM	0	107	68	0
MM	0	65	41	0
FM	0	0	0	0
ISO	0	0	0	0
INL-				
GF	0	4	14	0
CM	0	6	3	0
MM	0	6	4	1
FM	0	0	0	0
ISO	0	0	0	0
Other	10	8	11	0
f) B2 C				
GF-CM	44	6	1	0
GF-MM	9	1	0	0
GF-FM	1	1	0	0
GF-ISO	17	31	46	0
CM-MM	5	0	0	0
CM-FM	3	0	0	0
CM-ISO	3	28	15	1
MM-FM	8	0	0	0
MM-ISO	5	15	7	0
FM-ISO	0	0	0	1
INS-				
GF	0	275	113	1
CM	0	146	65	0
MM	0	38	27	0
FM	0	2	1	0
ISO	0	0	1	0
INL-				
GF	1	15	7	0
CM	0	11	5	1
MM	0	8	8	0
FM	0	1	0	0
ISO	0	0	1	0
Other	6	10	14	0

g) B2 IC	T	FU	FI	UF
GF-CM	15	1	0	0
GF-MM	14	4	0	0
GF-FM	7	3	7	0
GF-ISO	38	40	94	0
CM-MM	0	0	0	0
CM-FM	0	0	0	0
CM-ISO	2	14	5	0
MM-FM	25	3	5	0
MM-ISO	10	11	18	0
FM-ISO	5	1	7	0
INS-				
GF	0	202	180	1
CM	0	56	31	0
MM	0	55	33	0
FM	0	3	4	0
ISO	0	0	2	1
INL-				
GF	2	14	26	0
CM	0	2	0	0
MM	0	4	6	0
FM	0	0	1	0
ISO	0	0	0	1
Other	12	12	27	0
h) C2 VC				
GF-CM	23	3	0	0
GF-MM	21	3	1	0
GF-FM	3	8	9	0
GF-ISO	38	62	61	1
CM-MM	6	0	0	0
CM-FM	2	3	5	0
CM-ISO	6	32	18	0
MM-FM	14	8	6	0
MM-ISO	11	26	28	1
FM-ISO	2	11	4	0
INS-				
GF	2	176	91	0
CM	0	79	39	1
MM	0	79	44	0
FM	0	1	0	0
ISO	0	0	2	0
INL-				
GF	0	7	6	0
CM	0	6	2	0
MM	0	8	6	0
FM	0	0	0	0
ISO	0	0	0	0
Other	6	18	11	0

i) C2 75V	T	FU	FI	UF
GF-CM	49	4	0	0
GF-MM	16	4	0	0
GF-FM	1	1	0	0
GF-ISO	35	49	50	0
CM-MM	11	0	0	0
CM-FM	3	1	0	0
CM-ISO	7	27	13	0
MM-FM	8	0	0	0
MM-ISO	8	11	14	0
FM-ISO	2	0	0	0
INS-				
GF	0	268	111	2
CM	0	116	38	0
MM	0	32	17	0
FM	0	0	0	0
ISO	0	1	0	0
INL-				
GF	0	11	7	0
CM	0	15	4	0
MM	0	6	7	0
FM	0	1	0	0
ISO	0	0	1	0
Other	13	26	10	0
j) C2 C				
GF-CM	32	7	1	0
GF-MM	11	1	2	0
GF-FM	4	0	1	0
GF-ISO	13	47	36	0
CM-MM	5	0	0	0
CM-FM	2	1	1	0
CM-ISO	4	13	11	0
MM-FM	10	0	0	0
MM-ISO	5	8	15	0
FM-ISO	2	0	1	0
INS-				
GF	0	236	132	3
CM	1	131	62	1
MM	0	48	39	0
FM	0	1	5	0
ISO	0	0	0	0
INL-				
GF	0	12	10	1
CM	0	13	13	0
MM	0	6	7	1
FM	0	0	0	0
ISO	0	0	4	0
Other	8	23	9	0

k) C2 50V	T	FU	FI	UF
GF-CM	35	4	1	0
GF-MM	11	2	0	0
GF-FM	4	12	14	1
GF-ISO	20	28	20	0
CM-MM	6	0	0	0
CM-FM	1	5	10	0
CM-ISO	2	26	18	3
MM-FM	10	10	9	0
MM-ISO	1	9	12	1
FM-ISO	1	7	3	0
INS-				
GF	3	218	101	1
CM	0	137	62	2
MM	0	55	26	0
FM	0	0	0	0
ISO	0	0	1	1
INL-				
GF	0	14	6	0
CM	0	8	9	0
MM	0	9	8	0
FM	0	0	0	0
ISO	0	0	1	0
Other	7	24	13	0
l) C2 IC				
GF-CM	18	3	0	0
GF-MM	10	1	2	0
GF-FM	3	1	2	0
GF-ISO	41	37	52	1
CM-MM	6	1	0	0
CM-FM	4	0	1	0
CM-ISO	5	11	20	0
MM-FM	21	2	4	0
MM-ISO	13	15	18	0
FM-ISO	2	0	0	0
INS-				
GF	0	153	135	0
CM	0	93	77	0
MM	0	69	59	0
FM	0	6	3	0
ISO	0	3	4	0
INL-				
GF	0	14	30	0
CM	0	3	4	0
MM	0	11	7	0
FM	0	1	0	0
ISO	0	0	5	0
Other	6	11	14	2

Table A3.6 Results from the 1000 Point by Components Interface Count on Sample Series 2.1

Sample	Interface	Pts counted
A2B2 37	T	90
	FU	224
	FI	180
	UF	6
A2C2 37	T	84
	FU	210
	FI	202
	UF	4
B2A2 25	T	130
	FU	110
	FI	251
	UF	9
B2A2 37	T	109
	FU	178
	FI	207
	UF	6
B2C2 25	T	109
	FU	217
	FI	169
	UF	5
B2C2 37	T	92
	FU	218
	FI	181
	UF	9
B2C2 50	T	91
	FU	205
	FI	192
	UF	12
BD 25	T	144
	FU	142
	FI	207
	UF	7
C2A2 25	T	103
	FU	237
	FI	158
	UF	2

Sample	Interface	Pts counted
C2A2 37	T	116
	FU	188
	FI	191
	UF	5
C2B2 25	T	77
	FU	216
	FI	199
	UF	8
C2B2 37	T	81
	FU	216
	FI	197
	UF	6
C2D2 25	T	142
	FU	207
	FI	146
	UF	5
D2A2 25	T	105
	FU	186
	FI	200
	UF	9
D2A2 37	T	97
	FU	168
	FI	230
	UF	5
D2B2 25	T	115
	FU	122
	FI	255
	UF	8
D2B2 37	T	106
	FU	162
	FI	227
	UF	5
D2C2 25	T	113
	FU	140
	FI	234
	UF	13

Table A3.7 Results from the 500 Point Simple Interface Count on Sample Series 2.2

	R-R				R-S				R-L			
	T	FU	FI	UF	T	FU	FI	UF	T	FU	FI	UF
A2B2 37	122	62	47	0	0	136	70	8	5	21	27	2
A2C2 37	100	61	61	1	0	133	97	4	1	22	15	5
B2A2 25	125	37	78	1	0	113	107	8	2	11	16	2
B2A2 37	124	62	27	1	0	135	84	9	6	21	27	4
B2C2 25	141	58	67	1	0	131	55	2	2	22	18	3
B2C2 37	107	63	62	2	0	152	49	3	3	24	32	3
B2C2 50	86	72	46	0	0	149	72	5	3	29	36	2
B2D2 25	175	42	61	1	0	94	88	6	0	16	15	2
C2A2 25	144	78	37	2	0	119	45	6	10	34	23	2
C2A2 37	107	70	47	2	0	129	71	10	2	27	27	8
C2B2 25	136	54	56	1	0	132	57	12	3	24	24	1
C2B2 37	129	51	53	2	0	138	57	11	8	30	19	2
C2D2 25	205	68	44	5	0	80	47	4	10	18	17	2
D2A2 25	61	20	27	1	0	63	37	8	2	8	18	5
D2A2 37	61	20	31	0	1	43	63	8	0	7	13	3
D2B2 25	130	33	103	2	0	91	82	7	8	12	30	2
D2B2 37	125	54	99	1	0	73	92	11	3	11	25	6
D2C2 25	87	27	43	0	0	28	33	7	4	5	12	4

Table A3.8 Results from the 500 Point Split Interface Count on Sample Series 2.2

a) A2B2 37	T	FU	FI	UF
GF-CM	22	1	1	0
GF-MM	24	0	3	0
GF-FM	1	3	1	0
GF-ISO	37	65	70	2
CM-MM	4	0	0	0
CM-FM	0	0	0	0
CM-ISO	0	5	5	0
MM-FM	15	1	0	0
MM-ISO	3	11	8	0
FM-ISO	0	0	0	0
INS-				
GF	2	371	154	3
CM	0	49	11	0
MM	0	36	17	1
FM	0	0	2	0
ISO	0	6	6	0
INL-				
GF	3	19	22	0
CM	0	3	0	0
MM	0	6	5	0
FM	0	1	1	0
ISO	0	0	2	0
Other	10	11	11	1
b) A2C2 37				
GF-CM	20	1	0	0
GF-MM	15	0	0	0
GF-FM	8	3	3	0
GF-ISO	56	64	78	0
CM-MM	1	0	0	0
CM-FM	1	1	0	0
CM-ISO	2	11	5	0
MM-FM	9	1	0	0
MM-ISO	0	4	3	0
FM-ISO	0	1	1	0
INS-				
GF	5	307	174	1
CM	0	45	19	0
MM	0	22	15	0
FM	0	0	5	0
ISO	0	0	12	0
INL-				
GF	1	22	23	1
CM	0	3	2	0
MM	0	4	3	1
FM	0	0	0	0
ISO	0	0	5	2
Other	17	16	12	0

c) B2A2 25	T	FU	FI	UF
GF-CM	53	2	2	0
GF-MM	28	2	1	0
GF-FM	4	0	1	0
GF-ISO	30	38	72	0
CM-MM	7	0	0	0
CM-FM	2	1	2	0
CM-ISO	14	18	27	0
MM-FM	19	0	0	0
MM-ISO	8	12	9	0
FM-ISO	3	0	2	0
INS-				
GF	1	185	137	1
CM	0	125	51	0
MM	0	45	19	0
FM	0	0	3	0
ISO	0	0	0	0
INL-				
GF	0	4	11	0
CM	0	7	5	1
MM	0	4	4	0
FM	0	0	0	0
ISO	0	0	0	1
Other	11	11	15	1
d) B2A2 37				
GF-CM	24	5	0	0
GF-MM	19	3	0	0
GF-FM	5	4	2	0
GF-ISO	21	45	47	0
CM-MM	3	0	0	0
CM-FM	3	0	0	0
CM-ISO	1	7	9	0
MM-FM	18	1	1	0
MM-ISO	8	21	9	0
FM-ISO	2	2	2	0
INS-				
GF	2	290	170	3
CM	0	85	41	0
MM	0	51	24	2
FM	0	2	1	0
ISO	0	1	2	0
INL-				
GF	0	8	17	0
CM	0	12	5	0
MM	0	6	3	0
FM	0	0	0	0
ISO	0	0	1	0
Other	16	14	13	0

e) B2C2 25	T	FU	FI	UF
GF-CM	47	2	0	0
GF-MM	25	3	1	0
GF-FM	7	2	6	0
GF-ISO	40	46	64	0
CM-MM	8	0	0	0
CM-FM	3	4	1	0
CM-ISO	12	35	12	0
MM-FM	21	5	4	0
MM-ISO	8	28	11	0
FM-ISO	1	1	5	0
INS-				
GF	3	179	89	1
CM	0	117	30	1
MM	0	66	13	0
FM	0	1	0	0
ISO	0	0	1	1
INL-				
GF	0	8	11	0
CM	0	7	4	0
MM	0	10	3	1
FM	0	0	4	1
ISO	0	0	2	0
Other	12	19	14	0
f) B2C2 37				
GF-CM	33	4	1	0
GF-MM	23	1	0	0
GF-FM	6	0	2	0
GF-ISO	12	37	52	0
CM-MM	14	0	0	0
CM-FM	2	1	0	0
CM-ISO	3	28	15	0
MM-FM	14	0	1	0
MM-ISO	13	19	22	0
FM-ISO	1	0	3	0
INS-				
GF	1	181	103	1
CM	0	140	53	1
MM	0	73	32	0
FM	0	2	0	0
ISO	0	0	2	0
INL-				
GF	1	17	13	0
CM	0	10	6	0
MM	0	17	8	1
FM	0	0	0	0
ISO	0	1	1	0
Other	8	13	9	0

g) B2C2 50	T	FU	FI	UF
GF-CM	33	5	0	0
GF-MM	22	3	0	0
GF-FM	6	2	0	0
GF-ISO	20	42	37	0
CM-MM	6	0	0	0
CM-FM	1	1	2	0
CM-ISO	1	18	15	0
MM-FM	17	1	1	0
MM-ISO	6	8	8	0
FM-ISO	1	0	3	0
INS-				
GF	2	205	91	5
CM	0	108	50	2
MM	0	93	58	0
FM	0	1	6	1
ISO	0	2	1	0
INL-				
GF	1	17	23	1
CM	0	10	4	1
MM	0	8	5	0
FM	0	0	0	0
ISO	0	0	3	0
Other	10	22	20	0
h) C2A2 25				
GF-CM	29	5	0	0
GF-MM	18	0	0	0
GF-FM	3	4	1	0
GF-ISO	32	79	62	0
CM-MM	8	0	0	0
CM-FM	5	1	2	0
CM-ISO	7	30	20	1
MM-FM	16	1	2	0
MM-ISO	7	18	9	0
FM-ISO	3	1	0	0
INS-				
GF	1	234	109	2
CM	0	93	39	0
MM	0	33	14	1
FM	0	3	2	0
ISO	0	0	5	0
INL-				
GF	1	12	12	0
CM	0	7	3	0
MM	0	4	1	0
FM	0	1	0	0
ISO	0	0	1	0
Other	14	32	15	0

i) C2A2 37	T	FU	FI	UF
GF-CM	30	1	0	0
GF-MM	17	3	1	0
GF-FM	11	2	2	0
GF-ISO	46	61	64	0
CM-MM	3	1	0	0
CM-FM	5	1	0	0
CM-ISO	6	17	6	0
MM-FM	16	0	1	0
MM-ISO	5	12	10	0
FM-ISO	1	1	1	0
INS-				
GF	2	238	130	1
CM	0	78	47	0
MM	0	41	28	0
FM	0	6	3	0
ISO	0	1	5	0
INL-				
GF	2	18	16	0
CM	1	4	2	0
MM	0	2	4	0
FM	0	1	0	0
ISO	0	1	2	1
Other	16	14	11	1
j) C2B2 25				
GF-CM	45	1	1	0
GF-MM	21	1	1	0
GF-FM	9	4	0	0
GF-ISO	23	53	63	1
CM-MM	7	0	0	0
CM-FM	5	0	2	0
CM-ISO	9	29	28	0
MM-FM	15	5	4	0
MM-ISO	4	14	13	0
FM-ISO	3	1	0	0
INS-				
GF	3	180	107	2
CM	1	115	53	0
MM	0	47	22	1
FM	0	2	4	0
ISO	0	0	3	0
INL-				
GF	1	11	12	1
CM	0	11	8	0
MM	0	1	3	1
FM	0	1	0	0
ISO	0	0	0	1
Other	11	17	19	0

k) C2B2 37	T	FU	FI	UF
GF-CM	30	1	1	0
GF-MM	15	5	0	0
GF-FM	3	5	3	0
GF-ISO	16	52	63	0
CM-MM	4	0	0	0
CM-FM	5	2	3	0
CM-ISO	1	22	16	0
MM-FM	8	1	1	1
MM-ISO	5	15	6	0
FM-ISO	1	0	3	0
INS-				
GF	0	231	130	2
CM	0	113	49	1
MM	0	55	29	0
FM	0	5	2	0
ISO	0	0	2	0
INL-				
GF	4	13	19	0
CM	0	8	6	0
MM	0	7	5	0
FM	0	0	1	0
ISO	0	0	3	0
Other	13	25	17	0

Table A3.9 Results from the 1000 Point by Components Interface Count on Sample Series 2.2

			Add1				Add2			
%Add			T	FU	FI	UF	T	FU	FI	UF
0%	A2	R	137	28	39	1				
		S	0	87	158	8				
		L	0	13	29	0				
		AS								
	B2	AL								
		R	154	18	17	1				
		S	1	170	105	7				
		L	1	18	24	4				
		AS								
	C2	AL								
		R	78	34	17	0				
		S	0	240	103	0				
		L	0	12	16	0				
		AS								
	Blend	AL								
		R	134	50	35	1				
		S	0	119	115	3				
		L	1	19	22	1				
10%	A2	AS								
		AL								
		R	192	33	16	0	142	29	24	0
		S	0	113	70	8	0	93	81	3
	B2	L	0	17	11	1	1	13	18	0
		AS	0	14	17	6	0	41	36	5
		AL	0	0	0	2	0	5	5	4
		R	127	9	12	0	95	15	5	0
	C2	S	0	117	83	7	0	156	43	2
		L	0	15	18	1	1	21	16	1
		AS	7	48	27	9	1	66	41	15
		AL	8	3	12	5	0	8	8	6
	Blend	R	65	23	3	0	52	31	3	0
		S	0	232	49	0	0	223	15	0
		L	0	9	3	0	0	20	2	0
		AS	0	71	16	0	1	92	23	2
		AL	2	16	10	1	0	16	14	6
		R	106	31	12	0	107	40	27	0
		S	0	144	73	1	0	121	63	0
		L	0	16	10	1	1	12	12	0
		AS	1	53	16	2	0	33	40	8
		AL	0	22	11	1	0	9	13	4

cont. overleaf

30%	A2	R	149	35	24	1	155	21	14	0
		S	0	88	84	1	0	83	81	4
		L	0	19	15	0	1	20	24	0
		AS	0	34	23	12	0	38	41	4
		AL	1	5	5	4	0	4	3	3
	B2	R	106	8	6	0	84	14	3	0
		S	0	120	49	1	0	128	37	0
		L	1	17	17	2	1	19	11	3
		AS	1	72	46	12	0	79	56	9
		AL	9	20	11	2	0	25	15	12
	C2	R	35	20	3	0	46	15	5	0
		S	0	175	16	0	0	135	81	1
		L	0	14	3	0	0	7	16	1
		AS	0	135	41	0	1	55	81	14
		AL	2	38	16	2	0	12	24	7
	Blend	R	91	19	13	0	95	28	15	2
		S	0	92	39	1	1	129	58	1
		L	1	17	13	0	0	23	14	0
		AS	1	119	53	4	0	43	50	6
		AL	3	17	15	2	0	12	16	5
50%	A2	R	178	32	18	0				
		S	0	106	47	5				
		L	3	14	6	0				
		AS	1	52	35	15				
		AL	0	5	7	0				
	B2	R	119	6	3	0	84	14	4	0
		S	0	83	56	4	0	127	36	0
		L	0	13	20	0	2	19	13	0
		AS	2	77	51	11	36	65	40	24
		AL	13	28	13	1	0	14	18	14
	C2	R	40	22	9	0	49	25	5	0
		S	1	146	39	0	0	149	38	0
		L	1	9	4	0	1	14	8	0
		AS	0	128	44	3	0	83	53	14
		AL	5	26	20	3	0	17	34	10
	Blend	R	115	23	15	0	97	22	5	0
		S	0	86	39	0	0	120	46	0
		L	1	19	9	0	1	18	12	1
		AS	0	108	42	12	28	63	31	12
		AL	4	15	11	1	0	15	30	5

Table A3.10 Results from the 500 Point Split Interface Count on Sample Series 3

a) INL									
	% Add	Add1				Add2			
		T	FU	FI	UF	T	FU	FI	UF
A3	0	0	108	125	18				
	10	1	120	101	28	0	65	170	15
	30	0	99	116	35	0	80	145	25
	50	0	78	130	43	0	0	0	0
B3	0	10	136	95	9	0	0	0	0
	10	7	105	122	16	0	103	118	30
	30	8	114	113	16	0	100	120	30
	50	6	105	122	18	0	95	113	43
C3	0	0	156	85	9				
	10	5	164	75	6	20	175	53	3
	30	0	144	96	10	10	125	105	10
	50	0	108	128	15	10	113	113	15
Blend	0	15	125	103	8				
	10	18	135	88	10	5	118	106	21
	30	15	138	88	10	0	100	125	25
	50	15	128	93	15	0	115	103	33

b) INS									
	% Add	Add1				Add2			
		T	FU	FI	UF	T	FU	FI	UF
A3	0	0	153	75	23				
	10	0	145	83	23	0	133	113	5
	30	0	130	85	35	0	136	113	1
	50	0	93	108	50	0	0	0	0
B3	0	1	171	71	8	0	0	0	0
	10	0	167	69	14	0	156	76	18
	30	0	166	70	14	0	150	74	25
	50	0	161	74	15	0	124	99	28
C3	0	3	213	33	3				
	10	0	226	21	3	3	213	34	1
	30	0	220	26	4	3	210	34	4
	50	0	179	61	10	3	195	51	1
Blend	0	0	178	65	8				
	10	3	186	55	6	1	180	58	11
	30	3	203	44	1	0	154	68	29
	50	3	179	56	13	0	133	98	20

c) AddL									
	% Add	Add1				Add2			
		T	FU	FI	UF	T	FU	FI	UF
A3	0								
	10	0	25	100	125	0	80	95	75
	30	8	81	77	85	0	85	105	60
	50	3	50	93	103	0	0	0	0
B3	0								
	10	10	89	117	34	0	63	100	88
	30	9	91	109	55	0	53	75	123
	50	8	78	116	61	0	28	74	149
C3	0								
	10	3	170	59	19	0	105	118	28
	30	0	124	104	23	0	55	130	65
	50	0	103	126	21	0	70	130	50
Blend	0								
	10	18	125	90	18	0	85	100	65
	30	18	113	105	15	0	59	96	95
	50	5	108	100	38	0	34	123	94

d) AddS									
	% Add	Add1				Add2			
		T	FU	FI	UF	T	FU	FI	UF
A3	0								
	10	0	60	108	83	0	125	111	14
	30	0	95	85	70	0	144	89	18
	50	0	100	68	82	0	0	0	0
B3	0								
	10	0	148	66	36	0	95	100	55
	30	0	143	76	31	0	83	71	96
	50	0	141	79	30	0	69	78	116
C3	0								
	10	6	210	29	5	0	191	58	1
	30	3	199	39	10	0	155	81	14
	50	0	154	84	13	0	148	85	18
Blend	0								
	10	0	189	56	5	0	149	65	36
	30	0	156	80	14	0	105	88	58
	50	0	160	60	30	0	81	114	55

Table A3.11 Results from the 250 Point Interface Count targeting Large Inerts, Small Inerts, Large Additive Particles and Small Additive Particles on Sample Series 3

